

LA-5227-PR

PROGRESS REPORT

RCC1.951228.001

Dr. Kervin

Annual Report of the
Biological and Medical Research Group (H-4)
of the
LASL Health Division
January through December 1972



los alamos
scientific laboratory
of the University of California
LOS ALAMOS, NEW MEXICO 87544

This report was prepared as an account of work sponsored by the United States Government. Neither the United States nor the United States Atomic Energy Commission, nor any of their employees, nor any of their contractors, subcontractors, or their employees, makes any warranty, express or implied, or assumes any legal liability or responsibility for the accuracy, completeness or usefulness of any information, apparatus, product or process disclosed, or represents that its use would not infringe privately owned rights.

This report presents the status of the research program of LASL's Biomedical Research Group. The four most recent reports in this series, all unclassified, are:

LA-3432-MS
LA-3610-MS

LA-3848-MS
LA-4923-PR

In the interest of prompt distribution, this progress report was not edited by the Technical Information staff.

Printed in the United States of America. Available from
National Technical Information Service
U. S. Department of Commerce
5285 Port Royal Road
Springfield, Virginia 22151
Price: Printed Copy \$3.00; Microfiche \$0.95

LA-5227-PR
Progress Report
UC-48

ISSUED: March 1973



Annual Report of the
Biological and Medical Research Group (H-4)
of the
LASL Health Division
January through December 1972

Compiled by

C. R. Richmond
G. L. Voelz

Contributions from the staff are indicated by section.

Experimental animals used in work presented in this report were maintained in animal care facilities that are fully accredited by the American Association for Accreditation of Laboratory Animal Care.

TABLE OF CONTENTS

| | <u>Page</u> |
|--------------------------------------------------------------------------------|-------------|
| ABSTRACT | vi |
| TABLE OF ORGANIZATION | vii |
| TEMPORARY APPOINTMENTS | viii |
| LOS ALAMOS SCIENTIFIC LABORATORY | x |
| HEALTH RESEARCH LABORATORY | xi |
| LABORATORY RESOURCES | xiii |
| INTRODUCTION | xiv |
| THE HOT PARTICLE PROJECT | |
| INTRODUCTION | 1 |
| EXPERIMENTAL CONDITIONS | 1 |
| Exposure of Animals | 1 |
| Distribution of Spheres in the Lung by Microradiography of Hamster Lungs | 3 |
| Retention and Excretion | 4 |
| Dosimetry | 5 |
| BIOLOGGICAL RESULTS | 9 |
| PROSPECT | 11 |
| MOLECULAR RADIOBIOLOGY SECTION | |
| INTRODUCTION | 12 |
| SYNTHESIS AND RADIOSENSITIVITY OF MODEL DNA | 13 |
| Chemical Synthesis of Oligodeoxyribonucleotides | 13 |
| Enzymatic Synthesis | 15 |
| Numerical Analysis of Gel Permeation Chromatograms | 17 |
| X-Irradiation | 18 |
| RADIATION AND GENETIC INFORMATION TRANSFER | 19 |
| Replication | 19 |
| Transcription | 20 |
| Effects of X-Irradiation on RNA Polymerase | 21 |
| Ultraviolet-Induced Cross-Links between RNA Polymerase and DNA | 23 |
| EFFECTS OF IONIZING RADIATION ON CHROMATIN STRUCTURE AND THE MITOTIC APPARATUS | 13 |
| Effects of Ionizing Radiation on Chromatin Structure and Metabolism | 25 |
| Effects of Ionizing Radiation on Components of the Mitotic Apparatus | 26 |

CELLULAR RADIOBIOLOGY SECTION

| | |
|------------------------------------------------------------------------------------------------------------------------------------------------------------------------------------|----|
| INTRODUCTION | 27 |
| REGULATORY AND CONTROL MECHANISMS IN THE MAMMALIAN CELL CYCLE | 28 |
| Informosomes in Cultured Chinese Hamster Cells: Cycloheximide-Mediated Polysome Superformation is Accompanied by Association of Informosomes with Ribosomes | 28 |
| Modified Bases of Mammalian RNA | 32 |
| Response of Histone Metabolism to X-Irradiation | 35 |
| Detailed Analysis of Biochemical Events Associated with Mammalian DNA Replication | 42 |
| SURFACE PHENOMENA AND CELLULAR INTERACTION | 45 |
| Flow Microfluorometric (FMF) Studies of Lectin Binding to Mammalian Cells | 45 |
| CHROMOSOME STRUCTURE AND FUNCTION | 46 |
| DNA-Membrane Associations in Cultured Chinese Hamster Cells: Nature of the DNA-Membrane Association and its Involvement in Temporal and Spatial Organization of DNA in the Nucleus | 46 |
| Band Analysis of the Chinese Hamster Cell Line CHO | 52 |
| Repair of Radiation Damage, Derepression, and Replication of a Bacterial Virus Chromosome | 57 |
| Packaging of a Bacterial Virus Chromosome: A Model Supported by Reactivation of Radiation-Damaged Virus DNA | 58 |

MAMMALIAN RADIOBIOLOGY SECTION

| | |
|----------------------------------------------------------------------------------------------------------------|----|
| INTRODUCTION | 61 |
| MAMMALIAN RADIOBIOLOGY | 62 |
| Biological Effects of Gamma-Ray Dose Protraction during Continuous Exposure with Fixed and Changing Dose Rates | 62 |
| Comparative Biological Effects of Radiation Dose Protraction in Dogs and Monkeys | 65 |
| Radiobiological Pilot Investigations for the Negative Pion Radiotherapy Program | 68 |
| MAMMALIAN METABOLISM | 71 |
| Retention of Tin-113 in Mice after Oral, Intraperitoneal, and Intravenous Injection | 71 |
| Cesium-137 Activity in a Normal New Mexico Population | 71 |

PHYSICAL RADIOBIOLOGY SECTION

| | |
|----------------------------------------------------------------------------------------------|----|
| INTRODUCTION | 75 |
| AUTOMATION OF DATA COLLECTION | 75 |
| NaI (Tl) Spectrometer and Transuranium Element Chest Counter Interface with PDP-8/I Computer | 75 |
| HUMCO II Interface with PDP-8/F Computer | 76 |
| Graf-Pen Interface to PDP-8/E Computer | 76 |
| ANALYTICAL SUPPORT | 76 |
| Chest and Whole-Body Counting Data Analysis | 76 |
| Flow Microfluorometric (FMF) Data Analysis | 77 |
| HUMCO II Data Analysis | 78 |
| KARYOLOGY | 78 |
| Semi-Automatic Chromosome Analysis | 78 |
| ELECTRONICS DEVELOPMENT | 79 |
| Cell Separator and Counting Logics | 79 |
| V ^{2/3} Generator | 79 |
| Amplifier with Base-Line Restoration | 80 |
| PION BEAM CHARACTERISTICS | 80 |

BIOPHYSICS SECTION

| | |
|-----------------------------------------------------------------------------------------------------------------------------|----|
| INTRODUCTION | 81 |
| CELL ANALYSIS AND SORTING INSTRUMENTATION DEVELOPMENT | 82 |
| Differential Light-Scattering Signatures of Mammalian Cells | 82 |
| Multiparameter Cell Sorter | 86 |
| A Dual-Parameter Cell Microphotometer | 88 |
| BIOLOGICAL APPLICATIONS OF CELL ANALYSIS AND SORTING | 91 |
| Fluorescent DNA Distributions in MCA-1 Tumor Cell Populations | 91 |
| Tumor Cell Identification and Separation | 92 |
| Use of Flow Microfluorometry for Analysis and Evaluation of Synchronizing Protocols and Drug Effects on Cell-Cycle Traverse | 94 |
| Application of Biophysical Instrumentation to Animal Disease Diagnosis | 96 |
| Normal and Tumor Cell Kinetic Studies Using Flow Microfluorometry (FMF) | 98 |

ISOTOPE APPLICATIONS SECTION

| | |
|-------------------------------------------------------|-----|
| INTRODUCTION | 102 |
| PREPARATION OF COMPOUNDS LABELED WITH STABLE ISOTOPES | 103 |
| Organic Synthesis | 104 |
| Biosynthesis | 114 |
| STABLE ISOTOPES IN BIOMEDICAL RESEARCH | 119 |
| Clinical Applications | 119 |
| Biochemistry | 121 |

ANIMAL COLONY ACTIVITIES

| | |
|------------------------------|-----|
| INTRODUCTION | 125 |
| DISEASE SURVEILLANCE | 125 |
| SUPPORT ACTIVITIES | 125 |
| PATHOLOGY | 126 |
| HAMSTER ANESTHESIA | 126 |
| COMPLIANCE WITH FEDERAL LAWS | 126 |

APPENDIX

| | |
|-----------------------------------------------------------------------------|-----|
| 1972 BIBLIOGRAPHY FOR BIOMEDICAL RESEARCH GROUP | 128 |
| Hot Particle Project | 128 |
| Molecular Radiobiology Section | 128 |
| Cellular Radiobiology Section | 129 |
| Mammalian Radiobiology Section | 131 |
| Physical Radiobiology Section | 131 |
| Isotope Applications Section | 132 |
| TALKS PRESENTED AT SEMINARS AND MEETINGS BY BIOMEDICAL RESEARCH GROUP STAFF | 134 |
| Cellular Radiobiology Section | 134 |
| Molecular Radiobiology Section | 135 |
| Biophysics Section | 136 |
| Mammalian Radiobiology Section | 137 |
| Isotope Applications Section | 137 |
| RESEARCH INTERESTS OF BIOMEDICAL RESEARCH GROUP DIRECTIVE STAFF MEMBERS | 139 |
| COMMITTEES ASSOCIATED WITH THE BIOMEDICAL RESEARCH PROGRAM | 141 |

ABSTRACT

This report summarizes research activities of the Los Alamos Scientific Laboratory's Biomedical Research Group for calendar year 1972. We have included information on organization of the group, research interests of the staff, and supporting facilities available at the Los Alamos Scientific Laboratory. Although for administrative purposes the group is comprised of seven sections, the technical portion of this report is based upon major areas of research and reflects the multidisciplinary

approach to problem solving, which is a basic ingredient of our research philosophy.

The format is akin to that of Science with the goal of transmitting a maximum of information in a concise manner with a minimum of technical detail. Work which has been published or submitted for publication has not been duplicated in this report. A list of publications for 1972, which follows as an appendix, allows the reader to consult the published literature for additional specific technical detail.

BIOMEDICAL RESEARCH GROUP

December 31, 1972

C. R. Richmond, Ph.D., Group Leader
D. G. Ott, Ph.D., Alternate Group Leader
E. C. Anderson, Ph.D., Assistant Group Leader for Special Problems
C. Richman, Ph.D., Biophysics Specialist
E. M. Sullivan, Administrative Specialist
T. M. Brittt, Secretary
H. L. Barrington, Clerk-Typist
J. M. Verre, Receptionist-Telephone Operator

CELLULAR RADIOBIOLOGY SECTION

D. F. Petersen, Ph.D.,
Section Leader

Staff Members

B. J. Barnhart, Ph.D.
E. W. Campbell, B.S.
S. H. Cox, B.A.
M. D. Enger, Ph.D.
L. R. Gurley, Ph.D.
C. E. Hildebrand, Ph.D.
P. M. Kraemer, Ph.D.
P. C. Sanders, Ph.D.
A. G. Saponara, Ph.D.
R. A. Tobey, Ph.D.
R. A. Walters, Ph.D.

Postdoctoral Appointee

L. L. Deaven, Ph.D.

Chemistry Technician

J. L. Hanners

Cell Culture Technician

J. G. Valdez

MOLECULAR RADIOBIOLOGY SECTION

F. N. Hayes, Ph.D.,
Section Leader

Staff Members

G. T. Fritz, B.S.**
J. M. Hardin, M.S.
D. E. Hoard, Ph.D.
A. M. Martinez, B.S.
E. L. Martinez, B.S.
B. J. Noland, B.A.
R. L. Ratliff, Ph.D.
G. R. Shepherd, Ph.D.*
D. A. Smith, Ph.D.
D. L. Williams, M.S.

Postdoctoral Appointee

G. F. Strniste, Ph.D.

Chemistry Technicians

V. E. Mitchell
E. C. Wilmoth

* Leave of absence.

** Casual.

*** Half-time.

BIOPHYSICS SECTION

P. F. Mullaney, Ph.D.
Acting Section Leader

Staff Members

L. S. Cram, Ph.D.
J. C. Forslund, B.S.
P. K. Horan, Ph.D.
J. C. Martin, B.A.
A. Romero, B.S.
J. A. Steinkamp, Ph.D.
T. T. Trujillo, B.S.
M. A. Van Dilla, Ph.D.*

Postdoctoral Appointee

H. A. Crissman, Ph.D.

Electronics Technicians

J. L. Horney
W. T. West

VETERINARY SECTION

L. M. Holland, D.V.M.,
Section Leader

Staff Members

S. G. Carpenter, B.A.
P. M. Labauve, B.A.
J. R. Prine, D.V.M.
Animal Colony Assistant
Manager
E. A. Vigil

Medical Stenographer

B. B. Gettemy**

Histopathology Technician

R. H. Wood

Animal Technicians

J. E. Atencio
F. Benavidez
J. Cordova**
J. S. Martinez
R. Martinez
E. C. Rivera
L. Salazar
J. B. Sanchez
F. Valdez

MAMMALIAN RADIOBIOLOGY SECTION

J. F. Spalding, Ph.D.,
Section Leader

Staff Members

M. R. Brooks, B.Ch.E.
G. A. Drake, B.S.
J. E. Furchner, Ph.D.
O. S. Johnson, B.S.
J. Langham, B.S.
J. E. London, B.S.
J. S. Wilson, B.S.

Biology Technicians

R. F. Archuleta

Undergraduate Co-op Students

E. G. Adams
M. A. Nevares

PHYSICAL RADIOBIOLOGY SECTION

P. N. Dean, M.S.,
Section Leader

Staff Members

J. H. Jett, Ph.D.
J. H. Larkins, B.S.***
J. D. Perrings
M. R. Raju, Ph.D.

Electronics Technicians

M. T. Butler
L. J. Carr
W. D. Jinks

(alternate 6 months at Highlands University; are LASL SCP-4 chemistry technicians)

TEMPORARY APPOINTMENTS

ASSOCIATED WESTERN UNIVERSITIES, INC.

The Los Alamos Scientific Laboratory, as a participant in the Associated Western Universities, Inc., serves the intended purpose of the U. S. Atomic Energy Commission of providing support for education and training of advanced students and faculty participation appointees. The function of AWU is to promote and coordinate orientation and training on projects of a regional nature that require inter-university cooperation. AWU is particularly concerned with organization and management of programs and facilities that cannot be undertaken with equal effectiveness by a single institution. One such area of interest is the promotion of orientation and training in recent and specific trends in the biological sciences.

It is felt that increasing opportunities for collaboration would serve the best interests of the universities, LASL, and the biological sciences. University personnel benefit by increased opportunities for training and teaching, by access to unique or specialized LASL facilities, and by use of Los Alamos as a focus, or catalyst, for multi-institutional cooperative efforts. Los Alamos biologists benefit from greater contact with university faculties and graduate students. All biologists participating in this program benefit from mutual collaborative efforts, cross-fertilization of ideas, and by sharing specialized expertise, unique capabilities, and costly equipment.

A truly functional relationship between LASL and other AWU members is of great potential value to research, continued professional development, and graduate training. Following is a list of participants in the AWU-LASL biomedical research program for 1972.

AWU Faculty Participant

U. Hollstein, Ph.D., University of Amsterdam (1956).
Department of Chemistry, University of New Mexico,
Albuquerque, New Mexico

AWU Laboratory Graduate Participant

A. W. Harmon, Ph.D., Oklahoma State University
(1972). Department of Chemistry, Oklahoma State
University, Stillwater, Oklahoma

AWU Graduate Fellow

A. Brunsting, M.S., University of New Mexico (1969).
Department of Physics, University of New Mexico,
Albuquerque, New Mexico

POSTDOCTORAL RESEARCH PROGRAM

A limited number of research assignments are available for young individuals with a Ph.D. degree at the Laboratory. These LASL fellowships are awarded on a competitive basis for one year with the possibility for renewal for a second year. The following is a list of postdoctoral appointees who participated in the LASL biomedical research program during part or all of 1972, with their previous academic affiliations and major research interests.

H. A. Crissman, Ph.D., Pennsylvania State University (1971)

Application of cytology and histochemistry
techniques to high-speed, flow-system cell
analysis instrumentation

C. E. Hildebrand, Ph.D., Pennsylvania State University (1970)

Synthesis of cell-free protein

G. F. Strniste, Ph.D., Pennsylvania State University (1971)

Identification of molecular effects of
various ionizing radiations upon carefully
characterized model systems

UNDERGRADUATE CO-OP STUDENTS

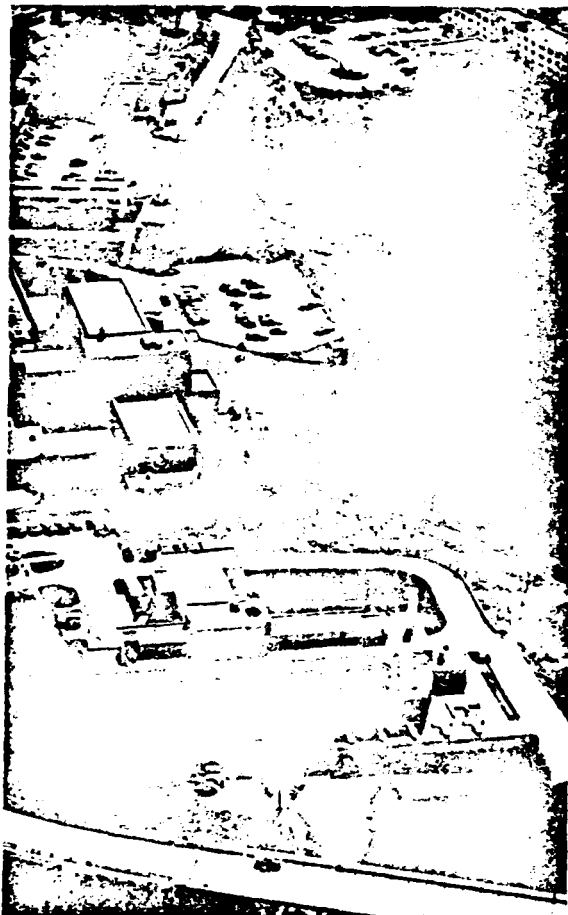
Several persons participated in the Biomedical Research Group's activities during 1972 as part of the Laboratory's Undergraduate Co-Operative Program. The participants are hired as pairs and spend 6-month periods between the participating university and LASL. Attempts are made to continue periodic employment for successful candidates from the beginning of the sophomore year through graduation. The current participants, Mr. M. A. Nevarez and Mr. E. G. Adams, both matriculated at Highlands University at Las Vegas, New Mexico, and function as chemistry technicians in the Isotope Applications Section of Group H-4.



LOS ALAMOS SCIENTIFIC LABORATORY

A rather spectacular aerial photograph shows the bridge over Los Alamos canyon which links the major Laboratory sites and facilities with the Biomedical Research Laboratory-Los Alamos Medical Center complex and town site. To the east (top) of the bridge are located the airstrip on the left and the Clinton P. Anderson Meson Physics Facility

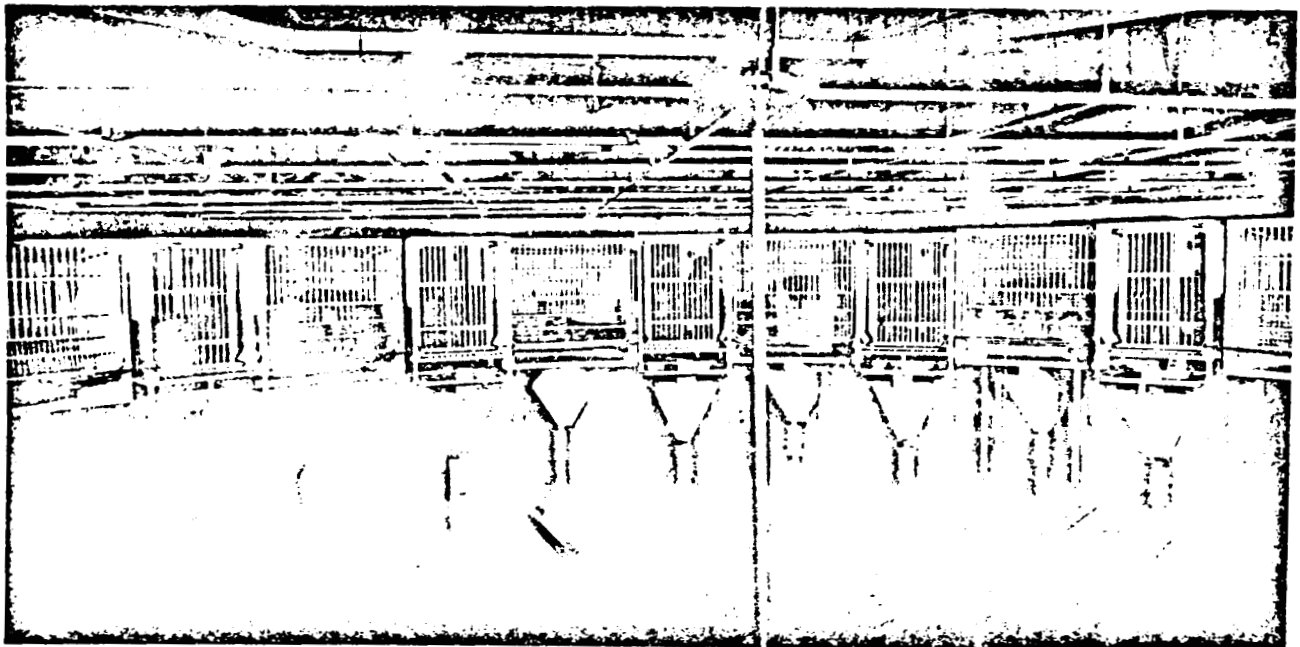
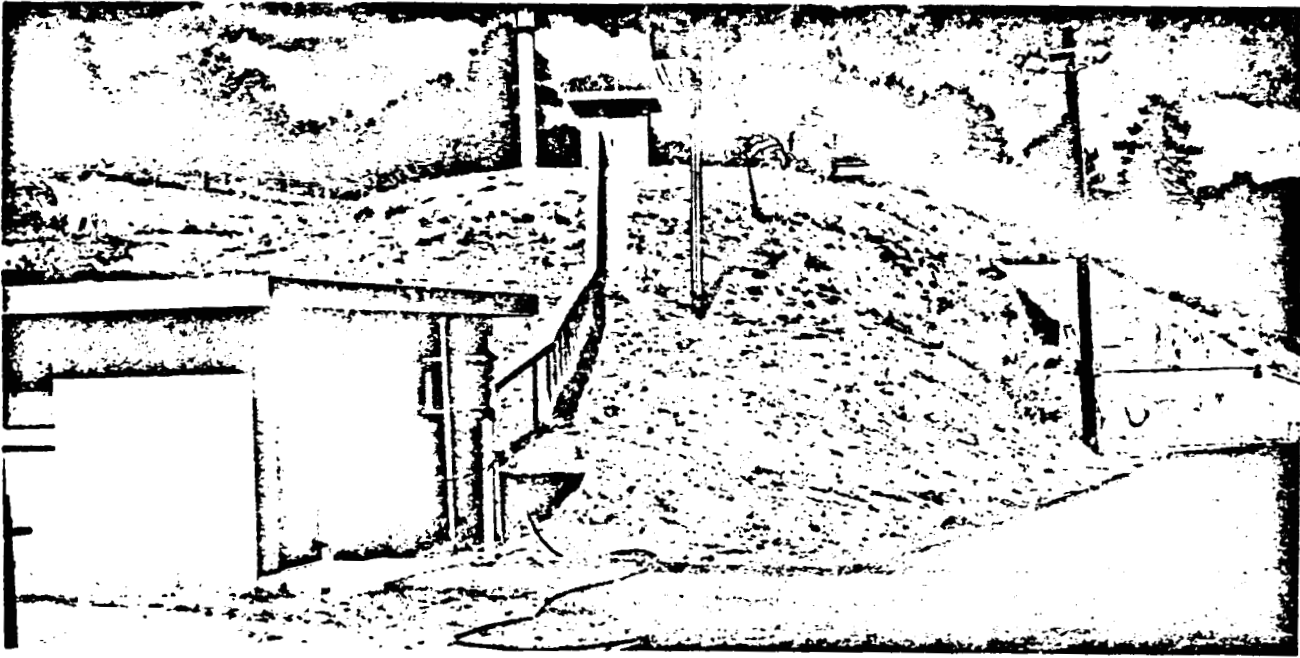
(LAMPF) on the right of the prominent Los Alamos canyon. Within the area shown are reactors, accelerators, sophisticated computing facilities, machine shops, and all the related equipment and technology associated with a large, well-established laboratory concerned with research in the physical sciences.



HEALTH RESEARCH LABORATORY

Two aerial views of the Health Research Laboratory, which houses the Biomedical Research Group (H-4) of the Los Alamos Scientific Laboratory's Health Division, are shown above. The left photograph shows the close proximity of the Health Research Laboratory to the bridge which spans Los Alamos canyon. The main multistoried building was constructed in 1952, and the single-level annex used to house experimental animals was added in 1960. Immediately above the Health Research Laboratory is shown the 84-bed Los Alamos Medical

Center, administered by the Lutheran Hospital and Home Society of Fargo, North Dakota, which serves Los Alamos and surrounding communities. The close physical relation between the Los Alamos Medical Center and the Health Research Laboratory fosters the exchange of ideas and interests among respective staffs. Shown in the right photograph is the Health Research Laboratory and Los Alamos Medical Center complex and its spatial relationship to the main centralized Laboratory complex across Los Alamos canyon.



The upper photograph shows the Biomedical Research Group's satellite Radiation Exposure Facility located in a remote area of the Laboratory about 10 miles from the main Health Research Laboratory. Built in 1962, the 1800-square foot facility houses cobalt-60 sources of 10, 100, and 1000 Ci encased in steel capsules which can be raised or lowered into a lead shield beneath the floor from another building about 50 yards away. The octagonal concrete igloo, 40 feet in diameter and 20 feet in

height, is buried in the side of a hill and is accessible through a 50-foot long tunnel. Studies of the biological effects of radiation delivered in different total doses, dose rates, or fractionations are conducted in this building.

The lower photograph shows the holding cage arrangement within the Radiation Exposure Facility which permits simultaneous exposure of dogs and monkeys to a wide range of cobalt-60 gamma rays.

LABORATORY RESOURCES

Although the Los Alamos Scientific Laboratory had its beginning as a weapons laboratory during the Second World War, about half of the Laboratory's effort currently is directed toward basic research in the physical and biological sciences. The Laboratory has some unusual research tools available to all Laboratory personnel, graduate students, and visiting scientists.

LIBRARIES

LASL maintains a system of libraries to meet specialized needs of the various research groups. The main library, with its branches, constitutes the largest technical library between the Mississippi and Pacific coast. The Medical Branch Library of the Health Research Laboratory has complete holdings of about 750 current periodicals in biochemistry and biophysics, radiation biology, cell biology, medicine, etc., including clinical medicine, through the Library's affiliation with the Los Alamos Medical Center serving the community.

STABLE ISOTOPE PROGRAM

LASL has unexcelled facilities for the production of large quantities of highly enriched stable isotopes: nitrogen-15, oxygen-17, and carbon-13. It is anticipated that sulfur-33 production will begin in the near future. Since these are all magnetically active nuclei, they can be detected by magnetic resonance techniques as well as by conventional mass spectrometry. A program of biochemical studies utilizing these isotopes and organic and biological syntheses, in conjunction with sophisticated nuclear magnetic resonance spectrometers and other advanced techniques of physical biochemistry, is just beginning to gain momentum.

RESEARCH REACTORS

Two research reactors located near the Health Research Laboratory are available as radiation sources: the "Water Boiler," a homogenous reactor capable of operation at all power levels from 0 to 25 kilowatts, and the 8-megawatt Omega West reactor.

ACCELERATORS

Several electrostatic accelerators, including

a 23-MeV tandem Van de Graaff, 28-MeV e^- linear accelerator, and a 25-MeV cyclotron, are available for radiation experiments. The particles available are electrons, protons, deuterons, and alphas. The linear accelerator can provide very intense X-ray beams up to about 2×10^5 rads/minute. The Van de Graaff accelerator can be used to provide copious quantities of high-energy neutrons.

CLINTON P. ANDERSON MESON PHYSICS FACILITY

A unique accelerator capable of producing an 800-MeV proton beam of unusually high intensity (1 ma average current) which, in turn, will be used to produce negative π mesons is now under construction. A biomedical research building is under construction in the target area for investigating the theoretically promising medical applications of these particles for cancer therapy. Preclinical radiobiological studies using negative π mesons are in the planning stage, and some comparative studies and work on exposure systems are in progress.

INSTRUMENT DEVELOPMENT

LASL maintains a large and unusually competent electronics group for the adaptation and creation of instrumentation needed for today's highly specialized research. The main machine shop, foundry, glass fabrication unit, and branch shops constitute one of the nation's unique experimental facilities. A branch shop with full-time machinists is available within the Health Research Laboratory.

COMPUTER FACILITY

One of the largest computer installations in the world, including three CDC 6600's, two CDC 7600's, and several smaller machines, is available to all Laboratory personnel as are programming and other support services. A special computer, MANIAC II, also is available. In addition, several smaller computers, a PDP 8/I, and a PDP 8/E are in use at the Health Research Laboratory dedicated to shared, real-time use in data acquisition and processing. The Health Research Laboratory also has a MUX (Multiple Use Experiment) terminal that communicates directly with one of the Laboratory's CDC 6600 computers.

INTRODUCTION

A significant historical event which altered the course of mankind occurred on February 23, 1941, when Dr. G. T. Seaborg and colleagues discovered the element plutonium in room 301 of Gilman Hall at Berkeley. The isotope of mass-238 and not the more familiar mass-239 was first discovered at that time; the plutonium isotope of mass-239 was not isolated until the spring of 1941, and element 94 remained unnamed until March of the following year. On March 28, 1941, 0.5 μg of plutonium-239 was fissioned by thermal neutrons, and the enormous effort to produce plutonium-239 in quantity for military purposes was begun. The potential toxicity of plutonium was recognized soon after its discovery and availability in quantities for biomedical research.

It is worth recalling that only extremely small quantities of this precious material were available for experimentation during the early 1940's. As an example, the following memorandum written to the Director of the Health Division of the Metallurgical Laboratory is indicative of the early concern about the potential toxicity of plutonium. The memorandum states in part: "It has occurred to me that the physiological hazards of working with plutonium and its compounds may be very great. Due to its alpha radiation and long life it may be that the permanent location in the body of even very small amounts, say 1 milligram or less, may be very harmful. The ingestion of such extraordinarily small amounts as some few tens of micrograms might be unpleasant, if it locates itself in a permanent position. In the handling of the relatively large amounts soon to begin here and at site Y (Los Alamos), there are many conceivable methods by which amounts of this order might be taken in unless the greatest care is exercised. In addition to helping set up measures in handling so as to prevent the occurrence of such accidents, I would like to suggest that a program to trace the course of plutonium in the body be initiated as soon as possible. In my opinion, such a program should have the very highest priority."

The writer of this memorandum was Dr. Glenn T. Seaborg, and the date was January 1944.

The biomedical research program at Los Alamos has evolved from its conception in 1943 as a small Health Group established to protect the health of the workers, to develop safe working procedures, and to establish tolerance levels for exposure to radioactivity, plutonium, and other radionuclides. In 1944, once significant amounts of plutonium began to accumulate at Los Alamos, the Laboratory Director, Dr. J. Robert Oppenheimer, at the request of the Health Group, authorized the temporary establishment of a group of four people to initiate a research program designed to develop tests for setting exposure limits for plutonium. Several months later, this small group was absorbed by the Health Group as a Biochemistry Section, and the Laboratory's biomedical research program was born. In 1945, the Section moved into a small building of its own, and its members established the urine assay procedure for diagnosing exposure of Laboratory personnel to plutonium. Experiments were conducted which led to the first successful labeling of a biologically important compound (nicotinic acid) with reactor-produced carbon-14. The first measurement of carbon-14 by scintillation counting procedures was accomplished here and formed the basis for the present generation of commercially available liquid scintillation counting systems.

By 1948, the Health Group was a Division in the Laboratory, and the Biochemistry Section became Group H-4, the Biomedical Research Group. In



Fig. 1. Makeshift building used for biomedical research activities during the war years (photographed in 1946 showing three additions to the original structure).

October 1952, the group moved from temporary wooden structures (Fig. 1) into its present building and by the end of that decade had established itself in both national and international circles as an authority on the effects of radiation from nuclear weapons, worldwide fallout, and the physiology and toxicology of tritium and plutonium.

The Biomedical Research Group pioneered in and became a recognized authority on liquid scintillation counting, synthesis of isotopically labeled organic compounds, use of radioactive tracers in biology and medicine, and whole-body counting techniques and applications to biomedical research. By utilizing the development of large-volume liquid scintillation detectors, the group contributed significantly to the field of anthropometry through its capability to measure total-body potassium by quantitating the natural level of potassium-40 within the human body. By exploiting the whole-body counting systems designed for both research animals and man and making use of the Laboratory's significant computer capabilities, the Biomedical Research Group contributed significantly to the field of radiation protection by conducting studies on the uptake, distribution, and excretion of radioisotopes by animals and man. The interest in metabolic kinetics was also applied to the emerging field of nuclear medicine during the late 1950's.

Shortly after the discovery in 1955 of the presence of cesium-137 in man from worldwide nuclear fallout, measurements were begun on a controlled population of subjects residing in the Los Alamos area. These studies have continued to the present time and represent perhaps the most meaningful documentation of the temporal changes in man of a radioactive material released to the environment.

Beginning in the early 1960's, more emphasis was placed on the fundamental research aspects of the biomedical research program. Although investigations continued in the Mammalian Metabolism and Mammalian Radiobiology Sections related to the response of higher organisms to ionizing radiations and radioactive materials, a major emphasis was directed toward research in the fields of molecular and cellular biology.

The late 1960's also marked the start of a research program related to the question of the probable biological effects resulting from

nonuniform dose distribution of alpha-emitting particulates in the lung. Interestingly, this very difficult problem has received considerable attention but little resolution since the mid-1940's. This particular problem is now one of the highest priority because of the vast potential applications of the element plutonium as regards breeder reactors, space nuclear power systems (radioisotopic thermoelectric generators), medical applications such as the heart pacer and artificial heart, as well as production, transportation, and deployment of this material for national defense. It is interesting in a sense that part of the group is now actively working on the problem which relates to plutonium efforts conducted some 20 years previously at LASL.

The 1970's have witnessed the emergence of an interest in the stable isotope program designed to exploit the use of stable elements in the general field of biomedical research. In 1971, an Isotope Applications Section was formed within the group to concentrate on the biomedical aspects of the ICONS (Isotopes of Carbon, Oxygen, Nitrogen, and Sulfur) program which involves several groups within the Los Alamos Scientific Laboratory.

The Molecular Radiobiology Section is engaged in a variety of organic synthesis procedures to assemble polynucleotides having known base sequences. Certain enzymes that catalyze polynucleotide synthesis are not only being isolated and purified but are also being studied as biofunctional proteins participating in information transfer reactions. The structure, function, and metabolism of both acidic and basic nuclear proteins, believed to be involved in readout of genetic specifications and thus differentiation, are being investigated.

Biologists and biochemists in the Cellular Radiobiology Section are investigating the temporal sequence of a variety of cellular processes in relation to specific phases of the cell life cycle using synchronized cultures of mammalian cells. A method has been developed in this Laboratory for producing relatively large quantities of cultured mammalian cells synchronized with respect to period in the life cycle. Using these cultures, mechanisms controlling synthetic processes, energy metabolism, recovery from ionizing radiation, cell-surface phenomena, and mathematical methods of cell growth are

being investigated. Several members of the Molecular Radiobiology Section are using synchronized cultures to examine the synthesis, turnover, and structural alterations of nuclear and cytoplasmic basic proteins. In addition to studies on animal cells, investigations are in progress on survival of microorganisms exposed to ultraviolet and ionizing radiations and the biochemistry of bacterial genetic transformation.

The Biophysics Section is mainly concerned with development and improvement of instrumentation for cell biology research. In collaboration with the Cellular Radiobiology Section, electronic instruments have been developed for high-speed electronic cell counting and cell sizing. A high-speed sorter has been invented which can physically separate living cells in suspension according to cell volume. A fluorescent cell spectrometer has been developed which utilizes a laser to provide the high intensity

and collimation of the light of excitation required to determine rapidly and quantitatively the DNA content of individual cells of a cell population. Both cell sensing and sorting efforts are currently being extended to other optical and multiparameter methods. The Biophysics Section also provides general electronics, mechanical engineering, radiological physics, and computer science support for the group.

On 1 July 1972, the Pion Radiobiology Group (H-9) was disbanded and incorporated into the Biomedical Research Group (H-4) to consolidate the research effort on the applications of negative π mesons to radiation therapy and pretherapy radiobiological research. This action added four people to H-4.

In September 1972, an Agricultural Biosciences Group (H-6) was formed within the Health Division, resulting in the loss of one person from the Biomedical Research Group.

THE HOT PARTICLE PROJECT

INTRODUCTION

The objective of this project is to study possible carcinogenesis and other hazards resulting from localized irradiation of tissue by highly radioactive, insoluble microparticles with emphasis on PuO_2 in the lung. The program is two-fold: (1) measurement of tumor incidence in experimental animals, and (2) development of mathematical models. Our previous annual report¹ discussed the preparation and characterization of the ceramic $\text{ZrO}_2\text{-PuO}_2$ spheres used as radiation sources, the injection of some 1000 golden hamsters with 2000 to 20,000 microspheres per animal (lung burdens of 0.14 to 360 nCi), the determination of distribution of spheres within the lung, and a few cases of mild biological response.

In calendar year 1972, progress has been made along several lines: (1) four additional dose levels have been injected, and observations have continued with exposure times now approaching 2 years in some cases; (2) ultrasoft X-radiography has been used to visualize structure and sphere distribution in excised whole lungs; (3) a Monte Carlo study of the effect of lung structure on dose distribution has begun; and (4) consideration has been given to the use of collateral insults to increase tumor incidence.

EXPERIMENTAL CONDITIONS

Exposure of Animals

(E. C. Anderson, G. A. Drake, L. M. Holland, J. E. London, J. D. Perrings, and J. S. Wilson)

For the convenience of the reader, we repeat here the protocol for preliminary experiments as given in last year's annual report¹ (pp. 26-27). Table 1 gives the plutonium content of 10 batches of ZrO_2 microspheres which have been prepared, and Table 2 summarizes the 8 exposure levels which were injected last year. These experiments were planned as an exploratory survey covering a wide dynamic

range and using 60 animals per group. When the dose range of interest is located, those groups will be expanded to 150 animals, and additional dose levels will be interpolated. This has not yet been done, since the unexpectedly low frequency and intensity of biological response observed thus far suggest that expectation may be in error in the assumed "worst dose" or in the maximum probability, or both. Therefore, it seemed more economical to extend the range of the preliminary experiment with a modest number of animals and to postpone full-scale commitment until more positive results are observed. Thus, in March 1972, one group of 150 animals was injected with 6000 spheres, each using Level 2 activity (0.22 pCi/sphere). The total lung burden for these animals is 1.3 nCi (similar groups using Levels 4 and 6 spheres previously had been started in November 1971). Compared with the original groups, the 2.5-fold increase in animal number and 3-fold increase in sphere number gave a total increase of 7.5-fold in sensitivity for low-level damage.

More immediate lung damage and higher tumor incidence rates than those we have observed have been reported for other animals exposed to comparable total doses of plutonium. The main difference appears to be that aerosols were inhaled in the other experiments, thus giving exposures to much larger numbers of smaller (and more mobile) particles. This would result in a more nearly uniform irradiation of and damage to a much larger fraction of the lung. In an attempt to approach these conditions, we have increased greatly the number of spheres administered using our lower specific-activity spheres. Although this action defeats our original intention of keeping the number of spheres small enough to minimize overlapping of radiation fields, it provides a comparison of our test system with those used elsewhere and will offer a direct comparison of localized versus diffuse irradiation and give a direct indication of the inefficiency of concentrated sources which should be of value in selection of additional exposure conditions. Once

TABLE 1. PLUTONIUM CONTENT OF MICROSPHERES

| Isotope | Level | Batch number | Specific activity | | Equivalent diameter pure ²³⁸ PuO ₂ (μm) | PuO ₂ weight fraction |
|-------------------|-------|--------------|-------------------|--------------|---------------------------------------------------------------|----------------------------------|
| | | | pCi/sphere | α/min/sphere | | |
| ²³⁹ Pu | 1 | Zr24 | 0.07 | 0.16 | 0.09 | 4.3 x 10 ⁻⁴ |
| | 2 | Zr25 | 0.22 | 0.49 | 0.13 | 1.4 x 10 ⁻³ |
| | 2A | Zr27 | 0.42 | 0.92 | 0.16 | 2.9 x 10 ⁻³ |
| | 3 | Zr22 | 0.91 | 2.0 | 0.21 | 5.8 x 10 ⁻³ |
| | 3A | Zr28 | 1.6 | 3.6 | 0.26 | 1.1 x 10 ⁻² |
| ²³⁸ Pu | 3A | Zr29 | 2.1 | 4.7 | 0.28 | 4.8 x 10 ⁻⁵ |
| | 4 | Zr31 | 4.3 | 9.5 | 0.36 | 1.0 x 10 ⁻⁴ |
| | 4A | Zr30 | 8.9 | 19.5 | 0.46 | 2.0 x 10 ⁻⁴ |
| | 5 | Zr32 | 13.3 | 29.3 | 0.52 | 3.3 x 10 ⁻⁴ |
| | 6 | Zr33 | 59.4 | 131.0 | 0.86 | 1.3 x 10 ⁻³ |

TABLE 2. EXPOSURE CONDITIONS FOR PRELIMINARY EXPERIMENT (2000 SPHERES/ANIMAL, 60 ANIMALS/GROUP)

| Isotope | Level number | nCi/Animal | "Averaged dose rate" ^b (rads/yr) | Local dose rate at | | Possible tumor incidence ^a (tumors/group) |
|-------------------|--------------|------------|---------------------------------------------|-----------------------------|-----------------------------|------------------------------------------------------|
| | | | | Surface of sphere (rads/hr) | 40 μm from center (rads/hr) | |
| ²³⁹ Pu | 1 | 0.14 | 13 | 4.2 x 10 ¹ | 6.8 x 10 ⁻¹ | 2 |
| | 2 | 0.44 | 42 | 1.2 x 10 ² | 2.2 x 10 ⁰ | 10 |
| | 2A | 0.84 | 81 | 2.5 x 10 ² | 4.1 x 10 ⁰ | 40 |
| | 3 | 1.82 | 175 | 5.5 x 10 ² | 1.0 x 10 ¹ | 60 |
| | 3A | 3.2 | 310 | 1.0 x 10 ³ | 1.7 x 10 ¹ | 40 |
| ²³⁸ Pu | 4 | 8.6 | 875 | 2.5 x 10 ³ | 4.2 x 10 ¹ | 10 |
| | 5 | 26.6 | 2,710 | 8.4 x 10 ³ | 1.3 x 10 ² | 0 |
| | 6 | 119.0 | 12,100 | 3.6 x 10 ⁴ | 5.8 x 10 ² | 0 |

^aUsing NUS structure lung, ρ = 0.19.²

^bAssuming 1 g of lung irradiated.

conditions are found which result in tumor production, the attempt to produce effects with isolated sources will be resumed. Thus, on July 2 additional groups of 30 animals each were injected with total lung burdens of about 100 nCi. One group received from 1,000,000 to 2,000,000 spheres/animal of Level 1 spheres (0.07 pCi/sphere), and the other received 200,000 spheres/animal of Level 2A (0.42 pCi/sphere). These 2 groups, along with the original Level 6 2000-sphere/animal group, will be compared with the observation³ that 0.1 μCi lung

burden resulted in a survival time of only 1 year with rats.

To investigate possible differences in foreign-body response to particles on opposite sides of the alveolar-capillary wall, we have introduced spheres directly into the alveoli to supplement previous jugular injections. No plutonium has been used pending a determination of the contamination problem posed by excretion; however, in June 1972, 24 animals received ⁵⁷Co-labeled spheres by intratracheal insufflation to study this problem.

Since the incidence of lung damage in the hamster has so far been lower than anticipated, a small number of rats was exposed to determine if this species, which has more natural lung disease than the hamster, showed a higher incidence of radiation damage possibly as a result of synergistic effects. In this experiment, 115 rats were injected with 6000 spheres/animal via the jugular route using Level 4 spheres (specific activity 4.3 pCi/sphere). Thus, the lung burden was 26 nCi/animal.

Distribution of Spheres in the Lung by Microradiography of Hamster Lungs

[S. G. Carpenter, L. M. Holland, J. R. Prine, and R. H. Wood (H-4), and L. E. Bryant and J. R. London (M-1)]

The determination of distribution of microspheres within the lung was previously reported¹ (pp. 28-30). Uniformity of average concentration was established by gamma-ray counting of the subdivisions (down to 1/64ths) of a left lung. Distribution of nearest-neighbor distances was shown to be essentially random by visual measurements on thin sections. This method is tedious and, because few spheres can be detected in any one section, it is very difficult to determine sphere location in relation to major lung anatomy. An elegant method of visualizing both the microspheres and lung microstructure in excised whole lung has been developed using ultrasoft X-radiographs. In this procedure, a previously injected animal is sacrificed and exsanguinated. The trachea is exposed and an intratracheal cannula fixed in place. The lungs are then removed from the thorax, and the specimen is enclosed in a plastic bag and suspended from a ring stand. Dry helium gas is allowed to flow through the cannula at a rate adjusted to allow the lungs to inflate to approximately their normal size (about 16 liters/hour or enough so that 300 liters pass through the specimen in 18 hours). This process dries and fixes the lung in an inflated configuration. While continuously maintaining the helium atmosphere, the lung or lobe of choice (usually the entire left lung) is dissected from the specimen. In some cases, one side of the lung may have to be trimmed slightly to achieve a flat surface for stable positioning.

Microradiography is done by Group M-1 (Non-

destructive Testing) of the Los Alamos Scientific Laboratory. Lung tissue is placed directly on the emulsion of a Kodak high-resolution spectrographic plate and placed in a Lucite chamber sealed to the X-ray tube head (Fig. 1). The chamber is evacuated and then filled with helium. Target-to-plate distance is 36 in. (0.91 meter), and the exposure is made at 15 kVp, 20 ma, for 40 minutes. The entire radiographic procedure is performed in a darkened, safe-light environment as the emulsion of the plate is exposed. Emulsion is on one side only to reduce unsharpness due to parallax. Parallax and vibration during the long exposures are important factors

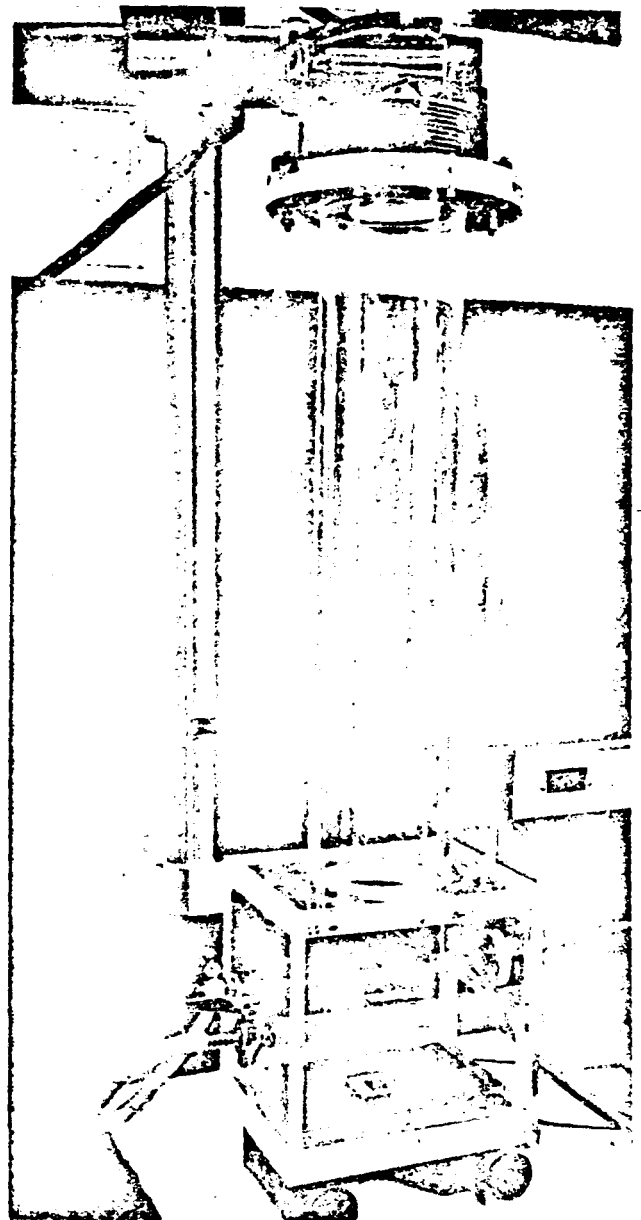


Fig. 1. Soft X-ray exposure system.

limiting resolution. Helium gas is used to reduce atmospheric absorption of the soft X-ray beam. The developed plate is placed on an enlarging shadowgraph and magnified up to 200 X. Photographs of regions of interest are then taken for permanent record. Examples are given in Figs. 2a and 2b, in which one can identify the 10- μ m ZrO₂ spheres and their locations relative to both macrostructure and microstructure of the lung airways.

If desired, the entire radiograph can be photographed on the shadowgraph, producing a montage visualizing the complete lung. In addition, we have made stereoradiographs which, when photographically enlarged and viewed with a stereoviewer, afford a three-dimensional image of the microspheres in situ. It is possible to obtain similar results from thick (0.25-mm) sections of paraffin-embedded specimens. A shorter target-to-plate distance (ca. 12 in.) and lower energies (ca. 8 kVp) can be used

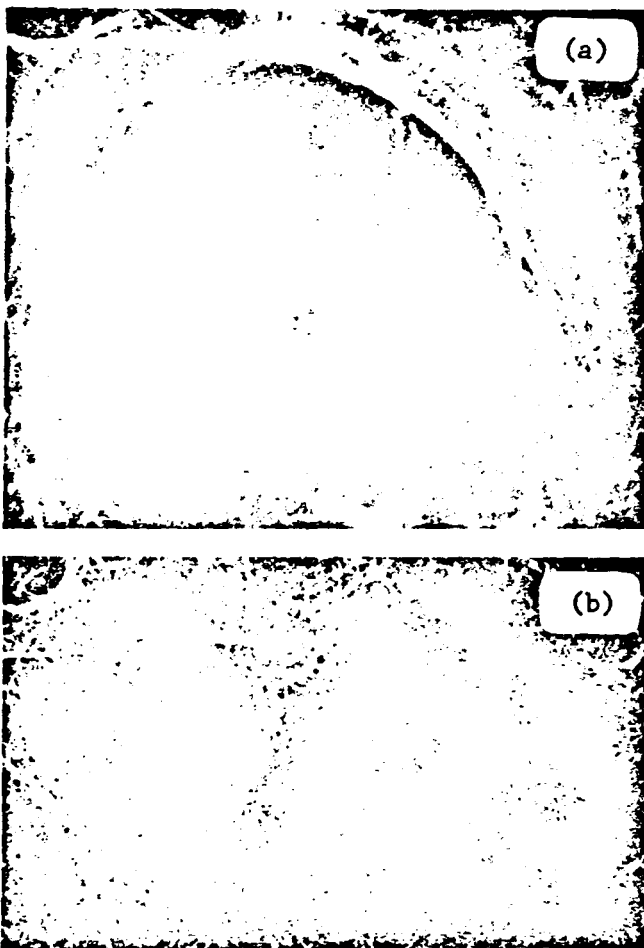


Fig. 2. Soft X-radiographs of (a) lung with microspheres (200 X), and (b) lung parenchyma with microspheres (50 X).

in a normal air atmosphere. This technique, particularly the shorter target-to-plate distance, creates more penumbra and, hence, a less sharp image.

A further advantage of the helium atmosphere technique is that, after radiography, the lung can be infiltrated with celloidin and studied histologically with acceptable preservation of configuration and microanatomy. Because the lung is inflated to an approximation of its normal size and the photographic enlargement factors are known, intersphere distances can be measured accurately either as projections or, with stereopairs, in three-dimensional space.

Retention and Excretion

(E. C. Anderson, P. N. Dean, G. A. Drake, L. M. Holland, J. E. London, and J. S. Wilson)

We have estimated previously the excretion rate over the first month's post injection to correspond to a biological half-time of about 7000 days for plutonium and about 400 days for ⁵⁷Co. Retention studies over an 11-month period with ⁵⁷Co now indicate an initial rapid loss of about 5 percent of the activity (presumably by surface leaching), followed by a slight decline corresponding to a half-time of about 4600 days (13 years), as shown in Fig. 3 (upper curve). The animals still retain over 90 percent of initial ⁵⁷Co activity at 1 year, confirming that these spheres are essentially permanently trapped in the capillary bed.

On the other hand, animals given ⁵⁷Co-labeled spheres by intratracheal insufflation show a higher excretion rate (Fig. 3, lower curve), corresponding to a biological half-time of about 270 days. This is comparable with the range of half-times reported for oxides of plutonium and uranium in rats (135 to

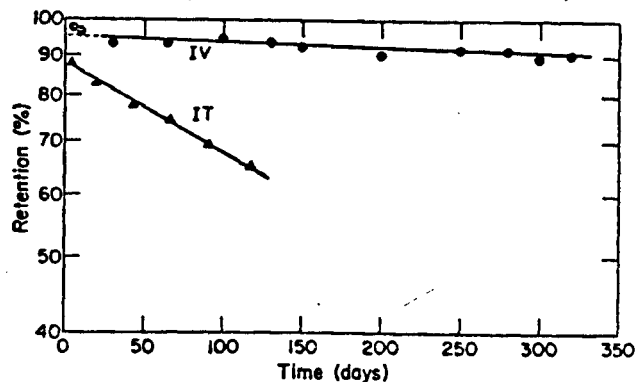


Fig. 3. Retention of microspheres in hamster lung following IV injection (upper curve) and IT insufflation (lower curve).

289 days) as summarized by the Task Group on Lung Dynamics.⁴

Dosimetry

[E. C. Anderson, P. N. Dean, and D. M. Matsakis, with essential contributions from H. J. Trussel (C-5) and from Group M-2]

To quantitate overall biological responses in terms of mechanisms at the cellular level, it is desirable to know the distribution function giving the number of cells which receive a given radiation dose as a function of distance from the microsphere. Because of highly localized deposition of energy along an alpha track and the possibility of sub-cellular targets, it is not obvious in what terms this "dose" should be expressed (e.g., by averaging the energy deposition over some critical volume or by using some form of hit theory). In either event, it is necessary first to know the fundamental effect of lung structure on radial distribution of encounters between alpha tracks and tissue. This distribution we will call the "radial interaction" function. Inverse-square effects are not included and would enter in the calculation of such dosimetric concepts as the probability of multiple hits to single targets, interactions between hits to neighboring cells, or local dose in rads. The purpose of the radial interaction function is to isolate the contribution of lung geometry in a form useful for later calculation of "dose." Variation of dE/dx along the alpha path is not included in the present calculations.

During the past year, we have developed a versatile system for numerical evaluation of the radial interaction function by a Monte Carlo technique based on a high-resolution photodigitizer and a library of image-processing computer programs developed elsewhere at the Los Alamos Scientific Laboratory. We are indebted to H. J. Trussel of Group C-5 (Statistical Services) for programming and to D. H. Janney and R. C. Bagley of Group M-2 (PHERMEX) for photodigitizing.

The procedure is first to prepare conventional photomicrograph negatives of thin-sections of lung tissue taken at magnifications of 50 X to 200 X. This has been done using both normal gray-scale and very high contrast films. These films are then scanned by a high-speed digital densitometer which

records on magnetic tape the optical densities of the square picture elements ("pixels") into which the image is decomposed.

Our objective is to identify parameters of the lung which determine the radial interaction function so that this function can be deduced from simple stereological measurements. Therefore, we have been interested in manipulating the digitized images to vary such parameters as density and mean intercept lengths in air and tissue in a controlled manner. This approach also has the advantage of bypassing the problem of obtaining sections which have exact properties of the in vivo lung (at some phase of the respiration cycle). Computer modification of the data using image-processing codes permits correction for some of the effects of shrinkage during preparation of the lung sections.

The first problem in digitization of a photomicrograph of a lung section is that of field size and resolution. The former should be large enough to be representative (of at least a local region of the lung parenchyma) and to permit termination of the alpha tracks (range 40 μm in tissue of unit density). In a typical lung section, density after fixation and embedding may be 0.22 g/cm^3 ; therefore, the average alpha range is 179 μm . Fewer than 1 percent of the alpha tracks are found to survive beyond 400 μm ; therefore, an image 600 μm square will contain most of the alpha tracks. If the points of origin of the tracks are confined to the central portion of the image (for example, to one-half the area), then about 20 percent of the tracks will reach the edge of the image and can be reflected. Because of the thinness of many alveolar walls, a resolution of better than 1 μm is desirable. Using 0.6 μm for the size of a pixel gives a 10^3 square array of 10^6 pixels to reproduce the image. With an original photomicrograph negative at 85 X diameter, this requires a 50- μm square aperture to scan a 50-mm square area of the negative. A scanning time of about 20 minutes is required to digitize and record on magnetic tape the optical density (OD) of 1,000,000 pixels.

Because of the requirement for frequent and rapid random access to any element of the million-word array, it is necessary to condense the information so that it can be stored in the central memory of the computer. This is accomplished by replacing

each 60-bit OD word with a single binary integer (0 = air, 1 = tissue), depending on whether or not the OD exceeds a given value. As discussed elsewhere, interesting and useful modifications of lung structure can be accomplished by varying the OD cutoff. The single bits of information are then packed 60 per word into a much smaller array of 17K words, which are unpacked for bit retrieval as needed.

The condensed image is then analyzed by a Monte Carlo program (ALFLUNG, written by H. J. Trussel of Group C-5) which selects a random point of origin (limited to tissue for most of our analyses) and projects an alpha-particle path in a random direction. The length of this path through each pixel is calculated, and the contents of the pixel (air or tissue) are determined. A record is kept of encounters with tissue as a function of distance from origin, and the path is terminated after 40 μm in tissue (reflecting at the edge of the image, if necessary). The process is repeated until a sufficiently large number of paths has been scanned to give the desired statistical accuracy. For distances to about 300 μm , 10^3 paths are usually adequate; 10^4 paths are required for 400 μm . Running times on a CDC-7600 computer are about 10 and 100 seconds, respectively.

The image of the lung resulting from selection of a given OD cutoff can be reconstructed by plotting the condensed bit array. Varying the cutoff changes the physical density of the section by varying the apparent thickness of the alveolar walls. Figures 4 and 5 show the images which are derived from a single photomicrograph with the OD varied so as to give lung densities of 0.23 and 0.34 g/cm^3 , respectively. The images, of course, are quite similar, and a better display of location of the tissue added by the OD change can be obtained by plotting only those pixels whose ODs lie in the incremental range. Figure 6 is such a plot for the tissue added when the apparent lung density was increased from 0.23 to 0.27 g/cm^3 . Note that this material is rather uniformly distributed around the alveoli and that the main effect is to increase alveolar wall thickness in a rather uniform way.

An interesting selection process occurs in the lung which results in a nonrandom distribution of those alpha paths which survive at large distances

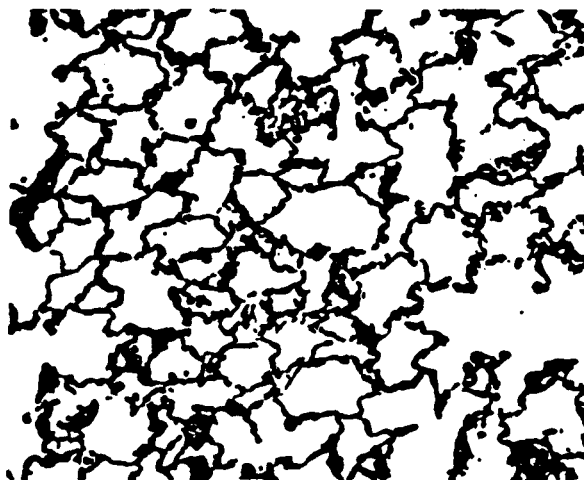


Fig. 4. Image of lung section played back at density = 0.231.

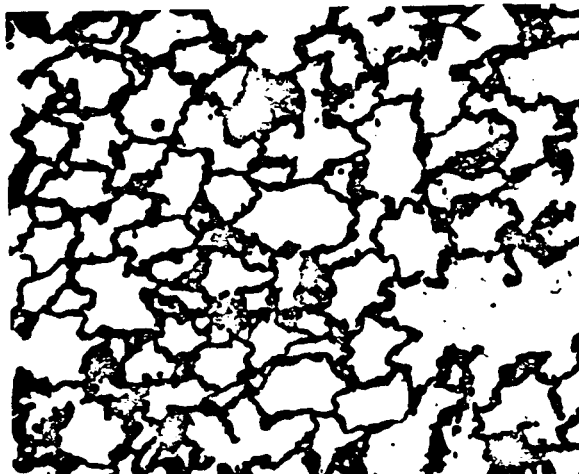


Fig. 5. Image of lung section played back at density = 0.345.

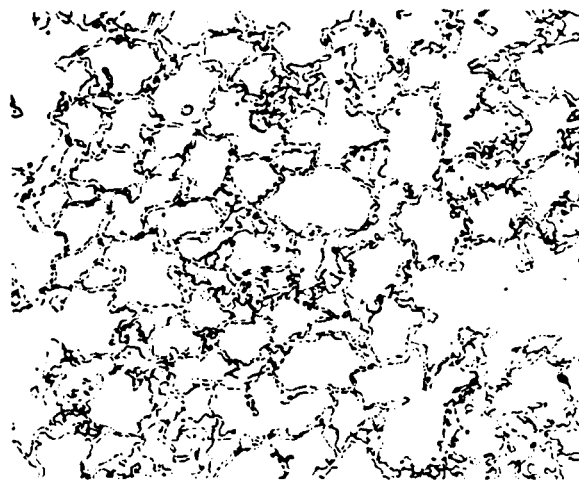


Fig. 6. Image of lung section showing tissue added to increase density from 0.231 to 0.273.

from their points of origin. The survivors are those whose paths were directed along the airways, and a collimation of direction results in addition to a nonuniform localization. This effect is illustrated in Figs. 7 and 8. Figure 7 shows the points and directions of origin for 10,000 alpha tracks chosen at random but with the restriction that the origin lies in tissue and in the central half of the image, resulting in a kind of "autograph" of lung structure. Figure 8 shows the locations and directions of 1000 alpha tracks which survive from the above after traveling 245 μm . The effects of collimation are clearly visible, and the structures responsible can be identified by comparison of the two figures.

Because of this selection effect, the fraction of alpha tracks surviving at a given distance from their origin is not a good measure of the interaction probability between alpha tracks and tissue. Alpha tracks do not pass through a medium of constant density; they begin in regions of higher than average density (their origins must be in tissue), and at large distances they are in regions of lower

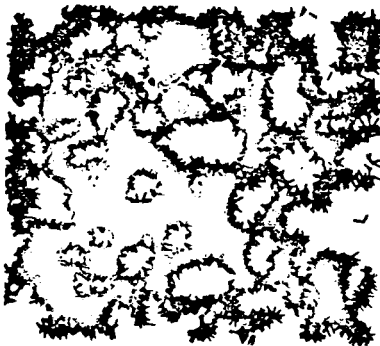


Fig. 7. Points and directions of origin (limited to tissue and to center of image) for 10,000 random alpha tracks.



Fig. 8. Locations and direction of those 1000 alpha particles surviving at 245 μm from their origins.

than average density (because of selection and collimation). Thus, the Monte Carlo code must evaluate the radial interaction function by tabulating the actual rate of encounter of tissue by alpha particles as a function of distance from origin and then averaging over many random source positions. A typical resulting histogram based on 10,000 paths is shown in Fig. 9. The ordinate (i.e., fractional tissue intercept length) is the fraction of original alpha paths actually traversing tissue at a given distance from the source. Because all origins are placed in tissue, the ordinate value is unity at zero distance and falls rapidly at short distances (as most of the tissue is in thin alveolar walls) and levels out at a value equal to the average lung density (here 0.223 g/cm^3). Inside 40 μm , the alpha range, there can be no terminations of paths, and all effects are due to lung structure. Beyond 40 μm , terminations begin and the shape of the curve is the result of three factors: (1) loss of alpha tracks; (2) collimation of the survivors; and (3) local lung structure.

Cells close to the alpha source undoubtedly will be killed and sterilized by the extraordinarily high dose rates. Thus, we are concerned only with the evaluation of dose at larger distances, say beyond 40 μm . Therefore, in what follows we will consider only that portion of the curve. We shall also normalize the variables by average density of

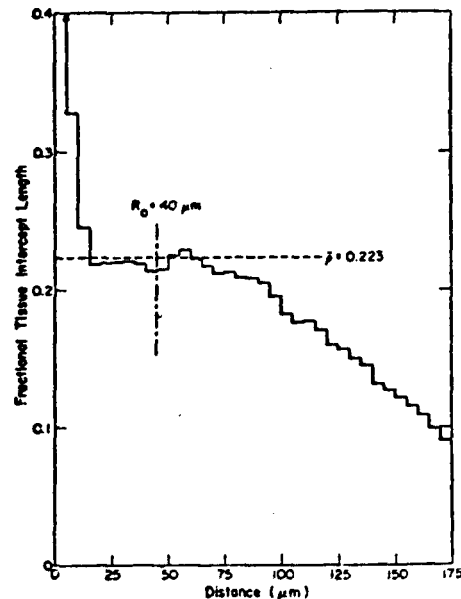


Fig. 9. Histogram of the radial interaction function for alpha tracks in a lung section.

the lung section under investigation. The ordinate divided by density becomes "relative path in tissue," and a value of unity corresponding to the plateau in Fig. 9 implies that tissue is being traversed at a rate equal to that of unattenuated source alpha paths in a medium of constant average density. The abscissa multiplied by density assumes the usual mass/area dimension. Because $\text{pg}/\mu\text{m}^3 = \text{g}/\text{cm}^3$, a convenient unit is $\text{pg}/\mu\text{m}^2$; dividing by density recovers the distance in units of μm .

Figure 10 shows a family of unnormalized curves for 4 lung images (the first and last of which were shown in Figs. 4 and 5) obtained from a single photomicrograph by varying the OD cutoff. The density of the image, as indicated, ranged from 0.23 to 0.34, and the curves are clearly quite different. Figure 11 shows the same data as normalized. Note that most of the differences are eliminated, the maximum residual variability being about ± 15 percent. Thus, for a given structural pattern (i.e., for a given distribution of alveolar sizes and shapes), effects of varying alveolar wall thickness, to a first approximation, are eliminated by appropriate density normalization. The curves shown in Figs. 10 and 11 are smoothed through the actual computer results which, of course, have the statistical fluctuations characteristic of all Monte Carlo calculations. Typical sets of primary data are shown in Fig. 12 to illustrate the statistical variations for calculations of 10^3 and 10^4 paths, respectively.

Another important parameter of a lung section is the "scale factor," the ratio of mean intercept length to alpha range. This parameter varies considerably during lung inflation as well as between species and, of course, also during the process of lung removal, fixation, and embedding. Therefore, it is important to understand the effects of these changes on the radial interaction function. This variation can be simulated easily by changing the assumed magnification factor for the digitized image while keeping the alpha range and density constant. Results of such calculations for a magnification range of about 100-fold for a typical lung section are shown in Fig. 13. The "true" magnification is 85 X, and the number on each curve gives the magnification assumed. The rectangular distributions labeled 0 and ∞ are the limiting functions expected at these extremes. At very low magnifications, the

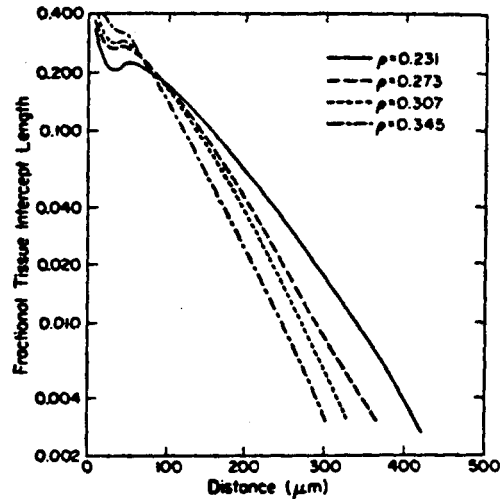


Fig. 10. Smoothed histograms of radial interaction functions for lung sections of 4 different densities (derived from a single photomicrograph).

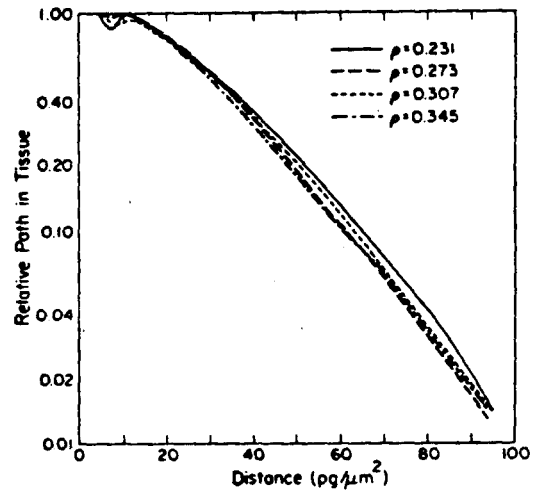


Fig. 11. Curves from Fig. 10 normalized by density.

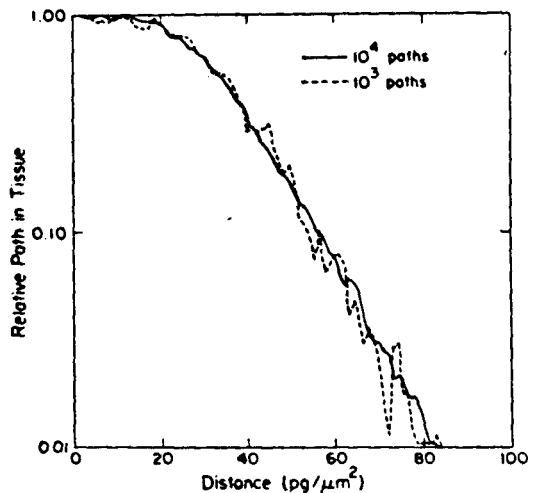


Fig. 12. Radial interaction functions showing statistical fluctuations for 10^3 and 10^4 paths.

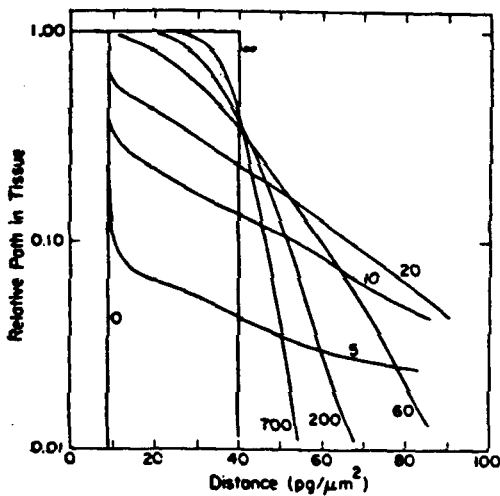


Fig. 13. Radial interaction functions as a function of scale factor. Numbers on the curves indicate the assumed magnification factor for the image.

lung structure becomes extremely coarse compared with the alpha range. In our model, all alpha tracks begin in tissue so that, when the alveolar walls become very thick, the alpha paths never leave tissue and a sharp range cutoff is observed at $40 \mu\text{m}$ distance from the source. The abscissa has been normalized by multiplying by the average density of the section (in this case, 0.23); therefore, the cutoff appears at $9 \text{ pg}/\mu\text{m}^2$. At very high magnifications, the structure becomes fine compared with the alpha range, and the lung is effectively homogeneous. Again, all alpha paths have the same range with uniform interaction probability along their paths, and the sharp cutoff is now at $40 \text{ pg}/\mu\text{m}^2$. Preliminary evidence suggests that lung sections which are quite different in preparation and appearance may produce the same family of curves as assumed magnification is varied.

The problem is now to identify an appropriate mathematical expression to represent at least the important members of this family of curves and to relate the adjustable parameters of the function to easily measured properties of a given lung section. One could then predict the radial interaction function for any given lung (or modification thereof) without the complexities of digitization and Monte Carlo analysis. The mathematical expression could be chosen on either mechanistic or heuristic grounds, the former being more rewarding but perhaps more complicated. We presently incline to the view that the generalized binomial distribution is

a promising function.⁵ It is not mechanistic but does imply an interesting mixture of structure and chance (the two possible outcomes of Bernoulli trials corresponding to encounter of air or tissue). The number and identity of the properties to be determined to characterize the lung section are not yet established but probably will be the parameter(s) characterizing the distribution of mean intercept lengths in air and in tissue. These can be determined easily, of course, by automatic electronic or optical scanning devices, a far simpler task than Monte Carlo analysis of digitized photographs.

BIOLOGICAL RESULTS

(S. G. Carpenter, G. A. Drake, L. M. Holland, J. E. London, J. R. Prine, J. S. Wilson, and R. H. Wood)

Last year we reported on the inertness of ZrO_2 microspheres. At that time only animals in the two highest dose groups showed any biological response to the presence of the spheres, in the form of small accumulations of macrophages in the proximity of individual spheres. We continue to see such accumulations of phagocytes but have not observed any capsules of fibrous connective tissue like those seen in our earlier work with larger, more radioactive spheres.⁶ Many of the animals in our earlier experimental groups are approaching the end of their anticipated life span, and we can expect to see more spontaneous deaths in the next few months.

In January 1972, we injected 105 rats [CRL:CD-(SD)SPF] with about 6000 microspheres of activity Level 4. These animals have been kept separated under barrier conditions from other rodents. During the subsequent 10 months, we have sacrificed 4 of these animals and have observed no pulmonary disease of any kind. There have been no spontaneous deaths or any signs of clinical disease in this group of animals.

Blood samples taken from all animals (hamsters and rats) have not revealed any effect upon the formed elements of blood even after long exposure. Earlier in the experiments, we anticipated that we might see an increasing lymphopenia from constant exposure of the blood as it circulated through the lungs. This has not been the case. In addition, we have not observed any effects on regional lymph nodes.

TABLE 3. HAMSTERS DYING FROM NEOPLASTIC DISEASE

| <u>Animal Number</u> | <u>Exposure group</u> | <u>Exposure duration (months)</u> | <u>Diagnosis</u> |
|----------------------|-----------------------|-----------------------------------|----------------------------------------------------------------------------------------|
| 647 | Control | 15.5 | Pancreatic carcinoma with abdominal extensions; no pulmonary metastases |
| 330 | Level 2A | 9.5 | Hemangio-endothelial sarcoma of lung |
| 694 | Level 2A | 11.5 | Undifferentiated sarcoma, abdominal viscera; no lung lesions |
| 705 | Level 2A | 12.0 | Undifferentiated sarcoma of lung |
| 870 | Level 4 | 15.0 | Undifferentiated sarcoma, multiple metastases, no lung lesions; primary not determined |
| 1368 | Level 6 | 7.5 | Fibrosarcoma, abdominal viscera; pulmonary metastases |

Thus far, 5 animals from the experimental groups and 1 from a control group have died of neoplastic disease. Of these, only 2 have had a primary lung lesion. Table 3 lists the neoplasms found, dose levels involved, and duration of the exposure in each case. One of the primary lung lesions was a hemangio-sarcoma (Fig. 14) in an animal from one of the lower dose groups (Level 2A) with an exposure time of 9.5 months (287 days). This tumor replaced almost entirely the left lung and severely compressed the adjacent normal lung tissue. There was no evidence of metastases to the rest of the lung or to any other organ.

The other primary lung lesion was an undifferentiated sarcoma (Fig. 15) in an animal from the same dose group and was found after about 1 year (354 days) of exposure time. In this case, there were multiple nodules in both lungs. Microspheres were found in adjacent normal lung tissue around each tumor site. No metastatic lesions were found in other organs. An animal from a control group showed the only case of a well-differentiated carcinoma (Fig. 16). This particular tumor had originated in the pancreas with extension to several other organs with no pulmonary metastases.

Because most of the neoplasms found have been sarcomas originating in the abdominal viscera, the question arises as to whether a significant number of microspheres may have passed through the lung and been picked up in the reticulo-endothelial



Fig. 14. Hemangio-sarcoma in hamster lung at Level 2A.

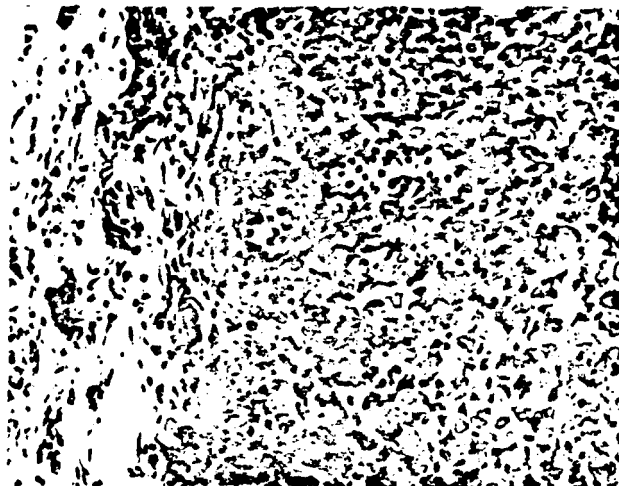


Fig. 15. Undifferentiated sarcoma in hamster lung at Level 2A.

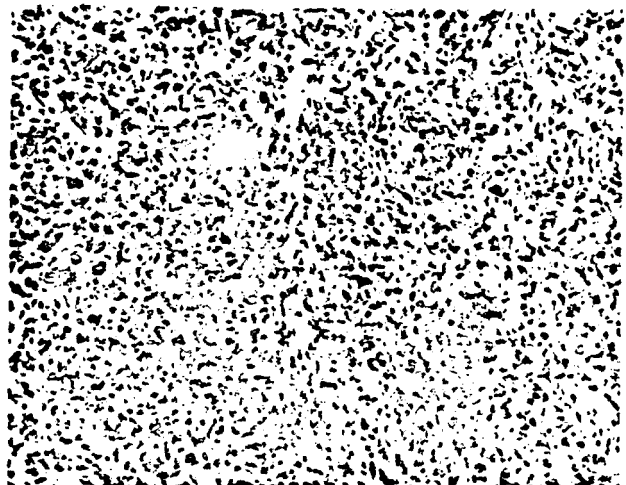


Fig. 16. Pancreatic carcinoma in a control hamster.

systems of the liver, spleen, etc. Counting of these separated organs in a NaI (Tl) twin-crystal counter (for plutonium and ^{57}Co gamma rays) and alpha radiography of selected tissues have been negative in this regard.

PROSPECT

During the coming year, the primary objectives are:

- (1) To continue the sphere injection program and to expand interesting exposure groups as indicated by forthcoming results.
- (2) To investigate additional insults to promote the incidence of lung damage.
- (3) To extend theoretical studies on effects of lung structure on dose distribution, especially on the correlation of structural parameters and the dose-distribution function.
- (4) To continue histological and pathological studies of exposed lungs.
- (5) To study the effects of a more uniform distribution of radiation dose to the lung (e.g., by use of beta radioactivity instead of alpha irradiation).

REFERENCES

1. C. R. Richmond and G. L. Voelz, eds., Annual Report of the Biological and Medical Research Group (H-4) of the LASL Health Division, January through December 1971, Los Alamos Scientific Laboratory report LA-4923-PR (1972).
2. J. R. Coleman and L. J. Perez, Jr., Considerations of a Tumor Probability Function and Micro-Dosimetry for the Deep Lung, Part II of Final Report of Radiological Safety Studies for the SNAP Program for Safety Branch, SEPO, USAEC, Environmental Safeguards Division, NUS Corporation, Rockville, Maryland (1969), report NUS-596.
3. B. O. Stuart, W. J. Bair, W. J. Clarke, and E. B. Howard, Acute Toxicity of Inhaled Plutonium Oxide-238 and -239 in Rats, Battelle Memorial Institute, Air Force Weapons Laboratory technical report AFWL-TR-68-49 (1972).
4. Task Group on Lung Dynamics. Health Phys. 12, 173-207 (1966).
5. W. Feller, An Introduction to Probability Theory and Its Applications, Vol. 1, John Wiley and Sons, Inc., New York (1950), pp. 104-110.
6. C. R. Richmond, J. Langham, and R. S. Stone, Biological Response to Small Discrete Highly-Radioactive Sources. II. Morphogenesis of Microlesions in Rat Lungs from Intravenously Injected $^{239}\text{PuO}_2$ Microspheres. Health Phys. 18, 401-408 (1970).

MOLECULAR RADIOBIOLOGY SECTION

INTRODUCTION

Efforts in molecular radiobiology are divided into three major areas, all of which involve both radiation studies and the essential fundamental investigations that yield information relative to which radiation data become meaningful. The three areas of research are model DNA, genetic information transfer, and chromatin structure and the mitotic apparatus. The objective of these studies is to understand the radiobiological mechanisms for inception, progress, and repair of radiation damage.

Synthetic work, utilizing procedures both from organic chemistry and enzymology, has supplied oligo- and polydeoxyribonucleotides to replenish stocks of much needed materials and to provide new base sequences. Numerical analysis of gel permeation chromatograms has proved to be a valuable procedure in all aspects of the preparation and use of model DNA. The major requirements this year for radiation and transcription studies have been homopolynucleotides with a variety of established average molecular weights. Reaction of poly d(G-T) with osmium tetroxide has converted part of the thymine bases to the 5,6-dihydro-5,6-dihydroxy structure that is one of the products resulting from the action of ionizing radiation upon DNA in anaerobic solution. Primary attention has been focused on radiation damage occurring at constant dose but with changing concentration of target molecule in order to find out the mechanism of damage. We have some data that suggest concomitant direct and indirect action for both base damage and chain breaks.

This year in studies of effects of radiation on genetic information transfer, we have continued the investigations on X-irradiated RNA polymerase. The D_{37} values observed for inactivation of enzymatic activity varied with different template molecules used in the assay. In some cases, observed inactivation also was dependent upon substrate concentration. Through a combination of experimental approaches in which we separately studied the effects of X-irradiation on the ability of RNA polymerase to bind templates, to initiate RNA chains, and to add onto chains already started, we

came to the conclusion that the initiation step is the most sensitive to X-irradiation. Furthermore, we found that X-irradiated RNA polymerase has a greater tendency to insert the "wrong" base into RNA than does unirradiated enzyme. In another study, we have evidence that ultraviolet irradiation produces covalent bonds between RNA polymerase and DNA; the utility of this reaction in the isolation of DNA binding sites is being investigated. In another direction, we have investigated parameters of the initiation of RNA synthesis by deoxyribosyl oligomers. These oligomers are covalently incorporated into the RNA chain. Presence of the deoxyribosyl oligomers in the reaction, by circumventing the normally rate-limiting step of initiation, greatly stimulates the rate of RNA synthesis. The amount of stimulation is a function of oligomer concentration, substrate concentration, and metal ion cofactor used.

In the area of chromatin structure, experiments conducted during the past year have clearly demonstrated that structural alterations of histones by acetylation, methylation, and phosphorylation occur at defined times within the cell cycle of cultured mammalian cells. The effects of ionizing radiation upon these reactions in cultured cells show that, with the decline of DNA and histone biosynthesis several hours post-irradiation, histone acetylation and methylation cease. Results of these studies support the hypothesis that radiation-induced division delay results from a blockage of cells in the G_2 portion of their life cycle. In order to test the hypothesis that irradiation of mammalian cells destroys a component or potential for division, standard microtubule assays have been adapted for use with cultured cells. Investigations have established the temporal pattern of intracellular microtubule protein levels in synchronized cultures of mammalian cells. Evidence has been obtained to indicate that the levels of microtubule protein in X-irradiated cells follow closely that of other functional proteins.

SYNTHESIS AND RADIOSENSITIVITY OF MODEL DNA

(F. N. Hayes, D. L. Williams, R. L. Ratliff, C. DeLisi, G. T. Fritz, W. B. Goad, D. E. Hoard, U. Hollstein, E. L. Martinez, V. E. Mitchell, and E. C. Wilmoth)

Chemical Synthesis of Oligodeoxyribonucleotides

As part of our continuing program, homooligodeoxyribonucleotides of any specific size are synthesized¹ from mononucleotides and made available for radiation studies and fundamental biological investigations. Many of these polymers are kept in stock at low temperature. Oligodeoxynucleotides of known base sequence are prepared by stepwise chemical condensation reactions² using functional blocking groups for amino groups and for 5'-phosphate and 3'-hydroxyl groups, where applicable. Protected dinucleotides are synthesized and are either chemically polymerized to obtain polydimers or are used in the synthesis of trimers² or longer oligonucleotides. Chemical polymerization³ of the trimers, followed by anion exchange chromatography, affords polytrimers in the size range from hexamer to dodecamer in addition to the larger unresolved polymers.

In the stepwise chemical synthesis of oligonucleotides of known base sequence, if purity of base sequence is to be maintained, the ideal protective group for phosphate should remain intact during the condensation and isolation steps and should be removable at the desired time without alteration of other parts of the product structure. The widely used 2-cyanoethyl group⁴ does not meet these requirements, since it is partially lost during the chemical condensation step and partially removed during subsequent hydrolysis of the 3'-hydroxyl-protecting group. When two different nucleotide bases are used in preparing the initial dimer, the first mentioned loss may result in contamination of the desired sequence and applies to many of the new protective groups for phosphate which have appeared in the recent literature. However, in no case has the degree of retention of a suggested group, under reaction conditions, been demonstrated directly. We have evaluated⁵ a number of these groups which appeared to have satisfactory removal conditions, together with a new group of our own design. Our new group, 1,1,1-trichloro-2-methyl-2-propyl, has proven to be superior, in terms of retention, to all those

evaluated under test conditions analogous to those which would be used for diester bond formation.

Two new protective groups for phosphate,^{6,7} which are designed for rapid isolation of the growing protected oligonucleotide, will also be evaluated. The *N,N*-dimethyl-*p*-phenylenediamino group⁶ renders the protected oligonucleotide selectively adsorbable on Amberlite IR-45 resin, and the unreacted incoming nucleotide with free phosphate can be washed out, together with anions from the condensing agent. The 2-phenylmercaptoethyl group⁷ imparts to the protected oligonucleotide product sufficient affinity for benzoylated DEAE-cellulose or DEAE-Sephadex that unreacted mononucleotides and by-products with free phosphate groups can be eluted first from the column. 2-Phenylmercaptoethyl 5'-thymidylate has been prepared and purified for stability evaluation by our testing method.

The extremely good stability of the 1,1,1-trichloro-2-methyl-2-propyl (trichloro-*tert*-butyl) derivatives of nucleotides, under the conditions of diester bond synthesis, is probably due in large part to steric hindrance. This characteristic of the group is also apparent in preparation of the protected nucleotides. As illustrated in Table 1, the rate of application of the trichloro-*tert*-butyl group is slow, and yields are poor to fair due to side reactions.

Removal of the trichloro-*tert*-butyl group from nucleotides is effected by reduction with zinc/copper couple in dimethylformamide solvent at 50° C. Removal is essentially quantitative from the mononucleotides in 1 hour (see Table 2). Removal is less nearly quantitative from the oligonucleotides tested but appears to reach a maximum. This apparently is due to formation of a zinc salt insoluble in DMF, since the residual material is reduced when recovered and converted to a soluble trialkylammonium salt. During reduction of a fully blocked nucleotide, amino blocking groups such as benzoyl and anisoyl are partially lost. This makes it necessary to reacylate oligonucleotides containing the base cytosine before further condensation or chemical polymerization reactions are carried out, since the cytosine amino group forms phosphoamide linkages with nucleotide phosphate. This apparently is not the case with guanine and adenine⁸ (i.e., the now blocked amino groups are not involved in the above,

TABLE 1. PREPARATION OF TRICHLORO-TERT-BUTYL ESTERS OF DEOXYNUCLEOTIDES

| <u>Nucleotide</u> | <u>Millimoles^a</u> | <u>Condensing agent</u> | <u>Millimoles</u> | <u>Time (days)</u> | <u>Yield (%)</u> |
|------------------------|-------------------------------|-------------------------|-------------------|--------------------|------------------|
| d-pTOAc | 0.5 | DCC ^b | 2.5 | 3 | 28.8 |
| | 0.5 | DCC | 2.5 | 5 | 34.7 |
| | 0.2 | DCC | 0.5 | 26 | 69.6 |
| | 0.2 | DCC | 0.4 | 26 | 61.0 |
| | 5.0 | TPS ^c | 10.0 | 12 | 56.7 |
| d-pC ^{Ac} OAc | 4.7 | DCC | 14.1 | 25 | 34.4 |
| | 3.6 | DCC | 18.1 | 26 | 35.6 |
| | 0.2 | TPS | 0.4 | 23 | 37.0 |
| d-pG ^{Ac} OAc | 4.88 | DCC | 15.0 | 28 | 40.8 |

^aA 50-fold excess of trichloro-tert-butyl alcohol was used in every case.

^bDCC, dicyclohexylcarbodiimide.

^cTPS, trisopropylbenzenesulfonyl chloride.

TABLE 2. REMOVAL^a OF TRICHLORO-TERT-BUTYL PHOSPHATE BLOCKING GROUP WITH ZINC-COPPER COUPLE

| <u>Nucleotide with block</u> | <u>Free nucleotide (%)</u> | <u>Residual blocked nucleotide (%)</u> | <u>Total recovery (%)</u> | <u>Time (hours)</u> |
|------------------------------|----------------------------|----------------------------------------|---------------------------|---------------------|
| d-pT | 100.0 | -- | 99.2 | 1 |
| | 96.5 | 3.5 | 95.5 | 2 |
| d-pG | 100.0 | -- | 100.0 | 2 |
| d-pC | 92.7 | 7.3 | -- | 1 |
| | 87.1 | 6.1 | 94.4 | 1 |
| d-pCpA | 92.0 | 8.0 | 100.0 | 2 (53° C) |
| d-pCpCpT | 51.6 | 44.5 | 93.9 | 1 |
| | 59.2 | 24.8 | 96.7 | 3 |
| | 67.9 | 22.4 | 100.0 | 6 |

^aAll experiments were run in DMF solution at 50° C.

TABLE 3. SYNTHESIS OF PROTECTED DINUCLEOTIDES AND TRINUCLEOTIDES

| <u>Phosphate protected component^a</u> | <u>Amount (mmoles)</u> | <u>O^{3'}-A nucleotide</u> | <u>Amount (mmoles)</u> | <u>TPS (mmoles)</u> | <u>Time (hours)</u> | <u>Product</u> | <u>Yield (%)</u> |
|--------------------------------------------------|------------------------|------------------------------------|------------------------|---------------------|---------------------|---------------------------------------------|------------------|
| d-CBpG ^{iBu} | 0.191 | d-pA ^{Bz} OAc | 0.433 | 0.80 | 3 | d-CBpG ^{iBu} pA ^{Bz} OAc | 47 |
| d-CBpT | 0.123 | d-pG ^{iBu} iBu | 0.104 | 0.208 | 19 | d-CBpTpG ^{iBu} OiBu | 67 |
| d-CBpC ^{An} | 1.36 | d-pC ^{An} OAc | 1.32 | 2.63 | 16 | d-CBpC ^{An} pC ^{An} OAc | 31 |
| d-CBpC ^{An} pC ^{An} | 0.198 | d-pT | 1.02 | 1.95 | 4 | d-CBpC ^{An} pC ^{An} pTOAc | 69 |

^aCB = trichloro-tert-butyl.

type of reaction).

As illustrated in Table 3, good to excellent yields of oligonucleotides are realized in chemical synthesis reactions. During isolation of these products by anion exchange column chromatography, a minimum of by-products is observed.

REFERENCES

1. H. G. Khorana and J. P. Vizsolyi, Studies on polynucleotides. VIII. Experiments on the polymerization of mononucleotides. Improved preparation and separation of linear thymidine polynucleotides. *J. Amer. Chem. Soc.* **83**, 675-685 (1961).
2. S. A. Narang, T. M. Jacob, and H. G. Khorana, Studies on polynucleotides. LXII. Deoxyribo-polynucleotides containing repeating trinucleotide sequences (4). Preparation of suitably protected trinucleotides. *J. Amer. Chem. Soc.* **89**, 2158-2166 (1967).
3. S. A. Narang, T. M. Jacob, and H. G. Khorana, Studies on polynucleotides. LXIII. Deoxyribo-polynucleotides containing repeating trinucleotide sequences (5). The polymerization of protected deoxyribopolynucleotides. *J. Amer. Chem. Soc.* **89**, 2167-2177 (1967).
4. G. M. Tener, 2-Cyanoethyl phosphate and its use in the synthesis of phosphate esters. *J. Amer. Chem. Soc.* **83**, 159-168 (1961).
5. C. R. Richmond and C. L. Voelz, eds., Annual Report of the Biological and Medical Research Group (H-4) of the LASL Health Division, Los Alamos Scientific Laboratory Report LA-4923-PR (1971), pp. 36-38.
6. T. Hata, K. Tajima, and T. Mukaiyama, A simple protecting group protection-purification "handle" for polynucleotide synthesis. I. *J. Amer. Chem. Soc.* **93**, 4928-4930 (1971).
7. S. A. Narang, O. S. Bhanat, J. Goodchild, R. H. Wightman, and S. K. Dheer, A new general method for the synthesis of phosphate-protected deoxy-ribooligonucleotides. IV. *J. Amer. Chem. Soc.* **94**, 6183-6189 (1972).
8. S. A. Narang, K. Itakura, and R. H. Wightman, A simplification in the synthesis of deoxyribo-oligonucleotides. *Canad. J. Chem.* **50**, 769-770 (1972).

Enzymatic Synthesis

Syntheses of mixed ribo- and deoxyribonucleotide polymers have been accomplished¹ using terminal deoxyribonucleotidyltransferase and an oligodeoxy-ribo-nucleotide initiator. Depending upon the ratio of deoxyribonucleoside triphosphate to ribonucleoside triphosphate, the percent of ribonucleotide in the mixed polymer can vary from less than 1 percent to as much as 38 percent (equal molar concentrations

of dATP and rGTP, see Tables 1 and 2). The fact that the ribonucleotide occurs internally was demonstrated by nearest-neighbor analyses using α -³²P-labeled deoxyribonucleoside triphosphates and by size distribution before and after alkaline hydrolysis (Tables 1 and 3).

The mixed ribo- and deoxyribonucleotide polymers have been used as templates for RNA polymerase from *Escherichia coli*. Both the deoxyribonucleotide and ribonucleotide are transcribed, giving a ribonucleotide polymer with nucleotide content similar to the original mixed polymer (Table 4).

Although no attempt has been made at this time to determine if the DNA polymerase from calf thymus will replicate the mixed ribo- and deoxyribonucleotide polymers in the presence or absence of the proper initiator, it will be interesting to compare the results with previous experimental work.⁵ The mixed ribo- and deoxyribonucleotide polymers should also have some value in determining conditions for chain elongation (addition to oligonucleotide) and replication of polydeoxynucleotides by DNA polymerases from *E. coli* and *Micrococcus luteus*. If chain elongation by the above two enzymes depends entirely on the first few nucleotides at the 3'-hydroxyl terminus, then the ribonucleotides in the mixed polymer should only exert an effect upon catalytic reaction if they are at or near the 3'-hydroxyl terminus. If the ribonucleotides are at the 3'-hydroxyl terminus and chain elongation is prevented, then replication should take preference over chain elongation. This might happen especially if the ribonucleotide is not complementary to the deoxyribonucleotides [e.g., $d(A_n, rC_m) \cdot d(T_n, rC_m)$]. Studies on the effect of ribonucleotide content in the mixed polymers on the above reactions, as well as one-fold or more replication of the deoxyribonucleotides, can also be determined.

Additional studies with $d(AAT)_n \cdot d(ATT)_n$ have been done, where the transcribed ribopolymer $r(AAU)_n \cdot r(AUU)_n$ has been isolated after pancreatic DNase digestion of the deoxyribonucleotide polymer. Circular dichroism spectra of $d(AAT)_n \cdot d(ATT)_n$ and $r(AAU)_n \cdot r(AUU)_n$ have been determined by Dr. Donald Gray (University of Texas at Dallas) and compared with their respective isomers: $dA_n \cdot dT_n$, $d(AT)_n \cdot d(AT)_n$, $rA_n \cdot rU_n$, and $r(AU)_n \cdot r(AU)_n$. This is the first instance where such a comparison has been

TABLE 1. NEAREST-NEIGHBOR ANALYSES OF $d(A_n, rN_m)^a$

| Ribonucleoside triphosphate concentration (pmoles) | Percent of radioactivity in nucleoside 3'-phosphates | | | | | |
|----------------------------------------------------|------------------------------------------------------|------|------|------|------|------|
| | rCTP | | rGTP | | rUTP | |
| | rCp | dAp | rGp | dAp | rUp | dAp |
| 10 | 0.1 | 99.9 | 0.3 | 99.7 | 0.9 | 99.1 |
| 10 ² | 0.1 | 99.9 | 0.4 | 99.6 | 0.7 | 99.3 |
| 10 ³ | 0.2 | 99.8 | 0.9 | 99.1 | 1.0 | 99.0 |
| 10 ⁴ | 1.5 | 98.5 | 5.2 | 94.8 | 1.6 | 98.4 |
| 10 ⁵ | 13.0 | 87.0 | 37.3 | 62.7 | 4.9 | 95.1 |

^aThe reaction mixtures contained the following components in a total volume of 0.2 ml: 10⁵ pmoles α -³²P-dATP, 10³ pmoles of the hexamer of 5'-deoxythymidylic acid, 40 mM potassium cacodylate (pH 6.8), 8 mM MgCl₂, 1 mM 2-mercaptoethanol, 200 units terminal deoxyribonucleotidyltransferase, and from 10 to 10⁵ pmoles ribonucleoside triphosphate. The mixtures were incubated at 37°C for 2 hr, and nearest-neighbor analyses were determined as previously described by Josse *et al.*² and Ratliff *et al.*³

TABLE 2. NEAREST-NEIGHBOR ANALYSES OF $d(A_n, rN_m)^a$

| Ribonucleoside triphosphate concentration (pmoles) | Percent of radioactivity in nucleoside 3'-phosphates | | | | | |
|----------------------------------------------------|------------------------------------------------------|------|----------------------------------|------|----------------------------------|------|
| | rCTP- α - ³² P | | rGTP- α - ³² P | | rUTP- α - ³² P | |
| | rCp | dAp | rGp | dAp | rUp | dAp |
| 10 | 0.6 | 99.4 | 0.4 | 99.6 | 2.4 | 97.6 |
| 10 ² | 0.2 | 99.8 | 0.8 | 99.2 | 0.9 | 99.1 |
| 10 ³ | 0.2 | 99.8 | 0.9 | 99.1 | 1.3 | 98.7 |
| 10 ⁴ | 2.2 | 97.8 | 9.0 | 91.0 | 3.2 | 96.8 |
| 10 ⁵ | 15.8 | 84.2 | 38.1 | 61.9 | 7.0 | 93.0 |

^aThe conditions were identical to those described in Table 1 except that each of the ribonucleoside triphosphates was labeled with α -³²P.

possible using spectra of double-strand RNA sequences, and the agreement between measured and approximated spectra for $r(AAU)_n \cdot r(AUU)_n$ is surprisingly good.⁶

The $d(AAT)_n \cdot d(ATT)_n$ circular dichroism spectrum has provided the first independent test of the spectral procedure of Allen *et al.*⁷ for obtaining first-neighbor frequencies. In this first independent test of the procedure, we found that the spectral analysis does infer the existence of a majority of 86 percent $d(ApA)$, $d(TpT)$, $d(ApT)$, and $d(TpA)$ first-neighbors.

REFERENCES

1. R. L. Ratliff, Synthesis of mixed polynucleotides containing ribo- and deoxyribonucleotides by terminal deoxynucleotidyltransferase. *Federation Proc.* **31**, 425 (1972).

TABLE 3. SIZE DISTRIBUTION OF $d(A_n, rA_m)$ BEFORE AND AFTER ALKALINE HYDROLYSIS

| Ratio dATP/rATP (pmoles) | Nucleotide length at peak of absorbance | |
|--------------------------|-----------------------------------------|-----------------------------|
| | (before alkaline hydrolysis) | (after alkaline hydrolysis) |
| 10 ⁵ to 1 | 140 | 120 |
| 10 ⁴ to 1 | 140 | 120 |
| 10 ³ to 1 | 140 | 100 |
| 10 ² to 1 | 115 | 20 |
| 10 to 1 | 62 | 4 |

^aThe reaction mixture described in Table 1 was scaled up 100-fold for preparation of $d(A_n, rA_m)$. After incubation, the reaction mixtures were deproteinized with isoamyl alcohol and chloroform and dialyzed against water. One-half of the isolated polymer was hydrolyzed with 0.3 N KOH for 18 hr at 37°C and then neutralized with 5 N HCl. Lengths at peaks of absorbance were determined for both untreated and alkaline-treated ribodeoxyribocopolymers as previously described.⁴

TABLE 4. NEAREST-NEIGHBOR ANALYSES OF THE RIBOPOLYMER TRANSCRIBED FROM $d(A_n, rN_m)^a$

| RNA | α - ³² P-labeled triphosphate | Radioactivity in ribonucleoside 2'- and 3'-phosphates (%) | | | |
|----------------|-------------------------------------------------|-----------------------------------------------------------|------|------|------|
| | | rGp | rUp | rCp | rUp |
| $r(G_m, rU_n)$ | rGTP | 28.5 | 71.5 | -- | -- |
| | rUTP | 38.4 | 61.6 | -- | -- |
| $r(C_m, rU_n)$ | rCTP | -- | -- | 28.1 | 71.9 |
| | rUTP | -- | -- | 26.1 | 73.9 |

^aThe reaction mixtures contained per ml: 40 μ moles of Tris-HCl buffer (pH 8.0), 4 μ moles MgCl₂, 1 μ -mole MnCl₂, 12 μ moles 2-mercaptoethanol, 100 nmoles ribonucleoside triphosphates, with each labeled in turn with α -³²P, 0.5 A₂₆₀ units of the mixed ribodeoxyribopolymer, and 300 units of RNA polymerase. The reaction mixtures were incubated at 37°C for 2 hr and were terminated by placing in boiling water for 10 min and dialyzed against 0.01 M sodium pyrophosphate (pH 7.0) and then distilled water. The polymers were hydrolyzed with 0.3 N KOH at 37°C for 18 hr and neutralized with 5 N HCl, and the mononucleotides were separated by paper electrophoresis.^{2,3}

2. J. Josse, A. D. Kaiser, and A. Kornberg, Enzymatic synthesis of deoxyribonucleic acid. VIII. Frequencies of nearest neighbor base sequences in deoxyribonucleic acid. *J. Biol. Chem.* **236**, 864-875 (1961).
3. R. L. Ratliff, A. W. Schwartz, V. N. Kerr, D. L. Williams, D. G. Ott, and F. N. Hayes, Heteropolydeoxynucleotides synthesized with terminal deoxyribonucleotidyltransferase. II. Nearest neighbor frequencies and extent of digestion by

Micrococcal deoxyribonuclease. *Biochemistry* **7**, 412-418 (1968).

4. F. N. Hayes and V. E. Mitchell, Gel filtration chromatography of polydeoxynucleotides using agarose columns. *J. Chromatog.* **39**, 139-146 (1969).
5. F. N. Hayes, E. Hansbury, V. E. Mitchell, R. L. Ratliff, D. A. Smith, and D. L. Williams, Early stages in complementary synthesis directed by synthetic single-stranded polydeoxyribonucleotide templates and catalyzed by calf thymus deoxyribonucleic acid polymerase. *J. Biol. Chem.* **246**, 3631-3638 (1971).
6. D. M. Gray, R. L. Ratliff, and D. L. Williams, The circular dichroism of poly d(AAT)·d(ATT) and poly r(AAU)·r(AUU). A test of the first neighbor hypothesis. *Biopolymers* (1972), submitted.
7. F. S. Allen, D. M. Gray, G. P. Roberts, and I. Tinoco, Jr., The ultraviolet circular dichroism of some natural DNAs and an analysis of the spectra for sequence information. *Biopolymers* **11**, 853-879 (1972).

Numerical Analysis of Gel Permeation Chromatograms

Data from gel permeation chromatography are being used to derive molecular size distribution patterns for polydeoxyribonucleotides. Some of the kinds of samples for which size distributions are valuable are those newly isolated, those kept long in storage, or those subjected to known sources of damage. However, gel permeation chromatography suffers from incomplete resolution between fragments of various lengths. Nevertheless, if one knows the elution profile that each of the expected molecular species gives when present alone, in principle, he can find the superposition of them necessary to account for the observed elution profile of any sample of interest (that is, he can infer its composition).

To carry this through, two classes of difficulties have to be dealt with. First, if one tries to find precisely what sum of overlapping contributions give a particular profile, uncertainties and imprecisions in definition of the profile are so magnified in the result as to defeat the effort. One has errors of measurement, uncertainties from definition of the profile by a limited number of finite fractions, and errors in definition of elution profiles of individual species present. A typical composition inferred in this way consists of large positive and negative numbers of adjacent species. Therefore, we must instead consider that

the observed elution profile with its associated uncertainties could have been produced by a range of sample compositions and select from this range those that are probable by physical criteria. So far we have applied two kinds of criteria. The least prejudiced is to optimize a measure of smoothness of molecular weight distribution in the sample; this amounts to assuming that the process that generates the molecular weight distribution is continuous in the sense of not sharply changing as between a polymer of N units and one of the next higher and lower numbers. The second means of selection is to limit the form of molecular weight distribution to that generated by a specific model of the process generating it -- breakage of the polymer at random points in the case of an irradiated sample -- a generalization of the Michaelis-Menten process in the case of a sample generated by the enzyme, terminal deoxyribonucleotidyltransferase.

The second class of difficulties lies in defining the individual elution profiles of each expected species. These, of course, have to be calibrated by direct experimental determinations with homogeneous molecular samples, but for two reasons it is not feasible to rely entirely on experimental data. In the first place, it would require an enormous amount of experimental work; in the second place, if magnification of the errors discussed above is to be minimized, it is essential that the form of individual elution profiles vary consistently and accurately from one species to the next. In the face of experimental uncertainties, this latter requirement is most readily met by understanding the mechanisms that determine the shape of the profile and, therefore, how its form, of necessity, varies with molecular size.

We have made a detailed analysis of coupled hydrodynamic and diffusion processes by which molecules are transported down the column, through the tubing and monitor, and into the collecting test tubes. The gel particles are sufficiently small (~100 microns) that, for the range of polymers of interest here, each molecule samples the volume accessible to it sufficiently often that its dispersion along the column is Gaussian, the mean-square dispersion being the sum of four terms: one independent of molecular diffusion, one dependent

on the free diffusion coefficient, one dependent on volume accessible to the molecule within the gel particles and its diffusion coefficient there, and a correlation term between the last two. (For polydeoxynucleotides, it appears that the two diffusion coefficients are different.) In the tubing needed to convey the sample to and from the column, the situation is more complicated, and the form of its modification of the profile has been directly calculated by a Monte Carlo method. A Monte Carlo calculation has also been employed to determine some of the coefficients in column dispersion (i.e., those that cannot be determined by calibration with experiment).

These results are being assembled into the computer code that performs the compositional analysis outlined above, which has been in use with individual elution profiles as determined earlier more crudely. The earlier experience, plus the completeness of new information on individual elution profiles, gives grounds for expecting the emergence of a reasonably satisfactory analysis.

X-Irradiation

Irradiation studies have been extended to dTMP, poly dT, and poly dA to facilitate interpretation of data that we have already obtained from poly d(A-C) and poly d(G-T). Thus far, we have carried out ultraviolet absorption analyses on all samples and gel permeation chromatography and T_m studies on the polymers. Controlled chemical alteration of d(G-T)₂₀ has yielded products containing known extents of a type of base damage found after irradiation.

We have measured the change in absorbance of dTMP at $\lambda_{(\max)} = 267$ nm versus solute concentration, C_0 , at a constant 25 krad of X-irradiation. The range of C_0 was 18 to 1000 μM . The concentration of dTMP that had lost its chromophore, C^* , was found to increase rapidly from zero across the lowest values of C_0 and then to assume a gradual linear increase. The linear portion extended between C_0 values of 400 to 1000 μM . The rapid change of C^* for C_0 values less than 400 μM is in accord with an expected lowering of the radical concentration by recombination at very low solute concentrations.¹ An equation that is the least-squares fit to all the experimental points is:

$$C^* = 0.0296 C_0 + 35.3 [1 - \exp(-0.0175 C_0)]. \quad (\text{Eq. 1})$$

It is surprising that this equation contains a linear term relating C^* and C_0 ; if, according to expectation, inactivation had occurred entirely through indirect action, the value of C^* should have become constant at high values of C_0 .² One way to interpret the results is that the linear term in Eq. 1 is concerned with direct action and that the exponential term covers uniquely that part of the inactivation caused by indirect action. The calculated values for G rose slowly through C_0 values of 400 to 1000 μM ; the average value of G in that range was 2.26.

Gel permeation chromatograms have been obtained for various size distributions of synthetic polydeoxyribonucleotides both before and after X-irradiation. These model DNAs have the following sequences: poly dA, poly dT, poly d(A-C), and poly d(G-T). Final analyses of the data await completion of the computer program described above. Preliminary analysis, as expected through strand breakage, not only shows that X-irradiation lessens the arithmetic mean of a size distribution and does this somewhat in proportion to the dose³ but that at constant dose, quite interestingly, the effect continues, with almost identical degree of breakage, even up to polymer concentrations of 6000 mono- μM . This dependence is quite different from what was observed in radiation-induced loss of chromophore incurred by dTMP. Therefore, as concluded exclusively from the test of concentration dependence, strand breakage in solution largely results from the direct effect. Further elucidation of this argument will be most valuable toward increased understanding of the effect of ionizing radiation upon nucleic acids.

One identified major product of radiation-induced hydroxyl radical attack upon the thymine ring in DNA under anaerobic conditions is the 5,6-dihydro-5,6-dihydroxy derivative.⁴ By use of osmium tetroxide⁵ in neutral phosphate buffer at 37° C, we have converted d(G-T)₂₀ to products that are identically hydroxylated, d(G-T*)₂₀, and in which varying percentages of the thymine bases have been altered. Gel permeation chromatography showed that very little if any strand breakage occurred. It is known that the guanine ring is not attacked by osmium tetroxide.⁵ The products were analyzed for both ultraviolet absorption and phosphorus content from which were calculated $\epsilon(p)$ values; these

were lower than the $\epsilon(p)$ of $d(G-T)_{20}$, indicating that the thymine chromophore was partially destroyed. One sample was studied in detail; it contained only an average of 6 unaltered thymines out of the original 20, as shown from its $\epsilon(p)$. A mixture with $d(A-C)_{200}$ in 0.02 M Na^+ buffer (pH 7.0) gave a melting curve whose T_m (40° C) was 26 degrees lower than that from the original $d(G-T)_{20}$. This proved to be a valuable data point in establishing a practical explanation for T_m values from X-irradiated polydeoxyribonucleotides.

Two mathematical approaches have been used for explanation of T_m values. One is an empirical modification of an earlier empirical equation⁶ relating T_m to unirradiated strand length

$$T_m = A - B/n \quad (\text{Eq. 2})$$

to give the new Eq. 3

$$T_m = A - (1 + ka) B/n, \quad (\text{Eq. 3})$$

where n is the mean strand length from gel permeation chromatography, a is the number of bases per strand that have been altered to make them ineffective toward stabilization of double-stranded association, and A , B , and k are constants that are evaluated by melting suitable standards. The other approach was to derive thermodynamically an average molecular structure for which would be calculated, from summed free energy values, a T_m equal to the experimental T_m .⁷ There is too little evidence yet to show whether this second approach will be feasible. Using Eq. 3, whose constants were established by melting data from unirradiated samples of various mean lengths and also the $d(G-T^*)_{20}$ mentioned above, we have been able to compare base damage in poly $d(G-T)$ with that in poly $d(A-C)$. The ratio proved to be 1.54, with poly $d(G-T)$ sustaining more damage. The early work by Hems⁸ gave relative damage to all four bases in DNA. Summing G with T and calculating the ratio of this to the sum of A and C gives 1.59. At 50 krads, we calculated that 19 percent of the bases in poly $d(G-T)$ either had been altered or had been eliminated without concurrent strand breakage.

REFERENCES

1. R. B. Setlow and E. C. Pollard, Molecular biophysics, Addison-Wesley Publishing Company, Reading, Massachusetts (1964), p. 335.
2. W. M. Dale, L. H. Gray, and W. J. Meredith, The inactivation of an enzyme (carboxypeptidase)

by X- and α -radiation. *Phil. Trans. Roy. Soc. London Ser. 242A*, 5-62 (1950).

3. U. Hagen, Bestimmung von einzel- und doppelbrüchen in bestrahlter desoxyribonukleinsäure durch die molekulargewichtsverteilung, *Biochim. Biophys. Acta* 134, 45-58 (1967).
4. R. Latarjet, B. Ekert, S. Apelgot, and N. Rabeyrotte, Radiobiochemical studies of deoxyribonucleic acid (DNA). *J. Chim. Phys.* 58, 1046-1057 (1961).
5. M. Beer, S. Stern, D. Carmalt, and K. H. Mohlenrich, Determination of base sequence in nucleic acids with the electron microscope. V. The thymine-specific reactions of osmium tetroxide with deoxyribonucleic acid and its components. *Biochemistry* 5, 2283-2288 (1966).
6. F. N. Hayes, E. H. Lilly, R. L. Ratliff, D. A. Smith, and D. L. Williams, Thermal transitions in mixtures of polydeoxyribodinuclotides, *Biopolymers* 9, 1105-1117 (1970).
7. C. DeLisi, Conformational changes in transfer RNA. I. Equilibrium calculations. *Biopolymers* (1973), in press.
8. G. Hems, Chemical effects of ionizing radiation on deoxyribonucleic acid in dilute aqueous solutions. *Nature* 186, 710-712 (1960).

RADIATION AND GENETIC INFORMATION TRANSFER

(D. A. Smith, F. N. Hayes, A. M. Martinez, V. E. Mitchell, R. L. Ratliff, and G. F. Strniste)

Replication

We have used calf thymus DNA polymerase to prepare synthetic polynucleotides.^{1,2} Such polymers have been used in several kinds of studies including, for example, investigations into the physical and template properties of polydeoxyribonucleotides.^{3,4} The lack of nuclease activity associated with calf thymus DNA polymerase and the strictly repair replication property of its catalytic activity make it ideal for preparation of model double-stranded DNAs. However, the lability of this enzyme in storage and the considerable expense, time, and effort entailed in its purification have caused us to look at DNA polymerases from other sources as possible replacements for calf thymus DNA polymerase. We have recently made highly purified preparations of DNA polymerase from Micrococcus luteus. The ability of this enzyme to perform accurate repair replication has been demonstrated in preliminary studies (see Table 1). Accurate repair replication of poly dT in the presence of a dA_{33} initiator took place at

TABLE 1. REPAIR REPLICATION OF POLY dT^a

| Monomer template (nmoles) | dATP- ¹⁴ C dA ₃₃ (nmoles) | Replication (%) |
|---------------------------|-------------------------------------------------|-----------------|
| <u>Experiment 1</u> | | |
| 98 | 88 | 91 |
| <u>Experiment 2</u> | | |
| 196 | 176 | 90 |
| <u>Experiment 3</u> | | |
| 98 | 0 | 0 |

^aPoly dT with average length of 208 was incubated with dATP-¹⁴C and calf thymus DNA polymerase. In experiments 1 and 2, a dA₃₃ initiator also was included in the reaction mixture. No dA₃₃ was included in experiment 3.

5° C and 0.15 M KCl. At higher temperatures and lower KCl concentrations, "over-replication" was usually observed. The ability of the enzyme to perform accurate repair replication of more complicated templates is now under investigation.

In addition, we are studying some other properties of *M. luteus* DNA polymerase. A nitrocellulose membrane assay for complex formation between the enzyme and DNA has been developed. The ability of the enzyme to bind d(A-T)_n·d(A-T)_n, as well as the influence of ionic strength upon the amount of polymer bound, has been measured. The binding reaction is very sensitive to ionic strength with the amount of d(A-T)_n·d(A-T)_n bound decreased by 50 percent as the KCl concentration in the binding buffer is raised from 0.05 M to 0.3 M. We have also initiated studies on the role of sulfhydryl groups in binding and catalytic activities of *M. luteus* DNA polymerase. Results to date have shown that some sulfhydryl reagents do not inhibit binding or activity. These reagents include p-chloromercuribenzoate and N-ethylmaleimide. On the other hand, some inorganic reagents such as HgCl₂, which react with sulfhydryl groups, do inhibit catalytic activity of the enzyme but not its ability to bind polydeoxyribonucleotides. Since rather high concentrations of these inorganic reagents are required to produce the effects, it may be that the observed inhibition is due to some mechanism other than a reaction with putative polymerase sulfhydryl groups.

REFERENCES

1. F. W. Hayes, E. Hansbury, V. E. Mitchell, R. L. Ratliff, D. A. Smith, and D. L. Williams, Early stages in complementary synthesis directed by synthetic single-stranded polydeoxyribonucleotide templates and catalyzed by calf thymus deoxyribonucleic acid polymerase. *J. Biol. Chem.* **246**, 3631-3638 (1971).
2. F. W. Hayes, U. Hollstein, V. E. Mitchell, and R. L. Ratliff, Polydeoxythymidylate as template for complementary synthesis. *FEBS Letters* **19**, 15-18 (1971).
3. F. W. Hayes, E. H. Lilly, R. L. Ratliff, D. A. Smith, and D. L. Williams, Thermal transitions in mixtures of polydeoxyribodinucleotides. *Biopolymers* **9**, 1105-1117 (1970).
4. D. A. Smith, F. W. Hayes, A. M. Martinez, R. L. Ratliff, and D. L. Williams, Concerning the role of pyrimidine clusters in transcription. In: Abstracts of the 160th National Meeting of the American Chemical Society, Chicago, Illinois (September 14-18, 1970), Abstract No. Biol. 63.

Transcription

Initiation of RNA synthesis in vitro normally takes place with ATP or GTP serving as the first nucleotide in the RNA chain. Subsequent nucleotides are added to the 3'-hydroxyl group of ATP or GTP, and the RNA chain is extended by this mechanism. When RNA homopolymers serve as template for RNA synthesis, complementary oligoribonucleotides stimulate the rate of RNA synthesis, and they can serve to initiate RNA chains by being covalently incorporated into the growing RNA chain.¹ Straat et al.² recently observed that complementary deoxyribosyl oligomers also stimulate RNA synthesis. They thought it unlikely that deoxyribosyl oligomers were covalently incorporated into the RNA chain. We have investigated the parameters involved in stimulation of RNA synthesis by deoxyribosyl oligomers and the question of their covalent incorporation into RNA.³

Deoxyribothymidylate oligomers stimulate poly U synthesis directed by poly A or poly dA and catalyzed by *Escherichia coli* RNA polymerase. The amount of stimulation observed is a function of oligomer concentration, substrate concentration, and metal ion used. Figure 1 shows stimulation of poly A-directed poly U synthesis by d(pT)₈ as a function of UTP concentration. At low UTP concentrations where the initiation step is severely rate-limiting, the stimulatory effect of d(pT)₈ on the reaction is highest. Other experiments which utilized γ-³²P-UTP

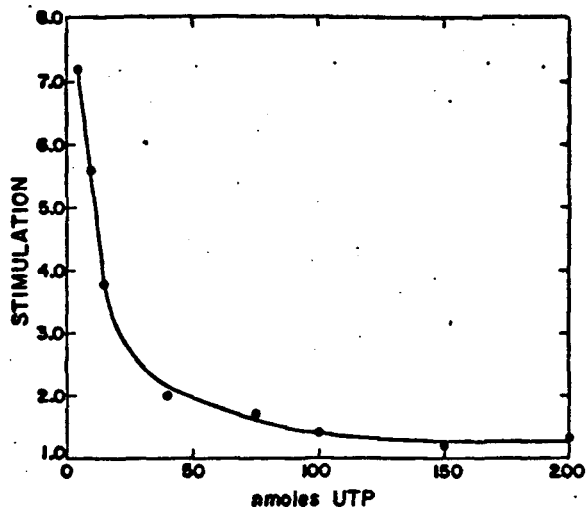


Fig. 1. Stimulation of poly A-directed poly U synthesis by $d(pT)_8$ as a function of UTP concentration. Stimulation is defined as the ratio of $UMP-^{14}C$ polymerized in the presence of $d(pT)_8$ divided by the amount polymerized in the absence of $d(pT)_8$.

as substrate showed that initiation of poly U chains with UTP is greatly decreased when oligodeoxythymidylate is included in the reaction mixture. Direct evidence for oligodeoxythymidylate incorporation into poly U chains was obtained in the following way.

Poly A, 3H -UTP, and RNA polymerase were incubated in two reactions, one of which also contained $d(pT)_8$. The reaction mixtures were hydrolyzed in 0.3 N KOH at 37° C for 20 hours and neutralized, and the hydrolysates were chromatographed on DEAE-cellulose. The reaction which contained $d(pT)_8$ gave rise to a radioactive peak with chromatographic properties expected of $d(pT)_8pUp$ (Fig. 2). Such a peak was not seen in the other reaction. We also have somewhat similar types of evidence that much longer poly dT also serves to initiate poly U synthesis. In some reactions, all poly U chains appear to be initiated with deoxythymidylate oligomers. Oligomer initiation of RNA synthesis seems to occur independently of the presence of the sigma subunit of RNA polymerase.

The role *in vivo*, if any, of initiation of DNA synthesis with RNA or DNA oligomers is not known. However, this reaction suggests the possibility that *in vivo* initiation of RNA synthesis might occur sometimes at single-stranded breaks on DNA and thus produce DNA-RNA covalent hybrids. The occurrence of this reaction also requires that most studies of *in vitro* initiation of RNA synthesis be reinterpreted.

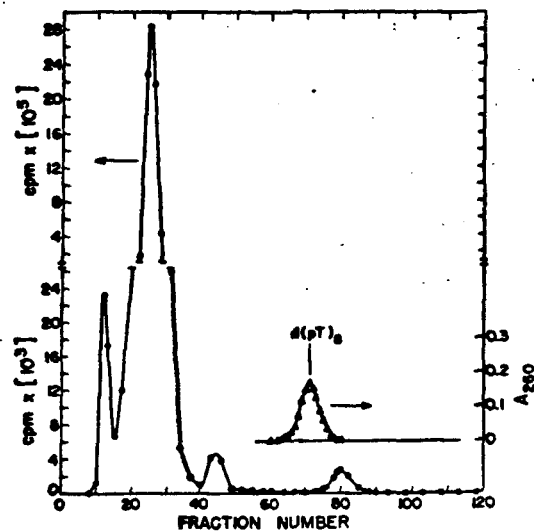


Fig. 2. DEAE-Cellulose chromatography of the hydrolysate of a $d(pT)_8$ -stimulated poly U synthesis reaction. A $d(pT)_8$ marker was added to the neutralized hydrolysate prior to chromatography. The radioactive peak that is eluted after the $d(pT)_8$ is presumed to be $d(pT)_8$ to which an additional tritiated pUp remains attached after alkaline hydrolysis. This peak was not seen in reactions which did not contain $d(pT)_8$.

REFERENCES

1. S. K. Niyogi and A. Stevens, Studies of the ribonucleic acid polymerase from *Escherichia coli*. IV. Effect of oligonucleotides on the ribonucleic acid polymerase reaction with synthetic polyribonucleotides as templates. *J. Biol. Chem.* **240**, 2593-2598 (1965).
2. P. A. Straat, O. Pongs, and P. O. P. Ts'o, RNA polymerase from *Micrococcus luteus*: Comparative effect of ribosyl and deoxyribosyl oligomers on the homopolymer-directed reaction. *Biochem. Biophys. Res. Commun.* **44**, 905-911 (1971).
3. D. A. Smith, A. M. Martinez, and D. L. Williams, Initiation of *in vitro* RNA synthesis with oligodeoxyribonucleotides. In: Abstracts of the 164th National Meeting of the American Chemical Society, New York City, New York (August 27-September 1, 1972), Abstract No. 71.

Effects of X-Irradiation on RNA Polymerase

In the studies of Pollard and co-workers,¹ it has been shown that controlled transcription *in vivo* in the bacterium *Escherichia coli* is sensitive to ionizing radiation; furthermore, it was possible to correlate from critical target analysis the radio-sensitive structure responsible for utilization of the RNA precursor uracil with a structure similar in size to the RNA polymerase molecule. Accordingly,

we undertook an investigation of the radiosensitivity of that enzyme.

The effects of X-irradiation upon RNA polymerase from three strains of *E. coli* of varying radiosensitivities have been investigated using a variety of homopolymers and a natural double-stranded DNA as templates.²⁻⁴ The radioresponse of enzymatic activity of the polymerase was independent of the radiosensitivity of the cell from which it was extracted. D_{37} values obtained varied according to the template molecule used. This variability in dose-response of the enzyme could not be attributed to an effect on binding of irradiated enzyme to the template molecule; D_{37} values for inactivation of binding to poly U or poly dT were 4 to 8 times greater than corresponding D_{37} values for inactivation of enzymatic activity of the enzyme (Figs. 1 and 2).

When irradiated enzyme was assayed with ribohomopolymer templates, there was a substrate dependence of inactivation (i.e., D_{37} values for inactivation of enzyme activity of the RNA polymerase changed as substrate concentration in the reaction mixture was varied). At low substrate levels where the initiation step of RNA synthesis is rate-limiting, radiosensitivity of the enzyme is highest. With homodeoxyribopolymer templates, a substrate independence of inactivation was observed.

The ability of complementary ribosyl pentamers to bypass chain initiation and to stimulate poly A synthesis in poly U- and poly dT-directed reactions was examined. Utilizing this method of bypassing the rate-limiting step in *in vitro* RNA synthesis, the inactivation of enzymatic activity by X-irradiation was investigated. The substrate concentration dependence of D_{37} values for homoribopolymer templates is eliminated when these initiator molecules are included in the reactions. Furthermore, the irradiated enzyme, when assayed with homodeoxyribopolymers, becomes less radiosensitive in the presence of oligomer primers. These results suggest that the initiation step is the most radiosensitive in the process of RNA synthesis.

The fidelity of RNA synthesis by X-irradiated RNA polymerase was also examined. A linear increase in insertion of noncomplementary nucleotides into poly A as a function of dose for both poly U- and poly dT-directed reactions was observed. Misreading

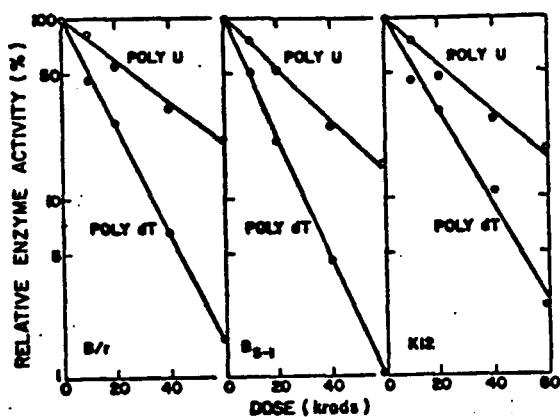


Fig. 1. Inactivation of the enzymatic activity of *E. coli* B/r, B₈₋₁, and K12 RNA polymerases by X-irradiation when assayed with either poly U or poly dT. The assays contained 375 nmoles ¹⁴C-ATP (4.5×10^5 cpm/ μ mole) per reaction. The nonirradiated polymerase samples (7.5 to 8.0 μ g) incorporated 4 nmoles ¹⁴C-AMP in 20 minutes using a poly U template plus Mn⁺⁺ or 18 nmoles ¹⁴C-AMP in 10 minutes using a poly dT template plus Mg⁺⁺.

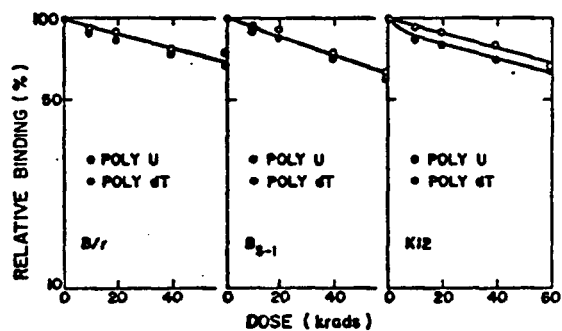


Fig. 2. X-ray inactivation of binding ability of *E. coli* B/r, B₈₋₁, and K12 RNA polymerases to either poly U or poly dT. The assays contained 2.6 nmoles ³H-poly U or 2.6 nmoles ³H-poly dT and 1.5 μ g or 3.0 μ g enzyme, respectively.

was 3 to 4 times more pronounced in poly dT-directed reactions compared to poly U-directed reactions (see Fig. 3). It is not known if damage to RNA polymerase is an important effect *in vivo* of X-irradiation. If so, it may be that decreased fidelity of transcription could account for some of the delayed effects of irradiation.

REFERENCES

1. E. C. Pollard, The effect of ionizing radiation on the molecular biology of *Escherichia coli*. In: *Current Topics in Radiation Research VI*, 51 (1970), M. Ebert and A. Howard, eds., North-Holland Publishing Company, Amsterdam.

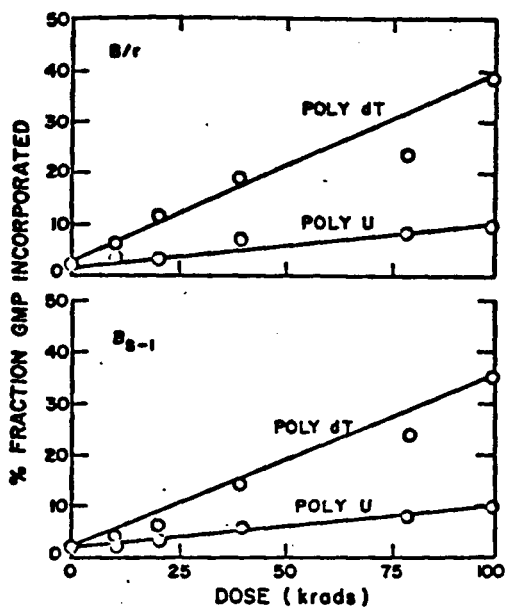


Fig. 3. Misreading or percent fraction of GMP incorporated in a poly U- or poly dT-directed poly A synthesis reaction by X-irradiated *E. coli* RNA polymerase as a function of dose. The percent fraction of GMP incorporated at a particular dose by either the B/r or B₈₋₁ RNA polymerase was calculated from the amount of GMP incorporated, compared to the amount of AMP incorporated, and multiplied by 100.

2. G. F. Strniste and D. A. Smith, *In vitro* studies on the synthesis of ribonucleic acid using X-irradiated RNA polymerase. In: Abstracts of the First Rocky Mountain Regional American Chemical Society Meeting, Fort Collins, Colorado (June 30-July 2, 1972), p. 17, Abstract No. 18.
3. G. F. Strniste, D. A. Smith, and F. N. Hayes, X-Ray inactivation of the *Escherichia coli* DNA-dependent RNA polymerase in aqueous solution. I. Studies on binding and substrate concentration dependence in the inactivation of enzymatic activity. *Biochemistry* (1973), in press.
4. G. F. Strniste, D. A. Smith, and F. N. Hayes, X-Ray inactivation of the *Escherichia coli* DNA-dependent RNA polymerase in aqueous solution. II. Studies on initiation and fidelity of transcription. *Biochemistry* (1973), in press.

Ultraviolet-Induced Cross-Links between RNA Polymerase and DNA

There are certain specific sites on DNA molecules which bind the RNA polymerase enzyme. Several attempts have been made in recent years to isolate RNA polymerase binding sites utilizing the property of nuclease resistance of those regions of the DNA molecule covered by bound polymerase. However, base analysis of the labeled DNA fragments

has not revealed any major differences in comparison with base composition of the entire DNA molecule. Among the many technical problems in this experimental approach is the possibility that the enzyme may migrate to other sites during the digestion process. If the RNA polymerase-DNA complex could be stabilized by formation of a covalent bond between the two, not only would migration be prevented but also more vigorous procedures could be utilized during purification of the complex. We have developed a method of stabilizing the RNA polymerase-DNA complex. It has been shown previously that ultraviolet light can induce, in addition to pyrimidine dimers, DNA-protein cross-links.¹ An ultraviolet-induced cross-link between bound RNA polymerase and a DNA might stabilize the enzyme at its initial binding site and allow purification and characterization of these sites.

In control experiments, we examined as a function of dose the ability of ultraviolet light to induce formation of a stable complex between *Escherichia coli* RNA polymerase and poly d(A-T)-d(A-T). A stable complex is defined as one which maintains its integrity in a high salt concentration (2 M KCl) which totally disrupts nonlinked polymerase-DNA complexes. Existence of such complexes is detected by nitrocellulose filter assay.² Their formation appears to be a biphasic response, consisting of an initial rapid formation followed by a more gradual increase of stable complex with dose. Irradiation of the enzyme and polymer separately does not promote formation of stable complexes upon mixing.

With poly d(A-T)-d(A-T) of an average length of 239 nucleotides, we examined ultraviolet-induced stable complex formation at two enzyme:polymer ratios (mole:mole). About 10 and 24 percent of the labeled polymer remained bound to the enzyme in high salt when enzyme:polymer ratios of 2.2:1.0 and 4.4:1.0, respectively, were irradiated with 150,000 ergs/mm². To characterize further these complexes, samples from the above experiment were centrifuged to equilibrium in cesium chloride. The results are shown in Fig. 1. The stable protein-polymer complex essentially floats in these gradients and, thus, can be readily separated from dissociable complexes. Work is in progress to characterize further these stable complexes prior

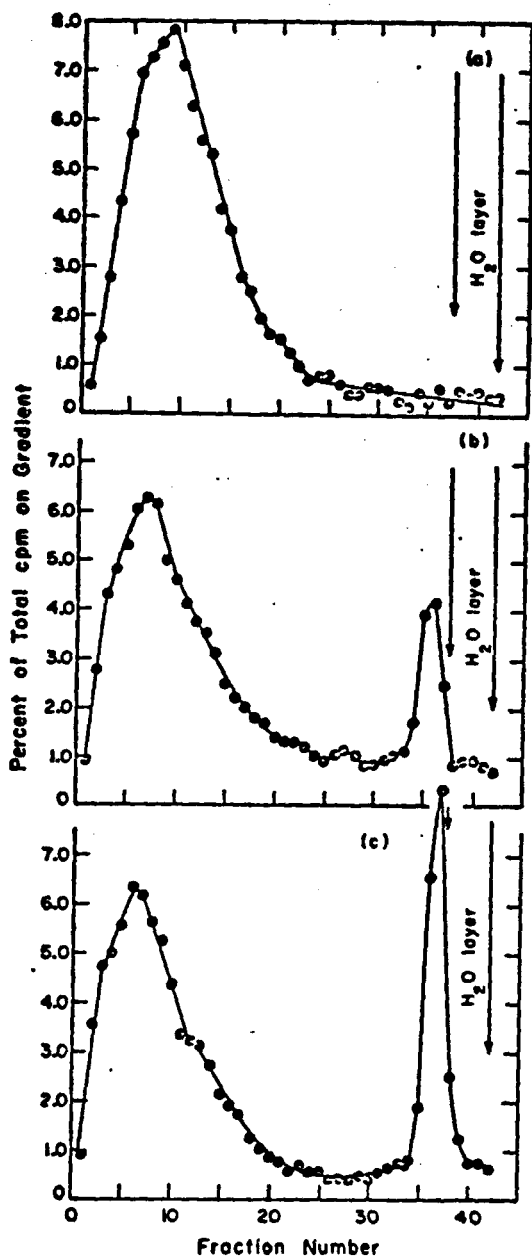


Fig. 1. Cesium chloride sedimentation equilibrium gradient analysis of ultraviolet-induced stable complex formation between RNA polymerase and ^{14}C -poly d(A-T)·d(A-T). Samples of irradiated polymer and irradiated enzyme:polymer complexes were mixed with cesium chloride to a final density of 1.46 g/cm^3 and centrifuged to equilibrium. After centrifugation, approximately 1 ml H_2O was layered onto each gradient, and the gradients were fractionated: (a) irradiated polymer; (b) irradiated enzyme:polymer (2.2:1.0); and (c) irradiated enzyme:polymer (4.4:1.0). In agreement with the nitrocellulose filter assay, about 10 percent of activity was found in the light peak in (b) and about 24 percent in (c).

to determining the utility of this approach in isolation of RNA polymerase binding sites on native DNA.

REFERENCES

1. K. C. Smith, The biological importance of UV-induced DNA-protein cross-linking *in vivo* and its probable chemical mechanism. *Photochem. Photobiol.* 7, 651 (1968).
2. O. W. Jones and P. Berg, Studies on the binding of RNA polymerase to polynucleotides. *J. Mol. Biol.* 22, 199 (1968).

EFFECTS OF IONIZING RADIATION ON CHROMATIN STRUCTURE AND THE MITOTIC APPARATUS

(G. R. Shepherd, J. M. Hardin, and B. J. Noland)

Ionizing radiation administered at sufficient dose levels gives rise, either directly or indirectly, to alterations in target molecules or sites within the living cell. These alterations are eventually expressed as such classical radiobiological phenomena as division delay, cell death, and chromosomal aberrations. The means by which these phenomena are effected at the molecular level are not clear, though it is by now quite apparent that multiple but interrelated factors contribute to these phenomena in nearly every case.

It is our purpose to (a) characterize *in vivo* and *in vitro* alterations in cellular biochemistry brought about by ionizing radiation; (b) determine the molecular mechanisms by which these changes are effected; and (c) attempt to determine the relevance of defined *in vitro* mechanisms with observed *in vivo* radiobiological phenomena. Our investigations have suggested two important biochemical areas in which ionizing radiation might contribute directly and significantly to cell death and division delay. In the first of these areas, the basic postulate suggests that ionizing radiation at sufficient levels brings about disruption of chromatin structure, resulting in alterations in template capacity and specificity of protein-bound genomic DNA. Chromatin disruption might well be evoked as a causative factor in radiation-induced cell transformation, viral induction, or cell death. In the second of these areas, the basic postulate is that radiation-induced division delay stems from the inability of the cell to undergo division and that

this inability results from induced alterations in cellular division mechanisms. We have concerned ourselves in the following studies with the effects of ionizing radiation upon components of chromatin and of the mitotic apparatus.

Effects of Ionizing Radiation on Chromatin Structure and Metabolism

The constant association of nuclear proteins with nucleic acids and ability of these proteins to affect the nature and rate of genomic transcription reactions have led to the suggestion that nuclear proteins may function as direct regulators or as intermediate moderators of gene expression. Nuclear proteins combine with nuclear DNA and RNA to form the chromatin of living cells. Alterations in the balance of any of these components within the chromatin or alterations in properties of these components can give rise to changes in ability of chromatin to serve as template in transcription reactions. It is the purpose of this study to (a) characterize *in vivo* and *in vitro* chromatin structural alterations brought about by ionizing radiation; (b) determine the molecular mechanisms by which these alterations are effected; (c) determine the result of these changes on normal chromatin functions; and (d) establish the relationship of these effects to classical radiobiological phenomena.

Histones are believed to be the molecular entities primarily responsible for compaction and structuring of chromatin. Structural alterations of these proteins via acetylation, methylation, and phosphorylation reactions occur at clearly defined times within the cell cycle, and these reactions appear to be regulated by availability of histones within the chromatin rather than intracellular effector enzyme levels. These results have been reviewed recently.¹

If these structural alterations are permanent, one might assume that the function they perform is also relatively constant. The stabilities of histone acetyl, methyl, and phosphoryl groups were determined. Both histone methyl² and acetyl³ groups appeared to be conserved in rapidly dividing cultured mammalian cells. Histone F2b phosphoryl groups also appeared to be conserved, while histone F1 phosphate appeared to turn over during G₂ in synchronized mammalian cells.⁴ Thus, the biological effects of histone acetylation and methylation and

phosphorylation of fraction F2b may well be relatively permanent, while phosphorylation and dephosphorylation of histone F1 may represent an ongoing process such as transport or derepression.

If alteration of histones represents the derepression of DNA prior to replication in S, one might predict that only "old" histones, the repressive products of an earlier division cycle, would be altered within a given cell cycle. We have demonstrated recently that the internal peptide 13-17 of histone fraction F2a1 is acetylated at residue 16 within the same cell cycle in which the histone was synthesized.⁵ This demonstration provides proof of the principle that new histones may be acetylated and renders it unlikely that acetylation of this site is solely involved in the derepression of DNA within that cell cycle. These observations agree with our previous correlation of radiation-induced inhibition of both DNA and histone biosynthesis and of histone acetylation and methylation.⁶ Thus, the observed effects of ionizing radiation upon histone synthesis and structural alterations may well be an effect rather than a cause.

REFERENCES

1. G. R. Shepherd, B. J. Noland, J. M. Hardin, and P. Byvoet, Structural modifications of histones in cultured mammalian cells. In: *The Biochemistry of Gene Expression in Higher Organisms*, D. Reidel, Dordrecht, Holland (1973), in press.
2. P. Byvoet, G. R. Shepherd, J. M. Hardin, and B. J. Noland, The distribution and turnover of labeled methyl groups in histone fractions of cultured mammalian cells. *Arch. Biochem. Biophys.* **148**, 558-567 (1972).
3. G. R. Shepherd, B. J. Noland, and J. M. Hardin, Turnover of histone acetyl groups in cultured mammalian cells. *Arch. Biochem. Biophys.* (1973), in press.
4. G. R. Shepherd, J. M. Hardin, and B. J. Noland, Dephosphorylation of histone fractions of cultured mammalian cells. *Arch. Biochem. Biophys.* (1973), in press.
5. G. R. Shepherd, Evidence for the biological coupling of biosynthesis and internal acetylation of histone fraction F2a1 (IV) in cultured mammalian cells. *Biochim. Biophys. Acta* (1973), in press.
6. G. R. Shepherd, R. A. Walters, J. M. Hardin, and B. J. Noland, The effects of X-irradiation on histone acetylation and methylation in cultured mammalian cells. *Arch. Biochem. Biophys.* **149**, 175-182 (1972).

Effects of Ionizing Radiation on Components of the Mitotic Apparatus

X-Irradiation of exponentially growing mammalian cells at intermediate dose levels induces the phenomenon of division delay. Irradiated cells typically cease division immediately for a period of time proportional to the dose of incident radiation, after which they resume their normal growth pattern for one or more generations. It has been shown that cells irradiated at these levels, while retaining their ability to synthesize RNA, DNA, and functional proteins, accumulate in G_2 or a G_2 -like state prior to resuming division. This accumulation has led to the suggestion that radiation-induced division delay arises from damage to cellular division mechanisms or to some component necessary for initiation of division. This component appears to be protein in nature.

We have determined the temporal pattern of intracellular microtubule protein levels in synchronized cultures of mammalian cells (Fig. 1). Cellular microtubule protein levels display two distinct maxima in late S and in late G_2 . It may be seen that these maxima correspond closely to maxima in total soluble protein content of the cells.

The effect of 1600 rads of X-irradiation upon intracellular RNA, total soluble protein, and microtubule protein levels may be seen in Fig. 2. All levels rose to maxima between 15 and 30 hours post irradiation as cells accumulated in G_2 and declined thereafter. It is believed that phosphorylation may precede assembly of microtubular protein into macrostructures. Radiation has been shown to cause transitory effects upon phosphorylation of a variety of metabolites within the mammalian cell. Techniques for isolation of pure microtubule protein from cultured mammalian cells have been established, and microassay techniques are now being developed to allow establishment of phosphorylation of tubulin as a precursor to microtubule assembly, to determine which of the subunits is phosphorylated, to determine the progress of phosphorylation within the cell, and ultimately to determine the effects of ionizing radiation upon tubulin phosphorylation.

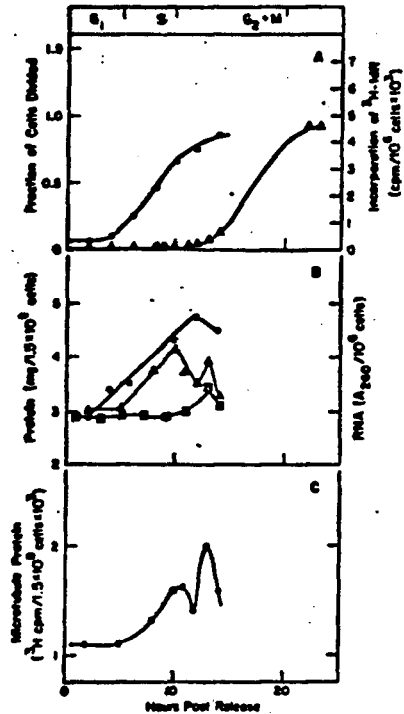


FIG. 1. Temporal profiles in a synchronized culture of mammalian cells (CHO) for (A) DNA synthesis (●-●-) and cell count (-▲-▲-); (B) RNA mass/cell (●-●-), total soluble protein (-▲-▲-), and total insoluble protein (-■-■-); and (C) cpm 3H colchicine incorporated into microtubule protein.

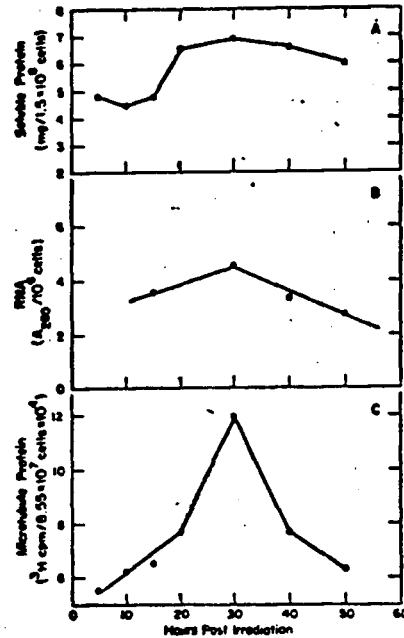


FIG. 2. Temporal profiles in an X-irradiated (1600-rad) culture of mammalian cells (CHO) are demonstrated for 50 hr post irradiation for (A) total soluble protein; (B) RNA mass/cell; and (C) cpm 3H colchicine incorporated into microtubule protein.

CELLULAR RADIOBIOLOGY SECTION

INTRODUCTION

Interests of the Cellular Radiobiology Section during the past year have continued to focus on three main areas employing cultured mammalian cells and microbial systems as test objects. Regulatory and control mechanisms, cell-cell interactions, and chromosome structure and function are general features of our overall objective of establishing well-defined test systems which can be exploited to determine (1) relevance of specific biochemical features to cell-cycle progression; (2) some sense of proportion regarding the importance of radiation or other toxic effects on specific features of cell metabolism to cell survival; and (3) practical applications of specific features of cell metabolism to problems of tumor cell biology and radiotherapy. Currently the most useful systems relate to RNA metabolism, histone metabolism, cell-cycle kinetics, cell-surface receptor sites, cytogenetic effects, and DNA synthesis. The general approach continues to be one of establishing a system and then measuring the effects of biologically important toxic agents or ionizing radiation of varying quality on various established, recognizable, and measurable features.

In our 1971 report¹ unique particulate-associated RNA species were characterized, and an attempt was made to ascribe functional requirements for these species in the cycling cell. In this report we summarize results which describe rapidly-labeled, high molecular-weight RNA from mammalian cytoplasm associated with protein or nucleoprotein to form two rapidly-sedimenting particulates (i.e., polysomes and informosomes) distinguishable by their differing densities. Conditions have been established which restrict messenger or messenger-like RNA available for ribosome association to messenger-like RNA of informosomes. Under these conditions, cycloheximide-mediated polysome superformation occurs in part as a result of association of ribosomes with RNA (and presumably

protein) of informosomes. Thus, at least part of the population of informosomal messenger-like RNA is true messenger RNA capable of participating in polysome formation. This observation is in accord with other evidence indicating that cytoplasmic mammalian messenger RNA exists as a nucleoprotein, not as free RNA, prior to association with ribosomes.

Further characterization of mammalian RNA species by identification of minor bases has been accomplished. For example, several RNA species contain distinctive quaternary nucleosides which are easily separable chromatographically. Three nuclear species contain trimethylguanosine, which is found in no other species. Ribosomal RNAs can be distinguished because 18S contains a single 7-methylguanosine but none of the other quaternary nucleosides, while 28S contains a single 1-methyladenosine and no others. Moreover, 18S RNA has for the first time been shown to contain a single hypermodified base, 1-methyl-3- γ -(α -amino- α -carboxypropyl)pseudouridine, of interest because hypermodified bases have thus far been found exclusively in the anticodon region of tRNA. In fact, tRNA of CHO cells has been found to contain a similar nucleoside, 3- γ -(α -amino- α -carboxypropyl)uridine.

Recent studies of radiation effects on histone metabolism have revealed that f2a2 phosphorylation is independent of f2a2 synthesis, f1 phosphorylation, and DNA synthesis. Histone f1 phosphorylation, although not related to either f1 or DNA synthesis, is nonetheless an exclusive S-phase phenomenon strongly inhibited by X-irradiation and, because of cycle-dependence, is probably not important in derepression of DNA template activity.

Improved control of experimental conditions for studying cycle-dependent biochemical effects has been achieved by tandem isoleucine deprivation and hydroxyurea treatment to yield large cultures suitable for biochemical analysis in which all cells are truly in G₁ and subsequently divide synchronously. Biochemical criteria for assessing the degree of perturbation exhibited by these cultures appear to

have general applicability for measuring the effects of a variety of stresses on any cell line.

Continued studies of cell-surface properties have focused on attempts to quantitate cell-surface binding of fluorescein-conjugated plant lectins employing flow microfluorometric techniques. The surface density of binding sites has been found to be nearly constant throughout the cell cycle, with some evidence for heterogeneity of binding sites and, generally, competition for binding sites between concanavalin A and wheat germ agglutinin. Agglutinability of virus-transformed lines and trypsin-treated parental lines could be readily demonstrated but not clearly correlated with binding.

The striking observation of DNA constancy despite marked variability in chromosome number in heteroploid mammalian cell lines utilizing flow microfluorometric techniques has been confirmed independently, in part by extensive karyologic comparison of euploid Chinese hamster fibroblasts with line CHO cells employing modern Giemsa banding procedures. Although no homologous pairs of chromosomes remain in CHO cells, virtually the entire genome can be accounted for in terms of extensive translocations and a pericentric inversion; however, most of a haploid set of chromosomes has retained normal configuration. Approximately 3 percent of the genome missing from CHO cells has been identified as the arms of the late-replicating X_2 chromosome. These observations have important genetic implications.

The evidence is now also clear that, although membrane-bound DNA replication sites do not occur in CHO, the sites for initiation of DNA synthesis may indeed be membrane-associated. Thus, the spatial arrangement of DNA within the nucleus might be regulated by association of specific regions with the nuclear membrane.

Details of phage DNA replication following derepression of prophage by ultraviolet light in Haemophilus influenzae are most consistent with a model in which both synthesis of a multiple phage-equivalent concatomer and subsequent reduction to phage-sized pieces occur on cell membrane. Excision repair capability of the host bacterium does not appear to be essential for triggering derepression, nor does it prevent derepression. However,

excision-repair capability is important at elevated ultraviolet doses for maintaining capacity for phage production in the derepressed lysogen. Repair capability has also been used to distinguish between alternative models for assembly of phage T4. The conclusion, based on differences in ultraviolet inactivation curves, suggests that T4 assembly proceeds by first constructing the protein shell into which DNA is subsequently inserted.

REFERENCE

1. C. R. Richmond and G. L. Voelz, eds., Annual Report of the Biological and Medical Research Group (H-4) of the LASL Health Division, January through December 1971, Los Alamos Scientific Laboratory Report LA-4923-PR (April 1972).

REGULATORY AND CONTROL MECHANISMS IN THE MAMMALIAN CELL CYCLE

(M. D. Enger, R. A. Tobey, L. R. Gurley, R. A. Walters, A. G. Saponara, and E. W. Campbell)

Informosomes in Cultured Chinese Hamster Cells: Cycloheximide-Mediated Polysome Superformation is Accompanied by Association of Informosomes with Ribosomes

Rapidly labeled, high molecular-weight RNA of mammalian cytoplasm is associated with protein or nucleoprotein to form two types of rapidly sedimenting particulate structures. In one instance, the RNA is messenger RNA and the association is with ribosomes to form polysomes. In the other instance, the association is with protein of unknown function. The resultant particle (~80 percent protein) is referred to as an informosome.¹ [Polysomes and informosomes are distinguished by their differing densities: 1.52 g/cc and 1.4 g/cc for fixed particles in cesium chloride, respectively.] Several lines of evidence suggest that the RNA of informosomes is also messenger. It is similar in size, stability, hybridization properties, and base composition to polysome-bound messenger^{1,2} and is thus referred to as messenger-like RNA. There is about as much messenger-like RNA (mlRNA) in informosomes as there is messenger RNA in polysomes.² Circumstantial evidence indicates that informosomes may represent the form in which messenger RNA exists during transport from nucleus to cytoplasm, during

association with ribosomes to form polysomes, and even during translation. First, informosome-like particles carrying nascent mRNA may be found in³ or extracted from⁴ nuclei. Also, nuclear heterogeneous RNA, which may in part represent messenger precursor, is similarly associated with protein.⁵ Second, all mRNA of the cytoplasm is found to be particulate; no free mRNA exists.² Third, the density of polysomes is less than that of ribosomes, indicating that nucleoprotein that is predominantly protein in composition must have associated with ribosomes to form polysomes.¹ Further, informosome-like particles may be dissociated from polysomes using EDTA.⁶⁻¹¹ Fifth, informosome-like particles are released from polysomes during and re-associated with ribosomes after mitosis.¹² Finally, the kinetics of RNA precursor incorporation are not inconsistent with a flow of messenger RNA through informosomes to polysomes.^{2,11} However, one cannot definitively establish such flow from kinetics alone, and pulse-chase experiments fail to demonstrate satisfactorily such a flow, since the incorporated label in RNA of polysomes and informosomes decays in concert subsequent to inhibition of further incorporation³ (Fig. 1). Thus, no direct evidence exists to show that the informosomes (or mRNA thereof) in the cytoplasm of interphase cells can or do associate with ribosomes to form polysomes. In this report we show that polysome superformation, achieved under conditions where informosomes are the only source of mRNA, is accompanied by an increase in polysomal-labeled mRNA and a decrease in informosomal mRNA -- that polysome superformation is achieved in part by association of ribosomes with informosomes (the majority of

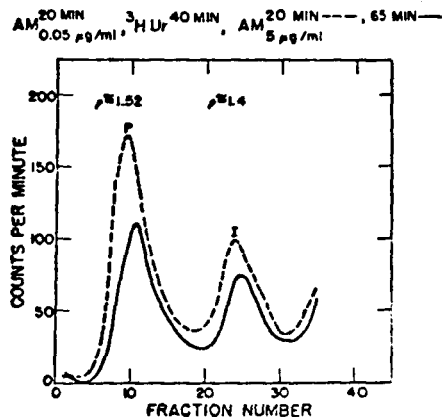


FIG. 1. Decay of RNA in polysomes and informosomes in the presence of actinomycin.

the superformation is apparently due to an increased packing of ribosomes on polysomes). We show further that polysomal messenger RNA and informosomal mRNAs are identical in Millipore retentivity and thus probably share the same content of poly A sequences.

In these experiments, synthesis of ribosomal RNA is preferentially inhibited by treating cultures with 0.05 µg/ml actinomycin (AM) for 30 min¹³ before exposing cultures to radioactive RNA precursors to ensure that most of the incorporation into cytoplasmic particulate-associated RNA is into messenger or messenger-like RNA (mRNA). Subsequent to exposure to labeled RNA precursor, further RNA synthesis is stopped by addition of actinomycin to 5 µg/ml. Because nuclear-cytoplasmic transport of messenger may continue for up to 15 min after synthesis inhibition in HeLa cells¹⁴ (in general, RNA transport and processing occur significantly more rapidly in CHO), cultures are held in the high level of actinomycin for 20 min before effecting superformation of polysomes by addition of cycloheximide (Cx) to 1 µg/ml.¹⁵ Thus, the first treatment with a low level of actinomycin allows one to equate the amount of RNA precursor incorporated into cytoplasmic particles of density 1.4 (informosomes) or 1.52 (polysomes) with their labeled messenger or mRNA contents. Treatment with a high concentration of AM after precursor incorporation prevents any further synthesis of messenger or mRNA and allows one (after establishing that no free mRNA is present) to look for association of informosomes with

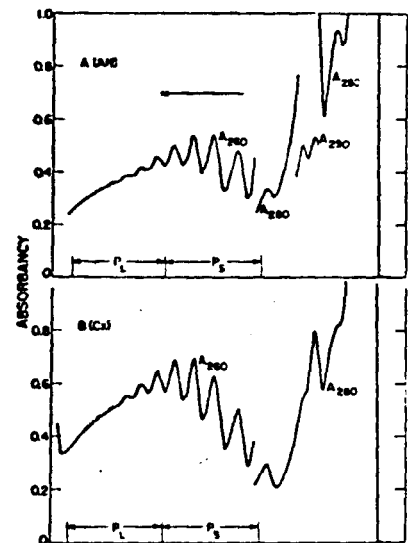


FIG. 2. Polysome superformation in 1 µg/ml cycloheximide.

ribosomes to form polysomes by measuring the amount of incorporated label transferred from 1.4-density material to 1.52-density material when superformation of polysomes is effected [measured as the ratio of label in the two density species after 45 min in Cx as opposed to holding in the high concentration of AM alone for 45 min (AH)]. As shown in Fig. 2, cycloheximide treatment results in a marked increase in polysome content and a corresponding decrease in free 80S ribosomes and ribosome subunits. When one looks at the effect of this superformation upon the relative amount of RNA label in 1.4- and 1.52-density species sedimenting in the region of small (P_S) or large (P_L) polysomes, there is indeed a conversion of label from informosomes to polysomes when superformation occurs (Fig. 3). That the 1.4- \rightarrow 1.52-density conversion effect is not as pronounced as polysome superformation probably is because most of the superformation is effected by a more dense packing of ribosomes (the effect is due apparently to slowing translation rate relative to initiation).

Reproducibility of this effect and a more detailed analysis in terms of including 1.4 and 1.52 particles from all sedimentation ranges are shown in another experiment (Figs. 4 and 5). Again, polysome superformation (Fig. 4) is accompanied by an increase in 1.52 density and a decrease in 1.4 density (Fig. 5, A + D). Because the effect is small, we must assure ourselves that prerequisite conditions obtain. First, we must have an absence of label incorporated into ribosomal RNA. Figure 5A shows this condition is met. That is, any synthesis of rRNA would be seen first in 18S RNA indigenous to the 40S RNA subunit and would produce label in the region of fraction 10; however, none is found. Second, we must consider the possibility

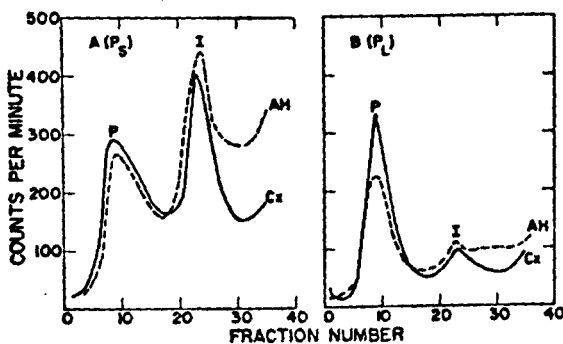


FIG. 3. Change in apportionment of radioactivity in 1.4 (I) and 1.52 (P) density species upon polysome superformation.

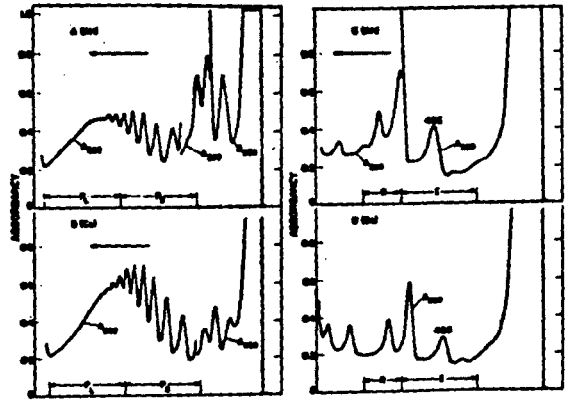


FIG. 4. Polysome superformation in 1 μ g/ml cycloheximide, including the effect on slowly sedimenting material.

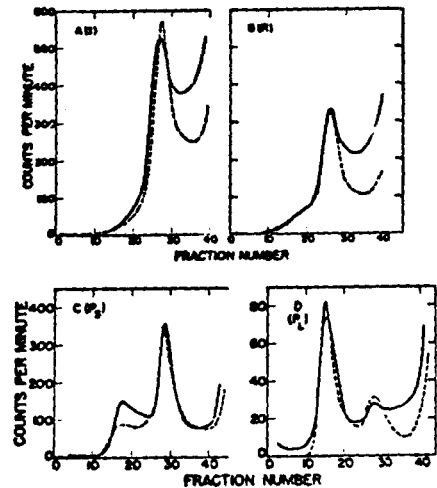


FIG. 5. Isopycnic analysis of the effect of polysome superformation on labeled RNA content of informosomes and polysomes from the region of ribosome subunits (A), 80S ribosomes (B), small polysomes (C), and large polysomes (D).

that the increase in 1.52 density label is due entirely to an increased packing of ribosomes on existing polysomes with concomitant increase in the amount of (labeled) polysomal rRNA. Analysis of RNA extracted from AH or Cx polysomes (Fig. 6A) shows that this is not so, as the label increase is in the mRNA peak (\sim 18S). A corresponding decrease is shown in the case of mRNA extracted from informosomes (Fig. 6B). Third, we must verify the absence of free mRNA or mRNA at the time superformation is initiated. This is shown in Fig. 7. No mRNA is extracted from the sedimentation region (of cytoplasm) which would be occupied by free mRNA.

Thus, at least part of the informosome population can associate with ribosomes to form

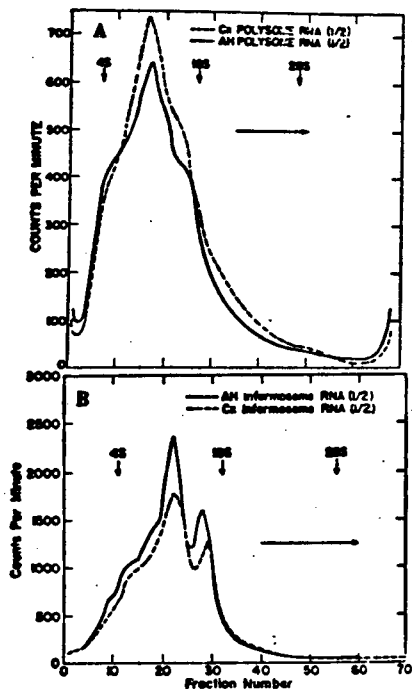


FIG. 6. Size (sedimentation rate) distribution of labeled RNA from polysomes and informosomes in samples treated with cycloheximide to superform polysomes (Cx) or held in actinomycin without cycloheximide (AH).

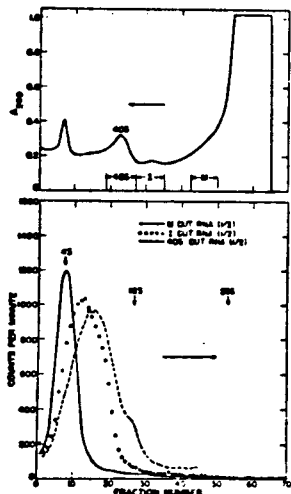


FIG. 7. Labeled RNA of cytoplasm in the region of free mRNA (M), informosomes (I), and 40S subunits (40S).

polysomes. Taken with the other evidence, association of true messenger RNA with protein to form particles of density 1.4 prior to association of messenger with ribosomes appears to be most probable. The question now raised concerns the relatively large amount of messenger in this form. If it represents a statistical sampling of all messenger destined for translation, then one would think that coupling between transcription and translation would

be extremely loose. More probably unbound informosomes represent either incompletely modified or processed forms which will be used eventually as processing is finished (the messenger in informosomes is in a "pipeline" rather than a "pool"), or most of the informosome population is differentially modified to preclude utilization. Such incomplete or differential modification could involve messenger RNAs and/or their associated protein(s).

A property apparently peculiar to mRNA of polysomes is a content of poly A sufficient to cause it to be partially retained on Millipore filters.¹⁶ Is the informosomal mRNA so modified? The data shown in Fig. 5 indicate that labeled RNA is obtained from informosome-density material alone when material in the 20 to 70S region is extracted; labeled RNA obtained from the large polysome fraction is primarily from polysome-density material. Therefore, we may use extracts of these fractions as sources of informosomal mRNA and polysomal mRNA. By comparing polysomal mRNA, informosomal mRNA, and ribosomal RNA by the procedure of Lee *et al.*,¹⁶ we found that no ribosomal RNA was retained on Millipore but that informosomal mRNA and polysomal mRNA were held up to the same extent (30 percent), indicating that the difference in informosomes bound or not bound to ribosomes is not a difference in modification of their RNA by preferential addition of poly A to those messengers designed for translation.

REFERENCES

1. A. S. Spirin, *Eur. J. Biochem.* **10**, 20 (1969).
2. G. Spohr, N. Granboulan, C. Morel, and K. Scherrer, *Eur. J. Biochem.* **17**, 296 (1970).
3. O. P. Samarina, E. M. Lukanidin, J. Molnar, and G. P. Georgiev, *J. Mol. Biol.* **33**, 251 (1968).
4. K. Köhler and S. Arends, *Eur. J. Biochem.* **5**, 500 (1968).
5. K. Scherrer, G. Spohr, N. Granboulan, C. Morel, J. Grosclaude, and C. Chezzi, *Symp. Quant. Biol.* **35**, 539 (1970).
6. R. P. Perry and D. E. Kelley, *J. Mol. Biol.* **35**, 37 (1968).
7. E. C. Henshaw, *J. Mol. Biol.* **36**, 401 (1968).
8. A. Burny, G. Huez, G. Marbaix, and H. Chantrenne, *Biochim. Biophys. Acta* **190**, 228 (1969).
9. S. Olsnes, *Eur. J. Biochem.* **15**, 464 (1970).

10. B. Lebleu, G. Marbaix, G. Huez, J. Temmerman, A. Burny, and H. Chantranne, *Eur. J. Biochem.* 19, 264 (1971).
11. E. C. Henshaw and J. Loebenstein, *Biochim. Biophys. Acta* 199, 405 (1970).
12. H. Fan and S. Penman, *J. Mol. Biol.* 50, 655 (1970).
13. R. P. Perry and D. E. Kelley, *J. Cell. Physiol.* 76, 127 (1970).
14. S. Penman, M. Rosbash, and M. Penman, *Proc. Nat. Acad. Sci. USA* 67, 1878 (1970).
15. C. P. Stanners, *Biochem. Biophys. Res. Commun.* 24, 758 (1966).
16. S. Y. Lee, J. Mendecki, and G. Brawerman, *Proc. Nat. Acad. Sci. USA* 68, 1331 (1971).

Modified Bases of Mammalian RNA

A major difficulty in the investigation of nucleic acids is lack of characteristics by which molecules can be discriminated. Hybridization has been employed in some circumstances to compare nucleic acid sequences, but the technique is demanding and fraught with the potential for artifact. Further, the relationship between nucleotide sequence similarities and hybridization competition has not been defined for complex sequences containing modified nucleosides. Nucleic acids can be separated according to their size and shape by sucrose density gradient stabilized centrifugation. The technique has been used successfully to study kinetics of RNA synthesis and to characterize effects of inhibitors; however, resolution is limited. The low molecular-weight region of sucrose gradients, traditionally attributed to tRNA, in fact consists of a complex mixture of RNA molecules which are resolvable by acrylamide gel electrophoresis.¹ Electrophoretic mobility of polynucleotides is also dependent upon molecular size, which has inherent difficulties as a standard stemming from ubiquity of degradative enzymes which may derive either from endogenous sucrose or from contaminating microorganisms. For this reason, we have sought chemical characteristics which would distinguish nucleic acids from one another. Our efforts have led to elucidation of structure of three previously unknown nucleosides. Two of these appear to be uniquely localized in specific RNA types, and the third is a hypermodified nucleoside of the type known to be confined to the anticodon region of tRNA.²

One of the newly discovered nucleosides belongs to the class of minor bases having a quaternary ring nitrogen. These are characterized by a basic dissociation constant near neutral pH; therefore, they bear a positive charge under physiological conditions. We were first alerted to the presence of quaternary nucleotides in RNA during our preliminary investigations of the nature of species of RNA, low molecular-weight, methylated RNA (LMM-RNA), with sizes intermediate between tRNA and 18S ribosomal RNA. Some of these RNAs contained methylated nucleosides; therefore, to prove that they were not breakdown products of rRNA or tRNA precursors, we employed DEAE-urea column chromatography of their alkaline degradation products. Our earlier studies had shown that rRNA gave a different methyl distribution pattern from tRNA by this procedure. The patterns given by the LMM-RNAs were totally unlike distributions given by either tRNA or rRNA. A large fraction of the methyl label was not adsorbed by the column and behaved in a manner expected for the non-phosphorylated nucleoside at the 3'-end of a polynucleotide chain. We now know that this unadsorbed material is a degradation product derived from internally located quaternary nucleotides which undergo an alkali catalyzed opening of the purine ring, followed by loss of the phosphate group which is responsible for adsorption to DEAE-cellulose. The quaternary nucleoside found in LMM-RNA was identified as N²,N²,7-trimethylguanosine, and we have shown that this hitherto unknown nucleoside is present in three of the isolated LMM-RNA species.³ None of the other known methylated RNAs contains this nucleoside. Therefore, we can eliminate the possibility that the LMM-RNAs are artifactually derived. Thus, excluding the possibility that a class of RNA which is not extractable by our phenol procedure (e.g., the chromosomal-RNA of Bonner *et al.*⁴) also contains trimethylguanosine, the three LMM-RNAs appear to be the sole RNAs so modified.

Our studies with trimethylguanosine led to development of a simple chromatographic system for separation of the quaternary nucleosides of RNA. Figure 1 shows a pattern representative of total RNA. The column packing is phosphocellulose which has been equilibrated with buffer at pH 7.0. All of the common nucleosides and most of the modified

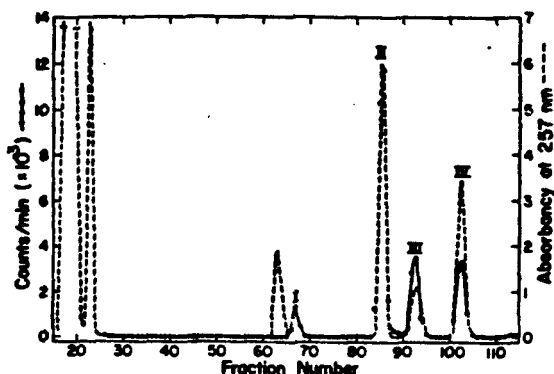


FIG. 1. Methylated quaternary nucleosides present in 2S to 10S RNA. The sample was prepared from cells labeled overnight with (^3H -methyl)methionine, purified by sucrose gradient centrifugation, digested with snake venom and alkaline phosphatase, and chromatographed on phosphocellulose at pH 7.0, as described previously.¹ Absorbancy from left to right is due to a digest of yeast nucleic acid added as a marker for emergence of nonadsorbed nucleosides and, commencing at fraction 62, added synthetic nucleosides 7-methylinosine, 1-methyladenosine, 3-methylcytidine, and 7-methylguanosine. Roman numerals refer to labeled nucleosides present in Chinese hamster RNA. The structures of the nucleosides are shown in Fig. 2.

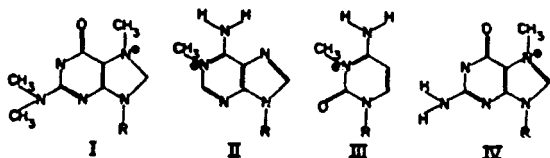


FIG. 2. Structures of the quaternary nucleosides present in Chinese hamster RNA. The compounds are (I) $\text{N}^2, \text{N}^2, 7$ -trimethylguanosine, (II) 1-methyladenosine, (III) 3-methylcytidine, and (IV) 7-methylguanosine. R represents ribose.

nucleosides are uncharged at pH 7.0 and, because they have no affinity for the column, elute in the first 25 fractions which we refer to as the void volume. The radioactive quaternary nucleosides found in Chinese hamster RNA are (I) $\text{N}^2, \text{N}^2, 7$ -trimethylguanosine, (II) 1-methyladenosine, (III) 3-methylcytidine, and (IV) 7-methylguanosine. Their structures are shown in Fig. 2. These four quaternary nucleosides appear to be the only ones present in RNA isolated from Chinese hamster cells by phenol extraction. We have not excluded the possibility that other quaternary nucleosides, which are too labile to survive our conditions of preparation or which are present in RNAs which are not extracted by our protocol, exist in Chinese hamster

RNA. Examination of separated 18S and 28S ribosomal RNAs has produced the results presented in Figs. 3 and 4. The 18S RNA contains mainly 7-methylguanosine, and the 28S RNA contains mainly 1-methyladenosine. The quaternary nucleosides are somewhat unstable, making the yields shown in Figs. 3 and 4 low. We have rerun the isolated quaternary nucleosides on phosphocellulose after subjecting them to manipulations mimicking those received by a typical RNA preparation following isolation.

The fraction of the nucleoside which adsorbed to phosphocellulose following such treatment was taken to represent the initial recovery. Values obtained were 71 percent for 1-methyladenosine, 90 percent for 3-methylcytidine, and 53 percent for 7-methylguanosine. These recoveries have been used

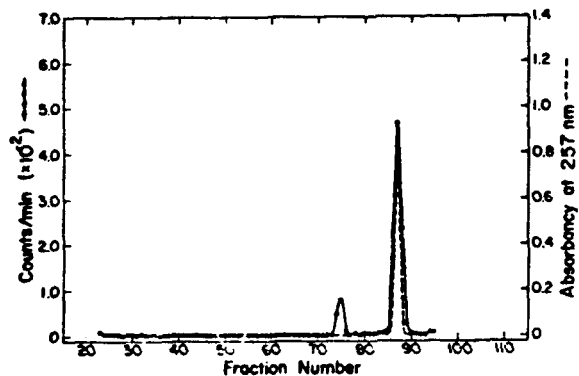


FIG. 3. Methylated quaternary nucleosides present in 18S RNA. The sample was taken from a sucrose gradient and run as described. Addition of 7-methylguanosine, a synthetically prepared nucleoside, is responsible for absorbancy.

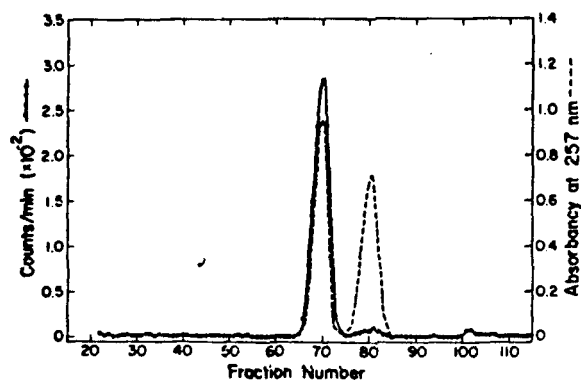


FIG. 4. Methylated quaternary nucleosides present in 28S RNA. The sample was taken from a sucrose gradient and chromatographed as described. Addition of synthetically prepared nucleosides 1-methyladenosine and 7-methylguanosine was responsible for absorbancy.

TABLE 1. RELATIVE ABUNDANCE OF METHYL GROUPS IN QUATERNARY NUCLEOSIDES AND IN THE REMAINING METHYLATED NUCLEOSIDES OF RNA

| RNA Species | Void | Corrected counts per minute | | | |
|-------------|-------------------|-----------------------------|---------------|------|---------------|
| | | TMG ^a | 1 MA | 3 MC | 7 MG |
| 18S | 301,729 (54.6) | — | 582 (0.11) | — | 5530 (1.0) |
| 28S | 472,680 (78.9) | — | 5966 (1.0) | — | 432 (0.07) |
| LMM IV | 13,650 | 2257 | — | — | — |
| LMM VII | 13,896 | 2894 | — | — | — |
| tRNA | 208,027 | — | 39,911 | 6326 | 23,797 |

^aTMG data have not been corrected, since we have not accumulated sufficient sample with which to obtain a recovery factor. Making the assumption that recovery is 50 percent (i.e., about the same as recovery for 7 MG), then we can calculate the total number of methyls per molecule in the same manner employed for ribosomal RNAs. LMM RNA IV would have 10 or 11 methyls per molecule and LMM VII 9 total methyls.

to correct the data presented in Table 1. This table was constructed from column chromatographic data such as that shown in Fig. 1 and Figs. 3-6. The numbers in parentheses are the calculated number of methyls attributed to each of the species, assuming that the quaternary nucleoside present in highest amount is represented once. The assumption appears to be correct, since independent estimates of total number of methyls per molecule are 55 per 18S and 85 per 28S. If one assumes that the ribosomal RNAs represent homogeneous molecules, then data in Table 1 indicate that each ribosomal species has a distinct quaternary nucleoside and that each has a single molecule of that nucleoside. The assumption of homogeneity appears to be valid for the small ribosomal RNA of *Escherichia coli* which Felner *et al.* have sequenced.⁵ They have shown that the *E. coli* species also has a single residue of 7-methylguanosine per molecule. Furthermore, although all of the remaining methylated species are clustered in the first third of the molecule from the 3'-end, the 7-methylguanosine is located very near the middle of the molecule.⁵

Figures 5 and 6 show quaternary nucleoside distribution of our isolated LMM species IV and an electrophoretically purified fraction enriched for tRNA. The figures demonstrate the absence of

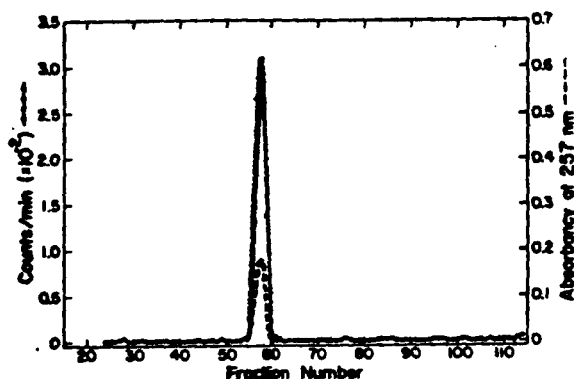


FIG. 5. Methylated quaternary nucleosides present in LMM species IV. RNA was isolated by preparative acrylamide gel electrophoresis and digested and chromatographed as described. Addition of synthetically prepared nucleoside N²,N²,7-trimethylguanosine was responsible for absorbancy.

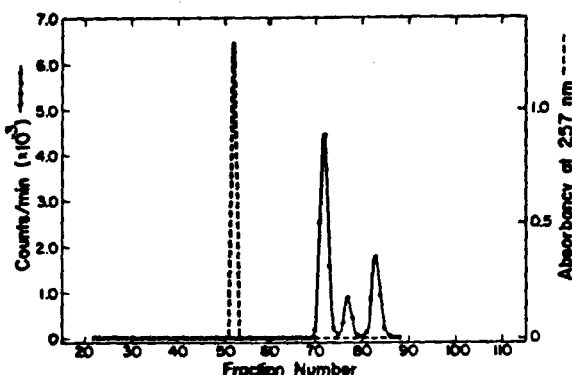


FIG. 6. Methylated quaternary nucleosides present in 4S RNA. RNA was isolated by preparative acrylamide gel electrophoresis. This fraction comprises the bulk of RNA present in the 2S to 10S region of sucrose gradients obtained from whole cells and was shown to have amino acid acceptance activity. Addition of synthetically prepared nucleoside 7-methylinosine is responsible for absorbancy.

trimethylguanosine in tRNA and its exclusive presence in species IV. LMM species VI and VII give patterns very similar to that shown for species IV.

The second class of nucleosides we have discovered is found in 18S ribosomal RNA and in an electrophoretic fraction which contains tRNA. These nucleosides are characterized by their content of an α -aminobutyrate residue which is derived from methionine probably via the agency of S-adenosyl-methionine, generally recognized as the active methyl donor. The presence of this class of nucleosides in RNA is demonstrated readily by allowing cells to incorporate methionine labeled in either the 1, 2, or 1,2,3 and 4 carbons.⁶ An illustrative sucrose gradient of RNA isolated from cells labeled

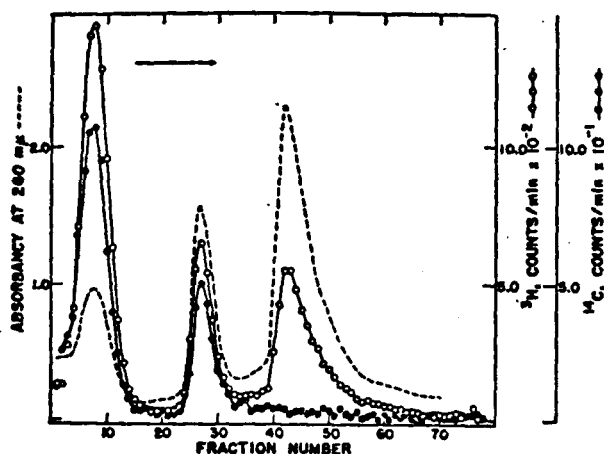


FIG. 7. Incorporation of (^3H -methyl)methionine and (^{14}C -methyl)methionine into total RNA of Chinese hamster cells. Isolated RNA was centrifuged in a sucrose gradient (arrow shows the direction of sedimentation).

with (^{14}C -methyl)methionine is shown in Fig. 7. The complete absence of (^{14}C -methyl)methionine label from 28S RNA excludes the possibility that labeling results from indiscriminate incorporation into purine or pyrimidine bases. We have made structural assignments of the nucleosides on the basis of (a) examination of incorporation of isotopic label from precursors, (b) degradation with anhydrous hydrazine and comparison of the products with synthetic material or with the hydrazinolysis products of known uridines, and (c) comparison of the unknowns as their hydantoin derivatives with the 5- β -(bromoethyl)hydantoin alkylation products of uridine and of 1- and 3-methylpseudouridine. The 4S unknown is heterogeneous. We identify one of the constituents as 3- γ -(α -amino- α -carboxypropyl)-uridine. Another of the 4S unknowns appears to give rise to the above substance after hydrolysis with 1 N HCl at 100°C ; therefore, it may be an amino-substituted derivative of that compound. A third labeled product is also present, which we have not yet attempted to characterize. We note that Nakanishi's structural assignment of the "Y" base,⁷ which is known to be located in the 3'-position to the anticodon region of phenylalanine tRNAs of higher organisms, has a derivatized α -aminobutyrate residue attached to the 10 position. We suggest the possibility that this residue is also derived from methionine and that our unidentified material may, in fact, be the "Y" base or its derivative. We further speculate that, although all known hypermodified bases adjacent to the anticodon are purine

derivatives, our aminobutyrate derivatized uridine may represent a related species of hypermodified pyrimidine and may serve a related function in Chinese hamster cells. Tentatively, we identify the unknown isolated from 18S ribosomal RNA as 1-methyl-3- γ -(α -amino- α -carboxypropyl)pseudouridine. The nature of our uncertainty in assignment is the relative position of the methyl and α -amino- α -carboxypropyl groups. There is a single molecule of this nucleoside in the 18S molecule.

REFERENCES

1. W. F. Zepisek, A. G. Saponara, and M. D. Enger, *Biochemistry* **8**, 1170 (1969).
2. R. H. Hall, In: "The Modified Nucleosides in Nucleic Acids," Columbia University Press, New York and London (1971), p. 318.
3. A. G. Saponara and M. D. Enger, *Nature* **223**, 1365 (1969).
4. D. S. Holmes, J. E. Mayfield, G. Saunder, and J. Bonner, *Science* **177**, 72 (1972).
5. P. Felner, C. Ehresmann, P. Stiegler, and J. P. Ebel, *Nature New Biology* **239**, 1 (1972).
6. M. D. Enger and A. G. Saponara, *J. Mol. Biol.* **33**, 319 (1968).
7. K. Nakanishi, N. Furutachi, D. Grunberger, and I. B. Weinstein, *J. Amer. Chem. Soc.* **92**, 7617 (1970).

Response of Histone Metabolism to X-Irradiation

Because of the involvement of histones in control of chromosome structure and genetic expression,¹ it is particularly important that we understand the radiosensitivity of these proteins. The normal biochemistry of histones in cultured Chinese hamster cells has been investigated extensively in this Laboratory.²⁻⁶ By integrating information obtained from this program with knowledge of the Chinese hamster cell cycle⁷⁻¹⁰ and radiobiology¹¹⁻¹⁷ previously described in this Laboratory, an investigation of the radiosensitive nature of histone metabolism was initiated.^{18,19}

Abnormal Accumulation of Histone f3 following X-irradiation.--We have shown previously that biologically significant doses of X-irradiation (800 rads) will result in an abnormally high accumulation of protein in the histone f3 fraction of chromatin.¹⁸ However, whether this abnormal excess of protein in

chromatin resulted from an increase in histone f3 per se or from an increase in some contaminant in the f3 preparations following irradiation remains to be answered. We have irradiated cells prelabeled with ^{14}C -amino acids and subjected their histones to purification by preparative electrophoresis (as shown in Fig. 1) and have demonstrated that at 10 hr following 800 rads (X-irradiation) the chromatin of irradiated cells contained 77 percent excess ^{14}C -labeled pure f3 (Table 1), in agreement with previous studies from this Laboratory.¹⁹ The loss of a small amount of prelabeled f1 (Table 1) during the 10-hr period after irradiation was the result of f1 turnover. Moderate increase in ^{14}C -f2b, ^{14}C -f2a1, and ^{14}C -f2a2 (Table 1) suggested that some reutilization of ^{14}C -amino acids occurred during the 10-hr post-irradiation period. Further experimentation revealed that half of post-irradiation ^{14}C -f3 accumulation resulted from reutilization of ^{14}C -amino acids and that the other half was from accumulation of presynthesized ^{14}C -f3 derived from

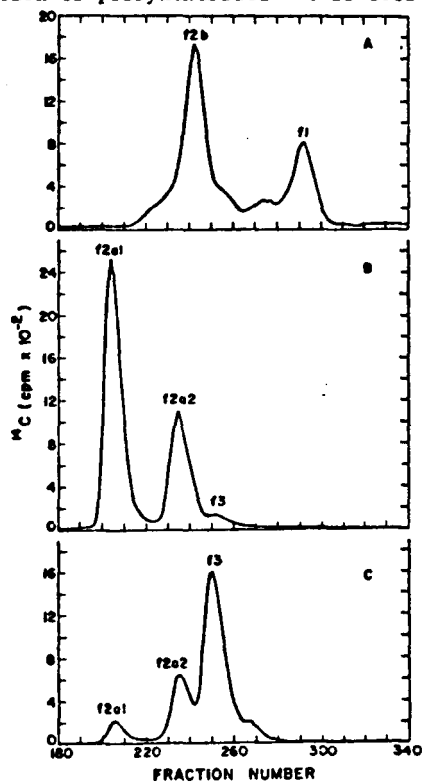


FIG. 1. Preparative electrophoresis of histones extracted from Chinese hamster cells as described by Gurley and Hardin:² (A) electrophoresis of a mixture of f1 and f2b; (B) electrophoresis of the f2a complex; and (C) electrophoresis of histone f3 prepared in the presence of 0.14 M 2-mercaptoethanol to prevent dimerization of f3.

TABLE 1. RECOVERY OF PRELABELED HISTONES BY PREPARATIVE ELECTROPHORESIS FOLLOWING X-IRRADIATION

| Histone fraction | Total ^{14}C recovered (cpm) ^a | | % Change |
|------------------|----------------------------------------------------|---------------------------------|----------|
| | Unirradiated culture (0 hr) | Post irradiated culture (10 hr) | |
| f1 | 11,510 | 10,811 | - 6.1 |
| f2b | 24,169 | 27,116 | + 12.2 |
| f2a1 | 20,774 | 25,514 | + 22.8 |
| f2a2 | 14,982 | 18,426 | + 23.0 |
| f3 | 12,426 | 22,025 | + 77.2 |

^aThe total ^{14}C counts per minute (cpm) in each electrophoretic peak shown in Fig. 1 were summed and tabulated. The total cpm recovered for each purified histone fraction was then obtained.

some nonchromatin source, where it was stored prior to irradiation (Fig. 2). Additional experiments will be necessary to determine if a relationship exists between excess histone f3 on chromatin and X-ray-induced division delay or the eventual death of these cells which occurs 2 to 3 generations after irradiation.¹⁷

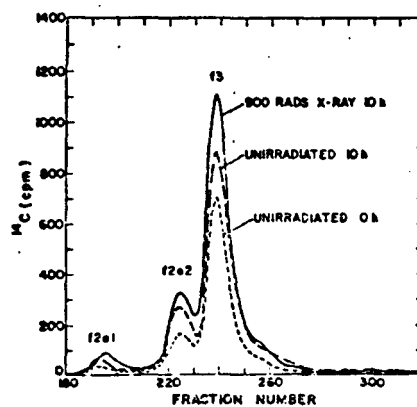


FIG. 2. Accumulation of prelabeled histone f3 in chromatin following X-irradiation. Chinese hamster cells were labeled with ^{14}C -amino acids and then resuspended into three cultures containing no carbon-14. One culture was irradiated with 800 rads and harvested 10 hr after irradiation (—); one unirradiated culture was harvested 10 hr after irradiation (---); and one unirradiated culture was harvested immediately as a zero-time control (----). Histone f3 was isolated and subjected to purification by preparative electrophoresis. Reutilization of ^{14}C -amino acids during the 10-hr post-irradiation period is indicated by the increased recovery of carbon-14 in the 10-hr unirradiated culture over the zero-time control.

Reduction of X-Ray Effects with Caffeine.--One of the first observable effects of X-irradiation on cultured Chinese hamster cells is the cessation of cell division. Correlating this phenomenon with specific biochemical events has been a primary objective of this Laboratory.¹¹⁻¹⁷ Recently we have shown that one of the early biochemical events occurring as a result of X-irradiation is a reduction of histone f1 phosphorylation.¹⁹ This radiosensitive phosphorylation is specific for histone f1 and does not occur in other phosphorylated histones. Experiments with caffeine suggest that X-ray-induced reduction of f1 phosphorylation may be directly coupled with X-ray-induced division delay. Treatment of X-irradiated cultures with caffeine shortened the division delay period to half that of untreated X-irradiated cultures (Fig. 3). Histone phosphorylation was measured by incorporating [³²P]-phosphate into cellular proteins for 1 hr following irradiation and treatment with caffeine. We extracted histones from these cells and fractionated them on a preparative electrophoresis column (Fig. 4)

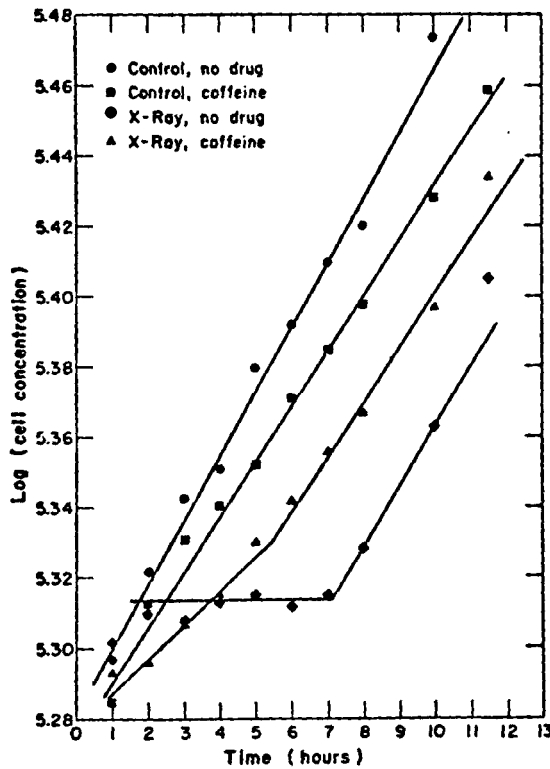


FIG. 3. Effect of caffeine on X-ray-induced division delay. Cultures were treated with 400 rads of X-irradiation and/or 2 mM caffeine at zero time. (○) control, no drug; (●) control, caffeine; (◇) X-irradiation, no drug; (△) X-irradiation, caffeine.

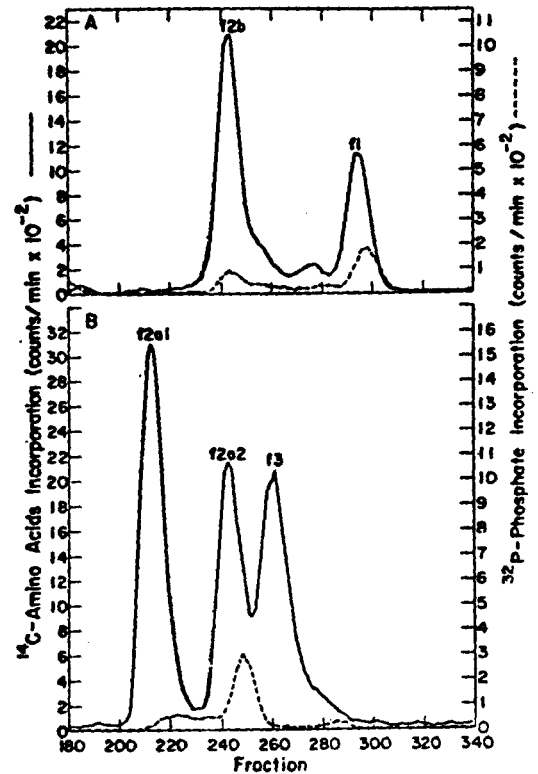


FIG. 4. Preparative electrophoresis of phosphorylated histones extracted from Chinese hamster cells. Cells were labeled for two generations with ¹⁴C-protein hydrolysate and then pulse-labeled with H₃³²PO₄ for 1 hr. Carbon-14 and phosphorus-32 were counted simultaneously in two channels on a liquid scintillation spectrometer. (A) Electrophoresis of the lysine-rich histones f1 and f2b; and (B) electrophoresis of the arginine-rich histones f2a1, f2a2, and f3. The arginine-rich histones were prepared in the presence of 0.14 M 2-mercaptoethanol to prevent dimerization of f3.

and found that caffeine also prevented X-ray-induced reduction of histone f1 phosphorylation by an amount similar to amelioration of division delay (Table 2). These data suggest that radiosensitive phosphorylation of histone f1 may be required for cell division and that, by restoring f1 phosphorylation, one can alleviate X-ray-induced division delay. Caffeine is thought to exert its action by inhibiting the phosphodiesterase which breaks down cyclic AMP,²⁰ thus causing an increase in cyclic AMP available to histone kinase which specifically phosphorylates histone f1.²¹ In turn, increased histone kinase activity would increase the degree of f1 phosphorylation and thus reduce division delay. Further investigations are being made to test this hypothesis.

TABLE 2. EFFECT OF CAFFEINE AND X-IRRADIATION ON HISTONE PHOSPHORYLATION^a

| Histone fraction | Culture treatment | ³² P/ ¹⁴ C | Unirradiated control (%) |
|------------------|----------------------------|----------------------------------|--------------------------|
| f1 | None | 0.226 | 100.00 |
| f1 | X-irradiation | 0.132 | 58.4 |
| f1 | Caffeine | 0.282 | 100.0 |
| f1 | Caffeine and X-irradiation | 0.223 | 79.1 |
| f2a2 | None | 0.176 | 100.0 |
| f2a2 | X-irradiation | 0.187 | 106.2 |
| f2a2 | Caffeine | 0.172 | 100.0 |
| f2a2 | Caffeine and X-irradiation | 0.172 | 97.7 |

^aChinese hamster cultures were prelabeled for two generations with 50 μ Ci of ¹⁴C-protein hydrolysate per liter culture to label their proteins uniformly. Cultures to be treated were X-irradiated with 800 rads¹¹ and/or subjected to 2 mM caffeine. Immediately after treatment, 20 mCi of H₃³²PO₄ was added per liter culture. After 1 hr in ³²P, the cells were harvested and histones extracted.² The histones were fractionated by preparative electrophoresis (Fig. 4). The total ¹⁴C and ³²P counts per minute (cpm) in the two major phosphorylated histones (f1 and f2a2) were summed. Phosphorylation rate was expressed as the ratio of 1-hr ³²P incorporation to 34-hr ¹⁴C incorporation.

Synthesis of Histones during the G₁-Phase of the Mammalian Life Cycle.—Experiments in this Laboratory indicate that cells, when released synchronously from an isoleucine-deficient state into the G₁ phase of the life cycle and then irradiated, show a significantly reduced division delay as compared with that observed in cells irradiated at similar times in the cell cycle after synchronization by mitotic selection. Because of the possible involvement of histones in X-ray-induced division delay, we started an investigation of histone metabolism in the G₁ phase to establish a foundation for future investigations into the mechanisms involved in reduction of X-ray-induced division delay by isoleucine deficiency.

When cells were synchronized in isoleucine-deficient G₁-arrest, the rate of histone synthesis was reduced, as expected, but not to zero (Fig. 5A). A small but detectable amount of synthesis continued for up to 50 hr in the absence of DNA synthesis (Fig. 6A) and without an increase in histone mass (Fig. 5B). This continuing histone synthesis was the result of histone turnover in the chromatin

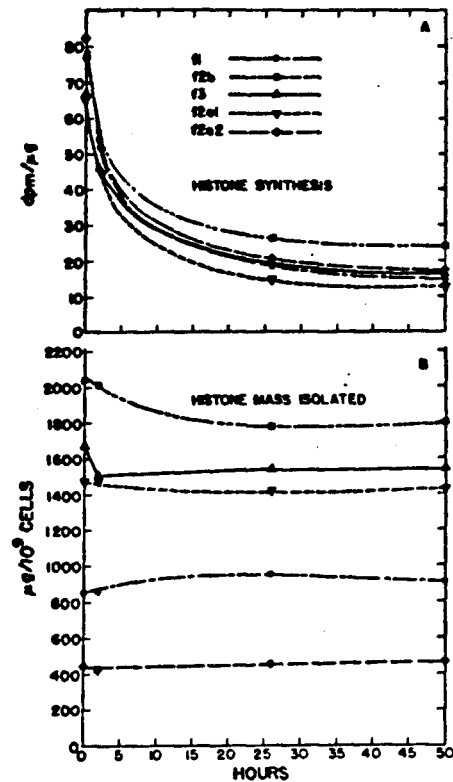


FIG. 5. Synthesis of histone fractions following resuspension of cells in isoleucine-deficient medium: (A) specific activity of histone fractions following a 2-hr pulse with ¹⁴C-protein labeling mixture containing no isoleucine; and (B) mass per cell of each histone fraction recovered in the isolation procedure.

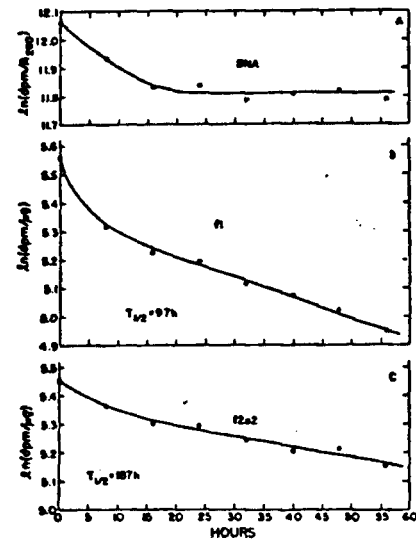


FIG. 6. Turnover of prelabeled DNA (A), histone f1 (B), and histone f2a2 (C) following resuspension of cells in isoleucine-deficient medium. DNA was prelabeled with [³H]-thymidine and histones with [¹⁴C]amino acid mixture. T_{1/2} is the half-life of the loss of ¹⁴C-prelabeled histone from the chromatin from 16 to 56 hr.

(Fig. 6B and C). When the various turnover rates were measured, we found that histone f1 had the fastest rate of turnover in cells arrested in G_1 (Table 3). This turnover rate is only slightly less than that previously measured for f1 in exponential cultures.^{3,4} Because DNA synthesis is completely turned off under these conditions, normal turnover of histone f1 apparently is not coupled in any obligatory way to DNA synthesis. This complements and confirms conclusions drawn from X-ray studies in which we observed that f1 turnover could be stopped by X-irradiation without stopping DNA replication.¹⁹

Loss of pre-labeled histone with no loss of pre-labeled DNA in G_1 -arrested cells (Fig. 6) indicates that the DNA-histone complex is not a static association *in vivo* but, rather, in equilibrium with its component parts. Therefore, when histone synthesis occurs in the absence of DNA synthesis, these newly synthesized histones can exchange with chromatin-bound histones. This interpretation agrees with conclusions we have reached after measuring significant histone turnover in cultures whose DNA synthesis was blocked by high concentrations of thymidine.^{3,4}

A comparison was made of histone synthesis rate in cells arrested in G_1 by isoleucine deficiency and cells actively traversing the G_1 phase following mitotic selection (Fig. 7). The rate of histone synthesis in G_1 -arrested cells was estimated to be only 2 percent of that of an S-phase cell.

TABLE 3. TURNOVER RATES OF HISTONE FRACTIONS DURING ISOLEUCINE-DEFICIENT G_1 -ARREST

| Histone fraction | ¹⁴ C-prelabeled histone half-life ^a (hr) |
|------------------|-------------------------------------------------------------------|
| f1 | 97 |
| f2b | 127 |
| f2a1 | 140 |
| f2a2 | 187 |
| f3 | 145 |

^aCells were labeled with ¹⁴C-amino acids for 2 days to prelabel their proteins. The cells were then resuspended in isoleucine-deficient medium without ¹⁴C-amino acids and allowed to enter G_1 -arrest. Turnover rates were measured for loss of ¹⁴C-prelabeled histone from the chromatin during the period 16 to 56 hr in isoleucine-deficient medium (as shown in Fig. 6).

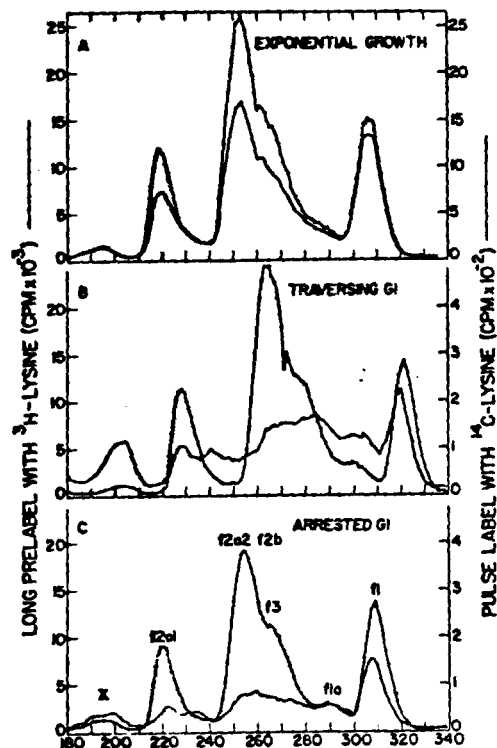


FIG. 7. Preparative electrophoresis of whole histones pre-labeled with [³H]lysine and pulse-labeled for 2 hr with [¹⁴C]lysine. Histones were isolated from cells in exponential growth (A), cells traversing G_1 pulsed from 1 to 3 hr following synchronization by mitotic selection (B), and cells arrested in G_1 pulsed from 34 to 36 hr following resuspension in isoleucine-deficient medium (C).

In G_1 cells traversing the life cycle, we could detect a synthesis rate of only 3.5 to 5.0 percent of an S-phase cell (Table 4). Therefore, we conclude that the high rate of histone synthesis during thymidine blockade observed in many different laboratories represents S-phase histone synthesis even though DNA synthesis cannot proceed because of feedback inhibition of deoxycytidine phosphate synthesis. The low rate of histone synthesis in arrested G_1 cells and in normal traversing G_1 cells further characterizes the isoleucine-deficient synchronized cells as truly G_1 in nature.

Phosphorylation of Histone Fractions during the Cell Cycle.--Radiation experiments in this Laboratory show that histone f1 phosphorylation is radio-sensitive, while histone f2a2 phosphorylation is not.¹⁹ As a result, we conclude that phosphorylation of these two proteins is related to two different functions *in vivo*. By relating histone phosphorylation to cell-cycle position, we have added

TABLE 4. ANALYSIS OF RADIOACTIVITY IN DOUBLE-LABELED HISTONE FRACTIONS PREPARED BY PREPARATIVE ELECTROPHORESIS^a

| Histone fraction | ¹⁴ C Pulse-label (cpm) | ¹⁴ C Pulse (% of exponential growth) | Theoretical S phase ^b ¹⁴ C pulse (cpm) | ¹⁴ C Pulse (% of S phase) |
|---------------------------------|-----------------------------------|-------------------------------------------------|--------------------------------------------------------------|--------------------------------------|
| <u>Exponential growth</u> | | | | |
| f2a1 | 11,941 | — | 46,331 | — |
| f2a2 + f2b | 22,302 | — | 86,532 | — |
| f3 | 15,347 | — | 59,546 | — |
| f1 | 18,219 | — | 70,690 | — |
| <u>Traversing G₁</u> | | | | |
| f2a1 | 2,478 | 20.6 | | 5.3 |
| f2a2 + f2b | 3,036 | 13.6 | | 3.5 |
| f3 | 2,479 | 19.4 | | 5.0 |
| f1 | 2,707 | 14.9 | | 3.8 |
| <u>Arrested G₁</u> | | | | |
| f2a1 | 1,069 | 9.1 | | 2.3 |
| f2a2 + f2b | 1,429 | 6.4 | | 1.7 |
| f3 | 1,263 | 8.2 | | 2.1 |
| f1 | 1,873 | 10.3 | | 2.6 |

^aTaken from Fig. 7.

^bAssuming an exponential culture contains 25.8 percent of its population in S phase, a culture containing all S-phase cells should incorporate 3.88 times the ¹⁴C-lysine of the exponential culture.

more support to this conclusion. When histone phosphorylation was measured in cells arrested in G₁ by isoleucine deficiency, we found that histone f1 phosphorylation was essentially non-existent (see Fig. 8A). However, histone f2a2 was actively phosphorylated in G₁-arrest (Fig. 8B). When these cells were released from G₁-arrest and allowed to traverse the cell cycle, their histone f1 phosphorylation remained inactive (Fig. 9A), while histone f2a2 phosphorylation continued active (Fig. 9B). However, when these cells enter the S phase, histone f1 phosphorylation became active (Fig. 10A), and histone f2a1 phosphorylation remained active in the S phase (Fig. 10B). These experiments demonstrate that histone f1 phosphorylation is cell-cycle dependent, not occurring in G₁ but rather in S, while histone f2a2 phosphorylation is cell-cycle independent, occurring at all times measured. We can analyze these observations in relation to knowledge acquired in this Laboratory on the Chinese hamster cell line^{2-6,8-10,18,19} and draw several conclusions:

(1) Histone f2a2 phosphorylation is

independent of f2a2 synthesis, occurring at equal rates in G₁ phase when f2a2 synthesis is extremely low and also occurring in S phase when f2a2 synthesis is active.

(2) Histone f2a2 phosphorylation is independent of histone f1 phosphorylation in synchronized cells and in X-irradiated cells.

(3) Histone f2a2 phosphorylation is independent of DNA synthesis, occurring at equal rates in G₁ phase when DNA synthesis is extremely low and also in S phase when DNA synthesis is active.

(4) Histone f1 phosphorylation is an S-phase phenomenon but is not directly involved in either DNA replication or f1 synthesis because f1 phosphorylation is inhibited by X-irradiation, but neither DNA synthesis nor f1 synthesis is affected by this treatment.

(5) Histone f1 turnover does not require f1 phosphorylation, as f1 phosphorylation is absent in cells held in isoleucine-deficient G₁-arrest, a state we have shown to exhibit f1 turnover (Fig. 6).

Langan²¹ has recently presented a model for induction of RNA synthesis involving histone

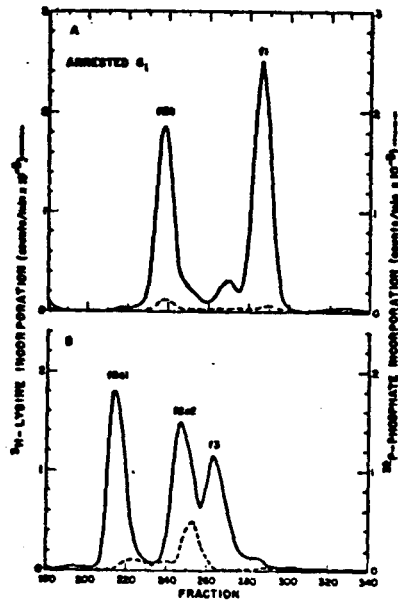


FIG. 8. Preparative electrophoresis of histones from cells arrested in the G_1 state by isoleucine deprivation. Individual lysine-rich histone fractions (A) and arginine-rich fractions (B) are indicated by the $[^3H]$ lysine long-term incorporation. The degree of phosphorylation of each fraction is indicated by the $[^{32}P]$ phosphate 1-hr pulse incorporation.

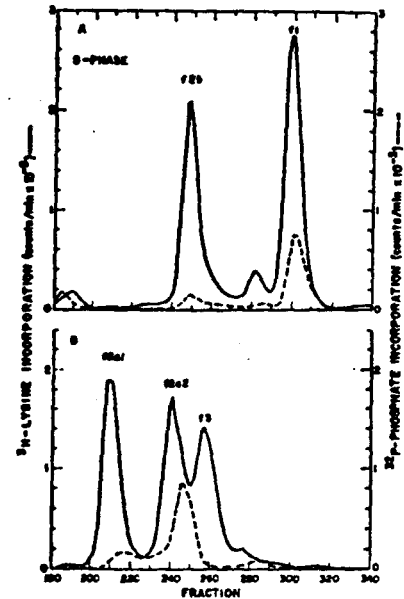


FIG. 10. Preparative electrophoresis of histones from cells traversing the S phase 10 hr following release from synchronization by the isoleucine deprivation method. The individual lysine-rich histone fractions (A) and arginine-rich histone fractions (B) are indicated by the $[^3H]$ lysine long-term incorporation. The degree of phosphorylation of each fraction is indicated by the $[^{32}P]$ phosphate 1-hr pulse incorporation.

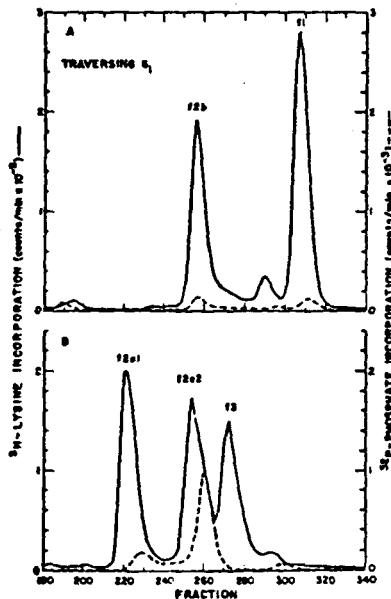


FIG. 9. Preparative electrophoresis of histones from cells traversing the G_1 phase 2 hr following release from synchronization by the isoleucine deprivation method. The individual lysine-rich histone fractions (A) and arginine-rich histone fractions (B) are indicated by the $[^3H]$ lysine long-term incorporation. The degree of phosphorylation of each fraction is indicated by the $[^{32}P]$ phosphate 1-hr pulse incorporation.

phosphorylation. In this model, interaction between DNA and histone is weakened by phosphorylation of histones, resulting in a derepression of the DNA template. We conclude from our investigations that histone f1 phosphorylation is not involved in such a control mechanism, as it does not occur in G_1 when RNA synthesis is very active. We feel that f2a2 phosphorylation, which does occur in G_1 , should continue to be considered in such models concerning activation of DNA template activity.

The S-phase-specific phosphorylation of histone f1 has led to speculations that histone f1 phosphorylation is involved in DNA replication. From studies using X-irradiation, we conclude that this is not the case.¹⁹ The caffeine amelioration of X-ray-induced division delay and X-ray-induced histone f1 phosphorylation reduction suggests that we look for an involvement of histone f1 phosphorylation in cell division.

REFERENCES

1. V. G. Allfrey, Functional and metabolic aspects of DNA-associated proteins, In: "Histones and Nucleohistones" (D. M. P. Phillips, ed.),

Plenum Press, New York (1971), pp. 241-294.

2. L. R. Gurley and J. M. Hardin, The metabolism of histone fractions. I. Synthesis of histone fractions during the life cycle of mammalian cells, *Arch. Biochem. Biophys.* 128, 285-292 (1968).
3. L. R. Gurley and J. M. Hardin, The metabolism of histone fractions. II. Conservation and turnover of histone fractions in mammalian cells, *Arch. Biochem. Biophys.* 130, 1-6 (1969).
4. L. R. Gurley and J. M. Hardin, The metabolism of histone fractions. III. Synthesis and turnover of histone f1, *Arch. Biochem. Biophys.* 136, 392-401 (1970).
5. L. R. Gurley, R. A. Walters, and M. D. Enger, Isolation and characterization of histone f1 in ribosomes, *Biochem. Biophys. Res. Commun.* 40, 428-436 (1970).
6. L. R. Gurley, R. A. Walters, and R. A. Tobey, The metabolism of histone fractions. IV. Synthesis of histones during the G₁-phase of the mammalian life cycle, *Arch. Biochem. Biophys.* 148, 633-641 (1972).
7. D. F. Petersen, E. C. Anderson, and R. A. Tobey, Mitotic cells as a source of synchronized cultures, In: "Methods in Cell Physiology," Vol. III (D. M. Prescott, ed.), Academic Press, New York (1968), pp. 347-370.
8. R. A. Tobey and K. D. Ley, Isoleucine-mediated regulation of genome replication in various mammalian cell lines, *Cancer Res.* 31, 46-51 (1971).
9. M. D. Enger and R. A. Tobey, Effects of isoleucine deficiency on nucleic acid and protein metabolism in cultured Chinese hamster cells. Continued RNA and protein synthesis in the absence of DNA synthesis, *Biochemistry* 11, 269-277 (1972).
10. R. A. Tobey, Production and characterization of mammalian cells reversibly arrested in G₁ by growth in isoleucine-deficient medium, In: "Methods in Cell Physiology," Vol. 6 (D. M. Prescott, ed.), Academic Press, New York (1973), in press.
11. R. A. Walters and D. F. Petersen, Radiosensitivity of mammalian cells. I. Timing and dose-dependence of radiation-induced division delay, *Biophys. J.* 8, 1475-1486 (1968).
12. R. A. Walters and D. F. Petersen, Radiosensitivity of mammalian cells. II. Radiation effects on macromolecular synthesis, *Biophys. J.* 8, 1487-1504 (1968).
13. R. A. Walters, B. R. Burchill, and D. F. Petersen, Radiosensitivity of mammalian cells. III. Effect of suboptimal growth temperatures on recovery from radiation-induced division delay, *Biophys. J.* 9, 1323-1328 (1969).
14. R. A. Walters and R. A. Tobey, Radiosensitivity of mammalian cells. IV. Effects of X-irradiation on the DNA synthetic period in synchronized cells, *Biophys. J.* 10, 556-562 (1970).
15. R. A. Tobey, D. F. Petersen, and R. A. Walters, Synthesis of functional proteins in X-irradiated mammalian cells, *Nature* 221, 191 (1969).
16. R. A. Tobey, J. Y. Hutson, R. A. Walters, and D. F. Petersen, Retention of functional coding properties by polyribosomes in the X-irradiated mammalian cell, *Int. J. Radiat. Biol.* 17, 487-492 (1970).
17. R. A. Walters, J. Y. Hutson, and B. R. Burchill, A new method of cloning mammalian tissue culture cells in suspension, *J. Cell. Physiol.* 76, 85-88 (1970).
18. L. R. Gurley, J. M. Hardin, and R. A. Walters, The response of histone fractions to X-irradiation in cultured Chinese hamster cells, *Biochem. Biophys. Res. Commun.* 38, 290-297 (1970).
19. L. R. Gurley and R. A. Walters, Response of histone turnover and phosphorylation to X-irradiation, *Biochemistry* 10, 1588-1593 (1971).
20. T. Posternak, Formation and metabolism of cyclic AMP, In: "Cyclic AMP" (G. A. Robinson, R. W. Butcher, and E. W. Sutherland, eds.), Academic Press, New York (1971), pp. 72-90.
21. T. A. Langan, Phosphorylation of histones *in vivo* under the control of cyclic AMP and hormones, In: "Role of Cyclic AMP in Cell Function, Advances in Biochemical Pharmacology," Vol. III (P. Greengard and E. Costa, eds.), Raven Press, New York (1970), pp. 307-323.

Detailed Analysis of Biochemical Events Associated with Mammalian DNA Replication

Regulation of mammalian cell proliferation is dependent to a large extent upon the capacity for initiation of DNA replication (that is, generally if a cell can replicate its DNA, it can also divide). Very little is known about the biochemical events in G₁ and at the G₁/S boundary that prepare a cell for replication of its genetic material, although such processes most likely play an integral role in the mechanisms which regulate DNA synthesis and cell proliferation. Part of the difficulty stems from an inability to produce sufficient quantities of pure G₁ cells synchronously preparing for cell division. We have developed a technique by which we can examine both preparative processes occurring during G₁ and boundary processes and biochemical operations coordinated with genome replication and late

interphase. In addition, a comparison is made of the perturbation introduced into cell-cycle progression capacity resulting from this and other techniques used for synchrony induction.

Large quantities (limited only by size of culture vessel) of Chinese hamster cells, line CHO, may be arrested reversibly in early G_1 by cultivation in isoleucine-deficient F-10 medium. These cells do not enter a state of gross biochemical imbalance even though biosynthetic capacities for major classes of macromolecules (except DNA) remain at high levels. Restoration of isoleucine in the arrested culture results in synchronous resumption of cell progression.¹ If hydroxyurea (10^{-3} M) is added at the time of isoleucine restoration, the previously arrested cells traverse G_1 but are unable to commence DNA synthesis,² as evidenced by the lack of labeling of DNA with 3 H-thymidine and lack of increase in relative DNA content as determined by flow microfluorometry (Fig. 1A). Upon removal of hydroxyurea after 10 hr, the cells begin synthesizing DNA almost immediately and subsequently divide in a highly synchronous fashion (Fig. 1B). Thus, cells released from isoleucine-mediated G_1 -arrest in the presence of hydroxyurea accumulate in very late G_1 , and this technique provides a unique opportunity to study events in G_1 which prepare a cell for DNA synthesis. The nearly immediate entry into S phase following hydroxyurea removal provides a second stage which can be exploited for studies of transition processes and S- and/or G_2 -correlated events.

Because such populations are subjected to two discrete biochemical insults (cultivation in isoleucine-deficient medium and exposure to hydroxyurea), questions arise regarding effects of the synchronizing protocol on capacity of the population to carry out subsequent cell-cycle operations. A technique is required that will provide a population distribution measure of a basic cycle-specific process, yielding information on capabilities of individual cells in the population. Standard biochemical measurements of biosynthetic capacities are not especially useful, as they yield only population averages rather than individual cell responses.

We have developed a technique which measures the capacity of populations to carry out cell-cycle progression subsequent to synchronization by

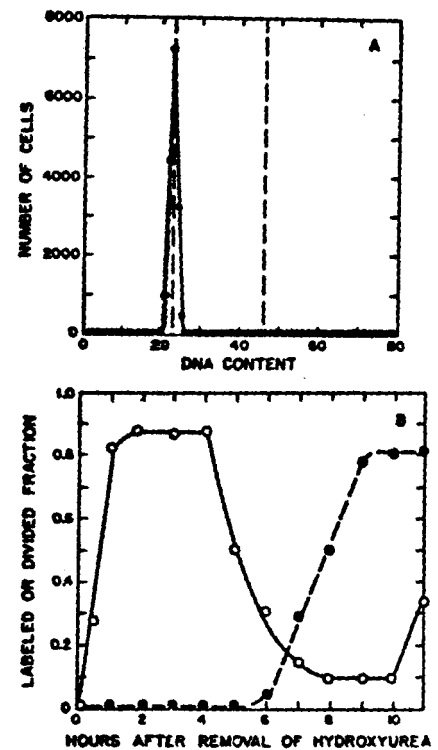


FIG. 1. Evidence for reversible accumulation of cells at the G_1/S boundary by the isoleucine deficiency/hydroxyurea technique. Chinese hamster line CHO cells cultivated for 30 hr in isoleucine-deficient F-10 medium were resuspended in fresh complete medium containing isoleucine and hydroxyurea to 10^{-3} M for 10 hr, at which time an aliquot was removed for flow microfluorometric analysis (A). Broken lines represent values for G_1 (2C) and $G_2 + M$ (4C) DNA calculated from controls. Immediately thereafter the cells were spun down, washed, and resuspended in fresh medium without hydroxyurea. At times thereafter aliquots were pulse-labeled for 15-min periods with 2 μ Ci/ml 3 H-thymidine, and autoradiographs were prepared for determination of labeled fractions (open figures). Aliquots were also removed for determination of cell number with an electronic particle counter (solid figures). Divided fractions represent $N/N_0 - 1$.

localization of cells in the cell cycle based upon relative DNA content as determined with the flow microfluorometer.³ In all cultures studied to date involving a variety of synchronizing techniques, the vast majority of cells traversed the cell cycle in a normal fashion; however, in all cultures there remained small subpopulations which, though remaining viable for several days, could not carry out normal cycle progression.

Figure 2A shows the flow microfluorometric DNA distribution pattern from a culture prepared by

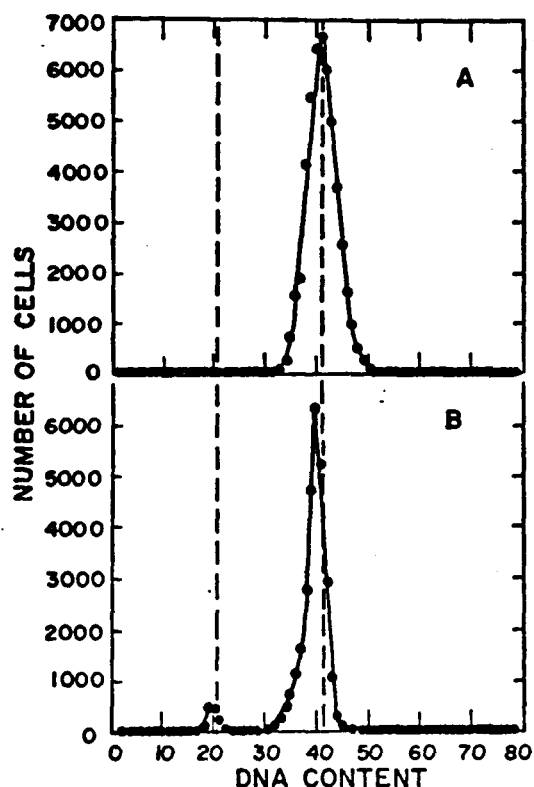


FIG. 2. DNA distribution pattern showing non-traversing fraction of cells in a culture prepared by mitotic selection. Broken lines represent values for G_1 (2C) and $G_2 + M$ (4C) DNA calculated from controls. Cells were prepared by mitotic selection with no drugs or temperature depression (DNA pattern shown in A) and were allowed to continue cell-cycle traverse in suspension culture. Colcemid was added at 9 hr (0.2 $\mu\text{g}/\text{ml}$), and an aliquot was analyzed for DNA distribution pattern at 18 hr (B).

mitotic selection. Such cells are minimally perturbed in a biochemical sense. All cells possessed the 4C DNA content expected for mitotic cells. Following selection, the cells were placed in a spinner culture to allow continued traverse of the cell cycle. After all the detached cells had escaped from mitosis and entered G_1 , colcemid was added 9 hr later to arrest normally traversing cells in mitosis and to prevent their reentering G_1 and obscuring detection of slowly or non-progressing subpopulations. Analysis of relative population DNA contents at 18 hr revealed a small subpopulation with a G_1 DNA content, clearly distinct from the bulk of the population which possessed the DNA content expected of cells arrested in mitosis. The non-traversing subfraction comprised 5.5 percent of the population, was highly reproducible, and

remained viable for at least 48 hr without entering S phase. Corresponding values for non-traversing fractions induced by a variety of synchronization techniques are shown in Table 1. It is of interest that the combination of isoleucine deficiency and hydroxyurea produced no greater perturbed fraction than isoleucine deprivation alone.

A term "traverse perturbation index" is proposed which is defined as the fraction of cells converted to a slowly or non-progressing state as the result of experimental manipulation. Determination of this value allows direct comparison of effects on cell-cycle traverse either induced by different protocols in the same cell line or induced by a common protocol in different cell lines. Based upon the data presented in Table 1, we conclude that the isoleucine deficiency/hydroxyurea treatment does not grossly perturb cell-cycle traverse capacity. This technique represents a major improvement in technique for the study of events involved with DNA replication and regulation of cell proliferation.

REFERENCES

1. M. D. Enger and R. A. Tobey, Effects of isoleucine deficiency on nucleic acid and protein metabolism in cultured Chinese hamster cells: Continued RNA and protein synthesis in the absence of DNA synthesis, *Biochemistry* 11, 269-277 (1972).
2. R. A. Tobey and H. A. Crissman, Preparation of large quantities of synchronized mammalian cells in late G_1 in the pre-DNA replicative phase of the cell cycle, *Exp. Cell Res.* (1973), in press.
3. R. A. Tobey, H. A. Crissman, and P. M. Kraemer, A method for comparing effects of different synchronizing protocols on mammalian cell-cycle traverse: The traverse perturbation index, *J. Cell Biol.* 54, 638-645 (1972).

TABLE 1. EFFECT OF DIFFERENT SYNCHRONY INDUCTION TECHNIQUES ON SUBSEQUENT CELL-CYCLE TRAVERSE CAPACITY

| Method of synchronization | Traverse Perturbation Index |
|-------------------------------------------------|-----------------------------|
| Mitotic selection | 0.055 |
| Isoleucine deficiency | 0.124 |
| Isoleucine deficiency/hydroxyurea | 0.120 |
| Isoleucine deficiency/single thymidine blockade | 0.134 |
| Double thymidine blockade | 0.170 |

SURFACE PHENOMENA AND CELLULAR INTERACTION

(P. M. Kraemer, H. A. Crissman, and M. A. Van Dilla)

Flow Microfluorometric (FMF) Studies of Lectin Binding to Mammalian Cells

Lectins such as concanavalin A (Con A) and wheat germ agglutinin (WGA) serve as useful reagents in studies of the cell surface because they bind specifically to cell-surface sugar moieties.¹ In some cases binding causes cellular agglutination, and in other cases it does not.²

Flow microfluorometry (FMF) techniques were used to quantitate cell-surface binding of fluorescein conjugated lectins (Con A-F and WGA-F) to a wide variety of cultured cell populations. These preparations included established cell lines CHO, HeLa, and L as well as euploid cell strains and tumor virus transformants. In addition, variables such as cell-cycle position, cell size, and the effects of pretreatment of the cells with enzymes were studied. The preparations were routinely monitored by fluorescence microscopy before FMF analysis to ascertain localization of binding to the cell surface.

Figure 1 illustrates the kinetics of binding of Con A-F to CHO cells. Frequency distributions of cell-surface binding, such as those illustrated in Fig. 1A, are summarized in Fig. 1B. It is evident that saturation of cell-surface sites occurred by 3 hr exposure and that modal cell-surface fluorescence, at saturation, can be used to summarize binding for any given cell population.

Figure 2 illustrates the analysis of binding of Con A-F to CHO cells synchronized by mitotic selection. When the data were analyzed to nullify the changes in cell size, we concluded that the surface density of binding sites was remarkably uniform throughout the division cycle.

Chemical heterogeneity of binding sites on each individual CHO cell was indicated by specific inhibition of Con A-F binding by α -methyl mannoside. Figure 3 illustrates saturation binding in the presence of 2-fold increases in added inhibitor. Because the active sites of Con A are homogeneous,³ if the cellular binding sites were also homogeneous, one would expect binding to decrease to one-half for each increment; this did not occur.

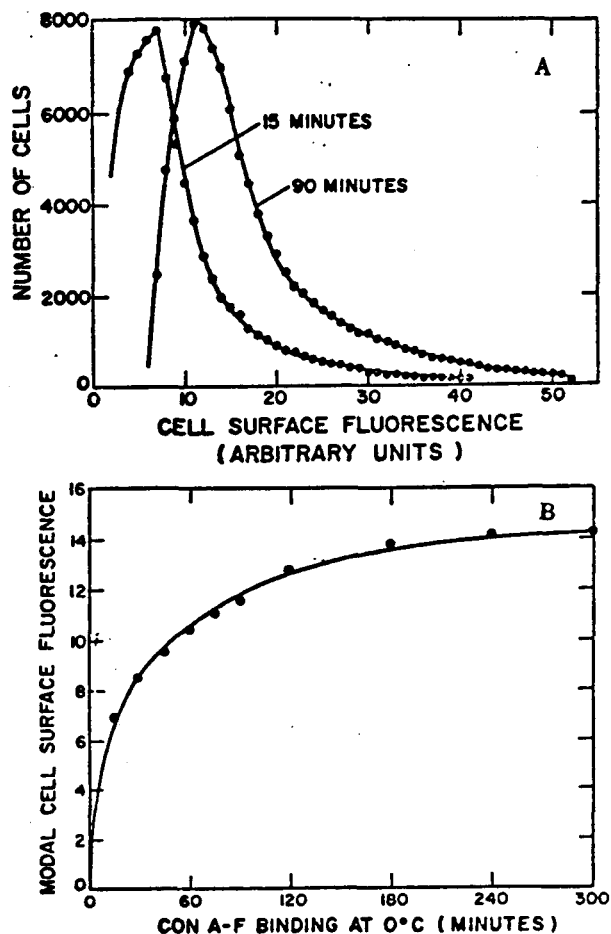


FIG. 1. Fluorescence distribution of CHO cells exposed to Con A-F at 0°C for 15 min and for 90 min (A). Modal cellular fluorescence of CHO cells exposed to Con A-F at 0°C for various times (B).

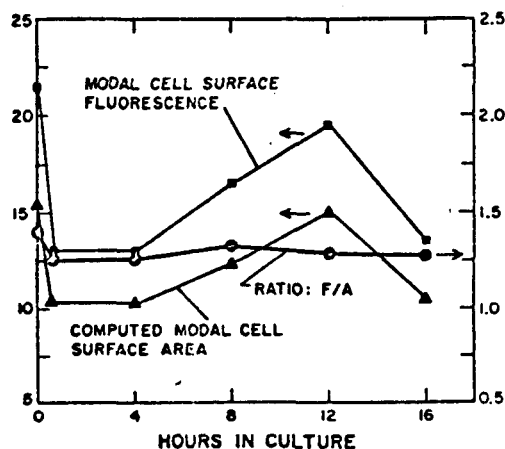


FIG. 2. Modal cell-surface fluorescence, computed modal cell-surface area, and ratio of fluorescence-to-area for CHO cells synchronized by mitotic selection and released into fresh warm medium at zero time.

In confirmation of other workers,⁴ agglutinability of virus-transformed cell lines or

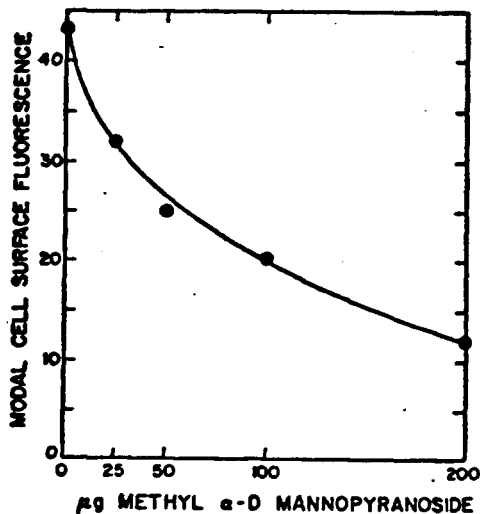


FIG. 3. Modal cellular fluorescence of CHO cells exposed to Con A-F under standard conditions but with addition of various amounts of α -methyl mannopyranoside.

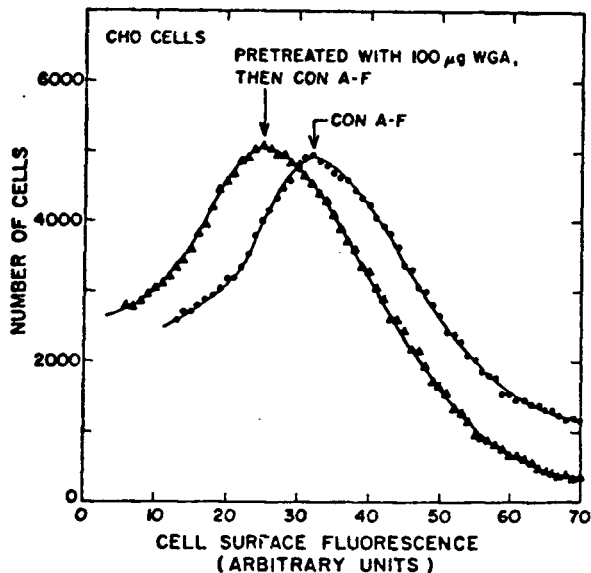


FIG. 4. Fluorescence distributions of growing CHO cells exposed to Con A-F under standard conditions, with or without prior exposure to unconjugated WGA.

trypsin-treated parental lines was demonstrated but could not be correlated with Con A-F or WGA-F binding. Ozanne and Sambrook's data⁴ on SV3T3 cells indicated that Con A and WGA sites were independent; we have come to a similar conclusion for mouse L cells. However, reciprocal inhibition was demonstrated for CHO and HeLa cells. One such experiment is illustrated in Fig. 4.

REFERENCES

1. N. Sharon and H. Lis, Lectins: Cell agglutinating and sugar specific proteins, Science

177, 949-959 (1972).

2. J. L. Wang, B. A. Cunningham, and G. M. Edelman, Unusual fragments in the subunit structure of concanavalin A, Proc. Natl. Acad. Sci. USA 68, 1130-1134 (1971).
3. L. L. So and I. J. Goldstein, Protein-carbohydrate interaction. XX. On the number of combining sites on concanavalin A, the phytohemagglutinin of the Jack bean, Biochem. Biophys. Acta 165, 398-404 (1968).
4. B. Ozanne and J. Sambrook, Binding of radioactivity labelled concanavalin A and wheat germ agglutinin to normal and virus-transformed cells, Nature New Biology 232, 156-160 (1971).

CHROMOSOME STRUCTURE AND FUNCTION

(B. J. Barnhart, C. E. Hildebrand, L. L. Deaven, R. T. Okinaka, R. A. Tobey, D. F. Petersen, S. H. Cox, and P. C. Sanders)

DNA-Membrane Associations in Cultured Chinese Hamster Cells: Nature of the DNA-Membrane Association and its Involvement in Temporal and Spatial Organization of DNA in the Nucleus

The fidelity of chromosome duplication in mammalian cells implies a large degree of organization for replication of DNA, packaging of DNA into chromatin, condensation of chromatin to form chromosomes, and segregation of chromosomes during mitosis. It is likely that well regulated temporal and spatial controls are required for these processes.

Temporal organization of DNA replication and chromosome segregation is indicated by restriction of these processes to specific parts of the cell growth (S phase) and division cycle (M). Further, temporal control of DNA replication within S phase has been documented by evidence from both cytological and biochemical studies.^{1,2} Spatial organization of DNA is implied in the finding that DNA (or chromatin) is attached to the nuclear membrane at multiple sites.³⁻¹⁶ This evidence was obtained by both biochemical and electron microscopic techniques. Results of several of these studies⁶⁻¹¹ suggested that newly replicated DNA was found predominantly in DNA-membrane complexes. On the basis of this evidence, it was concluded that DNA replication sites are attached to the nuclear membrane. More recently, several laboratories have reported findings which are at variance with this

conclusion.¹²⁻¹⁸ In view of these studies, it is unlikely that DNA-membrane attachment sites are directly involved in replication of DNA. However, the possibility that initiation of DNA replication takes place at the membrane attachment site is suggested by several of these studies.^{19,15,16} Studies of DNA-membrane complexes in cultured Chinese hamster ovary (CHO) cells have been made in an effort to examine the nature of the complexes and to investigate their functional role in the processes mentioned above.

Two independent techniques have been used to isolate and characterize DNA-membrane complexes of CHO cells. These methods include (a) the M-band procedure developed by Earhart *et al.*¹⁹ which utilizes attachment of membrane fragments to crystals of detergent, sodium lauroyl sarcosinate (sarkosyl), formed in the presence of Mg²⁺ ions, and (b) sucrose gradient sedimentation of cells or nuclei disrupted by limited sonication. Several experiments were performed to test for nonspecific attachment of free DNA or chromatin to sarkosyl crystals. In these studies unlabeled, exponentially growing CHO cells were harvested and washed by resuspension and centrifugation in TK buffer at 0°C [0.01 M Tris-Cl (pH 7.1 at 25°C), 0.1 M KCl] and lysed at a concentration of 10⁶ cells/ml in TK buffer with 0.1 percent sarkosyl. Either ³H-thymidine (TdR) labeled DNA or ³H-TdR labeled chromatin in TK buffer was mixed with the cell lysate. Sarkosyl crystals were formed by addition of 1.0 M MgCl₂ to a final concentration of 0.01 M. All operations were performed at 0°C. The sarkosyl crystals were isolated in discontinuous sucrose gradients [6 ml 20 percent sucrose (w/w) over 4 ml 47 percent sucrose (w/w) in TKM buffer (0.01 M Tris-Cl (pH 7.1 at 25°C), 0.1 M KCl, 0.01 M MgCl₂)] by centrifugation in a Spinco SW41 rotor at 15,000 rpm for 20 min in a Beckman L3-50 preparative ultracentrifuge at 4°C. Sarkosyl crystals sedimented to the 20/47 percent sucrose interface, and the gradients were fractionated from the top. Fractions were precipitated by addition of 10 percent TCA (trichloroacetic acid,) and 0.01 M sodium pyrophosphate and were assayed by filtration through Whatman GF-82 glass fiber filters. Filters were washed with 5 percent TCA and 0.01 M pyrophosphate, dried, and counted in toluene-POPOP-PPO liquid scintillation

counting fluid in a Packard liquid scintillation spectrometer. Results of these experiments are shown in Table 1. It is clear from these results that very little nonspecific aggregation of free or denatured DNA or chromatin takes place.

Subjecting the samples to shear by vortex mixing before or after crystal formation reduces the level of nonspecific attachment compared with the unsheared sample. For the control sample, whole cells or nuclei (isolated either by NP-40 treatment of whole cells or by hypotonic swelling followed by Dounce homogenization), the DNA of which was uniformly prelabeled with ³H-TdR, were carried through the sarkosyl lysis, shear, and crystallization procedures according to the preceding protocol. Shearing the samples before or after crystals are formed apparently removes DNA or chromatin not closely associated with the membrane fraction. Even after vortex mixing, 80 to 90 percent of the total membrane as assayed by ³H-choline incorporation into membranes remains with the sarkosyl crystals.

To study the macromolecular nature of the structure of the DNA membrane complex, both the M-band technique and sucrose gradient sedimentation of sonically disrupted cells or nuclei were used to determine the sensitivity of the complex to various agents. Results of the M-band analysis for these treatments are shown in Table 2. The two types of assay produced qualitatively similar results for all agents examined. In addition to

TABLE 1. NONSPECIFIC ATTACHMENT OF FREE OR DENATURED DNA OR CHROMATIN TO SARKOSYL CRYSTALS

| Sample | Total TCA-precipitable label in sarkosyl crystals (percent) | |
|-----------------------------------------------------------|-------------------------------------------------------------|------------------------|
| | No vortex mixing | Vortex mixing (20 sec) |
| Whole cells or nuclei prelabeled with ³ H-TdR | 80-95 | 10-20 |
| Unlabeled cells plus native ³ H-TdR DNA | 0.5 | 1.1 |
| Unlabeled cells plus denatured ³ H-TdR DNA | -- | 2.7 |
| Unlabeled cells plus ³ H-TdR labeled chromatin | 4.8 | 1.2 |

TABLE 2. SARKOSYL ASSAY FOR STABILITY OF DNA-MEMBRANE COMPLEXES FOLLOWING TREATMENT BY VARIOUS ENZYMES

| Treatment | $\frac{\text{DNA in sarkosyl crystals in treated sample (percent)}}{\text{DNA in sarkosyl crystals in untreated sample (percent)}} \times 100$ | |
|----------------------|------------------------------------------------------------------------------------------------------------------------------------------------|---------------------------|
| | Whole cells | NP-40 nuclei ^a |
| None ^b | 100 | 100 |
| DNase ^c | 3.3 | 0.6 |
| RNase ^d | 100 | - |
| Pronase ^e | 35 | 14 |

^aControl samples were handled exactly as treated samples except that enzyme was absent.

^bNuclei from exponentially growing cells prelabeled for 24 hr with ¹⁴C-TdR were isolated by treatment of whole cells at 5×10^6 cells/ml with the non-ionic detergent NP-40 in RSB [0.01 M Tris (pH 7.4 at 25°C), 0.010 M NaCl, 0.0015 M MgCl₂]. Nuclei were harvested by centrifugation, resuspended in TK buffer at a final concentration of 5×10^6 /ml, and quickly frozen in Dry Ice-acetone. Samples were stored at -70°C and diluted 5- to 10-fold before use.

^cSamples of sarkosyl-lysed cells or nuclei containing 0.05 M MgCl₂ were treated for 1 hr at 37°C with 40 units/ml of RNase-free DNase I. Samples were assayed for membrane-attached DNA as described in the text.

^dThe sarkosyl-lysed cell suspension in TK buffer was treated with 100 units/ml of RNase (freed of DNase by treatment at 80°C for 10 min before use) for 1 hr at 24°C and assayed as described in the text.

^eCell or nuclear lysates were digested with Pronase (60 units/ml) at 37°C for 1 hr. The samples were assayed as described in the text.

enzyme treatments, the detergent sodium dodecyl sulfate (SDS) completely dissolved the membrane-DNA complex as assayed by the sucrose gradient sedimentation method. Results of these treatments indicate considerable sensitivity of the DNA in the complex to release by DNase, Pronase, or SDS. The DNase treatment shows that no extended regions of DNA are protected from digestion by interaction with the membrane. RNase digestion has no effect indicating that RNA, although found in the complex, is not required for maintaining the structural integrity of the DNA-membrane complex.

To examine further the nature of DNA-membrane

interaction, sarkosyl-lysed cells were held at temperatures ranging from 0 to 65°C for 20 min following lysis. Samples were then chilled to 0°C and assayed for the amount of DNA remaining associated with the complex via the M-band procedure. Results of this experiment are shown in Fig. 1. Cells were uniformly labeled for several generations prior to treatment with ³H-choline and ¹⁴C-TdR so that the fate of both membrane and DNA could be followed. In Fig. 1a the percent of the TCA-precipitable membrane label is plotted relative to the percent found in the sample held at 0°C (approximately 83 percent of total membrane label), indicating that the membrane fragments isolated via the M-band procedure remain largely intact during treatments at temperatures up to 55°C. However, Fig. 1b clearly shows that a precipitous decrease in amount of DNA remaining in DNA-membrane complexes occurs over a narrow range of temperatures from 34 to 37°C. This phenomenon is indicative of a phase transition within the lipid component of the membrane which could destabilize the complex such that the DNA (or a protein mediating the DNA-membrane association) is released. Evidence for such lipid phase transitions has been reported to occur at 40 to 45°C.²⁰ Lowering of the transition temperature observed in this study could be attributed to the presence of the detergent sarkosyl.

Two experiments were performed to examine the alleged involvement in DNA replication of the

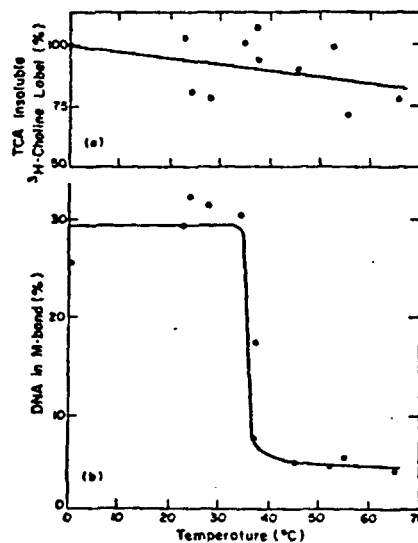


FIG. 1. Effect of temperature on stability of DNA-membrane complexes as assayed by the M-band technique.

DNA-membrane complexes isolated by the sarkosyl crystal method. First, cells prelabeled for approximately two generation times (24 to 36 hr) with ^{14}C -TdR were synchronized by mitotic selection.²¹ At 8.5 hr after cells were released from mitosis, a 2-min ^3H -TdR pulse label (20 $\mu\text{Ci}/\text{ml}$) was applied. The pulse label was stopped by pouring the aliquot over crushed frozen medium, and the cells were harvested as described above. Cell lysates were prepared and subjected to various amounts of shear by vortex mixing, and sarkosyl crystals were formed. Results of this experiment, shown in Fig. 2, show that the ratio of $^3\text{H}/^{14}\text{C}$ increases significantly as the lysates are subjected to increasing shear. We found similar results for exponentially growing cells, suggesting that some newly labeled regions of DNA are close to the site of attachment of DNA to membrane and are protected from shear degradation by the complex. If this is the case, a pulse label followed by a chase period of growth in nonradioactive medium supplemented with TdR should result in a decrease following vortex mixing of the fraction of newly labeled DNA in the membrane complex with increasing times in the "chase medium." The results of this experiment are illustrated in Fig. 3. Each sample was prepared for the sarkosyl assay with 20-sec intervals of vortex mixing. Figure 3 shows that the fraction of newly labeled DNA in the lipoprotein complex decreases with increasing "chase" times, while the fraction of ^{14}C -TdR prelabeled DNA remains approximately constant.

Results of the two experiments described are consistent with localization of some DNA replication

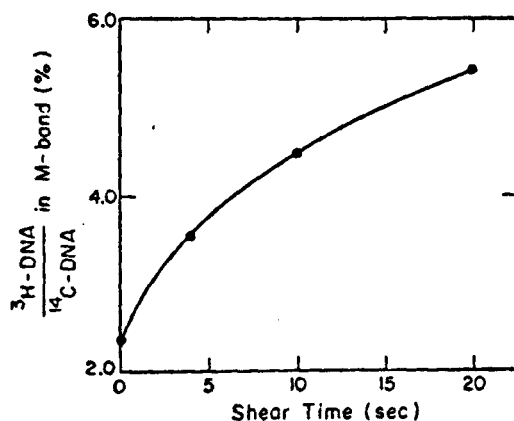


FIG. 2. Effect of shearing sarkosyl lysate for various times on the relative distribution of pulse-labeled DNA (^3H -DNA) and uniformly labeled DNA (^{14}C -DNA) between the M-band bound and the free fraction.

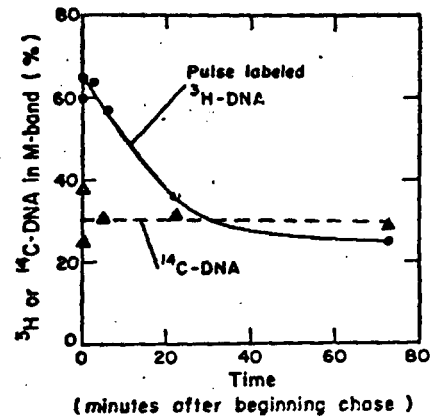


FIG. 3. Distribution of pulse-labeled DNA (^3H -DNA) and uniformly labeled DNA (^{14}C -DNA) between M-band bound and free fractions at various times during incubation of ^3H -TdR pulsed labeled cells with excess unlabeled TdR. The level of TdR in the chase medium (10^{-4} M) was not sufficient to block DNA synthesis.

sites at or near the nuclear membrane. In addition, results of the pulse-chase experiment suggest that not all DNA replication sites are associated with membrane complexes. If all replication sites were located in the complex, the amount of pulse-labeled DNA (^3H -TdT labeled DNA) remaining associated with the sarkosyl crystals after 60 min of chase would be considerably less than 50 percent of the amount found immediately after the pulse label. This observation indicates that some newly replicated DNA remains close to the membrane complex, while the replication site might continue to move away from the site of association. Such a situation could exist if DNA-membrane attachment sites are those for initiation of DNA synthesis but not for elongation.

Because of the apparent role of DNA-membrane complexes in some aspect of DNA replication (possibly initiation), experiments were performed using cultures of CHO cells synchronized by the mitotic selection procedure to determine if the amount of DNA in DNA-membrane complexes varied during the cell growth and division cycle in some way which would provide information regarding involvement of the complex in DNA replication. CHO cells were prelabeled for approximately two generation times with ^{14}C -TdR. Cells were synchronized by the mitotic selection procedure and released from mitosis at 0 hr by placing the mitotic cells in suspension culture at 37°C . The onset of the DNA

synthesis phase (S phase) of the growth cycle was measured by ^3H -TdR autoradiography (using an unlabeled population of cells) or incorporation of ^3H -TdR into TCA-insoluble material. Cell division was measured by counting aliquots of the culture with a Coulter counter; these results are plotted in Fig. 4a and 4b. Aliquots of cells were taken both before release from mitosis and at regular intervals after release and were assayed for amount of DNA in DNA-membrane complexes by the two procedures described earlier. Results of the M-band assay (shown in Fig. 4c) show that the amount of DNA closely attached to membrane increases during the latter part of the G_1 phase of the cell cycle. By comparison with parts a and b of Fig. 3, the increase in membrane-associated DNA appears to precede onset

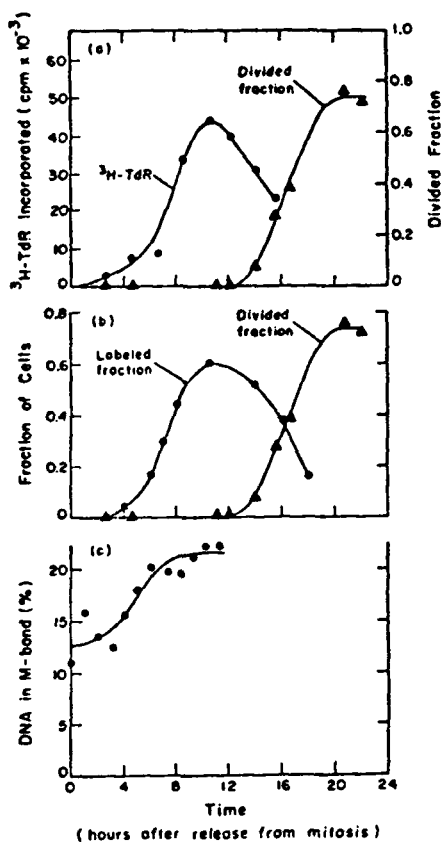


FIG. 4. Results of measurements of amount of DNA-membrane complex at various times are for mitotically synchronized cells which were released from mitosis. The quality of cell synchrony in going through S phase and cell division is shown in a and b. Aliquots of the synchronized culture were pulse-labeled with ^3H -TdR at 25 $\mu\text{Ci}/\text{ml}$ (52 Ci/mM) for 10 min at 37°C. The pulse was stopped by addition of 2 volumes of ice-cold cacodylate buffer (pH 7.1). The cells were harvested by centrifugation, and the TCA-insoluble material was measured as described in the text.

of DNA synthesis. In any case, timing of the increase in DNA complexed with membrane correlates strongly with entry of cells into the S phase of the cycle.

Similar results were found for the sucrose gradient sedimentation assay of sonicated cells or nuclei. Results of this assay for mitotic cells and S phase cells and nuclei are shown in Fig. 5. The S phase cells and nuclei clearly show a significantly greater amount of DNA complexed with membrane than mitotic cells. The fractions of material sedimenting to the 10/30 percent sucrose interface and the 30/55 percent interface have been operationally defined as DNA-membrane complexes according to the criteria described above. It should be mentioned that some variability was observed in the amount of DNA in rapidly sedimenting material in

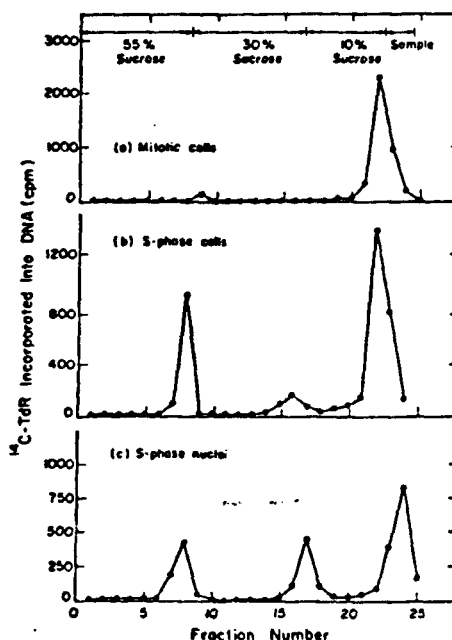


FIG. 5. Results of discontinuous sucrose gradient sedimentation analysis of mitotic cells (a) and S phase cells (b) or nuclei (c) disrupted by limited sonication. DNA-membrane complexes are found at the interfaces (10/30 and 30/55 percent) between the sucrose layers. Nuclei were prepared by hypotonic treatment of whole cells at 0°C for 15 min and by Dounce homogenization in TM buffer [0.01 M Tris (pH 7.1), 0.0005 M MgCl_2]. Washed cells or nuclei were then treated with limited sonication. Solid potassium citrate was added to a final concentration of 10 percent. Samples were layered on the sucrose gradients in the same buffer and centrifuged at 4°C for 4 hr at 33,000 rpm in a Spinco SW41 rotor using a Beckman L3-50 preparative ultracentrifuge. Fractions were collected from the bottom of the tube.

cell samples taken between 5 and 14 hr after release from mitosis. This variability can be attributed to irreproducibility of sonication conditions from sample to sample. No such variability was found in samples taken from 0 to 4 hr or from 14 to 17 hr after release from mitosis. The amount of DNA in rapidly sedimenting material was low (3 to 6 percent of total DNA) in samples taken early or late in the cell cycle, compared with a much higher level in samples taken from 5 to 13 hr (10 to 30 percent of total DNA). Hence, variability introduced by sonication would be more obvious in S phase samples where the amount of membrane-associated DNA is larger. Results of these studies suggest that the spatial arrangement of DNA within the nucleus is regulated by association of specific regions of DNA with the nuclear membrane. This proposal is supported by the findings of Harrison¹⁷ that indicate a preferential association of centromeric heterochromatin to the nuclear membrane.

Fujiwara concluded from his studies¹⁶ that initiation of DNA synthesis is regulated at the nuclear membrane. While the results presented here showing a correlation between increase in DNA associated with membrane and onset of DNA synthesis agree with his conclusion, other interpretations are compatible with these results. For example, it is possible that organization of DNA within the nucleus mediated by attachment of specific regions of DNA to the nuclear membrane may be required either for proper arrangement of DNA to assure fidelity of chromosome duplication or for proper timing of the sequence of DNA replication. Initiation of DNA synthesis might occur independently of this organizational event, while the same initiation sites might fortuitously lie close to the DNA-membrane attachment sites.

Other possible roles for attachment of DNA to nuclear membrane have been proposed.^{17,22} These studies implicate the attachment sites in control of genetic expression either by virtue of localization of DNA within the nucleus or by altering the activity of RNA polymerase required for transcription of DNA. In addition to these suggestions, other control mechanisms such as methylation of DNA could function as signals which specify which DNA should be attached to the nuclear membrane.¹⁷

REFERENCES

1. T. C. Hsu, W. Schmid, and E. Stubblefield, In: "Role of Chromosomes in Development," Academic Press, New York (1964).
2. G. C. Mueller and K. Kajiwara, *Biochim. Biophys. Acta* 114, 108 (1966).
3. M. G. Ormerod and A. R. Lehman, *Biochim. Biophys. Acta* 228, 331 (1971).
4. A. Cole, P. M. Corry, R. M. Humphrey, and A. T. Ansevin, Abstracts Sixteenth Annual Biophysical Society Meeting (1972), Abstract No. SuAM-C18, p. 237a.
5. D. E. Comings and T. J. Kakefuda, *J. Mol. Biol.* 33, 225 (1968).
6. D. E. Comings and T. A. Okada, *Exp. Cell Res.* 62, 293 (1970).
7. D. L. Friedman and G. C. Mueller, *Biochim. Biophys. Acta* 174, 253 (1969).
8. F. Hanoaka and M. Yamada, *Biochem. Biophys. Res. Commun.* 42, 647 (1971).
9. N. S. Mizumo, C. E. Stoops, and A. A. Sinha, *Nature New Biology* 229, 22 (1971).
10. N. S. Mizumo, C. E. Stoops, and R. L. Pfeiffer, Jr., *J. Mol. Biol.* 59, 517 (1971).
11. J. M. R. Hatfield, *Exp. Cell Res.* 72, 591 (1972).
12. P. R. Kay, M. E. Haines, and I. R. Johnston, *FEBS Letters* 16, 233 (1971).
13. S. Fakan, G. N. Turner, J. S. Pagano, and R. Hancock, *Proc. Natl. Acad. Sci. USA* 69, 2300 (1972).
14. C. E. Hildebrand and R. A. Tobey (manuscript in preparation).
15. C. E. Hildebrand and R. A. Tobey (manuscript in preparation).
16. Y. Fujiwara, *Cancer Res.* 32, 2089 (1972).
17. C. M. H. Harrison, *Tissue and Cell* 3, 523 (1971).
18. C. H. Ockey, *Exp. Cell Res.* 70, 203 (1972).
19. C. F. Earhart, G. Y. Tremblay, M. J. Daniels, and M. Schaechter, *Cold Spring Harb. Symp. Quant. Biol.* 33, 707 (1968).
20. J. M. Steim, M. E. Tourtellotte, J. C. Reinert, R. N. McElhaney, and R. L. Rader, *Proc. Natl. Acad. Sci. USA* 68, 1996 (1971).
21. R. A. Tobey, E. C. Anderson, and D. F. Petersen, *J. Cell. Physiol.* 70, 63 (1967).
22. I. A. Menon, *Canad. J. Biochem.* 50, 807 (1972).

Band Analysis of the Chinese Hamster Cell Line CHO

Chinese hamster cells (line CHO)¹ have been used extensively for metabolic, radiobiological, and genetic studies²⁻⁴ with only a superficial appreciation for the degree of aneuploidy characteristic of the line. The modal chromosome number and morphology were briefly described by Kao and Puck^{4,5} and classified on the basis of arm-length measurements as 12 normal and 9 altered chromosomes and an estimated 3 percent less total chromatin than normal cells.

Our current lack of understanding of aneuploidy, the widespread use of the cell line, and the previous report of a relatively large number of abnormal chromosomes⁴ prompted us to undertake a more extensive karyologic analysis utilizing autoradiographic and Giemsa banding techniques. Our observations demonstrate that no homologous pairs remain and that only 8 chromosomes appear normal when compared with the euploid Chinese hamster karyotype.⁶

The CHO cells used in this study were from the line obtained in 1962 from Dr. T. T. Puck.⁷ Euploid female Chinese hamster fibroblasts were from a strain designated LA-CHE[♀] and were propagated from an ear clipping. Autoradiographic analysis of DNA replication patterns employed conventional techniques using Kodak NTB emulsion.

The C-band technique was a modification of the method described by Arrighi and Hsu⁸ in which air-dry preparations were treated for 3 min with 0.01 N NaOH or saturated Ba(OH)₂ and incubated 17 hr in 6X SSC at 60°C. Preparations were stained 10 min with buffered Giemsa.

G-Band preparations were treated with trypsin by a modification of Seabright's method⁹ in which the major change was to treat fixed chromosomes with trypsin at 0°C. After drying, slides were stained as described for C-band staining. The cold trypsin treatment appears to reduce dramatically the variability characteristic of trypsin hydrolysis, particularly in cells blocked with colcemid.

Table 1 summarizes the chromosome number and relative DNA content of CHO and LA-CHE[♀]. Flow microfluorometric estimates on fluorescent Feulgen-stained cells¹⁰ indicate 4 percent less DNA in CHO than in LA-CHE[♀], in good agreement with the previous estimate of a 3 percent decrement reported by Kao and Puck.⁴ One of the X chromosomes appears

TABLE 1. CHROMOSOME NUMBER PER CELL AND RELATIVE DNA CONTENT FOR CHO AND LA-CHE[♀] CULTURES

| | Chromosome number | | | | |
|---------------------|-------------------|----|----|----|----|
| | Number of cells | | | | |
| CHO | 19 | 20 | 21 | 22 | 44 |
| | 1 | 6 | 38 | 4 | 1 |
| LA-CHE [♀] | 19 | 20 | 21 | 22 | 44 |
| | | | 1 | 46 | 3 |

Microfluorometric data

| | |
|-----------------------------------------|------|
| CHO G ₁ peak | 21.1 |
| G ₁ mode normalized | 0.96 |
| LA-CHE [♀] G ₁ peak | 21.9 |
| G ₁ mode normalized | 1.00 |

to be missing.

Figure 1 shows the untreated chromosomes of CHO and LA-CHE[♀] arranged according to Hsu and Zenkes.¹¹ Our CHO karyotype differs from the one presented by Kao and Puck⁴ only by substitution of a small metacentric chromosome (ours) for a small acrocentric (theirs). We have retained their

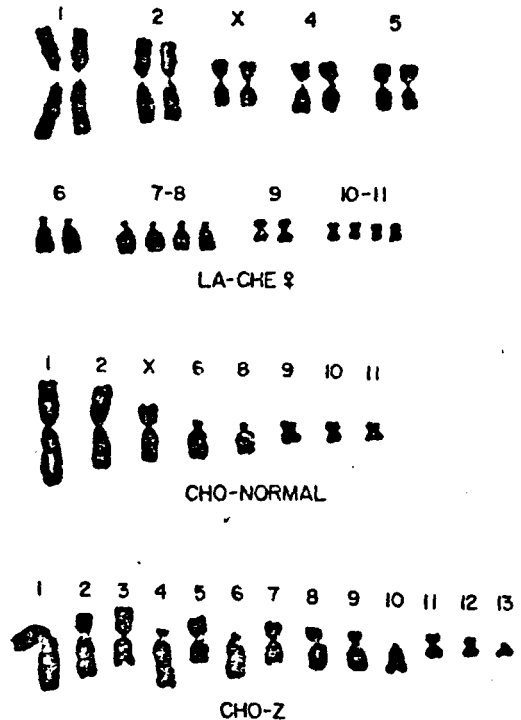


FIG. 1. Untreated karyotypes of euploid Chinese hamster fibroblasts (LA-CHE[♀]) and line CHO cells. The Z-group classification for altered chromosomes in CHO has been used previously⁴ but has been altered on the basis of chromosome banding patterns.

"Z-group" notation but, because we found evidence for several changes too small to be detected by arm-length measurements, have changed assignments to the "Z-group" accordingly.

The G-banding technique proved to be most informative of the methods used for detecting alterations in chromatin arrangement. Figure 2 shows a comparison of the chromosomes of CHO and LA-CHE^Q. Band patterns are similar to those induced by urea and NaCl or by 2-mercaptoethanol, urea, and SDS.¹² Notable exceptions are the terminal bands on the short arms of chromosome 4 and on the long arms of chromosome 5 which appear unstained in our preparation. In previous preparations, these terminal bands are heavily stained.¹² The differences are perhaps minor but are important for our analysis of the CHO chromosomes. Two karyotypes of CHO are shown: a prometaphase and a metaphase. Examination of the patterns gives an idea of the degree of variation encountered and indicates that bands are differentiated better in the small chromosomes of the prometaphase cell,

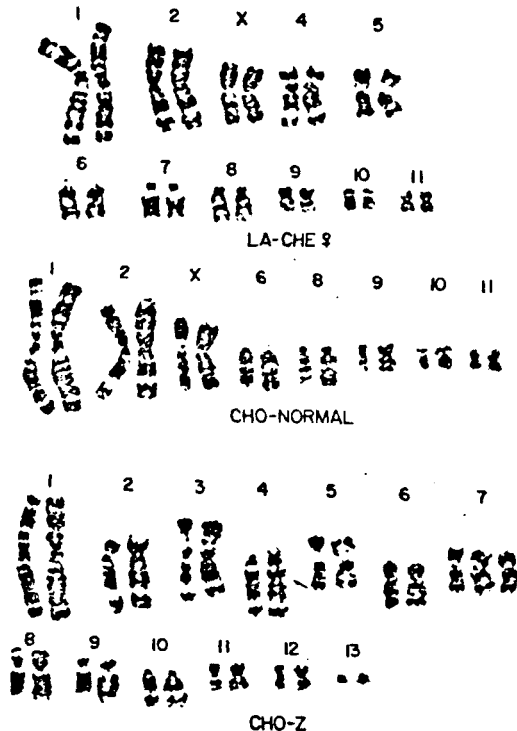


FIG. 2. Trypsin-induced Giemsa bands in LA-CHE^Q and CHO chromosomes. For the CHO chromosomes we present karyotypes from two cells; the first chromosome in each group is from a prometaphase cell and the second from a metaphase cell. The arrow at chromosome Z-4 indicates the point of reattachment of a pericentric inversion in a normal 4 chromosome (see text).

while resolution of bands in the larger chromosomes is superior in the metaphase cell.

Comparison of the G-bands in CHO and LA-CHE^Q reveals 8 apparently normal chromosomes, none of which are paired. The remainder have either major or minor deletions, additions, or rearrangements. In many of the Z-group chromosomes, the banding patterns permit identification of both the origin and destination of translocated chromatin, but some alterations which involve a single band lack sufficient information and are ambiguous. In addition to the G-band information, we have used arm-ratio measurements and data from C-band and autoradiographic examination to complete the analysis. We have published the detailed examination of the karyotypes⁶ and present here only major features. Chromosomes Z-3 and Z-7 are the products of an exchange between a normal 4 and a normal 5. Z-4 is a normal 4 which has undergone a pericentric inversion. The centromere is oriented upside down as compared with a normal 4. Z-6, which contains an extra dark and light band attached to the long arms, is of interest because a similar translocation can be seen in another aneuploid Chinese hamster line studied by Kato and Yosida.¹²

Two generalizations can be made from the G-band analysis. The first is that only one X chromosome is present in CHO cells; the other is that with relatively minor exceptions (namely, a light band added to the short arms of 8, a pericentric inversion of 4, and a small deletion in 5) one haploid set of chromosomes has remained intact in the CHO cell.

Although the C-bands shown in Fig. 3 are less informative than the G-bands, they have been useful in identifying several pairs of centromeres. The C-bands resemble those found by Hsu and Arrighi,¹³ but in our experience the amount of interstitial heterochromatin demonstrable was variable and dependent on experimental conditions. By varying the length of alkaline treatment, we could alter the number of bands and conclude, therefore, that the interstitial bands¹³ are remnants of patterns induced by the alkaline-saline-Giemsa technique of Schnedl.¹⁴ In our analysis, centromeric heterochromatin has been used for purposes of identification and interstitial bands, because of variability, have not been relied upon.

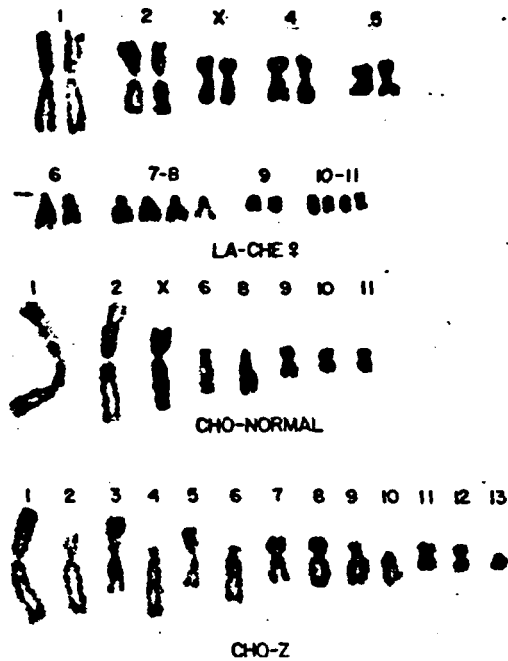


FIG. 3. Centromeric bands in LA-CHE⁺ and CHO cells following a DNA denaturation-renaturation procedure. The arrow at the number 6 chromosome in LA-CHE⁺ indicates the telomeric heterochromatin (see text).

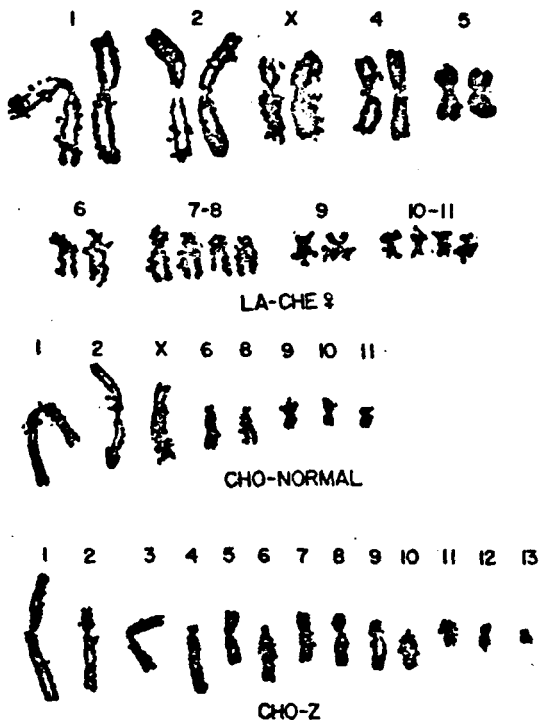


FIG. 4. Autoradiographs of late-replicating sites in LA-CHE⁺ and CHO chromosomes. ³H-Thymidine (2 μ Ci/ml) was added to exponential cultures for 1.5 hr; at this time colcemid (0.06 γ /ml) was added for 2 hr. Note the absence of label in the terminal areas of CHO chromosome 1 and the extra late-replicating sites in Z-group CHO chromosomes 6 and 10.

Identification of late-replicating DNA (Fig. 4) indicates that CHO cells possess an alteration in labeling sequence, particularly in chromosome 1. In our hands and in studies of others,^{15,16} euploid Chinese hamster cells replicate the terminal areas of the short arm of chromosome 1 late. However, in CHO these areas are consistently free of label. In addition to this difference, several other CHO chromosomes show late labeling patterns that are inconsistent with patterns of normal chromosomes but similar to patterns observed by Zakharov *et al.*¹⁷ These workers suggested that late-replicating areas were either derived from heterochromatic portions of the X chromosomes or that they originated by genetic inactivation of excess autosomal segments present in aneuploid cells. Because Z-group chromosomes Z-6 and Z-10 consistently label later than their normal counterparts 6 and 8, it is unlikely that Zakharov's explanation applies to CHO cells. We cannot rule out positively translocation of small portions of the X₂ chromosome to Z-6 and Z-10, but the general preservation of normal chromosome banding sequence in these two group members suggests that X₂ translocations have not occurred. The other hypothesis, that late-replicating elements are autosomal materials in excess of the normal complement, is contrary to the evidence both of the G-band analysis and the microfluorometric estimates of total DNA content. Finally, if heterochromatization is involved, it must be facultative because the C-bands show no differences between normal chromosomes and their late-replicating Z-group counterparts. Because of the unusual nature of these observations and their implications with respect to cellular control of DNA synthesis, an extensive study of the replication sequence across the entire S period is in progress.

These data clearly demonstrate that the remaining X chromosome is the early-replicating X₁, in contrast to Zakharov's¹⁷ observation that in hypodiploid hamster lines both X₁ and X₂ remain intact, while in both pseudo- and hyperdiploid lines one or both X chromosomes were absent.

Figure 5 is a diagrammatic representation of the major G-bands arranged for comparison of CHO and LA-CHE⁺. The arrangement is based on positive identification of centromeres (e.g., Z-1, Z-2, etc., were originally centromeres of the homologs now

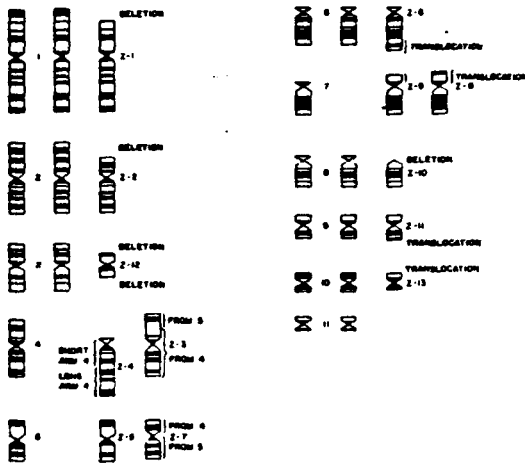


FIG. 5. Schematic summary of the major G-bands in LA-CHEP and CHO cells. The first and second chromosomes of each set are the normal diploid and apparently normal chromosomes from CHO. Chromosomes of the Z-group are arranged according to centromere of origin: (Z-1) deletion of the terminal portion of the upper arm; (Z-2) internal deletion from short arm with normal telomere; (Z-3) reciprocal translocation with Z-7; (Z-4) pericentric inversion; (Z-5) inversion deletion; (Z-6) translocation, origin uncertain; (Z-7) reciprocal translocation with Z-3; (Z-8) translocation, origin uncertain; (Z-9) translocation, origin uncertain; (Z-10) deletion; (Z-11) translocation, origin uncertain; (Z-12) ambiguous, best evidence is centromere from X_2 ; and (Z-13) translocation, origin uncertain.

altered in the karyotype). The first column shows one normal chromosome from LA-CHEP. The second represents those chromosomes of CHO in which no abnormalities can be detected. In columns 3 and 4, the chromosome with fewer abnormalities is displayed to the left and the major translocations, deletions, and rearrangements are indicated.

An outstanding feature of the G-banding pattern comparisons outlined here is the reproducibility achieved by drastically reducing the hydrolytic activity of the trypsin. The assumption that proteolytic enzymes, in general, cause alterations in Giemsa staining by cleavage of peptide bonds is supported by the general observation that banding patterns are similar following treatment with other proteolytic enzymes (e.g., Pronase which, on the one hand, should produce rather nonspecific hydrolysis and, on the other, by treatment with urea and mercaptoethanol which might be expected to produce more specific effects on sulfhydryl linkages). One notion, not yet emphasized but supported by both the

very limited conditions for enzymatic digestion and by brief urea-mercaptoethanol treatment,¹² is that few bonds are broken, and it is likely that in the best preparations little if any material is removed by the treatment. In each case, the most delicate and revealing patterns arise after the gentlest treatment, with typical fuzzing of the patterns the major consequence of prolonged treatment.

Differentiation of chromosomal segments into light, intermediate, and dark staining areas suggests that metaphase chromatin is organized in a specific way with regard to chromosomal proteins. This concept is supported by studies of isolated chromatin which have demonstrated that dense chromatin has a higher proportion of disulfide bonds than diffuse chromatin¹⁸ and that histones are bound to template-active and template-inactive chromatin in different ways.¹⁹ For these reasons, we conclude that G-bands are a result of protein hydrolysis and have little to do with denaturation of DNA, as proposed previously.^{14,20}

Kato and Yosida¹² found positive correlations between Giemsa bands and chromosome spiralization. We have made similar observations, and the studies of Stubblefield¹⁶ of segmented chromosomes also indicate that G-banding patterns result from chromosomal condensation processes. We should note that, while there are similarities between segmented chromosomes and G-bands (the patterns of dark and light bands are similar, and both suggest that light areas are late-replicating while dark areas are early-replicating), there are also clear differences. The segmentation patterns suggest that euploid Chinese hamster 1 chromosomes are not homologous¹⁶ and that the long arms of the X_1 and X_2 chromosomes may be differentiated.²¹ Neither difference is detected by the G-band technique.

The C-band mechanism apparently is involved in selective denaturation and renaturation of DNA.^{13,22,23} Bianchi and Ayres²⁴ contend that an increased amount of C-banded material (constitutive heterochromatin) occurs in an aneuploid line of African green monkey cells. Much of this excess material appeared as interstitial bands. We found no such increase or localization of this heterochromatin in aneuploid CHO cells but did see an increase in late-replicating sites. Ris and Kubai²⁵ concluded that chromatin may be rendered

inactive without heterochromatic condensation. Taken together, these observations suggest that two separate mechanisms may be present during aneuploid transformation. One mechanism inactivates portions of the genome by heterochromatization, the other by altering the time of replication. Further studies of aneuploid cell lines should elucidate these processes.

Zakharov *et al.*¹⁷ studied the structural and numerical variation of chromosome complements of 9 aneuploid Chinese hamster lines and concluded that "the viability of these lines depends on a rather narrow limit of the total amount of chromosomal material present." A similar concept emerges from a study of the DNA content of 14 cell lines from 8 different species.^{10,26} In total DNA content these lines cluster at points equivalent to haploid units of DNA for mammalian cells. Our present results show that, while numerous rearrangements have occurred in the CHO chromosomes, essentially all of the template-active genome is retained with intact sequences of bands. Also, when the Z-group chromosomes are arranged according to size, they are also arranged according to the sequence of chromosomes in the normal karyotype with respect to the centromere region (i.e., each centromere seems to carry a given amount of chromatin material regardless of the extent of rearrangement). These trends suggest that transition from euploidy to aneuploidy is rather sharply controlled. Both the total amount and organization of cellular DNA into chromosomes appear to be restricted. Presumably violations of these constraints are lethal.

Studies of the kind reported here should help to elucidate the control mechanisms involved in evolution of aneuploid lines²⁷ and may ultimately explain the observed differences in mutagenic behavior between euploid Chinese hamster fibroblasts and CHO cells.⁴

REFERENCES

1. T. T. Puck, S. J. Cieciora, and A. Robinson, Genetics of somatic mammalian cells. III. Long-term cultivation of euploid cells from human and animal subjects, *J. Exp. Med.* 108, 945-956 (1958).
2. D. F. Petersen, R. A. Tobey, and E. C. Anderson, Synchronously dividing mammalian cells, *Federation Proc.* 28, 1771-1779 (1969).
3. R. A. Walters and D. F. Petersen, Radiosensitivity of mammalian cells. II. Radiation effects on macromolecular synthesis, *Biophys. J.* 8, 1487-1504 (1968).
4. F. Kao and T. T. Puck, Genetics of somatic mammalian cells. IX. Quantitation of mutagenesis by physical and chemical agents, *J. Cell. Physiol.* 74, 245-257 (1969).
5. F. Kao and T. T. Puck, Genetics of somatic cells: Linkage studies with human-Chinese hamster cell hybrids, *Nature* 228, 329-332 (1970).
6. L. L. Deaven and D. F. Petersen, The chromosomes of CHO, an aneuploid Chinese hamster cell line: G-band, C-band, and autoradiographic analyses, *Chromosoma (Berlin)* (1973), in press.
7. T. T. Puck, P. C. Sanders, and D. F. Petersen, Life cycle analysis of mammalian cells. II. Cells from the Chinese hamster, *Biophys. J.* 4, 441-450 (1964).
8. F. E. Arrighi and T. C. Hsu, Localization of heterochromatin in human chromosomes, *Cytogenetics* 10, 81-86 (1971).
9. M. Seabright, A rapid banding technique for human chromosomes, *Lancet* 2, 971-972 (1971).
10. P. M. Kraemer, D. F. Petersen, and M. A. Van Dilla, DNA constancy in heteroploidy and the stem line theory of tumors, *Science* 174, 714-717 (1971).
11. T. C. Hsu and M. T. Zenzes, Mammalian chromosomes *in vitro*. XVII. Idiogram of the Chinese hamster, *J. Natl. Cancer Inst.* 32, 857-870 (1964).
12. H. Kato and T. H. Yosida, Banding patterns of Chinese hamster chromosomes revealed by new techniques, *Chromosoma (Berlin)* 36, 272-280 (1972).
13. T. C. Hsu and F. E. Arrighi, Distribution of constitutive heterochromatin in mammalian chromosomes, *Chromosoma (Berlin)* 34, 243-253 (1971).
14. W. Schnedl, Analysis of the human karyotype using a reassociation technique, *Chromosoma (Berlin)* 34, 448-454 (1971).
15. T. C. Hsu, Mammalian chromosomes *in vitro*. XVIII. DNA replication sequence in the Chinese hamster, *J. Cell Biol.* 23, 53-62 (1964).
16. E. Stubblefield, Mammalian chromosomes *in vitro*. XIX. Chromosomes of Don C, a Chinese hamster fibroblast strain with a part of autosome 1b translocated to the Y chromosome, *J. Natl. Cancer Inst.* 37, 799-817 (1966).
17. A. F. Zakharov, E. S. Kakpakova, N. A. Egolina, and H. E. Pogosiyan, Chromosomal variability in clonal populations of a Chinese hamster cell strain, *J. Natl. Cancer Inst.* 33, 935-956 (1964).

18. M. G. Ord and L. A. Stocken, Metabolic properties of histones from rat liver and thymus gland, *Biochem. J.* 98, 888-897 (1966).
19. K. Marushige and J. Bonner, Fractionation of liver protein, *Proc. Natl. Acad. Sci. USA* 68, 2941-2944 (1971).
20. M. E. Drets and M. W. Shaw, Specific banding patterns of human chromosomes, *Proc. Natl. Acad. Sci. USA* 68, 2073-2077 (1971).
21. A. F. Zakharov and N. A. Egolina, Asynchrony of DNA replication and mitotic spiralization along heterochromatic portions of Chinese hamster chromosomes, *Chromosoma (Berlin)* 23, 365-385 (1968).
22. M. L. Pardue and J. G. Gall, Chromosomal localization of mouse satellite DNA, *Science* 168, 1356-1358 (1970).
23. M. L. Mace, S. S. Tenethia, and B. R. Brinkley, Differential immunofluorescent labeling of chromosomes with antisera specific for single strand DNA, *Exp. Cell Res.* (1973), in press.
24. N. O. Bianchi and J. Ayres, Heterochromatin location on the chromosomes of normal and transformed cells from the African green monkey (*Cercopithecus eathlops*). DNA denaturation-renaturation method, *Exp. Cell Res.* 68, 253-258 (1971).
25. H. Ris and D. F. Kubai, Chromosome structure, *Ann. Rev. Genet.* 4, 263-294 (1970).
26. P. M. Kraemer, L. L. Deaven, H. A. Crissman, and M. A. Van Dilla, DNA constancy despite variability in chromosome number, In: "Advances in Cell and Molecular Biology," Vol. II (E. J. DuPraw, ed.), Academic Press, New York (1972), pp. 47-108.
27. T. C. Hsu, Chromosomal evolution in cell populations, *Int. Rev. Cytol.* 12, 69-161 (1961).

Repair of Radiation Damage, Derepression, and Replication of a Bacterial Virus Chromosome

We have studied the development of bacteriophage HPlc1 in the bacterium *Haemophilus influenzae* following derepression of the prophage by ultraviolet radiation. Our results support a model which places phage DNA replication on the cell membrane, where a relatively high molecular-weight concatomer of phage DNA is synthesized and subsequently degraded to phage-equivalent DNA, the majority of which is membrane-free. These results led us to conclude that the cell membrane not only is the site of DNA replication during which phage DNA is synthesized in multiple phage-equivalent concatomers but is also the site at which these concatomers are correctly sized and reduced to phage-sized pieces.¹

We use ultraviolet light irradiation of lysogenic cells to derepress the prophage. The cell which harbors the prophage is capable of excision-repair; therefore, several obvious questions can be asked of this repair capability relative to prophage derepression. The action of repair enzymes, particularly endonuclease, on the irradiated bacterial chromosome could trigger the prophage derepression event. First, we can ask if repair is necessary for derepression. Second, we can consider the possibility that repair does just the opposite.

We were concerned with the question of whether repair prevents prophage derepression. Possible involvement of excision-repair in ultraviolet-light derepression of the *Haemophilus* phage HPlc1 is investigated by analyzing and comparing derepression in lysogens of a uvr^+ strain and a uvr^- derivative which lacks the endonucleolytic activity of the excision-repair scheme.²

Lysogens of these two strains were exposed to varying doses of ultraviolet light (254 nm) and assayed on a phage-sensitive indicator strain (Rd) for infective centers (i.e., those cells in an irradiated population that produce phage) and for the titer of infective phage particles produced by each infective center. From the results shown in Fig. 1 one can see that the increase in infective centers is similar for strains with and without excision-repair capability. This suggests that excision-repair capability is not necessary for prophage derepression, a conclusion which has also been reported for phage lambda *Escherichia coli* lysogens,³ and does not prevent derepression. In addition, the uvr^+ strain, while quite capable of excision-repair, apparently does not repair those pyrimidine dimers which cause derepression. If dimers which trigger prophage derepression were rendered ineffective in the uvr^+ strain, the plot of infective centers versus radiation dose would be shifted downward relative to the uvr^- curve, indicative of a dose reduction. Clearly, this is not the case.

At higher doses of ultraviolet light, the frequency of derepressed lysogens increases in the uvr^+ culture but decreases in the uvr^- strain (Fig. 2). The curve showing decreasing infective centers for the uvr^- strain is similar to a survival curve showing that, at doses above 10 ergs/mm², these bacteria incur a sufficient number of lesions

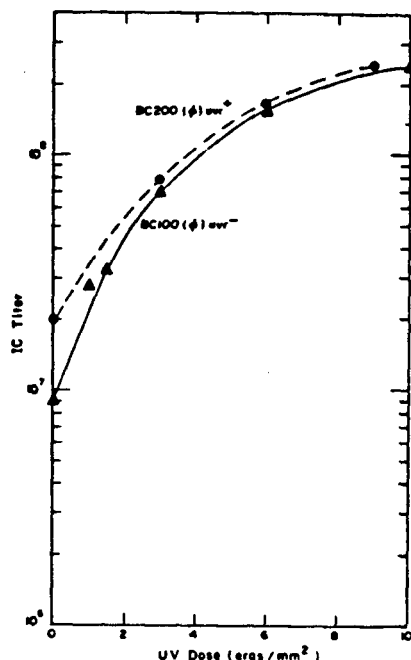


FIG. 1. Fractions of infective centers in irradiated cultures as a function of ultraviolet light dose. Exponentially growing cultures of *H. influenzae* strains BC200 and BC100 lysogenic for phage HPlc1 were resuspended in 0.01 M phosphate-buffered saline (pH 7.0) and exposed to light of wavelength 254 nm emitted from a 15-watt General Electric germicidal lamp under conditions permitting 93 percent transmission through the bacterial suspension. Aliquots were removed after the desired times of exposure and assayed for phage-producing bacteria on lawns of a phage-sensitive strain (i.e., *H. influenzae* Rd). (—●—) BC100 (HPlc1), and (---▲---) BC200 (HPlc1).

to render them biologically inactive with respect to phage-producing ability. However, the frequency of infective centers continues to increase with dose in the *uvr*⁺ culture, suggesting that the difference in these curves above 10 ergs/mm² results from DNA repair, which does indeed function in this strain to remove dimers and permits survival of phage-producing ability.

Our results on prophage derepression in *Haemophilus* indicate that excision-repair capability is not necessary for triggering derepression or preventing derepression. In addition, it appears that a cell which is capable of DNA repair and which does excise pyrimidine dimers does not remove the dimer(s) which results in derepression of the prophage state. However, excision-repair is important in sustaining the capacity of the derepressed lysogen to support phage production when bacteria are

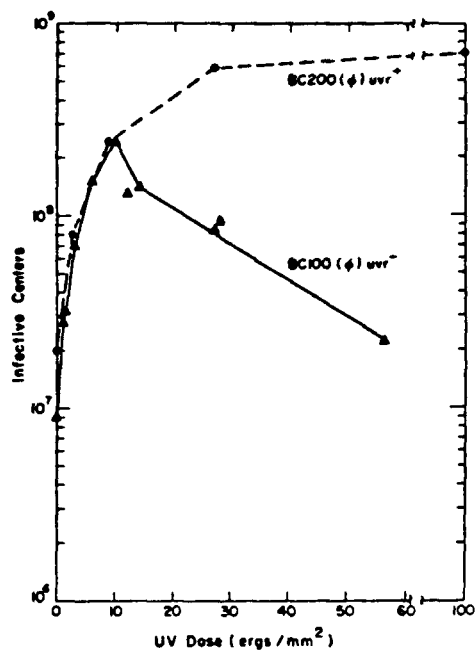


FIG. 2. Fractions of infective centers as a function of elevated doses of ultraviolet light. The bacterial strains and experimental conditions were the same as described in Fig. 1.

exposed to doses of ultraviolet-light greater than 10 ergs/mm.²

REFERENCES

1. B. J. Barnhart and S. H. Cox, DNA replication of induced prophage in *Haemophilus influenzae*, *J. Virology* (1972), submitted.
2. B. J. Barnhart and S. H. Cox, Recovery of *Haemophilus influenzae* from ultraviolet and X-ray damage, *Photochem. Photobiol.* **11**, 147-126 (1970).
3. M. Monk and J. Gross, Induction of prophage λ in a mutant of *E. coli* K12 defective in initiation of DNA replication at high temperature, *Mol. Gen. Genetics* **110**, 299-306 (1971).

Packaging of a Bacterial Virus Chromosome: A Model Supported by Reactivation of Radiation-Damaged Virus DNA

Recent evidence suggests that the complex, DNA-filled head of the bacterial virus T4 is assembled by first constructing a protein shell and then inserting DNA into this preformed structure.¹ This model for head maturation stems from experiments which indicate the following: (1) heads which appear to lack full DNA complements (by electron microscopy and sucrose gradient analysis) can

accumulate in cells infected under the proper conditions (i.e., with ts or am mutants or by treatment with certain drugs), and (2) in some cases, heads which accumulate under these conditions can serve as precursors to complete, viable phage upon removal of the block.¹ One such system is described below.

The maturation of T4 can be blocked by addition of acridine dyes such as 9-aminoacridine. This maturation block can be released to begin production of phages by removal of acridine from the medium.² Others have indicated that the amount of DNA and proteins synthesized in the presence of the dye is not significantly altered.³ These findings prompted our investigations to determine the nature of the structures synthesized under these conditions.

The electron micrographs shown in Fig. 1 illustrate the phage components synthesized in T4-infected cells grown in the presence of 9AA for 30 min (Fig. 1A) and then released from the 9AA block and grown for an additional 30 min (Fig. 1B). The cell section in Fig. 1A reveals the presence of many "diffuse" head-like particles lacking the intense staining property of DNA-filled heads. Upon removal of the dye and subsequent incubation, the cells reveal the presence of many dense, DNA-filled heads (Fig. 1B). Isotopic labeling and sucrose gradient analysis indicate that the diffuse heads seen in sections are converted to viable phage when the dye is removed.⁴ The conclusion implied by these experiments is that the sequence of events in head assembly may be an empty precursor to full-head pathway.

A critical argument against these studies is that the diffuse-appearing heads were once filled heads which became "empty" upon preparation for electron microscopy or sucrose gradient analysis. Kellenberger and co-workers have long suggested that T4 heads may exist in such a "fragile-filled state," which favors a model where DNA is first condensed and later enclosed by the protein subunits.⁵

From the discussion above, precursors of T4 heads probably are present in one of two forms when maturation is blocked by the drug 9AA: (a) the protein shells are filled with a tightly coiled DNA, but this protein shell is not stable and can readily lose this DNA, or (b) the protein shells are not filled, and the phage DNA is still in the DNA pool of the cell.

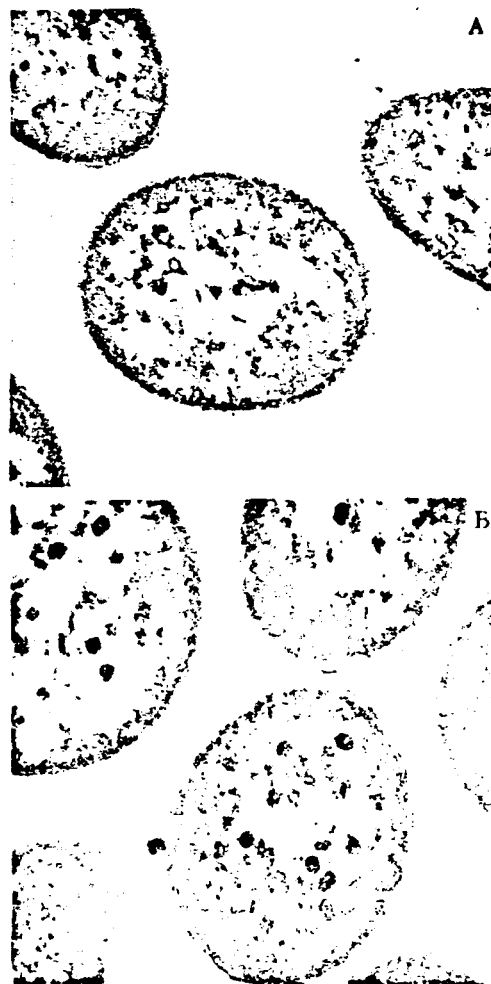


FIG. 1. Thin-section of T4-infected Escherichia coli B grown in the presence of 1 μ g/ml 9-aminoacridine. Cells were fixed in O_5O_4 , embedded, thin-sectioned, and stained with a $KMnO_4$ -lead citrate double stain. Cells grown for 30 min in 9AA-treated medium (A), and same cells removed from 9AA into fresh medium for 20 min before fixation (B).

Our approach to testing the validity of one of these models is based on the notion that radiation effects on these two systems will be dissimilar. Because fragile, filled precursors would be nearly complete heads, radiation inactivation curves of phages made from these heads should not differ significantly from those of free or complete phage. However, in the unfilled precursor the phage DNA probably remains in the DNA pool of the cell, where radiation-repair mechanisms are functioning. Under these conditions, the unfilled precursor would be more resistant to radiation than a fragile, filled precursor or viable phage.

T4-Infected cells were grown experimentally in

the presence and absence of 9AA. After 30 min, the control culture contained a sizable population of viable phage, while the 9AA-treated culture contained a sizable population of precursor (unfilled or fragile, filled heads). The cells were then exposed to increasing doses of ultraviolet radiation and assayed at appropriate times (doses) for surviving infective centers. The curves in Fig. 2 demonstrate that infective centers in the control culture are more sensitive to ultraviolet radiation than the 9AA-treated culture, suggesting that the DNA which accumulates in 9AA-treated cultures is more accessible to repair systems than is the DNA of phage grown under normal conditions. Such a finding is more consistent with a head-filling model than with a fragile, filled precursor model.

Because of the complexity and uncertainty of radiation effects on the cell system, this experiment would be more convincing if the precise repair mechanism in this system were known. The experiment was repeated with the excision-repairless mutant of *Escherichia coli*, B_{s-1}, with no significant differences in inactivation curves. Growth curves of phage development in 9AA-treated cells which were irradiated prior to 9AA removal indicate that the repair mechanism is quite rapid.

Experiments are in progress to establish whether recombination, DNA polymerase I repair, or a phage-mediated repair (γ -gene reactivation) is responsible for the bulk of rescue from ultraviolet radiation in the 9AA-treated cells. The possibility that the dye 9-aminoacridine protects the DNA from ultraviolet irradiation is being determined by comparing the thymine dimer content in control and 9AA-treated cultures. A correlation between ultraviolet resistance and a particular repair system should establish more distinctly the state of the viral chromosome prior to packaging into a compact head.

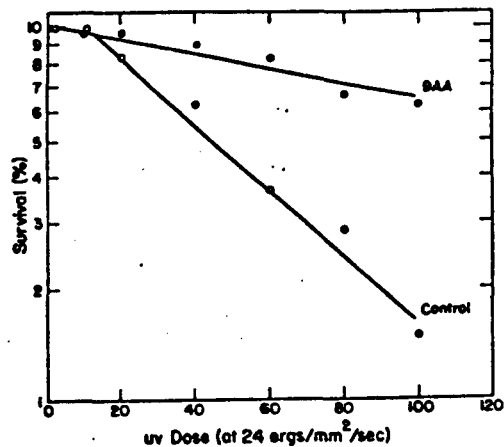


FIG. 2. Ultraviolet inactivation of infective centers of T4 grown in the presence and absence of 9-aminoacridine. Cells were ultraviolet-irradiated at 24 ergs/mm²/sec at 30 min after infection in simultaneous cultures (one control and one 9AA-treated). At times indicated on the abscissa, the cultures were plated for surviving infective centers.

REFERENCES

1. R. Luftig, W. B. Wood, and R. T. Okinaka, Bacteriophage T4 head morphogenesis. I. On the nature of 49-defective heads and their role as intermediates, *J. Mol. Biol.* **57**, 555-573 (1971).
2. M. Susman and M. M. Piechowski, Studies on phage development. I. An acridine sensitive clock, *Virology* **26**, 163-174 (1965).
3. M. M. Piechowski and M. Susman, Studies on phage development. II. The maturation of T4 phage in the presence of puromycin, *Virology* **28**, 386-395 (1966).
4. R. T. Okinaka, Morphogenesis of the Head of Bacteriophage T4, Ph.D. Thesis, University of California, Los Angeles (1971).
5. E. Kellenberger, J. Sechaud, and A. Ryter, Electron microscope studies on phage multiplication. IV. The establishment of the DNA pool of vegetative phage and maturation of phage particles, *Virology* **8**, 478 (1959).

MAMMALIAN RADIOBIOLOGY SECTION

INTRODUCTION

Research activities in mammalian radiobiology include the study of both internal effects (metabolism of radioisotopes entering the body by ingestion or injection) and effects of whole-body external exposure. Radiobiological experiments related to the negative pion radiotherapy program are also being done. These are mostly pilot studies designed to work out proven techniques, to develop new and improved techniques, and to establish X-ray-effect base lines for use when the meson facility becomes operational for biomedical research.

The primary objective of the whole-body exposure program is to gain knowledge about delayed or late biological effects of exposure to radiation under different total-dose and dose-rate conditions. The state-of-the-art and data deficiencies presented in 1968^{1,2} and in 1970³ are, for the most part, valid today. Recently contributed dose-rate-effect information suggests that the use of broad assumptions (in the absence of research data) concerning the prompt and long-term effects of exposure is unwarranted. Dose protraction by fractionation and continuous exposure may produce widely different responses in a given species⁴ and responses that differ significantly among species.⁵ Investigations at this Laboratory are programmatic in nature and designed to obtain needed acute- and low-dose-rate data in species with different radiation response characteristics. Because the primate (monkey) is a relatively long-lived animal that has not been used widely in low-dose-rate investigations, it is of primary interest as a research species in our long-range program.

The dog and monkey differ widely in their response to single high-dose-rate exposure and to low-dose-rate continuous exposure. Therefore, comparative dose-rate studies of the two species under the same exposure conditions should yield data that would be helpful in better understanding the kinetics of radiation injury and recovery.

Radiation effects data from these two species should also help to make extrapolations of prompt and long-term effects from animals to man more meaningful.

Projects being investigated include (a) large-animal studies using dogs and monkeys to compare response to gamma-ray exposure at different dose rates and residual injury that may reflect the species long-term effects, and (b) small-animal studies using mice to investigate the kinetics of radiation injury during changing (buildup and decay) and fixed dose-rate exposures and the effects of dose rate on residual injury.

Radiation Protection Guides (RPGs) have been established by the International Commission on Radiological Protection and afford a ready basis for evaluation of injury resulting from entrance of radioisotopes into the human body. Some of these values have been derived solely from observation of a nonhuman mammalian species because no other data were available. In order to avoid mere substitution of nonhuman data, this Laboratory has sought a rational basis for extrapolation from small animals to man in the interspecific relation based on various relevant metabolic parameters and whole-body weight. In a review dealing with comparative metabolism, Stara *et al.* conclude, "Extrapolations to man from animal data are admittedly difficult and sometimes inaccurate; however, the risks in not extrapolating are, unquestionably, much greater."⁶ Such extrapolations have been made for radioisotopes of zinc, iodine, manganese, silver, iridium, niobium, ruthenium,⁷ and beryllium, and other isotopes such as mercury-203 and selenium-75 are being investigated. The metabolic patterns determined with radioelements have useful relevance for questions concerning stable isotopes of these elements. Thus, the metabolic pathways followed by nonradioactive pollutants through a portion of the biosphere are indicated by these studies.

Determination of the course of whole-body activity after a single administration of a radio-nuclide gives metabolic data useful in estimation of

body burdens under conditions of chronic exposure. Distribution of such activity among various tissues (which is seldom uniform because of differential rates of uptake and loss) is also necessary for establishing the target tissue for the nuclide. Most RPGs which deal with chronic exposure are derived from data dealing with retention following a single exposure. It is useful to determine the accuracy of calculations based on single-dose data by comparison with data from animals exposed chronically. Chronic oral exposure is usually achieved by means of contaminated food or water. Factors associated with chronic oral exposure (multiple intakes per day, various levels of intake, external contamination) differ from those of a single administration by stomach tube, and estimates of body burdens and tissue distribution after chronic exposure that are based on single-exposure data may be erroneous.

Since 1956 a population of about 40 New Mexico residents has been monitored for the long-lived fallout product cesium-137, a portion of the radioactive debris of atmospheric nuclear tests. The rise and fall in human burdens correlate well with initiation and cessation of testing activity. A peak in body burdens reached in 1964 was followed by an almost linear decline until 1967.⁸ A somewhat reduced rate of loss in 1967-1968 was then followed by a relatively unchanging low-level body burden maintained until the present. A similar low level is maintained in foodstuffs. For instance, the average levels of cesium-137 contamination reported by the Pasteurized Milk Network of the U. S. Public Health Service for July 1969-June 1970 and for July 1970-June 1971 were 8 and 9 pCi/l., respectively.^{9,10} The continuing contamination in foodstuffs suggests that a reservoir more tenacious than the atmosphere (soil?) is responsible for the levels found in the biosphere. It is also possible that low levels in bone, formerly masked by high activities in soft tissues, are now becoming apparent.¹¹ The fate of cesium-137 in man and the biosphere is of interest not only as a radioactive fallout nuclide but also as a guide in the study of other pollutants of the atmosphere.

REFERENCES

1. J. B. Storer, In: *The Proceedings of a Symposium on Dose Rate in Mammalian Radiation Biology* (D. G. Brown, R. G. Cragle, and T. R. Noonan, eds.), UT-AEC Agricultural Research Laboratory and U. S. Atomic Energy Commission Report CONF-680410 (July 12, 1968), pp. 1.1-1.4.
2. N. P. Page, In: *The Proceedings of a Symposium on Dose Rate in Mammalian Radiation Biology* (D. G. Brown, R. G. Cragle, and T. R. Noonan, eds.), UT-AEC Agricultural Research Laboratory and U. S. Atomic Energy Commission Report CONF-680410 (July 12, 1968), pp. 12.1-12.23.
3. J. B. Storer and J. M. Yukas, In: *Conference on the Estimation of Low-Level Radiation Effects in Human Populations* (G. A. Sacher, ed.), Argonne National Laboratory Report ANL-7811 (December 1969), p. 31.
4. J. F. Spalding, W. J. Basmann, R. F. Archuleta, and O. S. Johnson, *Comparative effects of dose protraction by fractionation and by continuous exposure*, *Radiation Res.* 51, 608-614 (1972).
5. J. F. Spalding, L. M. Holland, and J. R. Prine, *The effects of dose protraction on hemato-poiesis in the primate and dog*, *Life Sciences and Space Research* 8, 155-164 (1972), Akademie Verlag, Berlin.
6. J. F. Stara, N. S. Nelson, R. J. Della Rosa, and L. K. Bustad, *Comparative metabolism of radionuclides in mammals: A review*, *Health Phys.* 20, 113-137 (1971).
7. J. E. Furchner, C. R. Richmond, and G. A. Drake, *Comparative metabolism of radionuclides in mammals. VII. Retention of ruthenium-106 in the mouse, rat, monkey and dog*, *Health Phys.* 21, 355-365 (1971).
8. C. R. Richmond and J. E. Furchner, *Cesium-137 body burdens in man: January 1956 to December 1966*, *Radiation Res.* 32, 538-549 (1967).
9. Section I. *Milk and Food, Milk Surveillance, June 1970*, *Radiological Health, Data and Reports* 11, 533-543 (1970).
10. Section I. *Milk and Food, Milk Surveillance, June 1971*, *Radiological Health, Data and Reports* 12, 501-510 (1971).
11. R. W. Anderson and P. F. Gustafson, *Concentration of cesium-137 in human rib bone*, *Science* 137, 668 (1962).

MAMMALIAN RADIOBIOLOGY

Biological Effects of Gamma-Ray Dose Protraction during Continuous Exposure with Fixed and Changing Dose Rates

(J. F. Spalding, R. F. Archuleta, J. E. London, and O. S. Johnson)

The modifying effects of dose protraction in rodents and larger animals have been reviewed extensively in recent symposia and colloquia.¹⁻⁹ To

assess and predict short- and long-term effects on man from exposure to terrestrial and space radiation, it is necessary to understand the modifying effects of a wide range of dose-rate conditions on a number of mammalian species. Effects of dose protraction by continuous exposure and by fractionation differ significantly.¹⁰ The dose rate most likely to be experienced in space or from fallout is continuous but changing. Comparative effects of continuously changing and continuously constant dose-rate exposures in the mammal are little known. Preliminary investigations reported in the annual report for last year¹¹ gave inconclusive results. Improvements in exposure technique and animal handling were indicated.

Two substrains of strain RFM mice (H-2^f and H-2^k) with different radiation-resistance characteristics^{12,13} were used. Mice were divided into 7 groups with 10 RFM H-2^f and 10 RFM H-2^k mice per group. Groups 1, 2, and 3 were housed 10 per cage (5 H-2^f and 5 H-2^k) and were subjected 20 each to three levels of continuous but changing gamma-ray exposure. Groups 4, 5, and 6 were housed 10 per cage (5 H-2^f and 5 H-2^k) and were subjected 20 each to three continuous and constant gamma-ray exposures. The seventh group of mice (10 of each substrain) was a nonirradiated control group. The continuous gamma-ray exposure regime provided for moving mice toward a cobalt-60 point source (up to a fixed distance), then moving them back to the fixed, most distant position. Round trips toward and away from the gamma-ray source were completed and automatically repeated every 46.4 hr. Dose rates increased and decreased according to the inverse-squares law. Three constant and three changing dose-rate regimes were used. Three replications of the high and medium and two of the low dose-rate regimes were completed, as shown in Table 1. Dose rates were measured at the nearest and farthest points from the source for each changing dose-rate condition and were calculated at 6-min intervals during exposure.

Lethality data were recorded twice daily, and mice were bled for hematology studies at 7-day intervals during exposure. Because the lethality data were cumulative, they were fitted (by nonlinear least squares) to a cumulative normal distribution. Mean values from each replication were obtained from the fitted equation and were used in the analysis of

TABLE 1. CHANGING AND FIXED DOSE-RATE CONDITIONS

| Fixed dose rate (rads/hr) | Equivalent changing dose rate (rads/hr) | | | Accumulated 46.4-hr dose (rads) |
|------------------------------------------|--------------------------------------------|-------|------|---------------------------------------|
| | Low | High | Mean | |
| <u>Low Dose Rate (2 replications)</u> | | | | |
| 2.03 | 0.61 | 6.79 | 2.03 | 94.4 |
| <u>Medium Dose Rate (3 replications)</u> | | | | |
| 2.91 | 0.69 | 12.22 | 2.91 | 135.0 |
| <u>High Dose Rate (3 replications)</u> | | | | |
| 4.45 | 0.80 | 22.72 | 4.45 | 206.4 |

TABLE 2. MEAN SURVIVAL TIMES

| Substrain | Dose-Rate Level and Exposure Method | | | | | |
|------------------|-------------------------------------|------------------|--------|------|------|------|
| | High | | Medium | | Low | |
| | CDR ^a | FDR ^b | CDR | FDR | CDR | FDR |
| H-2 ^f | 776 | 856 | 1185 | 1354 | 2268 | 2594 |
| H-2 ^k | 876 | 904 | 1272 | 1496 | 2526 | 3265 |

^aChanging dose rate.

^bFixed dose rate.

variance. Table 2 is a three-way table of mean survival times. The analysis of variance of mean survival times is shown in Table 3. There were significant differences in mean survival times among strains subjected to the three dose-rate levels and methods. These observations are consistent with radiation-resistance characteristics of the two RFM substrains used^{12,13} and suggest that the bone marrow was the critical target organ under all dose-rate conditions.

The two methods of exposure affected the animals differently at each of the three dose levels (Tables 2 and 3). Changing dose rates were more biologically damaging than equivalent constant or fixed dose rates. The 46.4-hr dose levels used in this investigation are somewhat higher than those that may be anticipated during space missions or recommended exposures in emergencies. However, Table 2 shows that as the dose rate is lowered the difference in mean survival time under the two exposure regimes increases. Although it was possible to demonstrate a significant difference in mean survival time of mice subjected to continuous

TABLE 3. VARIANCE OF MEAN SURVIVAL TIMES

| <u>Sources of variation</u> | <u>Degrees of freedom</u> | <u>Sum of squares</u> | <u>Mean square</u> | <u>F-ratio</u> |
|----------------------------------------------------|---------------------------|-----------------------|--------------------|----------------------|
| Method (CDR versus FDR) | 1 | 413,118 | 413,118 | 45.48 ^a |
| Strain (H-2 ^f versus H-2 ^k) | 1 | 279,098 | 279,098 | 30.73 ^a |
| Dose (high versus medium; medium versus low) | 2 | 16,200,993 | 8,100,496 | 891.79 ^a |
| Method x strain | 1 | 21,596 | 21,596 | 2.38 ^{n.s.} |
| Method x dose | 2 | 279,068 | 139,534 | 15.36 ^a |
| Strain x dose | 2 | 207,761 | 103,880 | 11.44 ^a |
| Method x strain x dose | 2 | 68,124 | 34,062 | 3.75 ^b |
| Error | 20 | 181,669 | 9,083 | |
| Total | 31 | | | |

^aSignificant at 0.01 level.

^bSignificant at 0.05 level.

n.s. not significant.

exposure using two exposure regimes, possible long-term-effect differences from nonlethal doses delivered by the two methods could not be estimated.

REFERENCES

- D. Grahn and G. A. Sacher, Fractionation and protraction factors and the late effects of radiation in small mammals, In: The Proceedings of a Symposium on Dose Rate in Mammalian Radiation Biology (D. G. Brown, R. G. Cragle, and T. R. Noonan, eds.), UT-AEC Agricultural Research Laboratory and U. S. Atomic Energy Commission Report CONF-68041 (July 12, 1968), p. 2.1.
- D. Grahn, Mechanisms of effect -- What is our understanding of recovery rates? In: The Proceedings of a Symposium on Dose Rate in Mammalian Radiation Biology (D. G. Brown, R. G. Cragle, and T. R. Noonan, eds.), UT-AEC Agricultural Research Laboratory and U. S. Atomic Energy Commission Report CONF-68041 (July 12, 1968), p. 24.1.
- D. Grahn, Biological effects of protracted low dose radiation exposure of man and animals, In: Proceedings of a Colloquium on Late Effects of Radiation, University of Chicago (R. M. Fry, D. Grahn, M. L. Griem, and J. H. Rust, eds.), University of Chicago Press (May 15-17, 1969).
- D. C. L. Jones, Responses of large animals to radiation injury, In: Proceedings of a Symposium on Survival of Food Crops and Livestock in the Event of Nuclear War, Brookhaven National Laboratory, USAEC Report CONF-700909 (December 1971), pp. 224-233.
- J. S. Krebs, Criteria for radiation injury, In: Proceedings of a Symposium on Survival of Food Crops and Livestock in the Event of Nuclear War, Brookhaven National Laboratory, USAEC Report CONF-700909 (December 1971), pp. 234-244.
- J. F. Spalding and L. M. Holland, Species recovery from radiation injury, In: Proceedings of a Symposium on Survival of Food Crops and Livestock in the Event of Nuclear War, Brookhaven National Laboratory, USAEC Report CONF-700909 (December 1971), pp. 245-258.
- N. P. Page and E. T. Still, Factors modifying the response of large mammals to low intensity radiation exposure, In: Proceedings of the National Symposium on Natural and Manmade Radiation in Space, Las Vegas, Nevada (E. A. Warman, ed.), National Aeronautics and Space Administration Report NASA TM X-2440 (1972), pp. 622-632.
- J. F. Spalding, L. M. Holland, J. R. Prine, D. N. Farrer, and R. G. Braun, Effect of continuous gamma-ray exposure on learned tasks and of subsequent fractionated exposure on performance of blood-forming tissue, In: Proceedings of the National Symposium on Natural and Manmade Radiation in Space, Las Vegas, Nevada (E. A. Warman, ed.), National Aeronautics and Space Administration Report NASA TM X-2440 (1972), pp. 633-640.
- C. C. Lushbaugh, Predicted levels of human radiation tolerance extrapolated from clinical studies of radiation effects, In: Proceedings of the National Symposium on Natural and Manmade Radiation in Space, Las Vegas, Nevada (E. A. Warman, ed.), National Aeronautics and Space Administration Report NASA TM X-2440 (1972).

10. J. F. Spalding, N. J. Basmann, R. F. Archuleta, and O. S. Johnson, Comparative effects of dose protraction at low dose rates by fractionation and by continuous exposure, *Radiation Res.* 51, 608-614 (1972).
11. C. R. Richmond and G. L. Voelz, eds., Annual Report of the Biological and Medical Research Group (H-4) of the LASL Health Division, January through December 1971, Los Alamos Scientific Laboratory Report LA-4923-PR (April 1972).
12. J. F. Spalding, D. M. Popp, and R. A. Popp, A within-strain difference in radiation sensitivity in the RFM mouse, *Radiation Res.* 40, 37-45 (1969).
13. J. F. Spalding, D. M. Popp, and R. A. Popp, A genetic effect on radiation sensitivity consistent with a single gene locus hypothesis, *Radiation Res.* 44, 670-673 (1970).

Comparative Biological Effects of Radiation Dose Protraction in Dogs and Monkeys

(J. F. Spalding, L. M. Holland, J. R. Prine, O. S. Johnson, P. M. LaBauve, and J. E. London)

A major goal in our mammalian radiobiology program is to obtain dose-rate-effects data on the monkey. This primate has received little attention as a research animal in studying the effects of dose protraction. This is perhaps partially because it is a difficult species to handle and restrain properly for prolonged periods in a radiation environment.

The dog is the most studied of our larger mammals, and much excellent radiation-effects data on the dog are being accumulated at other laboratories. To facilitate extrapolation of the effects of protracted whole-body gamma irradiation from one mammalian species to another, it is helpful to study two species simultaneously. During the last year, the Mammalian Radiobiology Section has modified its cobalt-60 gamma irradiation facility to accommodate 12 dogs and 12 monkeys for simultaneous whole-body exposures under nearly identical conditions. Figure 1 shows exposure arrangements used for dog-monkey investigations currently in progress.

Hematopoietic Response of Dogs and Monkeys to Whole-Body Protracted Exposure to Cobalt-60 Gamma Rays at 24 rads/day.--The modifying effects of dose protraction by fractionation have been reported for the monkey;¹⁻⁴ however, the effects on monkeys of dose protraction by continuous exposure are

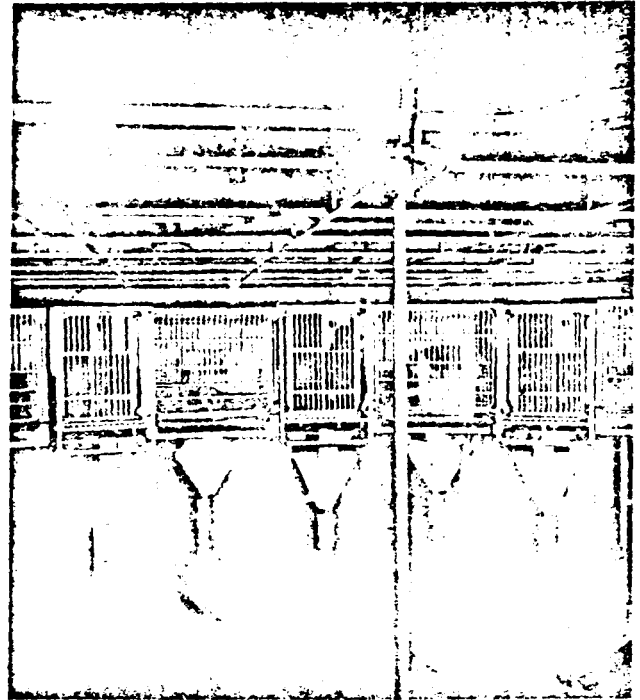


FIG. 1. The Biomedical Research Group's radiation exposure facility for dose protraction studies in dogs and monkeys.

little known. Comparative dose-rate studies on dogs and monkeys, two species with widely differing acute LD₅₀ values,⁵ have not been reported.

Six beagles and six monkeys (*Macaca mulatta*) were placed in a continuous gamma-ray environment at a dose rate of 24 rads/day until death. Blood samples were obtained by venipuncture from unanesthetized animals before exposure and at 7-day intervals during exposure.

Mean packed-cell volumes (PCV) and white-blood-cell counts (WBC) are shown in Fig. 2. These blood characteristics responded similarly in dogs and monkeys to whole-body gamma-ray exposure at 24 rads/day. This is in contrast to a quite different hematopoietic response between dogs and monkeys exposed continuously at 66 rads/day. At the higher dose rate, dog bone marrow appeared much less resistant to radiation injury than did that of the monkey.¹ Absolute numbers of neutrophils, expressed as percentages of pre-exposure values for dogs and monkeys, are shown in Fig. 3. Although the neutrophil (the predominant granulocyte) is the principal white cell in peripheral blood of the dog, it seems more radiosensitive than that of the monkey, whose principal white cell is the lymphocyte. This difference in neutrophil

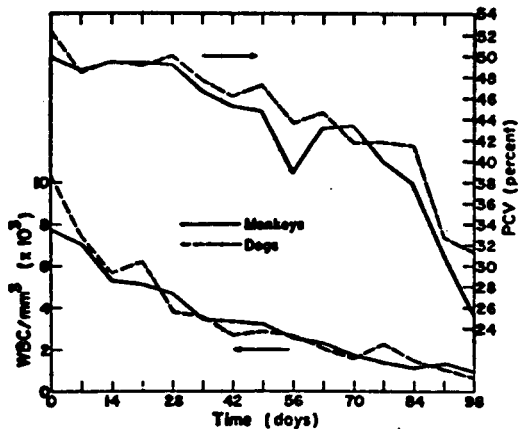


FIG. 2. Packed-cell volume and white-blood-cell count of dogs and monkeys during continuous gamma-ray exposure at 24 rads/day.

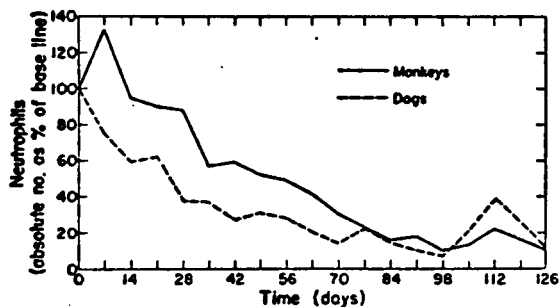


FIG. 3. Absolute number of neutrophils (percent of pre-exposure levels) of dogs and monkeys during continuous gamma-ray exposure at 24 rads/day.

response is observed at higher dose rates and has been reported using acute exposures.⁶ The characteristic neutrophil response in this study suggests that it is species-specific and that the severer response may be associated with acute radiation sensitivity or a low LD₅₀³⁰ value in larger mammals.

REFERENCES

1. J. F. Spalding, L. M. Holland, and J. R. Prine, Studies of the effects of dose protraction on hematopoiesis in the primate and dog, In: Program-Abstracts of the 14th Plenary Meeting of the COSPAR (Committee on Space Research), Seattle, Washington (June 17-July 2, 1971), Abstract L.3.2, p. 266.
2. J. F. Spalding, L. M. Holland, J. R. Prine, D. N. Farrer, and R. G. Braum, Effect of continuous gamma-ray exposure on performance of learned tasks and of subsequent fractionated exposures on performance of blood-forming tissue, In: Proceedings of the National Symposium on Natural and Manmade Radiation in Space, Las Vegas, Nevada (E. A. Warman, ed.), National Aeronautics and Space Administration Report NASA TM X-2440 (January 1972), pp. 633-640.
3. J. F. Spalding, L. M. Holland, and O. S. Johnson, Kinetics of injury and repair in monkeys and dogs exposed to gamma-ray fractionation, *Health Phys.* **10**, 11-17 (1969).
4. L. P. Kosichenko and E. K. Dzhikidze, Sensitivity of monkey bone marrow cells to prolonged daily irradiation in small doses, *Genetika* **8**, 160-164 (1966); *Biol. Abstracts* **50**, 129785 (1969).
5. N. P. Page, The effect of dose protraction on radiation lethality of large animals, In: Proceedings of a Symposium on Dose Rate in Mammalian Radiation Biology (D. G. Brown, R. G. Cragle, and T. R. Noonan, eds.), UT-AEC Agricultural Research Laboratory and U. S. Atomic Energy Commission Report CONF-680410 (1968), p. 12.1.
6. G. M. Suter, Response of Hematopoietic Systems to X-Rays, U. S. Atomic Energy Commission Report MDDC-824 (April 1947), 8 p.

Residual Injury in Dogs and Monkeys Exposed to

Whole-Body Cobalt-60 Gamma Rays.

Residual injury from nonlethal gamma-ray exposures as it may be reflected in life shortening has been demonstrated in the rodent in numerous reports¹⁻³ reviewed recently. Estimates of residual, long-term injury from exposure to ionizing radiation in larger mammals are needed. To estimate residual injury in species such as the dog and monkey, it is desirable to use an end point other than life shortening. Reduction in mean survival time during continuous gamma-ray exposure has been used as a measure of residual injury in mice⁴ and in larger animals such as sheep and swine.⁵ This technique of measuring irreparable or long-term injury in dogs and monkeys is being investigated.

Twelve beagles and 22 monkeys (*Macaca mulatta*) were used to test for possible long-term residual injury from a continuously delivered gamma-ray conditioning exposure (dogs and monkeys) and from large doses accumulated by the fractionation method of dose protraction (monkeys only).

Six beagles and six monkeys were exposed to 660 rads of gamma rays protracted over 10 days of continuous exposure. Ten monkeys were exposed to 2400 rads of gamma rays using the fractionation method of dose protraction, with 100-rad fractions being given at 56-day intervals. Eighty-four days after the 660-rad exposure of dogs and monkeys challenged by the continuous-exposure method and after the 24th 100-rad fraction administered to monkeys challenged by the fractionation method,

animals were placed in a gamma-ray environment at 24 rads/day continually until death. Six control dogs and monkeys with no challenge dose were also exposed continuously at 24 rads/day until death. Differences in mean survival time, if any, between challenged and unchallenged animals represented residual injury in the radiation-challenged animals.⁶ Two dogs (littermates) in the group challenged with 660 rads of gamma rays approached a "steady state" condition between hematopoietic-system cell renewal and radiation injury; therefore, they were not included in the mean survival time (MST) data of conditioned dogs.

Mean-survival data are shown in Tables 1 and 2. Residual injury in dogs 84 days after a 660-rad conditioning exposure protracted over 10 days was approximately 40 percent and was statistically significant at the 0.05 level. Monkeys showed 8 percent residual injury from the same conditioning exposure, but this was not statistically significant.

TABLE 1. MEAN SURVIVAL TIMES (MST) OF DOGS AND MONKEYS WITH AND WITHOUT A 660-RAD CONDITIONING DOSE IN A GAMMA-RAY FIELD OF 1 RAD/HR

| Treatment | MST (hr) | |
|------------------------------|-------------------------|-------------------------|
| | Monkeys | Dogs |
| No conditioning dose | 2260 ± 260 ^a | 2428 ± 334 ^a |
| Conditioning dose (660 rads) | 2070 ± 149 ^a | 1461 ± 231 ^a |
| Reduction in MST | 190 | 967 |
| Residual fraction | 8.4 | 39.8 |

^aStandard error of the mean value.

TABLE 2. MEAN SURVIVAL TIMES (MST) OF MONKEYS WITH AND WITHOUT 2400-RAD CONDITIONING DOSES IN A GAMMA-RAY FIELD OF 1 RAD/HR

| Treatment | MST (hr) |
|-------------------------------|-------------------------|
| No conditioning dose | 2260 ± 260 ^a |
| Conditioning dose (2400 rads) | 2437 ± 267 |
| Reduction in MST | -177 |
| Residual fraction | -7.8% |

^aStandard error of the mean value.

Monkeys with an accumulated gamma-ray dose of 2400 rads (approximately 4 times their acute LD₅₀³⁰) showed no residual injury in terms of a reduction in MST. Challenged monkeys actually lived slightly longer in the 1-rad/hr gamma-ray field than did unchallenged monkeys; however, the difference was not statistically significant.

These results are consistent with earlier reports that have demonstrated that the recovery rate of hematopoietic tissue, in terms of peripheral blood values, remained unchanged in these same monkeys from the first 100-rad exposure through the 24th 100-rad exposure. Long-term injury seems to vary greatly among species, and additional work remains before a rational basis for extrapolation of injury and recovery kinetics to man can be established.

REFERENCES

1. D. Grahn and G. A. Sacher, Fractionation and protraction and the late effects of radiation in small mammals, *In: Proceedings of a Symposium on Dose Rate in Mammalian Radiation Biology* (D. G. Brown, R. G. Cragle, and T. R. Noonan, eds.), UT-AEC Agricultural Research Laboratory and U. S. Atomic Energy Commission Report CONF-680410 (July 12, 1968).
2. C. D. Van Cleave, Late Somatic Effects of Ionizing Radiation, U. S. Atomic Energy Commission Report TID-24310 (1968).
3. R. M. Fry, D. Grahn, M. L. Griem, and J. H. Rust, Late effects of radiation, *In: Proceedings of a Colloquium held in the Center for Continuing Education, University of Chicago, May 15-17, 1969*, Taylor and Francis, Ltd., Publishing Company, London (1970), pp. 101-136.
4. J. F. Spalding, V. G. Strang, and F. C. V. Worman, Effect of graded acute exposures of gamma-rays or fission neutrons on survival in subsequent protracted gamma-ray exposures, *Radiation Res.* **13**, 415-423 (1960).
5. N. P. Page and E. T. Still, Factors modifying the response of large animals to low-intensity radiation exposure, *In: Proceedings of the National Symposium on Natural and Manmade Radiation in Space, Las Vegas, Nevada* (E. A. Warman, ed.), National Aeronautics and Space Administration Report NASA TM X-2440 (January 1972), pp. 632-662.
6. D. Grahn and G. A. Sacher, The measurement of residual acute injury from single exposure by survival following daily irradiation, *Ann. N. Y. Acad. Sci.* **114**, 158-168 (1964).

Radiobiological Pilot Investigations for the Negative Pion Radiotherapy Program

(M. R. Raju, R. F. Archuleta, L. M. Holland, and J. F. Spalding)

Pig, rat, and mouse skin has been used as a model for normal tissue renewal. Because of poor depth-dose distribution of fast neutrons, normal skin reactions could be serious when fast neutrons are used in radiotherapy; therefore, the radiation response of pig, rat, and mouse skin to X-rays and fast neutrons has been studied extensively.¹⁻⁵ Except for some slight differences, these skins can be used as a model for a cell-renewal system. Skin reactions in pigs and humans become significant 12 to 15 days after radiation exposure and peak at about 30 days. In mice and rats, the reaction begins 8 to 10 days after exposure and peaks at about 20 days. A second wave of skin reaction is observed in humans, pigs, and rats 10 to 14 weeks after exposure, whereas in mice no second wave of reaction is observed. Relative biological effectiveness (RBE) values from fast neutrons were found to be similar for pig and human skin; however, the single-dose RBE values for the mouse and rat foot are lower than those for pigskin. These low values could be due to the presence of subcutaneous fat in the pig and human.⁶ Thus, the difference in RBE on mouse foot and human skin from neutrons is mainly due to different neutron dose depositions in tissues with and without fat. This should not matter too much for negative pions. The mouse-foot system can be used to obtain quantitative results for negative pion beams of different peak widths used in different therapeutic situations. Because of linear-energy transfer (LET) variations for different peak widths, precise RBE estimates are necessary in systems such as this in order to understand and compare the results of late effects and tumor responses.

Kallman and his associates recently used the mouse foot as a model for cell renewal of normal tissue and KHT sarcoma from the same mouse, transplanted into the thighs of syngenic C₃H mice, to study the potential of a radiosensitizing drug (BCdR) for clinical radiotherapy.⁷ KHT is a sarcoma that arose spontaneously at the base of the ear of a C₃H/Km mouse in 1962 in Kallman's laboratory at Stanford. This line was maintained by serial subcutaneous

passage and has been studied extensively.^{8,9} Tomlinson¹⁰ has used the time the tumor takes to grow to a fixed size after irradiation as a criterion to study the effectiveness of radiation. He showed that this end point manifests itself chiefly through cellular response of neoplastic cells.¹¹ He also found that RBE values for growth delay agree very well with RBE values obtained from TCD₅₀ analysis.¹² Hence, tumor-growth measurements will be a quick and practical method for determining RBE for any new radiation such as negative pions.

Response of Normal Skin (Mouse Foot) to X-Irradiation.--Strain RFM female mice were used in this study. The white mouse can be scored more accurately than colored mice, and it is known that there are no significant variations from one strain of mouse to another.^{4,5} The hind left foot of the mouse, from the toe to halfway up the thigh, was irradiated. Groups of 6 mice each were irradiated simultaneously by 1000, 2000, 3000, 4000, 5000, and 6000 rads of 250-KVP X rays. Skin reactions were scored daily using an arbitrary scale developed by Fowler, with slight modifications made by Brown *et al.*⁷ as shown in Table 1. Results of skin reactions measured by this arbitrary scale are plotted as a function of time after exposure in Fig. 1. Reactions began about the tenth day and peaked at about 20 days. Also, the reaction from low doses began to heal sooner; hence, the maximum reaction occurred later with increasing dose. Therefore, the reaction at a given time will not be a good end point, and an average reaction during the time in which the reaction develops and subsides is generally used as an end point. Figure 2 shows the average skin reaction 13 to 34 days after each of the 6 doses. These data

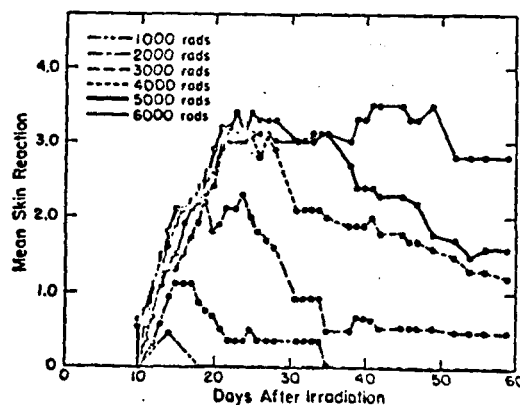


FIG. 1. Mean skin reaction in mice (scored by the scale shown in Table 1) plotted as a function of time after exposure.

TABLE 1. THE SYSTEM FOR SCORING SKIN REACTIONS IN MOUSE FOOT FOLLOWING X-IRRADIATION

| Score | Reaction increasing | Observation | Reaction subsiding |
|-----------|------------------------------------------------------------------------------------------|-------------|-------------------------------------------------------------------------|
| 0.5 | 50/50; doubtful if abnormal | | Hair slightly discolored |
| 1- (0.75) | Slight reddening, definitely not normal | | Patchy and/or discolored hair on foot |
| 1.0 | Definite reddening and/or slight edema and/or engorged blood vessels | | Very little hair on foot and lower leg; papery-thin skin |
| 1+ (1.25) | Severe reddening and edema and/or white scaling on bottom of foot (dry desquamation) | | No hair on foot and lower leg and/or club toes with no nails |
| 1.5 | First small area of moist breakdown; usually tips of two toes stuck (moist desquamation) | | As 1+ but with one small area of scab. May have two toes stuck |
| 1.5+ | Several small areas of moist desquamation | | Healing complete except for one medium scab or more than one small scab |
| 2.0 | Considerable moist desquamation with at least four toes stuck together | | Approximately one-fourth of foot unhealed (with scab) |
| 2+ | Very severe 2.0 (all toes stuck with much desquamation) | | Very severe 2.0 |
| 2.5 | Breakdown of half of the skin of foot (ulceration) | | Approximately one-half of foot unhealed |
| 2.5+ | Breakdown of three-fourths of skin of foot | | Approximately three-fourths of foot unhealed |
| 3.0 | Breakdown of almost all skin of the foot | | Minimal healing of foot |
| 3+ | Very severe 3.0 | | Almost complete necrosis of foot |
| 3.5 | Complete necrosis of foot in severe yellow moist exudate over foot | | Complete foot necrosis: "club" of yellow moist exudate over whole foot |

plotted as a function of dose show the sigmoidal curve similar to plots of cure rates and complications with dose in radiotherapy and agree with the results of Fowler et al.^{1,2,6} and Brown et al.⁷

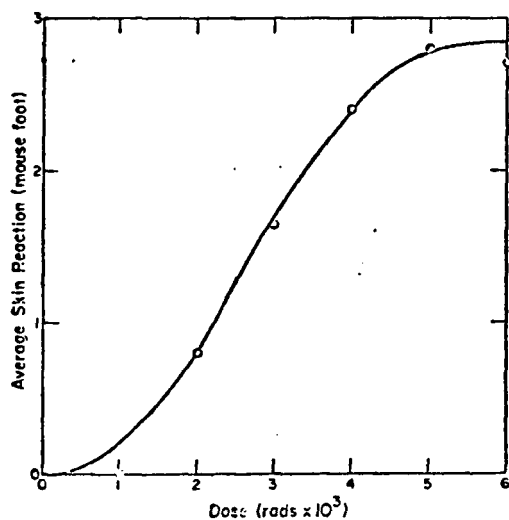


FIG. 2. Average skin reaction 13 to 34 days after each of 6 doses of X-irradiation.

Response of Malignant Tissue (Tumor) to X-Irradiation.--To obtain specific tumor-tissue response to X-ray exposure, it is necessary to isolate in vivo tumor tissue from normal tissue for exposure. Techniques have been developed to solve this problem. The KHT tumor normally carried in C₃H mice has been introduced and maintained in a hairless mutant strain of RFM mice. An ~12-mm-diameter tumor from a donor mouse is removed, placed in normal saline solution, and minced into small pieces (~1 mm³). These tumor pieces are transplanted into the backs of hairless RFM and C₃H mice by making a small incision in the skin after shaving the back. The back is used in preference to the thigh to permit isolating the tumor from the rest of the body during exposure. The tumor grows to about 6 mm in diameter on about the tenth day after transplantation. When the tumors are 6 to 8 mm in diameter, the mice are anesthetized (0.1 cm³/g body weight of Nembutal), and the tumors are exposed to X rays by shielding the rest of the mouse. Tumors

on the back do not adhere to the back muscle and may be stretched with surrounding skin several millimeters away from the back. Tumor diameters are measured in three perpendicular planes 3 times a week. The average geometric diameter is computed by assuming the tumor to be a sphere. Figure 3 shows results of the mean diameter on the tumor of C₃H mice, plotted as a function of dose (250-KVP X-rays, single dose) from time after exposure. After single doses of more than about 3500 rads, the tumor did not recur; after doses of less than 3500 rads, growth was slowed. Figure 4 shows results of the mean diameter of the tumor on the hairless RFM mouse, plotted as a function of dose (250-KVP X-rays, single dose) from time after exposure. This tumor in the bald mouse grows more slowly than it does in the C₃H strain, but there appears to be no significant histological difference among tumors grown in the two strains. The tumor in the hairless RFM mouse appears significantly more sensitive to radiation than it is in the C₃H strain. These pilot studies have established techniques for studying early skin reactions and tumor responses in mice which are of programmatic interest to negative-pion radiobiology. Experiments using more animals per point to obtain

the basic quantitative X-ray data are being planned.

REFERENCES

1. J. F. Fowler, E. L. Morgan, J. A. Silvester, D. K. Bewley, and B. A. Turner, Experiments with fractionated gamma ray treatment of the skin of pigs. I. Fractionation up to 28 days, *Brit. J. Radiol.* **36**, 188-196 (1963).
2. J. F. Fowler, K. Kragt, R. E. Ellis, P. J. Lindop, and R. J. Berry, The effect of divided doses of 15 MeV electrons on the skin response of mice, *Int. J. Radiat. Biol.* **9**, 241-252 (1965).
3. S. B. Field, T. Jones, and R. H. Tomlinson, The relative effects of fast neutrons and X-rays on tumor and the normal tissue in the rat. I. Single doses, *Brit. J. Radiol.* **40**, 834-842 (1967).
4. J. Denekamp, J. F. Fowler, K. Kragt, C. J. Parnell, and S. B. Field, Recovery and repopulation in mouse skin after irradiation with cyclotron neutrons as compared with 250-KV X-rays or 15-MeV electrons, *Radiation Res.* **29**, 71-84 (1966).
5. J. Denekamp and J. F. Fowler, Further investigations of the responses of irradiated mouse skin, *Int. J. Radiat. Biol.* **10**, 435-441 (1966).
6. J. F. Fowler, Effects of fractionated irradiation on the skin of pigs and other animals and on tumors in rats, In: *Proceedings of a Symposium on Dose Rate in Mammalian Radiation Biology*, UT-AEC Agricultural Research Laboratory and U. S. Atomic Energy Commission Report CONF-680410 (1968), pp. 21.1-21.25.

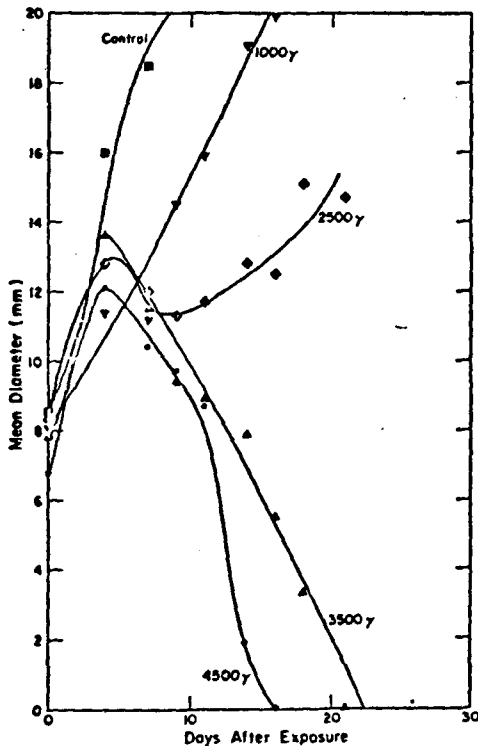


FIG. 3. Mean diameter of tumor body on C₃H mice plotted as a function of dose (250-KVP X-rays, single dose) from time after exposure.

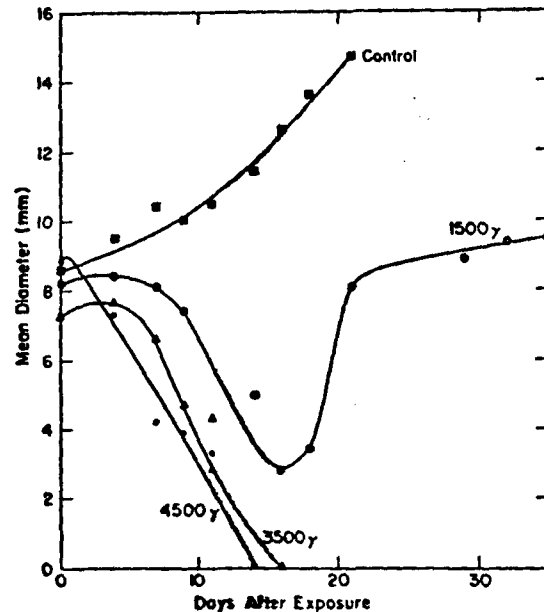


FIG. 4. Mean diameter of tumor body on RFM (hairless) mice plotted as a function of dose (250-KVP X-rays, single dose) from time after exposure.

7. J. M. Brown, D. R. Goffinet, J. E. Cleaver, and R. F. Kallman, Preferential radiosensitization of mouse sarcoma relative to normal skin by chronic intra-arterial infusion of halogenated pyrimidine analogs, *J. Natl. Cancer Inst.* 47, 75-89 (1971).
8. L. M. Van Putten and R. F. Kallman, Oxygenation status of a transplantable tumor during fractionated radiation therapy, *J. Natl. Cancer Inst.* 40, 441-451 (1968).
9. R. F. Kallman, G. Silini, and L. M. Van Putten, Factors influencing the quantitative estimates of *in vivo* survival of cells from solid tumors, *J. Natl. Cancer Inst.* 39, 539-549 (1967).
10. R. H. Tomlinson, An experimental method for comparing treatments of intact malignant tumors in animals and its application to the use of oxygen in radiotherapy, *Brit. J. Cancer* 14, 555-576 (1960).
11. R. H. Tomlinson and E. A. Craddock, The gross response of an experimental tumor to single doses of X-rays, *Brit. J. Cancer* 21, 108-123 (1967).
12. J. F. Fowler, J. Denekamp, A. L. Page, and A. C. Begg, Fractionation with X-rays and neutrons in mice: Response of skin and C3H mammary tumors, *Brit. J. Radiol.* 45, 237-249 (1972).

MAMMALIAN METABOLISM

Retention of Tin-113 in Mice after Oral, Intra-peritoneal, and Intravenous Injection

(J. E. London, G. A. Drake, J. S. Wilson, and J. E. Furchner)

Tin is found as a trace element in human tissues,¹ but it is considered to be only contaminant as no biological functions are attributed to this element, and it is relatively nontoxic. Tin-113 decay is an electron capture process with an associated 0.39-MeV gamma ray. The 118-day physical half-life makes this isotope a suitable tracer for metabolic studies.

Approximately 0.5 μCi of $^{113}\text{SnCl}$ in a 0.1 N HCl solution was administered to RF female mice, about 3 months old and weighing about 26 g. Three groups of 12 mice each were injected by the intravenous (IV), intraperitoneal (IP), or oral (IG) routes. Within 30 min of injection, the gamma activity was measured in a suitable detector, and the measurements were repeated periodically for more than 300 days in the IV and IP groups and for 4 days in the case of the IG group. The data were analyzed and fit to a sum of two or more exponentials. Average values

for the parameters of these retention functions are given in Table I. The best fit to all data is given for each route of administration. The best fit to the data for each of the IP mice is given in Table 2 to illustrate uniformity in metabolism of this nuclide within a group. It is obvious that very little tin was absorbed from the gut. Almost 99 percent was lost with a half-time less than 1 day and 1 percent with a 2-day half-time. Although the fast components of the retention functions for IP and IV data were different, in both cases about 30 percent was lost with a half-time of about 90 days (slow component). The radiation dose following injection of this nuclide by either route (IP or IV) would be the same as indicated by the time integral of the retention function, which is proportional to radiation dose. The effective half-times given refer to tracer atoms used and include radioactive decay. Holleman² suggests the use of turnover time in place of biological half-time to avoid ambiguity in usage. Turnover time (the time required to exchange a quantity equal to the pool) is the reciprocal of the rate constant and, for the long component for tin in mice, is given by $\tau = 1.0/k_3 - (0.693/118)$, where τ is the turnover time, k_3 is the rate constant for the long component (0.0077 day^{-1}), and 118 is the physical half-life of tin-113 and is equal to 546 days. The biological half-time computed by the usual method is 379 days.

REFERENCES

1. I. H. Tipton and M. J. Cook, Trace elements in human tissues. Part II. Adult subjects from the United States, *Health Phys.* 9, 103-145 (1963).
2. D. F. Holleman, Biological half-time and tracer experiments, *Int. J. Appl. Radiat. Isotopes* 23, 341 (1972).

Cesium-137 Activity in a Normal New Mexico Population

(J. S. Wilson and J. E. Furchner)

Measurements of low-level activity in a normal population of New Mexico residents have been made since 1956. About 40 individuals have been counted on a weekly or monthly basis (about 10 and 30, respectively). Results for the 1956-1967 period have been reported,^{1,2} and a report covering the period 1956-1972 is in preparation. Monthly

TABLE 1. AVERAGE EFFECTIVE RETENTION FUNCTIONS FOR TIN-113 IN MICE

| a_1^a (percent) | k_1^a (days ⁻¹) | $T_{1/2}$ (days) | a_2 (percent) | k_2 (days ⁻¹) | $T_{1/2}$ (days) | a_3 (percent) | k_3 (days ⁻¹) | $T_{1/2}$ (days) | EF ^b |
|------------------------------------|----------------------------------|---------------------|--------------------|--------------------------------|---------------------|--------------------|--------------------------------|---------------------|-----------------|
| <u>Intragastric Administration</u> | | | | | | | | | |
| 98.9 | 3.40 | 0.20 | 1.0 | 0.3490 | 2.0 | -- | -- | -- | 0.32 |
| <u>Intravenous Injection</u> | | | | | | | | | |
| 56.9 | 2.73 | 0.25 | 13.5 | 0.0534 | 13.0 | 29.6 | 0.00711 | 97.0 | 44.00 |
| <u>Intraperitoneal Injection</u> | | | | | | | | | |
| 43.9 | 1.09 | 0.63 | 25.1 | 0.0608 | 11.0 | 30.9 | 0.00776 | 89.0 | 44.00 |

^a a_1 and k_1 are the rate and intercept constants in the retention function: $R_t = \sum_{i=1}^n a_i e^{-k_i t}$, where t is time in days.

^bEF is the time integral of the retention function.

TABLE 2. EFFECTIVE RETENTION FUNCTION FOR TIN-113 AFTER INTRAPERITONEAL INJECTION IN MICE

| a_1^a (percent) | k_1^a (days ⁻¹) | $T_{1/2}$ (days) | a_2 (percent) | k_2 (days ⁻¹) | $T_{1/2}$ (days) | a_3 (percent) | k_3 (days ⁻¹) | $T_{1/2}$ (days) | EF ^b |
|----------------------|----------------------------------|---------------------|--------------------|--------------------------------|---------------------|--------------------|--------------------------------|---------------------|-----------------|
| 40.0 | 1.10 | 0.63 | 28.6 | 0.0695 | 10 | 31.5 | 0.00778 | 89 | 45 |
| 40.4 | 1.28 | 0.54 | 27.3 | 0.0740 | 9 | 32.2 | 0.00826 | 84 | 43 |
| 41.1 | 1.18 | 0.59 | 27.0 | 0.0599 | 12 | 32.0 | 0.00774 | 90 | 46 |
| 41.4 | 1.00 | 0.69 | 25.8 | 0.0590 | 12 | 32.7 | 0.00761 | 91 | 48 |
| 35.6 | 1.14 | 0.61 | 32.1 | 0.0690 | 10 | 32.1 | 0.00824 | 84 | 44 |
| 42.8 | 1.06 | 0.66 | 26.0 | 0.0590 | 12 | 31.2 | 0.00798 | 87 | 44 |
| 41.1 | 1.17 | 0.59 | 26.7 | 0.0552 | 13 | 32.2 | 0.00769 | 90 | 47 |
| 40.6 | 1.56 | 0.44 | 26.6 | 0.0651 | 11 | 32.7 | 0.00796 | 97 | 45 |
| 40.9 | 1.16 | 0.60 | 27.1 | 0.0581 | 12 | 32.1 | 0.00763 | 91 | 47 |
| 48.6 | 1.50 | 0.46 | 22.4 | 0.0724 | 10 | 29.1 | 0.00764 | 91 | 41 |
| 45.7 | 1.24 | 0.56 | 22.9 | 0.0593 | 12 | 31.5 | 0.00777 | 89 | 45 |

^a a_1 and k_1 are the rate and intercept constants in the retention function: $R_t = \sum_{i=1}^n a_i e^{-k_i t}$, where t is time in days.

^bEF is the time integral of the retention function.

average values for all subjects have fallen from a peak concentration of > 120 pCi/g K in 1964 to a level of about 20 pCi/g K and have remained there with only small variations during the past 4 years. Low levels in both foods and man³ suggest that a pool with a slower rate of loss than the stratosphere pool is the source of radiocesium contamination. Because cesium-137 is a fission product of high yield, long half-life (30 years), and is readily absorbed from the digestive tract, documentation of the time-course of cesium-137 burdens in humans is base-line data useful in assessment of radiation

exposures following further deliberate or inadvertent pollution of the biosphere. Fallout cesium-137 and natural potassium levels in a New Mexico population during 1972 are reported here.

The procedures used in collection and analysis have been reported.⁴ The results (Table 1) are presented as average monthly values with standard and relative standard deviation. Weight and potassium content changed little and showed no consistent change with the season of the year. Cesium-137 activity shows a peak twice a year in spring and fall (June and December), with two intervening

TABLE 1. BODY WEIGHT, POTASSIUM, AND CESIUM-137 IN A NEW MEXICO POPULATION SAMPLE (1972)^a

| | Jan | Feb | Mar | Apr | May | June | July | Aug | Sep | Oct | Nov | Dec | |
|----------------------|------------------|-------|-------|-------|-------|-------|-------|-------|-------|-------|-------|-------|-------|
| Body weight (kg) | \bar{x} | 68.2 | 68.0 | 67.8 | 69.6 | 68.6 | 67.9 | 67.8 | 68.1 | 67.9 | 70.0 | 67.2 | 69.5 |
| | σ | 11.1 | 10.8 | 10.8 | 11.7 | 11.1 | 11.4 | 11.6 | 10.7 | 11.9 | 14.2 | 11.5 | 12.7 |
| | σ/\bar{x} | 16.3 | 15.9 | 15.9 | 16.8 | 16.2 | 16.8 | 17.1 | 15.7 | 17.5 | 20.3 | 17.1 | 18.3 |
| Potassium (g) | \bar{x} | 132.3 | 131.4 | 125.7 | 129.4 | 128.6 | 125.4 | 125.4 | 129.3 | 128.6 | 124.6 | 125.8 | 128.0 |
| | σ | 29.4 | 30.3 | 29.5 | 27.6 | 28.4 | 31.3 | 28.8 | 27.7 | 20.4 | 31.2 | 22.8 | 28.1 |
| | σ/\bar{x} | 22.2 | 23.1 | 23.5 | 21.3 | 22.1 | 25.0 | 23.0 | 21.4 | 15.9 | 25.0 | 18.1 | 21.9 |
| Potassium (g/kg) | \bar{x} | 1.93 | 1.92 | 1.84 | 1.85 | 1.87 | 1.83 | 1.84 | 1.90 | 1.84 | 1.87 | 1.86 | 1.84 |
| | σ | 0.26 | 0.27 | 0.26 | 0.19 | 0.24 | 0.28 | 0.24 | 0.23 | 0.32 | 0.24 | 0.22 | 0.24 |
| | σ/\bar{x} | 13.5 | 14.1 | 14.1 | 10.3 | 12.8 | 15.3 | 13.0 | 12.1 | 17.4 | 12.8 | 11.8 | 13.0 |
| Cesium-137 (nCi) | \bar{x} | 2.71 | 2.46 | 2.34 | 2.62 | 2.70 | 2.61 | 2.34 | 2.35 | 2.36 | 2.71 | 2.62 | 2.65 |
| | σ | 0.51 | 0.61 | 0.59 | 0.56 | 0.63 | 0.60 | 0.63 | 0.54 | 0.60 | 0.61 | 0.68 | 0.60 |
| | σ/\bar{x} | 18.8 | 24.8 | 25.2 | 21.4 | 23.3 | 23.0 | 26.9 | 23.0 | 25.4 | 22.5 | 25.9 | 22.6 |
| Cesium-137 (pCi/g K) | \bar{x} | 21.1 | 19.0 | 18.8 | 20.6 | 21.5 | 21.4 | 18.6 | 18.6 | 19.3 | 22.5 | 21.0 | 21.1 |
| | σ | 4.1 | 3.1 | 3.0 | 3.7 | 4.8 | 4.2 | 4.1 | 4.0 | 4.0 | 4.0 | 3.6 | 3.8 |
| | σ/\bar{x} | 19.4 | 16.3 | 16.0 | 18.0 | 22.3 | 19.6 | 22.0 | 21.5 | 20.7 | 17.8 | 17.1 | 18.0 |
| Cesium-137 (pCi/kg) | \bar{x} | 40.3 | 36.3 | 34.4 | 37.8 | 39.6 | 38.4 | 34.4 | 35.0 | 34.9 | 39.5 | 39.0 | 38.5 |
| | σ | 7.4 | 7.4 | 6.2 | 6.5 | 7.8 | 6.3 | 7.1 | 7.1 | 7.7 | 7.0 | 7.8 | 9.7 |
| | σ/\bar{x} | 18.4 | 20.4 | 18.0 | 17.2 | 19.7 | 16.4 | 20.6 | 20.3 | 22.1 | 17.7 | 20.0 | 25.2 |

^aWhere \bar{x} is the mean, σ the standard deviation, and σ/\bar{x} the standard error.

"lows" in summer and winter (Fig. 1).

MacDonald *et al.*⁵ reported a very slowly decreasing level of cesium-137 in residents of Los Angeles, California, during 1968 and 1969. Shukla *et al.*⁶ reported a concentration of 18 to 20 pCi/g K for 1969 with "very little change in level in 1970 and 1971." Averages of the monthly values for total whole-body activity of cesium-137 for 1970,

1971, and 1972 were 2.49, 2.60, and 2.54 nCi, respectively. According to Sivintsev,⁷ this level would produce annual doses of 0.42, 0.43, and 0.42 mrem in a 70-kg body, less than 1/30th of the dose delivered by 120 g potassium to a 70-kg body.

REFERENCES

1. C. R. Richmond and J. E. Furchner, Cesium-137 body burdens in man: January 1956 to December 1966, *Radiation Res.* **32**, 538-549 (1967).
2. C. R. Richmond and J. E. London, Cesium-137 content of New Mexico control subjects: July 1966 through June 1967, *In: Los Alamos Scientific Laboratory Report LA-3848-MS* (1968), pp. 75-79.
3. Section I. Milk and Food, Milk Surveillance, June 1971, *Radiological Health, Data and Reports* **12**, 501-510 (1971).
4. C. R. Richmond, J. E. London, and J. S. Wilson, Cesium-137 content of New Mexico control subjects, *In: Los Alamos Scientific Laboratory Report LA-3610* (1966), pp. 170-176.
5. N. S. MacDonald, I. Ban, A. Flesher, and M. Hackendorf, ¹³⁷Cs levels in human adult population in California, 1960-1969, *Nature* **228**, 283-284 (1970).

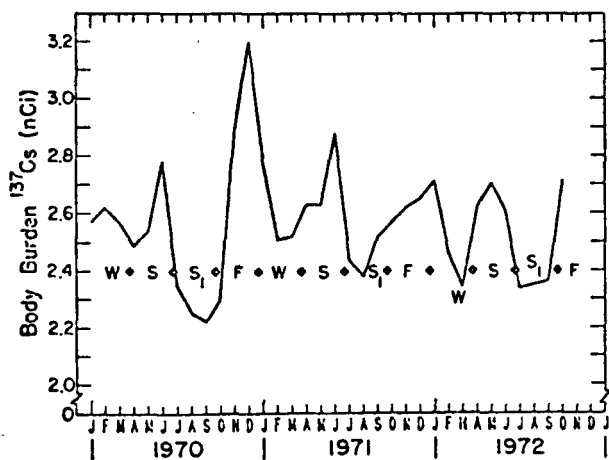


FIG. 1. Whole-body burden of cesium-137 in a New Mexico population sample. The closed diamonds separate the seasons: (W) winter, (S) spring, (S₁) summer, and (F) fall.

6. K. K. Shukla, C. S. Dombrowski, and S. H. Cohen, Fallout ^{137}Cs levels in man over a twelve year period, In: Brookhaven National Laboratory Report BNL-16927 (1972), pp. 1-9.

7. Y. V. Sivintsev, V. A. Kangreikin, and O. M. Arutinov, Change in the ^{137}Cs concentration in humans, Radiobiologiya 6, 822 (1966).

PHYSICAL RADIOBIOLOGY SECTION

INTRODUCTION

The Physical Radiobiology Section was formed in April 1972 to provide analytical and instrumentation support to the Biomedical Research Group. Personnel in the section are available to interact with all research programs in the group. Specific efforts of the section can be divided into the following six broad areas:

(1) Radionuclide assay, which includes whole-body counting, lung counting for transuranic elements, instrumentation for retention and excretion experiments (including Hot Particle Program), and production of radioactivity standard sources.

(2) Theoretical radiobiology, which includes computer models of dose and response, theoretical dose distribution in tissue (e.g., for hot particles and mesons), theoretical dose-response functions (based on empirical data and on cellular models), and support to Molecular Radiobiology Program.

(3) Dosimetry, which includes instrumentation for radiobiology experiments, including dosimetry of X rays, gamma rays, alpha particles, electrons, and negative pions.

(4) Dedicated computer developments, which include applications for whole-body and lung counting, chromosome analysis, lung structure and particle distribution studies, and biophysical applications.

(5) Consultation, which includes computer software for use by other sections of the Biomedical Research Group, including development, maintenance, and instruction in use of the local terminal for remote input to the central computer facility.

(6) Electronics development, which includes design and construction of specialized electronics as required.

As illustrated in the following examples, there has been considerable progress in each area. Although not reported below, members of the section provided some support in preparing the dosimetry

section of the grant application to the National Cancer Institute for preclinical studies for pic radiotherapy. Two members of the section are committed full-time to the dosimetry and radiobiology portions of this project. Another effort not described in this report, due to incomplete results, is a collaboration with the Molecular Radiobiology Section to attempt to understand and analyze DNA "melt" curves, an effort which should be completed within 1973. The chest counter for detecting low-energy photons (described in the previous annual report)¹ has been in routine use for the past year. All Laboratory personnel who work actively with transuranic elements are now counted at least once per year. Whole-body counting efforts have expanded somewhat in the past year. All personnel who work with the linear accelerator being constructed at LAMPF are being counted to obtain background information that will make it possible to interpret any future exposures that may occur when the accelerator is in operation.

AUTOMATION OF DATA COLLECTION

(M. T. Butler)

NaI (Tl) Spectrometer and Transuranium Element Chest Counter Interface with PDP-8/I Computer

A PDP-8/I computer with 12K core memory, a 32K disk, and oscilloscope display have been interfaced to the LASL total-body spectrometer and lung counter. The usual pulse-height analyzer has been replaced with two analog-to-digital converters and an interface to the computer. The interface includes a clock and switches that control the mode of operation of the system. These include codes for starting and stopping data collection and for selecting subgroup, counting time, type of output, and counting mode. There are two counting modes: one for chest counting, and one for whole-body counting using a 9-in. diameter by 5 in. thick NaI (Tl) crystal.

The end result is a 1054-channel pulse-height

analyzer with on-line data processing capabilities, ID inputs for subjects, presetable live counting time, large storage capability, visual display of counting data, high-speed printer, high-speed punched paper tape and teletype output, and counting programs which may be modified at will.

BUMCO II Interface with PDP-8/F Computer

This interface has progressed through the design stage and is now in the construction phase, and we expect completion by early 1973. The integrated system will consist of an amplifier, analog-to-digital converter (ADC), switch panel, ID panel, and a PDP-8/F computer with ASR-33 teletype. The ADC control section will plug directly into the computer and control transfer of pulse-height information from the ADC to the computer. The "interrupt" bus of the computer will be utilized with data being transferred through the accumulator. There will be a switch and ID panel external to the computer but connected to it by cables. Switches will be available for starting and stopping the counting and to set the counting time. Other switches will be available to enter information to identify the subject being counted.

Graf-Pen Interface to PDP-8/E Computer

A Graf-Pen, manufactured by Science Accessories Corporation, has been interfaced to a PDP-8/E computer to permit computerized on-line graphic analysis. The unit has a 14-in. square table with long microphones along two adjacent sides. Pressing a special pen against the surface of the table generates a spark and starts two scalars. Arrival of the sound wave from the spark at the microphones stops the scalars, the counts in which then represent the X and Y coordinates of the pen. This information can be read directly into the computer. The integrated system includes an oscilloscope for visual display of the data being entered, an ASR-33 teletype for data printout and communication with the computer, and a high-speed paper-tape reader.

The interface decodes computer instructions, generates gating signals, inputs data into the computer, accepts a "data-ready" signal from the Graf-Pen, notifies the computer that data are ready by providing appropriate control signals, and processes data and control signals between the Graf-Pen and computer to make them compatible. The interface was

built in a DEC Wire Wrap Board and plugs directly into the computer with connections to the Graf-Pen.

ANALYTICAL SUPPORT

(P. W. Dean and J. H. Jett)

Chest and Whole-Body Counting Data Analysis

During 1972, the dual-crystal, phoswich-type lung counter has been in routine operation. Recently two major changes in the system have been made: a new set of electronics is used for background suppression, and the multichannel pulse-height analyzer has been replaced with a PDP-8/I computer programmed to accomplish both data collection and analysis. The new method of background suppression based on pulse-shape discrimination is centered around an ORTEC-458 pulse-shape analyzer, a device which produces an output pulse whose amplitude is proportional to the rise time of the input pulse from the detector. The window of an internal single-channel analyzer (SCA) is set to provide gating pulses which correspond to interactions in the thin NaI (Tl) portion of the detector. The SCA output is used to gate the detector signal into an analog-to-digital converter (ADC). Large overload pulses caused by cosmic rays are detected by an integral discriminator whose output is used to block the counting system for 250 μ sec. Figure 1 shows a block diagram of the system.

The computer component of the lung-counting system is a PDP-8/I with 12K words of core memory, a 32K word disk, an oscilloscope display, and a LASL-built interface. The interface couples two ADCs to the computer and provides the computer with

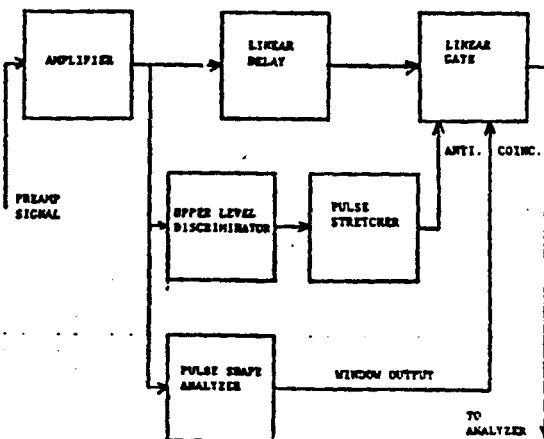


Fig. 1. Block diagram of electronics.

signals and codes for starting and stopping data collection, group selection, counting time selection, output selection, and counting mode selection. There are two counting modes: one for lung counting using the two dual-crystal assemblies, and one for whole-body counting with a 9-in. diameter by 4 in. thick NaI (Tl) crystal.

A computer program written for the system has the following capabilities. In the lung-counting mode, the number of channels per subgroup is set, the subgroup for data storage is determined from the switch panel, and counting for a preset time is initiated on receipt of a signal from the EXECUTE switch on the interface. During the counting period, data are displayed in a live time mode so that the complete incoming spectrum can be observed. Additionally, another spectrum can be displayed simultaneously either beside or overlapping the active spectrum.

Upon completion of the count period, data can be printed on a strip printer and are ready for analysis. The analysis part of the code proceeds as follows. After several items of bookkeeping data are recorded on the teletype, the subject's chest wall thickness measurements are entered and averaged, and calibration factors for the individual being counted are calculated. The background spectrum is then subtracted from the subject's spectrum and stored as a net spectrum. Count rates in the various regions of interest are calculated, as are lung burdens and standard deviations for ^{241}Am , ^{238}Pu , and ^{239}Pu . Results are printed on the teletype, and net spectra are displayed for photographing. In the 9 x 5-in. whole-body counting mode, the system operates in the same way except some of the constants are changed and the analysis consists of simply calculating net count rates.

The use of a dedicated computer in advanced chest- or whole-body counting systems provides more versatility and allows for on-line data analysis. Data can be obtained in real time by more personnel (including technicians), and radiation protection personnel are no longer dependent upon one or several people who, in the past, knew the required computer programming necessary to obtain estimates of body contamination.

As flow microfluorometry (FMF) systems are applied to a wide variety of biological experiments, the demand for improved methods of data analysis has increased. The primary objective in current experiments is to determine the number of cells in various phases of the cell life cycle. Some DNA distributions now being measured are basically different from distributions obtained with randomly growing CHO cells. Analysis of the latter has been accomplished by fitting with least-squares techniques the normal distributions to the G_1 and $G_2 + M$ populations and a second-degree polynomial to the S distribution. The polynomial is broadened to account for instrumental and preparation effects. A typical spectrum is shown in Fig. 2.

This method of analysis works well only for randomly growing cells. It cannot be used for synchronized populations such as those obtained when the cell system is arrested in G_1 and then released. Two methods of attacking this problem are being evaluated. The first method is to fit a G_1 control population (obtained by mitotic selection) with a normal distribution to determine peak coefficient of variation and mean. Ten normal distributions with constant coefficient of variation are then evenly spaced between the G_1 and $G_2 + M$ peak locations, and their areas are adjusted by a least-squares technique so that the sum of the 10 normal distributions yields the input spectrum. Although this method will accurately reproduce the input spectrum, 10 normal distributions do not provide enough resolution to determine accurately the proportions of the spectrum in G_1 , S, and $G_2 + M$. A

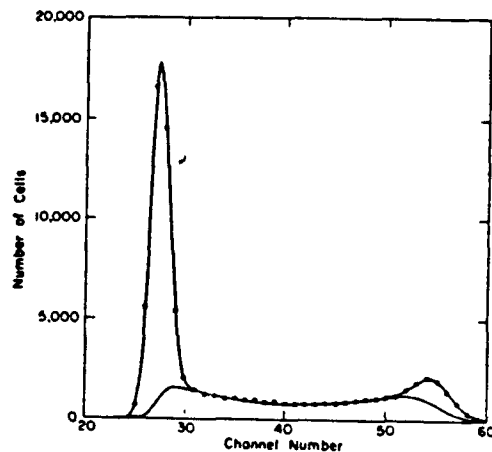


Fig. 2. Computer analysis of a randomly growing CHO cell population.

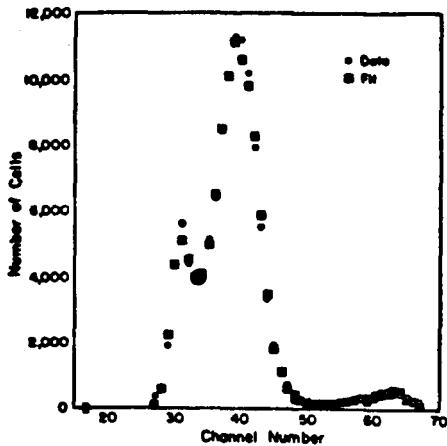


Fig. 3. Computer analysis of a synchronized cell population.

typical example of results obtained by applying this method is shown in Fig. 3. Variations of this method are now being studied.

A second method of analysis being studied utilizes a technique used in neutron physics called "spectrum unfolding," which basically consists of determining machine response for a pure G_1 population of cells and then solving the matrix equation relating true DNA spectrum to observed DNA spectrum through machine response functions.

HUMCO II Data Analysis

The LASL radioactivity counter for human subjects (HUMCO II), in routine operation since 1962, is used (1) to measure the amount of potassium and ^{137}Cs in humans; (2) to determine the biological half life of radioisotopes in both animals and man; and (3) for other counting problems where high counting efficiency is required and limited energy resolution can be tolerated. At present, the data collection system consists of 6 single-channel analyzers, scalars, and associated readout electronics which drive an IBM-526 card punch. Data are coded on cards and processed by the large computers in the LASL central computer facility (CCF).

Primarily because of age and obsolescence, the electronics recently have become unreliable. After examining the alternatives, we determined that the most economic replacement would be a small computer with a 4000-word memory, an analog-to-digital converter, and data input panel. The computer program which will control the system has been written and is awaiting arrival of the computer for final debugging. Initially, the system will be able to

store a 128-channel double-precision spectrum for a live time counting period that is entered on the data panel. At the end of the count period the spectrum is summed over 6 regions, and the count rates in each of the regions are calculated. Class codes which are read from the data panel are used to route the data so that background rates are stored in the proper location and calibration factors are calculated for the proper isotope and stored. When human subjects are counted, potassium and ^{137}Cs burdens are calculated. The data are printed and punched onto paper tape.

Future development of the computer program will include the capability of direct calculation of retention and excretion functions. We expect that within FY 1973 all required calculations will be performed on the small computer with no recourse to the large CCF computers required.

KARYOLOGY

(P. N. Dean)

Semi-Automatic Chromosome Analysis

A central question in the biological sciences is the mechanism by which eukaryotes maintain order in their genetic material. A technique for obtaining some information concerning the cell's manipulation of its genome involves study of the morphology of metaphase chromosomes of dividing cells. Such a technique permits continuous monitoring for ploidy drift in cultures carried for extended periods both as a control feature and as a means for determining whether specific segments of the genome are essential for survival.

Improvement in the technique for chromosome classification, described herein, was motivated by the requirement for still more rapid, routine karyotypic examination of a variety of diploid and heteroploid lines in culture. Recent studies at this Laboratory have raised further questions concerning the identity of chromosomes in heteroploid lines by apparently ruling out nondisjunction and supporting the idea that identical amounts of DNA may be incorporated in varying chromosome numbers through changes in chromosomal condensation-kinetichore development systems. One approach to testing this contention involves the precise karyotyping of as many of the chromosomes in heteroploid

of a monolithic integrated circuit; thus, they are very nearly identical electrically and, because of the common substrate, very close thermal coupling exists. LM-301 amplifiers were used because of low cost. The rise time of 5 μ sec and dynamic range of over one decade were adequate for the experiment. Greater range can be obtained by choosing an amplifier with lower input current.

Amplifier with Base-Line Restoration

Most detectors used to drive electronic amplifiers have a DC offset in terms of voltage or current upon which the real signal is superimposed. In some cases, this steady-state value may be many times larger than the signal and, in addition, may vary enough to make simple subtraction impractical. The usual solution is capacitive coupling, which blocks the DC effectively but introduces base-line shift as the repetition rate increases. Passive clipping circuits using diodes eliminate most of an "undershoot" but have an offset of several hundred millivolts. In addition, the amplitude of a closely following pulse will be reduced because recovery is not complete.

An active base-line restorer, using an operational amplifier with fairly high open loop gain, overcomes both problems. The base line can be adjusted for zero offset, and the recovery time is reduced to a very small value because the total output of the amplifier is available to "jerk" literally the base line back to zero.

Two amplifiers were required for the cell separator unit. The signals to be detected consist of a small change in aperture current (from a Coulter counter) and a change in photomultiplier anode current (fluorescence detector). For successful operation at high counting rates, base-line restoration is required. One amplifier uses 301 operational amplifiers for rise times of about 5 μ sec, and the other uses 715 operational amplifiers for rise times of less than 0.5 μ sec. The latter will handle repetition rates up to 3×10^5 pulses per second or paired pulses separated by only 1.5 μ sec.

PION BEAM CHARACTERISTICS

(C. Richman and W. D. Jinks)

Small silicon detectors (lithium-drifted and surface-barrier) are being tested for possible use

in studying contamination and properties of the pion beam at the LAMPF. Electronics used with these detectors are conventional NIM linear and logic modules with pulse-height analysis. However, because of various types of radiations occurring in the pion beam (components of varying linear energy transfer, LET), it will be necessary to have a detailed knowledge of the pulses being produced in the detectors. By choosing the thickness of the detectors appropriately, various properties of the beam can be brought to the foreground. Thus, in thin detectors of 100 μ or less, the large pulses will be due to stars. By this means, mapping of the stars will be determined which will be a direct measurement of the momentum spectrum of pions.

To study the pulses from electrons, a $\Delta E-E$ arrangement has been built with 2 silicon detectors. A ^{207}Bi test source is used, and the E detector selects the 2 high-energy conversion electrons (974 keV and 1047 keV) in the spectrum. The ΔE detector (300 μ thick) then measures energy loss of these electrons. Because these electrons produce minimum ionization, they give pulses that would be produced closely by 200-MeV contamination of the pion beam.

A clear line at around 110 keV is obtained for energy loss in this detector system, and the Landau width does not appear to be very serious. The Landau spread will be studied with different detector thicknesses. At present, we feel that electrons will be distinguishable from pions.

To prepare for the tumor therapy program, phantom materials in the form of slabs are being made in the LASL shops and in the Materials Technology Group (CMB-6). These specially formulated plastic compounds would approximate bone, lung, muscle, soft tissue, and fat. A movable probe with location readout also is being designed so that mapping of the beam can be studied in these mock tissues. We also plan to study transition regions from one tissue to another. At present, this aspect of the pion dosimetry program is funded from non-AEC sources.

REFERENCE

1. C. R. Richmond and G. L. Voelz, eds., Annual Report of the Biological and Medical Research Group (H-4) of the LASL Health Division, January through December 1971, Los Alamos Scientific Laboratory report LA-4923-PR (1972), pp. 116-118.

BIOPHYSICS SECTION

INTRODUCTION

During the past year, the Biophysics Section has been reorganized because of the formation of a new section, Physical Radiobiology, within the group. This new section assumed the responsibility for physical radiobiology, computer applications, and electronics support formerly charged to the Biophysics Section, and these activities are described elsewhere in this report. The Biophysics Section is now solely concerned with research and development programs in the general area of biophysics and instrumentation with the current major emphasis on development and application of rapid methods for cell analysis and sorting. This major effort is divided into three main areas: (1) physical investigations of the light scattering and other properties of mammalian cells that might be measurable by our instrumentation, (2) development of instrumentation for cell sorting and analysis, and (3) applications of these methods to biological problems. Our success, particularly in this latter area, has been possible because of excellent cooperation with members of the Cellular Radiobiology Section.

Flow microphotometry, the method of making rapid optical measurements on individual biological cells, is an exciting and important emerging technology in cell research and has been pioneered by personnel of the Biophysics Section at Los Alamos. This development grew from our early efforts in quantitating Coulter counting techniques which resulted in improved Coulter volume spectrometry and cell sorting based on cell volume. Flow microfluorometry (FMF) is our most important contribution to date in the area of optical measurements on single cells.

During 1972, FMF was used routinely by LASL personnel as well as by investigators from other laboratories who visited LASL (Salk Institute, Karolinska Institute, Cold Spring Harbor Laboratory, University of Houston, University of Texas at

Austin, University of New Mexico, University of Colorado, and University of California at Berkeley). In most of these experiments, cellular DNA was the important parameter measured. In such cases, FMF measurements were made on cells treated by the fluorescent Feulgen method.

A two-color fluorescence sensor has been incorporated into our multiparameter cell sorter. Use of the bi-color fluorescence detector has allowed us to study acridine orange-stained human leucocytes that exhibit bi-color fluorescence. We have used cell sorting techniques to show that the cells, based on their red fluorescence, can be classified as lymphocytes, monocytes, and granulocytes. We have also initiated work designed to obtain nuclear-to-cytoplasmic ratios based upon nuclear and cytoplasmic fluorescence; ethidium bromide-stained DNA yields red fluorescence, and fluorescein-stained protein produces green fluorescence.

A dual-parameter cell analysis photometer was also designed and constructed during 1972. This device measures fluorescence and small-angle light scattering simultaneously on each cell as it passes through the laser light in a flow photometer. Our present application uses light scattering to gate electronically for fluorescence analysis, permitting an electronic "clean up" of the signal in those cases where the signal would not be discernible from noise present in debris-laden biological samples.

More extensive theoretical studies on light scattered by biological cells were conducted during 1972. High-speed computers were used to calculate light scatter from coated spheres to simulate mammalian cells, the core representing the nucleus and the coating the cytoplasm. Results of the computer calculations indicate that the forward light scattering is dominated by gross size of the cell. Outside the forward direction, the scattering pattern is a function of both nuclear and cytoplasmic optical properties. Experimental scattering patterns also were obtained for suspensions of various cell types. In cases where cell

volume distribution, ratio of nuclear-to-whole cell diameter, and other properties are well defined (a.g., G₁ phase CHO cells), a high degree of correlation was obtained between experimental and theoretical scattering patterns. To our knowledge, this is the first time that such a complete physical description of light scattering from mammalian cells has been obtained. These studies hold promise for cell identification on yet another parameter measurable with our flow systems.

In addition to the experiments mentioned above, biological applications of our physical methods have been pursued with other personnel at the LASL and with others as part of our mutual-interest programs with the U. S. Department of Agriculture and the National Cancer Institute. These collaborative efforts include effects of stressing agents such as radiation, temperature, and chemicals on the life cycle of mammalian cells; ploidy studies on transformed mammalian cells; comparison of chromosome banding techniques with DNA determinations by FMF techniques; DNA determinations on several transplantable tumors; applications of cell sorting to human cervical material; improved methods of cell and tissue preparation for FMF applications; fluorescent antibody techniques; investigation of light scattering techniques as a possible indication of viral infection of mammalian cells; and binding of plant lectins such as fluorescein-tagged concanavalin A to cell surfaces.

The unique cell-analysis methods developed here at the LASL are receiving increasing attention within the scientific community. In this respect, one of us (M. A. Van Dilla) has been invited to participate in the establishment of a similar effort at the Lawrence Livermore Laboratory of the University of California. Dr. J. D. Watson of the Cold Spring Harbor Laboratory invited two of us (L. S. Cram and H. A. Crissman) to participate in the summer program at Cold Spring Harbor. These two scientists and an FMF unit were sent there to demonstrate the FMF technique. In addition to the institutions listed above, investigators from both the United States and abroad have sent us samples for FMF analysis as part of mutual-interest studies.

We are also pleased to report that A. Brunsting, an Associated Western Universities pre-doctoral fellow from the Physics Department at the

University of New Mexico, successfully completed the Ph.D. requirements in August 1972. During his stay at the LASL, Dr. Brunsting participated in the Biophysics Section's effort on the theoretical and experimental aspects of light scattering.

CELL ANALYSIS AND SORTING INSTRUMENTATION DEVELOPMENT

(A. Brunsting, J. R. Coulter, L. S. Cram, J. L. Horney, J. C. Martin, P. F. Mullaney, J. A. Steinkamp, M. A. Van Dilla, and W. T. West)

Differential Light-Scattering Signatures of Mammalian Cells

As we reported in the 1971 annual report,¹ mammalian cells have been simulated in computer models as coated spheres, the core representing the nucleus and the coating cytoplasm. Exact electromagnetic theory calculations² for individual particles with cell-like optical parameters indicate that light scattered in the forward direction is dominated mainly by the gross silhouette of the particle and contains information on particle size and that beyond the forward lobe the scattering pattern from a coated particle is significantly different from a simple homogeneous sphere. In the latter case, the scattering pattern is dependent upon optical properties of both the core and coat.

During 1972 some of our theoretical predictions have been tested with suspensions of mammalian cells. A simple but unique light-scattering photometer³ was constructed for this purpose and is shown schematically in Fig. 1. The photometer is housed in a 2.5-foot-diameter cylinder. Control of light from a 5-mW helium-neon laser (Spectra Physics Model 120) into the photometer is by shutter. The light then passes through a variable aperture to reduce extraneous nonlasing light and is reflected from a front surface mirror through a specially designed cuvette. The main laser beam and some forward scattered light are collected in a Rayleigh horn beam dump. Light scattered by the particles in the cuvette is recorded on high-speed, red-sensitive film (Kodak 2479 RAR ASA 400, 16-mm x 125-foot rolls) which is held in a track on the inside surface of the photometer. Approximately 34 exposures can be made from each roll of film. Fiducial markers on the film holder cast shadows on the film at 30°

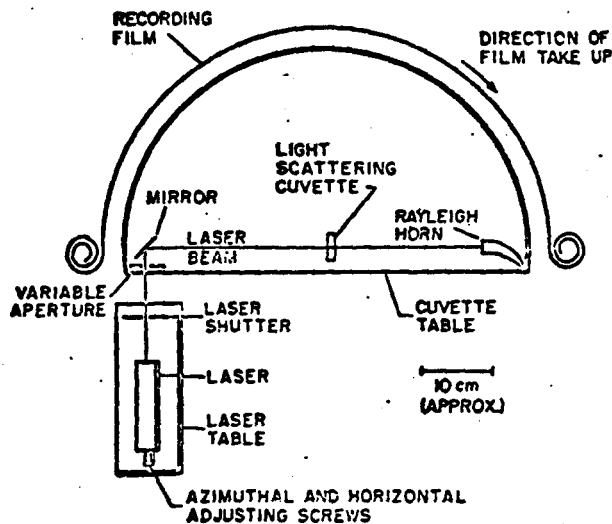


FIG. 1. Schematic diagram of the film photometer. The laser provides incident light to the scatterers in the cuvette. Most of the laser light is dumped into the Rayleigh horn while the film records the scattered light.

intervals, permitting film dispersion to be measured on each exposure. After exposure, the film is developed in a Kodak Versamat Model 11c using type B chemistry. This procedure produces a typical dynamic range of three decades, which can be extended by allowing some overlap between exposures and reducing intensity in the forward direction by use of neutral density filters. Developed film is read with a microdensitometer. Through the use of suitable calibration, film density as a function of distance on the film can be converted into scattering intensity as a function of scattering angle. Using these techniques, we have obtained scattering patterns for the angular range of 2.5 to 177°.

It is well known that angular positions of the maxima and minima in the scattering pattern are important functions of particle size.⁴ For this reason, in a suspension of particles which are similar in composition but not identical in size, some smearing out of the scattering pattern should be expected. Therefore, it is important that the mean size, size distribution, and refractive index of the particles are well characterized. One also needs to establish that the photometer has sufficient resolution to record the essential features of the scattering pattern of interest. This last consideration was accomplished by a calibration

procedure which uses extremely uniform diameter polystyrene microspheres produced at the Los Alamos Scientific Laboratory.⁵ The refractive index of the spheres was measured by an immersion technique and found to be 1.562 ± 0.002 (with respect to air). Optical microscopy and Coulter volume spectrometry measurements of the spheres provided information on mean diameter (10.5 microns) and coefficient of variation of volume (3 to 4 percent).

Light scattering measurements made at concentrations of 5×10^4 particles/ml are shown in Fig. 2. At this concentration, the particles behave as independent scattering centers (i.e., increasing the concentration produces a proportional signal increase with no change in shape of the scattering curve).

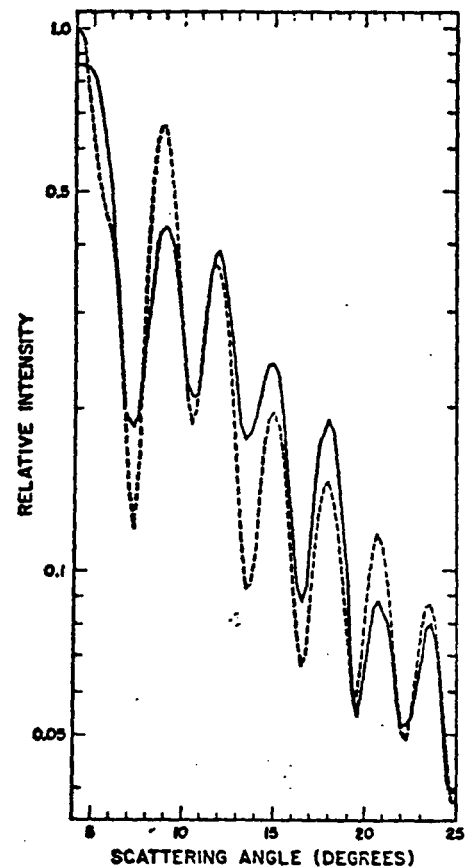


FIG. 2. A comparison of theory and experiment for the microspera scatterers. A semi-log scale of the relative intensity, computed (thin) and measured (thick), versus scattering angle, θ , in degrees. Theory accounted for the size distribution of the spheres and angular resolution of the photometer. The experimental curve was corrected for photometer scattering by transmission properties of the cuvette. Theoretical curves are given by dashed lines and experimental by a solid line.

Theoretical results are shown by the dotted curve and experimental results by the solid curve. Although the curves do not match exactly in shape, their maxima and minima agree quite well (Table 1). The agreement between theory and experiment confirms the accuracy of measured size distributions for the spheres based upon microscopic and Coulter volume spectrometric measurements. Light-scattering measurements yield a mean diameter of 10.3 microns as compared with 10.5 microns as determined by other methods.

The difference in relative intensity between the two curves (Fig. 2) is caused by a number of factors. Although uniform in diameter, the spheres are not smooth, and optical microscopy shows them to have a golfball-like surface. Theoretical calculations assumed a perfectly uniform sphere. In addition, there is an uncertainty of about 5 percent in measurement of film density response characteristics which is not a linear function of intensity. The fact that the maxima and minima agree so well demonstrates that the film photometer has sufficient resolution to measure the main characteristics in the scattering pattern obtained from particles with the dimensions of mammalian cells.

For all particles studied by this method, mean size, size distribution, and refractive index were measured. The computer codes written for individual particles were modified to account for size distributions. Thus, at each scattering angle, we could obtain the calculated intensity contribution from each particle in the distribution. These results were then weighted according to the measured diameter distribution and integrated across this distribution function to yield the theoretical curves

TABLE 1. LOCATIONS OF MAXIMA AND MINIMA FOR THEORY AND EXPERIMENT IN THE CASE OF PLASTIC MICROSPHERES (see Fig. 2)

| Theory ($\pm 0.15^\circ$) | | Experiment ($\pm 0.2^\circ$) | |
|-----------------------------|--------|--------------------------------|--------|
| Maxima | Minima | Maxima | Minima |
| 4.25 | 7.25 | 4.5 | 7.2 |
| 9.00 | 10.50 | 9.0 | 10.5 |
| 11.75 | 13.50 | 11.9 | 13.6 |
| 15.00 | 16.50 | 15.0 | 16.5 |
| 18.00 | 19.50 | 17.9 | 19.3 |
| 20.75 | 22.25 | 20.8 | 22.1 |
| 23.50 | 24.75 | 23.5 | 25.0 |

shown in this report. Details of this approach are given elsewhere.⁶

Measurements were made on several tissue culture cell lines and results for Chinese hamster cells (line CHO)⁷ are reported here. Using the technique of Tobey *et al.*,⁸ cells were synchronized in the M stage of the life cycle. Scattering measurements were made for these cells and for cells allowed to enter early G₁. Experimentally determined light-scattering curves then were compared with theoretically derived curves for coated spheres of the appropriate parameters and equivalent homogeneous spheres.

Mean cell volume and volume distribution information on both CHO cells and spheres was obtained with a laminar flow Coulter volume sensor.⁹ CHO cells in G₁ were found to have a mean diameter of 11.5 microns and a volume coefficient of variation of 13.6 percent. Photomicrographs of several hundred of these cells were made, and the ratio of nuclear diameter to whole cell diameter was calculated to be 0.73 ± 0.08 . Using a phase microscopy technique,¹⁰ the refractive index of the nucleus and cytoplasm (with respect to air) was found to be 1.392 and 1.3703, respectively. However, cells are immersed in a water-like medium; in which case, these figures become 1.030 (cytoplasm) and 1.047 (nucleus). Barer¹¹ has shown that the refractive index (n) of cells and their density (d) are related by $(n - 1) \cdot d^{-1} = k$. From the work of Anderson,¹² which demonstrated that the density of CHO cells is quite constant, we infer that the refractive index is not very variable among these cells. This information was used to calculate theoretical scattering curves for CHO cells in the G₁ stage of the cell cycle. The computer program treats the refractive indices of both nucleus and cytoplasm as being constant for the values stated above. The ratio of nuclear diameter to whole cell diameter was also assumed to be constant and equal to 0.73. Mean volume and volume distribution of these cells were also incorporated into the computer program. We also calculated light scattering from an equivalent homogeneous sphere in which the mean refractive index was equal to the volume-averaged refractive index of the nucleus and cytoplasm.⁶ A comparison of these two theoretical results with experimental data is shown in Fig. 3.

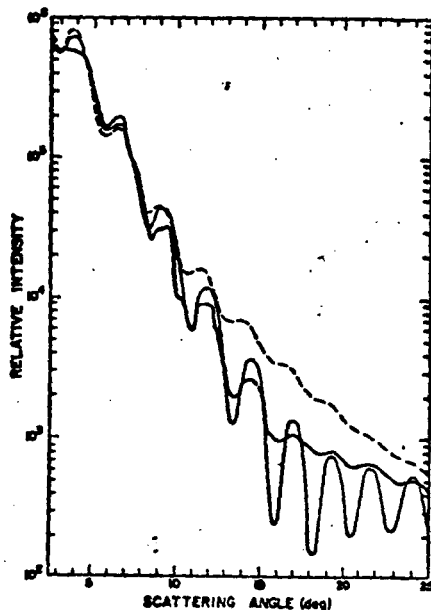


FIG. 3. Two theoretical plots and corresponding experimental results for the differential scatter patterns for G_1 Chinese hamster ovary cells. The coated sphere (thin solid line), the equivalent homogeneous sphere (thin dashed line) whose refractive index has been volume-averaged from the coated sphere, and the experimental results (thick solid line) are shown.

The log of the scattering intensity is plotted as a function of scattering angle. Experimental results are given by the heavy solid curve, coated sphere theoretical results by the light solid curve, and equivalent homogeneous sphere theoretical results by the dashed curve. Experimental results were obtained with cells in a concentration of 10^5 cells/ml. Below 7 to 8° all three curves agree quite well, indicating that gross size effects primarily dominate the scattering response in this angular region. Beyond 8° the light scattering from the coated sphere is considerably less than that from the equivalent homogeneous sphere. The position of the experimental maxima and minima agrees quite well with theoretical results for coated spheres, although there is some wash-out beyond roughly 15° , probably because of heterogeneity not accounted for in the model for CHO cells. The main feature of Fig. 3 is that actual cells behave much more like coated spheres than homogeneous spheres. Beyond the forward direction, the scattering curve reflects nuclear properties of the cell.

Figure 4 shows experimental scattering from CHO cells in M as compared with an equivalent homogeneous sphere. Unlike G_1 cells, these cells show

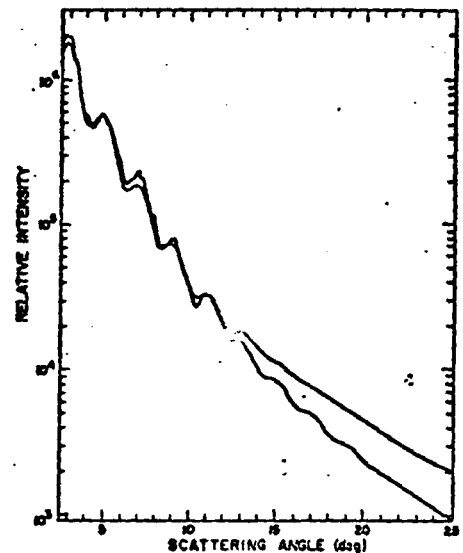


FIG. 4. Theoretical plot and corresponding experimental results for the differential scatter patterns for M Chinese hamster ovary cells in M. The equivalent homogeneous sphere (thin solid line) and experimental results are shown.

no well-defined nucleus. In this case, CHO cells in M are quite well modeled as homogeneous spheres over the angular range of interest. We should note that virtually all the scattering by cells is contained in the first 25° .

These preliminary studies were conducted on suspensions of living cells. Perhaps the most interesting result is that light scattering at larger angles is influenced by the internal structure of the cells. We plan to incorporate a wide-angle light-scatter sensor on our flow photometers to investigate the possibility of wide-angle scattering as another parameter for cell identification in flow-system analysis.

REFERENCES

1. C. R. Richmond and G. L. Voelz, eds., Annual Report of the Biological and Medical Research Group (H-4) of the LASL Health Division, January through December 1971, Los Alamos Scientific Laboratory report LA-4923-PR (April 1972).
2. A. Brunsting and P. F. Mullaney, *Applied Optics* **11**, 675 (1972).
3. A. Brunsting and P. F. Mullaney, *Rev. Sci. Instr.* (1973), in press.
4. H. H. Blau, D. J. McCleese, and D. Watson, *Applied Optics* **9**, 2522 (1970).
5. L. S. Cram, M. J. Fulwyler, and J. D. Perrings, *Biophysical Society Abstracts* **11**, 155a (1971).

6. A. Brunsting, "Light Scattering from Mammalian Cells," Ph.D. Thesis, Department of Physics, University of New Mexico (1972).
7. J. H. Tjio and T. T. Puck, *J. Exp. Med.* **108**, 259 (1958).
8. R. A. Tobey, E. C. Anderson, and D. F. Petersen, *J. Cell. Physiol.* **70**, 63 (1967).
9. J. T. Merrill, N. Veizades, H. R. Hulett, P. L. Wolf, and L. A. Herzenberg, *Rev. Sci. Instr.* **42**, 1157 (1971).
10. R. F. A. Ross, "Phase Contrast and Interference Microscopy for Cell Biologists," Edward Arnold Company, London (1967).
11. R. Barer and S. Joseph, *Q. J. Microsc. Sci.* **95**, 399 (1959).
12. E. C. Anderson, D. F. Petersen, and R. A. Tobey, *Biophys. J.* **10**, 630 (1970).

Multiparameter Cell Sorter

A multiparameter cell analysis and sorting system for use in cell biology research and possible clinical applications has been developed. Cell samples stained with a fluorescent dye that specifically labels biochemical components of interest are suspended in physiological saline and introduced into a flow chamber where optical and electrical sensors measure cell volume (Coulter method), single- or two-color fluorescence, and scattered light. Signals from the sensors are electronically processed in a variety of ways to provide optimum cell discrimination and are displayed as frequency distribution histograms. Processed signals are also compared with preselected standards, and this triggers sorting of the desired cells. Populations of mammalian tissue culture cells, human leucocytes, and other samples have been analyzed and sorted.

Figure 1 illustrates a cut-away sectional view of the multiparameter cell sorter. Fluorescently stained cells dispersed in saline are introduced (1000 cells/sec) into a dual sheath flow chamber via the sample inlet tube. Flowing coaxially around the inlet tube is a particle-free sheath fluid (sheath No. 1) of saline. Because the flow is laminar, the cell stream and surrounding sheath do not mix but move together through a Coulter volume sensing orifice, where cell volume is measured electronically. The flow next enters a fluid-filled viewing region where it intersects an argon-ion laser beam, causing light scattering and fluorescence. Both these

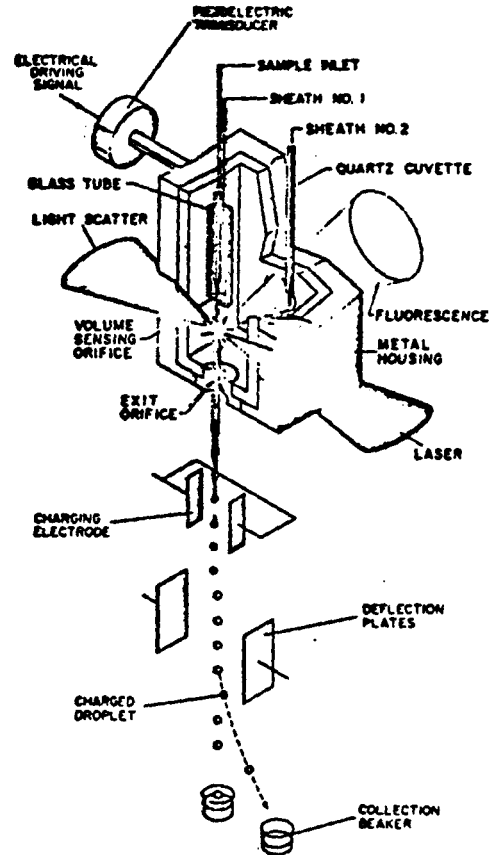


FIG. 1. The multiparameter cell sorter.

signals are electro-optically measured; the fluorescence sensor is a dual photomultiplier array which permits measurements of red and green fluorescence. Light scatter is measured in the forward direction by blocking the laser beam with an optical stop and focusing the forward scattered light onto a photodiode.

A second sheath fluid (sheath No. 2), also of saline, flows coaxially around the cell stream-sheath No. 1 flow. The total flow jets out into the air from an exit nozzle. A piezoelectric transducer mechanically coupled to the flow chamber and electrically driven at 45 kHz produces uniform liquid droplets (45,000/sec) by regularly disturbing the emerging jet. Cells are isolated effectively into single liquid droplets in this manner.¹ A group of droplets, one of which will contain a cell to be sorted, is electrically charged at the point of droplet formation (charging electrode) and is then deflected by a static electric field into a collection vessel.

Signals from the cell sensors are routed to a hard wired multiparameter analog signal processing

unit. Processed signals are then routed to a multichannel pulse-height analyzer, where frequency distribution histograms of cell volume, fluorescence, light scatter, or a combination of these parameters can be displayed. Processed signals also trigger cell sorting by comparing the amplitude of each processed signal pulse to a preset standard (i.e., if the signal amplitude falls within a preselected range, an appropriate electronic delay is activated which triggers a droplet charging pulse, causing the droplet containing the cell to be charged and subsequently deflected). A group of droplets, usually about 9, is then sorted from the main stream. Those cells failing to meet the criteria of the preset standards do not trigger sorting and are allowed to pass to a waste vessel. In a typical experiment 10^4 to 10^5 cells are sorted in a few minutes.

Figure 2a shows the volume and fluorescent Feulgen DNA histograms of Chinese hamster (line CHO)

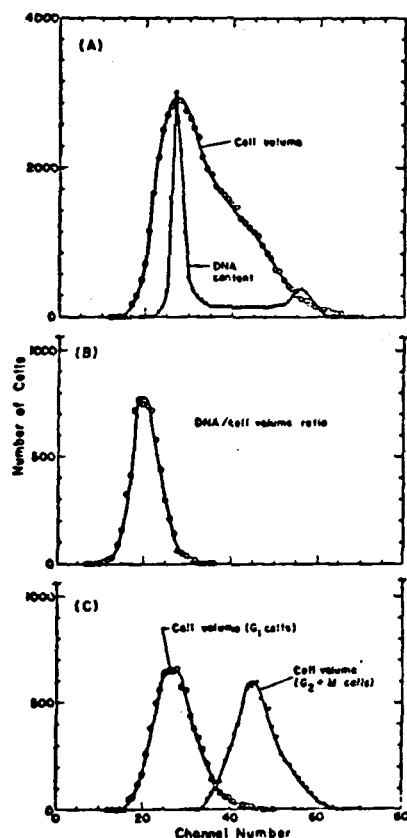


FIG. 2. Volume, DNA, and DNA-to-cell volume distribution histograms of Chinese hamster ovary cells growing asynchronously in suspension culture: (A) volume and DNA distribution; (B) DNA-to-cell volume distribution, and (C) volume distribution of G_1 and $G_2 + M$ cells.

cells growing asynchronously. These cells are stained with the fluorochrome acriflavine using the fluorescent Feulgen² procedure. DNA distributions show two peaks: the first represents the cells with diploid DNA (G_1 phase) having a coefficient of variation of 4 percent, and the second peak represents cells with tetraploid DNA content (G_2 and M phase). The region between the peaks represents cells synthesizing DNA (S phase). The ratio of G_1 and $G_2 + M$ modal fluorescence intensities of the two peaks is 2.04, very close to the expected value of 2.00. Cell volume distribution is broad, unimodal, and typical of a cell population in exponential growth. The DNA-to-cell volume ratio for this cell population, shown in Fig. 2b, is unimodal with a coefficient of variation of 15 percent. Volume distribution of G_1 cells (Fig. 2c) was obtained by analyzing only those Coulter sensor signals associated with the fluorescence signals indicating the G_1 amount of DNA (see Fig. 2a). Similarly, the volume distribution of $G_2 + M$ cells was obtained by analyzing only those Coulter sensor signals associated with the $G_2 + M$ fluorescence peak of the DNA distribution. Modal volume ratio ($G_2 + M$)/ G_1 is 1.7, less than the total volume increase over the life cycle of the cell (double) because the instrument is measuring average cell volume distributions of the G_1 and $G_2 + M$ phases.

The red and green fluorescence of human leucocytes supravivally stained with the metachromatic fluorochrome acridine orange³ is shown in Fig. 3. When leucocytes of diluted whole blood are stained according to this procedure, cytoplasmic granules exhibit red fluorescence whereas the nucleus fluoresces green. Erythrocytes do not take up the acridine orange stain. The bi-color fluorescence sensor was set to measure green and red fluorescence, and the cell sorting logic was adjusted to separate leucocytes having a red fluorescence corresponding to region 1. Differential microscopic counts on sorted leucocytes show that approximately 95 percent are lymphocytes. When the sorting logics are adjusted to separate cells lying within regions 2 and 3, subsequent microscopic counts show that 90 percent of the cells separated from region 2 are monocytes and that 95 percent separated from region 3 are granulocytes.

Because of the large ratio of erythrocytes to

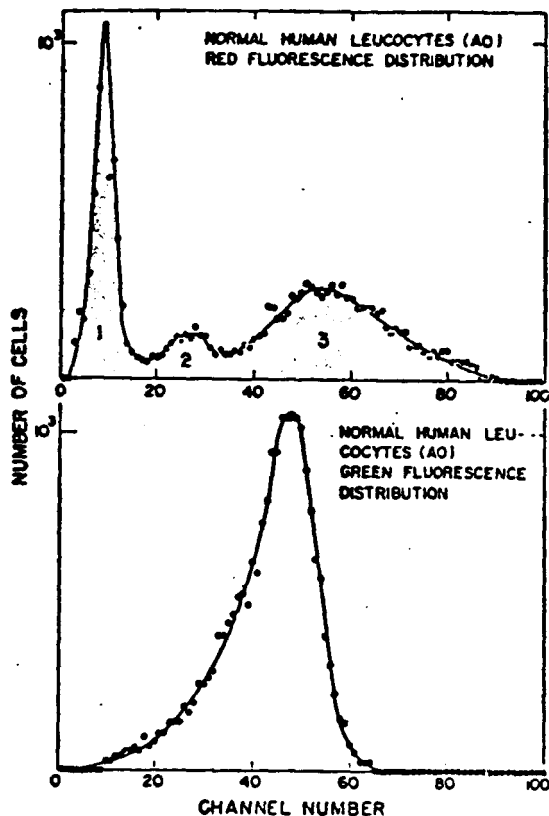


FIG. 3. Red and green fluorescence distribution histogram of normal human leucocytes supravivally stained with acridine orange.

leucocytes in normal human blood, leucocyte volume distributions cannot be obtained without prior saponin hemolysis of erythrocytes. This difficulty can be overcome by sorting all green fluorescing cells, thus producing a leucocyte-enriched sample. This sample is then reintroduced into the sorter, and the volume of cells showing only green fluorescence is measured.⁴ This method has the advantage of yielding a leucocyte volume distribution without requiring saponin hemolysis.⁵

A second multiparameter cell sorter is under construction presently, with a completion date of early 1973. This unit is intended to be dedicated to biological experiments, while the present sorter system continues to be used for some limited biological experiments coupled with instrument development (i.e., new cell sensing methods and determination of optimal detection parameters). Current experiments underway on the present cell sorter include ethidium bromide-fluorescein isothiocyanate (FITC) staining for DNA/cell protein studies, fluorescein-conjugated concanavalin A bound to membrane surface sites, continued study of

human and animal (hamster) leucocyte characterization with the metachromatic fluorochrome acridine orange, and work on cells from solid tumors and exfoliative material.

REFERENCES

1. M. J. Fulwyler, Electronic separation of biological cells by volume, *Science* **150**, 910-911 (1965).
2. R. A. Tobey, H. A. Crissman, and P. M. Kraemer, A method for comparing effects of different synchronizing protocols on mammalian cell-cycle traverse: The perturbation index, *J. Cell Biol.* **54**, 638-645 (1972).
3. L. R. Adams and L. A. Kamensky, Machine characterization of human leukocytes by acridine orange fluorescence, *Acta Cytol.* **15**, 289-291 (1971).
4. J. A. Steinkamp, A. Komero, and M. A. Van Dilla, Multiparameter cell sorting: Identification of human leukocytes by acridine orange fluorescence, *Acta Cytol.* (1973), in press.
5. M. A. Van Dilla, M. J. Fulwyler, and I. U. Boone, Volume distribution and separation of normal human leukocytes, *Proc. Soc. Exp. Biol. Med.* **125**, 367-370 (1967).

A Dual-Parameter Cell Microphotometer

During 1971, a dual-parameter microphotometer was developed and subjected to initial testing. The dual-parameter instrument described here represents a combination of the fluorescent microphotometer¹ and light-scattering photometer developed earlier.² Each cell stained with an appropriate fluorescent dye produces a pulse of fluorescent light, as well as a pulse of scattered light as it crosses a beam of blue light from an argon laser. These signals occur simultaneously and can be used as two descriptors for each cell. After detection, each signal is amplified and fed through a dual-parameter processing unit. If certain logical conditions are met, these two signals are then available for pulse-height analysis. The net result is a frequency histogram of fluorescence or light scatter of the cells of interest.

A schematic diagram of the dual-parameter photometer is shown in Fig. 1. The flow chamber is basically the same as that described previously.² Laminar flow is established within the chamber, and the cells are injected as the core of the main flow. Just prior to entering the viewing area, the entire

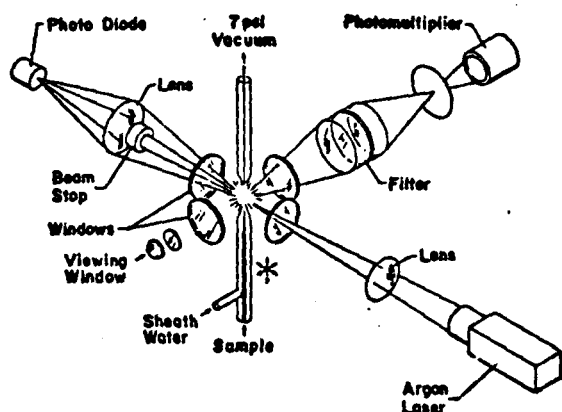


FIG. 1. Schematic of the dual-parameter flow micro-fluorometer. The argon-ion laser beam (lower right corner) is focused with a 20-cm lens to a 50-micron spot at the center of the flow chamber. Fluorescent light is detected at 90° to the incident direction. Light scattered in the forward direction between the central beam stop and outer stop is collected with a 10-cm lens and focused onto a photodiode.

flow moves through a constriction orifice which narrows the cell stream to a column about 20 microns in diameter. The cells are then lined up much as beads on a string as they intersect the laser light.

The light source for this photometer is a Coherent Radiation Laboratory Model 52GA argon laser operating at 1 watt at 488 nm. Laser light is focused with an 18-cm convex lens to form a 50-micron spot at the intersection with the cell stream at the center of the flow chamber. After passing through the laser beam, the cells exit out the top of the chamber and go to a waste vessel.

As each cell passes through the laser beam, it produces a 10-microsecond pulse of fluorescent and scattered light. The main laser beam is eliminated in a small trap. The cone of light scattered about this trap (approximately 0.7 to 2.0°) is collected with a 10-cm convex lens and focused on a photodiode. The resulting signal is then amplified.

The fluorescence signal is collected at 90° to the direction of the incident beam. Light then passes through a yellow barrier filter and is focused onto a 300-micron diameter pinhole. The fluorescent light emerging through the pinhole is viewed with an RCA Model C7164R photomultiplier tube selected for its extended red sensitivity. This signal is also amplified.

A box diagram of the dual-parameter signal

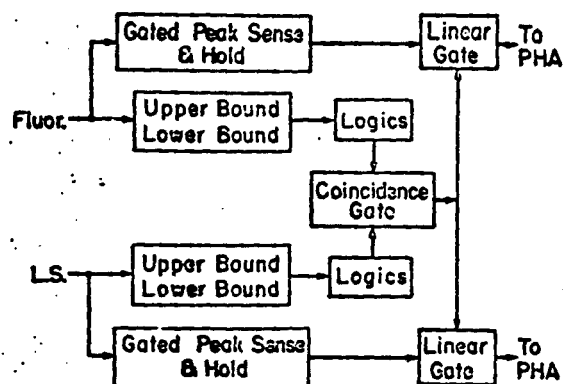


FIG. 2. Block diagram of dual-parameter signal-processing unit. When the conditions of coincidence and proper signal amplitude are met, both analog signals are passed for pulse-height analysis (PHA).

processing unit is shown in Fig. 2. In the present application, one signal is used to gate the second. After amplification, the signal from each of the two detectors is fed to separate adjustable discriminators. If both signals are within the appropriate amplitude range, they are then tested for coincidence. If both tests are positive, the analog signals are passed through a linear gate, and either or both signals are available for pulse-height analysis. The logics of Fig. 2 can be bypassed; in which case, the instrument functions as a single-parameter photometer.

A particularly useful application of the dual-parameter photometer is the analysis of fluorescence from weakly stained samples. Typically, 5×10^4 cells/min pass through the photometer, with each cell spending about 5 microseconds in the light beam. The total time that cells spend in the beam is then 5×10^{-1} seconds out of every minute; the photometer duty cycle is 0.83 percent. The remaining 99.17 percent of the time the photomultiplier is measuring noise due to fluorescence of non-cellular material in the cell stream. This noise may be from stained cellular debris or fluorescent dye in solution in the cell suspending medium.

Figure 3 shows the light-scattering frequency distribution obtained with Chinese hamster cells (line CHO) supravitaly stained with 10^{-8} M acridine orange. When viewed in the fluorescence microscope, these cells exhibit a weak green nuclear fluorescence and no detectable cytoplasmic fluorescence. The light-scattering signal is seen to be free from any debris which is comparable in size to

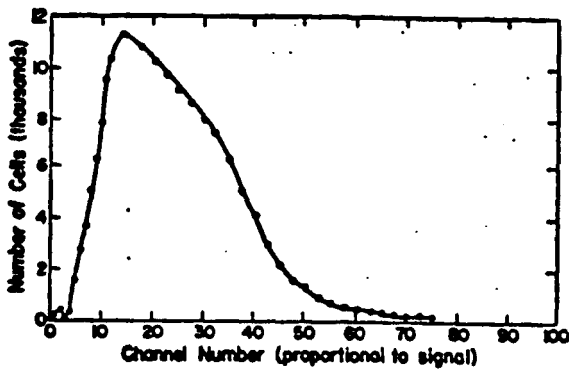


FIG. 3. Light-scattering distribution for random CHO cells stained with 10^{-8} M acridine orange.

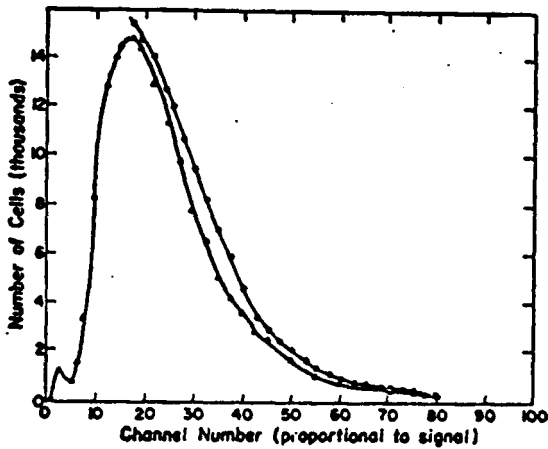


FIG. 4. Fluorescence distribution obtained for CHO cells stained with 10^{-8} M acridine orange: (---) when the instrument is used as an FMF; and (-A-A-) fluorescence gated on the light-scattering signal from each cell.

the cells. Figure 4 shows the fluorescence frequency distribution. When the dual-parameter photometer is operated as a single parameter, one obtains the upper curve which has the appearance of an exponential decay typical of a noise spectrum. However, when the fluorescence signal is gated by the light-scattering signal from the same cells, one obtains the lower curve. In this case, only the fluorescence of objects in the size range of cells is analyzed. This lower fluorescence frequency distribution is similar to that obtained for greater acridine orange concentrations ($> 10^{-5}$ M) where detection is no problem.

The instrument may be used also to identify particles based on the presence or absence of these two parameters. In Fig. 5, the light-scattering and fluorescent frequency distributions of paper mulberry pollen stained with acridine orange are shown. Both signals are free of noise.

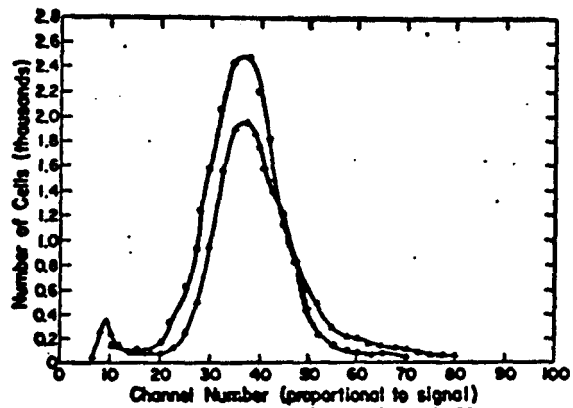


FIG. 5. Light scattering (-O-O-) and fluorescence (-A-A-) distributions for paper mulberry pollen stained with acridine orange.

Next, paper mulberry pollen was mixed with unstained CHO cells, and the light-scattering distribution of the ensemble was measured as shown in Fig. 6. Both particles are the same size (approximately 12 microns), but CHO cells show a much broader size distribution (cf. Fig. 3), hence broadening the distribution obtained from the combination. However, if light scattering from the combination is gated by the fluorescence of paper mulberry pollen, one obtains the scatter curve shown in Fig. 6, which is identical to that of paper mulberry pollen alone.

This instrument offers the possibility of improving the signal-to-noise ratios on samples that fluoresce poorly because of preparational difficulties and distinguishing one biological particle from another on the basis of differences in light-scattering and/or fluorescent properties. The

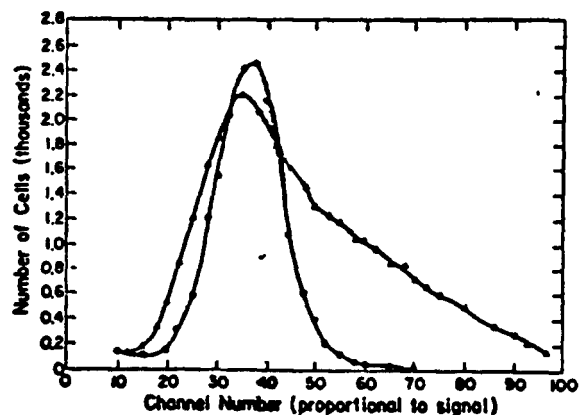


FIG. 6. Light-scattering distribution (-A-A-) obtained from a mixture of stained paper mulberry pollen and unstained CHO cells. Light-scatter distribution (-O-O-) obtained when the scattering signals from the mixture were gated by simultaneous fluorescent signals from the pollen.

first attribute permits measurements on samples not previously amenable to FMF analysis. The second feature greatly extends the FMF concept of cell identification.

REFERENCES

1. D. M. Holm and L. S. Cram, *Exp. Cell Res.* (1973), in press.
2. P. F. Mullaney, M. A. Van Dilla, J. R. Coulter, and P. N. Dean, Cell sizing: A light-scattering photometer for rapid volume determination, *Rev. Sci. Instr.* 40, 1029-1032 (1969).

BIOLOGICAL APPLICATIONS OF CELL ANALYSIS AND SORTING

(L. S. Cram, H. A. Crissman, J. C. Forslund, P. K. Horan, P. M. Kraemer, D. F. Petersen, M. R. Raju, A. Romero, R. A. Tobey, and T. T. Trujillo)

Fluorescent DNA Distributions in MCA-1 Tumor Cell Populations

The tumor cell line MCA-1 was derived in C3H mice by the application of the carcinogen methylcholanthrene to the skin. The resulting tumor was classified as a squamous cell carcinoma. Because of our interest in developing and separating squamous cell carcinoma for the cervical and uterine regions of humans, we felt that this tumor would serve as a good working model. For example, use of the MCA-1 tumor would allow us to have sufficient cells which are easily dissociated to determine the parameters which are most suited for cancer cell identification. Information gained with this model system would then be applied to an investigation of the identification of cancer in humans. One parameter or cell property considered acceptable for identifying abnormal cells in any cell population is the presence and extent of polyploid cells when analyzed for DNA content per cell. After working out a satisfactory single-cell suspension technique prior to fixation, fluorescent DNA distributions could be made from several animal tumors. The cells were stained by the acriflavine Feulgen reaction method¹ and measured by FMF techniques.² The fluorescent distribution histograms of these samples (Fig. 1) show three distinct peaks in a channel ratio of 1:2:4. The first peak corresponds to the normal diploid cells present with tumor cells. The position of this peak corresponds to that of diploid cells obtained from kidney and spleen from the same



FIG. 1. DNA distribution of MCA-1 tumor cells.

animal and to CHO cells in G_1 . The MCA-1 cell distribution pattern indicated the presence of cells with 2N, 4N, and 8N amounts of DNA. The second population (4N) appeared to be the most numerous. The three peaks seen in a single sample may also indicate the presence of two cell lines growing together: (1) normal diploid cells with the 2N amount of DNA, and (2) proliferating tumor cells as indicated by the G_1 (4N DNA) and $G_2 + M$ (8N DNA) peaks. We thought it would be interesting to investigate whether MCA-1 tumor cells could be grown in culture; this would not only provide a ready source of cells but might also lead to a selective line more suitable for the model system described above. This has been done with quite a degree of success. During the early passages (1 through 5), the fluorescent DNA distribution resembled the original tumor cells (Fig. 1); however, in later passages (6 through 10), we observed the disappearance of the first peak (2N) while the cell population was still at a nonconfluent state of growth (Fig. 2). However, a confluent population displayed only one peak at the 4N DNA level (Fig. 3).

From these preliminary data, we conclude that animal MCA-1 tumor tissue contains both normal diploid cells and polyploid tumor cells, with the former unable to survive and proliferate after a few passages in culture media. Also, when cultured MCA-1 tumor cells are allowed to grow to a confluent state, we see a typical G_1 arrest as observed by others³ in other mammalian cell lines. Because normal vaginal and cervical specimens produce typical diploid (2N DNA) histograms, it seems



FIG. 2. DNA distribution of MCA-1 cultured cells (nonconfluent).



FIG. 3. DNA distribution of MCA-1 cultured cells (confluent).

obvious that addition of varying amounts of G_1 (4N) tumor cells to these specimens will aid in determining the minimal levels of polyploid cells detectable with the currently used sensing and sorting equipment.

REFERENCES

1. T. T. Trujillo and M. A. Van Dilla, Adaptation of the fluorescent Feulgen reaction to cells in suspension for flow microfluorometry. *Acta Cytol.* **16**, 26-30 (1972).
2. D. M. Holm and L. S. Cram, An improved flow microfluorometer for rapid measurements of cell fluorescence. *Exp. Cell Res.* (1973), in press.
3. G. J. Todaro, G. K. Lazar, and H. Green, The initiation of cell division in a contact-inhibited mammalian cell line. *J. Cell. Comp. Physiol.* **66**, 325-334 (1965).

Tumor Cell Identification and Separation

A squamous cell carcinoma (MCA-1) growing in C3H mice was obtained from Dr. R. Malmgren of the National Cancer Institute. Tumors from these animals were removed using sterile procedures, minced, and placed into Ham's F-10 medium supplemented with serum and antibiotics. The resulting cells are epithelial in morphology and, when implanted in C3H mice, produce tumors in approximately one-third the time required for the original line to produce tumors in these animals. The purpose of this work was to determine if the multiparameter cell sorter¹ could distinguish normal tissue from neoplastic tissue based on cellular DNA content measurements and distinguish malignant cells from clumps of lymphocytes. Cell identification instruments designed for cancer screening have failed because of their inability to distinguish malignant cells from clusters of lymphocytes.² A great deal of lymphocyte activity is found in many tumors; therefore, it is of paramount importance to be able to distinguish tumor cells from white cells.

To test the capability of the instrument to distinguish these two cell types from each other, an artificial mixture was made from spleen cells and MCA-1 tumor cells grown in tissue culture. These cells were subjected to trypsinization, fixation, and acriflavine-Feulgen staining.³ Figure 1a and 1b shows that the modal channel of the G_1 spleen cells is less than the modal channel of the G_1 tumor cells, suggesting that it is indeed possible to distinguish the DNA distribution of tumor and spleen cells. A mixture of spleen and MCA-1 cells is shown in Fig. 1c. The mixed cells were then sorted and, as seen in Fig. 2, peak 1 is indeed representative of spleen cells, peak 2 is comprised mostly of tumor cells, and peak 3 is only tumor cells.

To check our capability to detect tumor cells *in vivo*, MCA-1 tumor cells grown in tissue culture were trypsinized and approximately 10^6 tumor cells inoculated subscapularly into each of 6 C3H mice. After 1.5 weeks, the animals were sacrificed and the tumors removed. The tumors were subjected to trypsinization, fixation, and acriflavine-Feulgen staining.³ Resulting DNA distributions of tumor cells are shown in Fig. 1d. The distribution is comprised of three peaks representing two

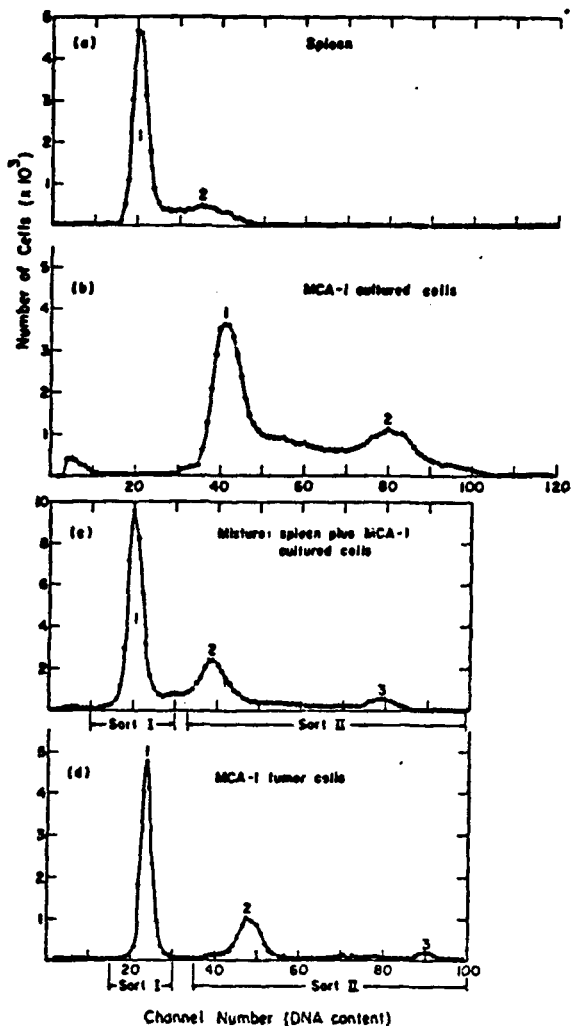


FIG. 1. Modal channel of G_1 spleen cells and G_1 tumor cells: (a) Mouse spleen cells which were trypsinized and fixed in formalin. The cells were stained with acriflavine-Feulgen. Cells in channel 20 represent G_1 spleen cells and those in channel 40 $G_2 + M$ cells. (b) MCA-1 cultured tumor cells, stained in the same fashion as the spleen cells. Note that the G_1 modal channel is 45, indicating that the DNA content of tumor cells is ≈ 2 times greater than diploid spleen cells. (c) Artificial mixture of cells from (a) and (b). The LASL cell sorter was adjusted to sort cells in channels 15 to 30 into one beaker and those in channels 35 to 100 into another beaker. (d) MCA-1 tumor cells taken from a C3H/HeJ mouse. Preparation was the same as in Fig. 1a.

overlapping bimodal distributions. The first peak on the left represents normal diploid cells, either fibroblasts or lymphocytes, within the tumor. The second or middle peak is representative of the G_1 tumor cells and the $G_2 + M$ diploid population, and the third peak is representative of $G_2 + M$ tumor

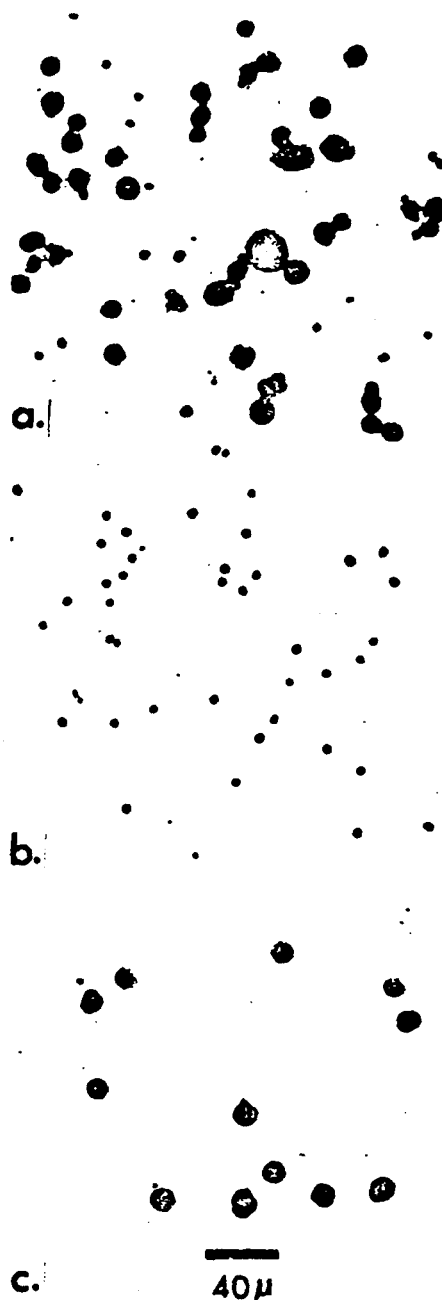


FIG. 2. Photomicrographs of cells described in Fig. 1c: (a) Unsorted mixture of cultured MCA-1 tumor cells and mouse spleen cells. (b) Sort I from distribution shown in Fig. 1c. (c) Sort II from distribution shown in Fig. 1c.

cells. From Fig. 3 it is obvious that tumor cell enrichment is possible if one uses the LASL cell sorter. It is also clear from Sort I (Fig. 3) that diploid cells within the tumor are lymphocytes and not fibroblasts.

While these preliminary studies suggest that measurement of DNA content alone is sufficient to detect tumor cells from normal diploid cells, many

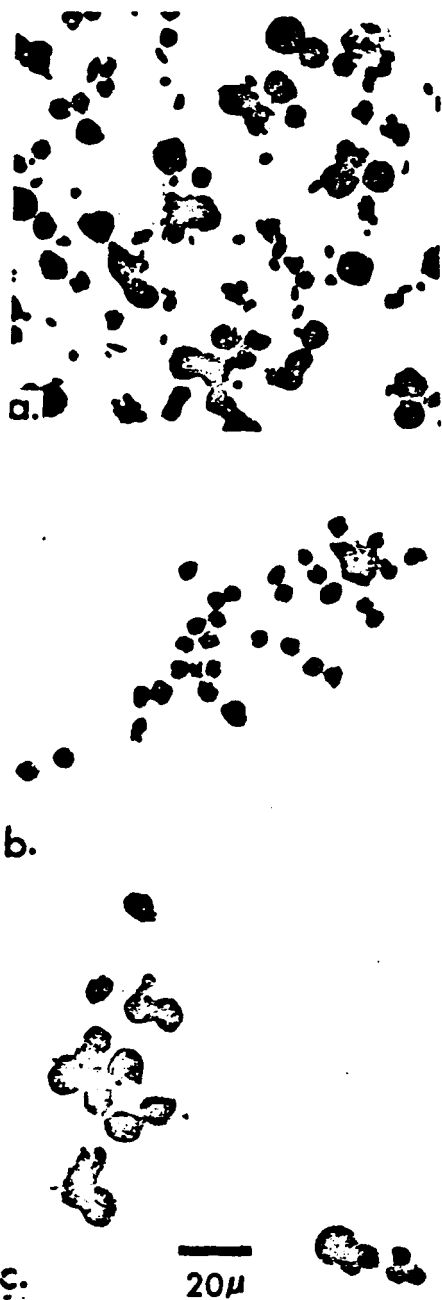


FIG. 3. Photomicrographs of cells described in Fig. 1d: (a) Unsorted tumor cells dispersed with trypsin. (b) Sort I from distribution described in Fig. 1d. (c) Sort II from distribution described in Fig. 1d.

other parameters must be investigated. Parameters such as nuclear-to-cytoplasmic ratio and tumor membrane antigens currently are of interest. Perhaps the use of multiparameter analysis (i.e., DNA content versus nuclear-to-cytoplasmic ratio⁴ might make unequivocal tumor cell detection a reality.

REFERENCES

1. J. A. Steinkamp, M. A. Van Dilla, and M. J. Fulwyler, A high-speed flow system for multi-parameter cell sorting (in preparation).
2. W. E. Tolles and H. P. Mansberg, Size and shape determination in scanning microscopy, In: *Scanning Techniques in Biology and Medicine*, Ann. N. Y. Acad. Sci. 97, 516-536 (1962).
3. P. M. Kraemer, L. L. Deaven, H. A. Crissman, and M. A. Van Dilla, Paradox of DNA constancy, In: *Advances in Cell and Molecular Biology*, Vol. 2 (E. J. DuPraw, ed.), Academic Press, New York and London (1972), pp. 47-108.
4. L. Wheelless, University of Rochester Medical School (1972), personal communication.

Use of Flow Microfluorometry for Analysis and Evaluation of Synchronizing Protocols and Drug Effects on Cell-Cycle Traverse

A number of cooperative studies with the Cellular Radiobiology Section were undertaken to determine the effects of various protocols on DNA synthesis. Flow microfluorometry (FMF) analysis offers the unique advantage of providing DNA distribution patterns of large numbers of cells, thereby revealing the relative number of cells in the various phases of the cell cycle under a variety of experimental conditions. FMF analysis, coupled with cell enumeration and autoradiography, provides a powerful method for analyzing the effects of various synchronizing protocols or drugs on cell-cycle traverse.

In a collaborative study with Drs. R. A. Tobey and P. M. Kraemer, the effects of three commonly used synchronizing methods, isoleucine deprivation,¹ double-thymidine blockade, and mitotic selection,^{2,3} were analyzed and evaluated with respect to their effects on subsequent DNA replication. In each case, we found a given fraction of cells was unable to complete genome replication following synchronization. The term "traverse perturbation index" was designated for the fraction of cells converted to a noncycle-traversing state because of experimental manipulation.⁴ Traverse perturbation indices for double-thymidine blockade, isoleucine deprivation, and mitotic selection were 17.0, 12.4, and 5.5 percent, respectively. A typical DNA distribution pattern revealing the noncycle cells following release from double-thymidine blockade is shown in Fig. 1. A knowledge of the traverse perturbation index will permit a direct comparison

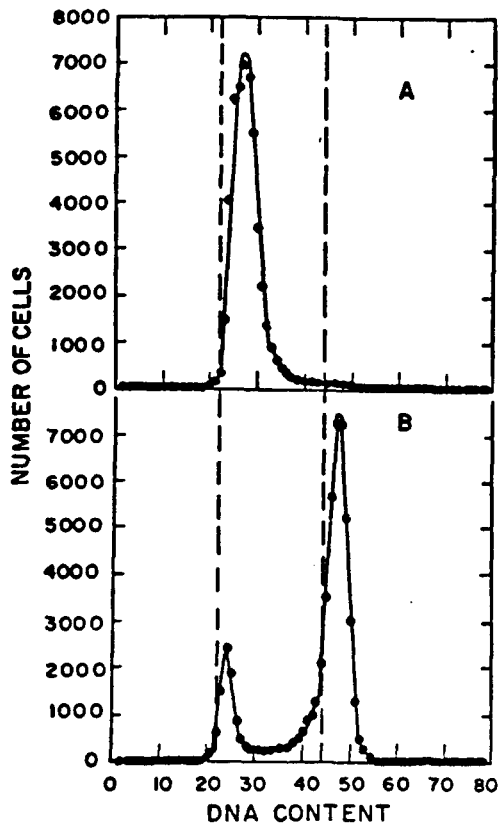


FIG. 1. DNA distribution patterns showing non-traversing fraction of cells after reversal of the double-thymidine blockade synchronizing technique. Broken lines represent values for G_1 and $G_2 + M$ DNA calculated from controls. Cells were prepared via the double-thymidine blockade technique. FMF patterns in the culture at time of removal of the second thymidine blockade (DNA pattern shown in A) and at 6 hr later, immediately before the first increase in cell number (shown in B). The numbers of cells examined in (A) and (B) were 51,000 and 52,000, respectively.

of the effects of various synchrony-induction protocols on cell-cycle traverse.

In another study conducted with Dr. R. A. Tobey, FMF techniques were used to evaluate a new protocol for preparing large quantities of synchronized mammalian cells in late G_1 of the pre-DNA replication phase of the cell cycle.⁵ This technique, a modification of the method described by Tobey and Ley,¹ employs hydroxyurea (to 10^{-3} M) or cytosine arabinoside (to 5 μ g/ml) for 10 hr following release of cells from isoleucine deprivation. Cells that are then washed and resuspended in fresh medium without drugs will initiate DNA synthesis and begin dividing within 7 hr. DNA distribution patterns for cells synchronized by this technique are shown in Fig. 2. This protocol offers the

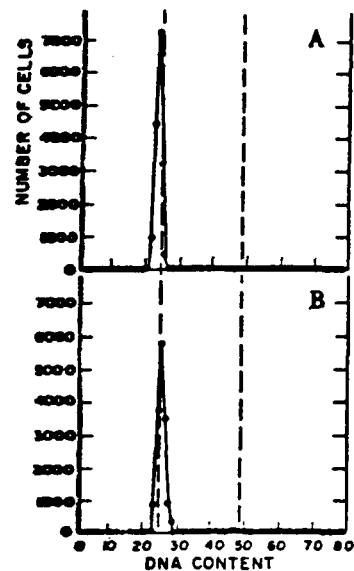


FIG. 2. DNA distribution patterns of various synchronized cell populations: (A) Cells were prepared by cultivation for 30 hr in isoleucine-deficient medium, then resuspended in fresh isoleucine-containing medium containing hydroxyurea to 10^{-3} M; the sample for FMF analysis was removed at 10 hr after resuspension of isoleucine-deficient cells in normal medium plus hydroxyurea. (B) Cells were prepared by cultivation for 30 hr in isoleucine-deficient medium, then resuspended in fresh isoleucine-containing medium containing cytosine arabinoside to 5 μ g/ml; the sample for FMF analysis was removed from the culture at 10 hr after resuspension of isoleucine-deficient cells in normal medium plus cytosine arabinoside. The number of cells examined in each culture was 19,000 (isoleucine-deficiency and hydroxyurea) and 17,000 (isoleucine-deficiency and cytosine arabinoside). Broken lines represent values for G_1 and $G_2 + M$ DNA peak values calculated from controls.

advantage of providing large quantities of cells near the G_1/S boundary suitable for studies of biochemical events associated with completion of interphase and initiation of genome replication.

In another cooperative study with Dr. R. A. Tobey, FMF techniques were used in experiments designed to determine effects of several chemotherapeutic agents on cell-cycle traverse.⁶ Four agents with differing effects on cell-cycle progression were examined: hydroxyurea, cytosine arabinoside, bleomycin, and camptothecin. Both hydroxyurea (10^{-3} M) and cytosine arabinoside (5 μ g/ml) grossly decreased the rate of progression of cells into S phase, resulting in accumulation of cells at the G_1/S boundary. Neither agent

completely prevented cells from initiating DNA synthesis. Bleomycin (100 $\mu\text{g/ml}$) allowed initiation and completion of genome replication to occur at a nearly normal rate, but cells accumulated in G_2 and most cells lost the capacity to enter mitosis. Camptothecin (1 $\mu\text{g/ml}$) reduced the overall rate of cycle progression and allowed a few cells to replicate a complete complement of DNA.

The DNA distribution patterns for cultures released from isoleucine-deficient G_1 -arrest and maintained in the various drugs are shown in Fig. 3.

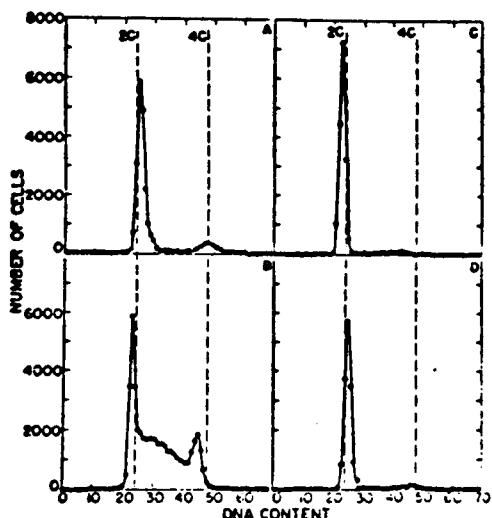


FIG. 3. DNA distribution patterns for cultures released from isoleucine-deficient G_1 -arrest and maintained for 10 hr in 100 $\mu\text{g/ml}$ bleomycin (B); 10^{-3} M hydroxyurea (C), or 5 $\mu\text{g/ml}$ cytosine arabinoside (D). (A) Control. The culture was maintained for 30 hr in isoleucine-deficient medium, at which time an aliquot was examined via FMF analysis. (B) Bleomycin. The culture was maintained for 30 hr in isoleucine-deficient medium; then the cells were resuspended in fresh, complete (isoleucine-containing) medium supplemented with bleomycin to 100 $\mu\text{g/ml}$, and after 10 hr a sample was removed for FMF analysis. (C) Hydroxyurea. The culture was maintained in isoleucine-deficient medium for 30 hr; then the cells were resuspended in fresh, complete medium containing hydroxyurea to 10^{-3} M, and after 10 hr a sample was removed for FMF analysis. (D) Cytosine arabinoside. After 30 hr in isoleucine deficient medium, the cells were resuspended in fresh, complete medium containing cytosine arabinoside to 5 $\mu\text{g/ml}$; 10 hr later an aliquot was removed for FMF analysis. The broken lines represent G_1 and $G_2 + M$ DNA peak values calculated from the exponential culture, which was the source of all cells used in these experiments. The number of cells examined in each culture was (A) 23,000; (B) 47,000; (C) 19,000; and (D) 17,000.

The combination of FMF, cell enumeration, and autoradiographic techniques provides a new approach to studying the effects of chemotherapeutic agents on cell-cycle traverse and provides valuable information to the clinician regarding drug dosage and times of application.

REFERENCES

1. R. A. Tobey and K. D. Ley, Isoleucine-mediated regulation of genome replication in various mammalian cell lines. *Cancer Res.* **31**, 46 (1971).
2. R. A. Tobey, E. C. Anderson, and D. F. Petersen, Properties of mitotic cells prepared by mechanically shaking monolayer cultures of Chinese hamster cells. *J. Cell. Physiol.* **70**, 63 (1967).
3. D. F. Petersen, E. C. Anderson, and R. A. Tobey, Mitotic cells: Source of synchronized cultures, In: "Methods in Cell Physiology," Vol. 3 (D. M. Prescott, ed.), Academic Press, New York (1968), p. 347.
4. R. A. Tobey, H. A. Crissman, and P. M. Kraemer, A method for comparing effects of different synchronizing protocols on mammalian cell cycle traverse. *J. Cell Biol.* **54**, 638-645 (1972).
5. R. A. Tobey and H. A. Crissman, Preparation of large quantities of synchronized mammalian cells in late G_1 in the pre-DNA replicative phase of the cell cycle. *Exp. Cell Res.* (1973), in press.
6. R. A. Tobey and H. A. Crissman, Use of flow microfluorometry in detailed analysis of effects of chemical agents on cell-cycle progression. *Cancer Res.* **32**, 2726-2732 (1972).

Application of Biophysical Instrumentation to Animal Disease Diagnosis

The Hog Cholera PK-15 System.--Investigative effort since last year's annual report describing our successful "proof-of-principle" experiments¹ has concentrated on adaptation of this system to fresh tissue techniques. The specific aim is one of direct detection of viral antigen from field submissions.

New problems were encountered in preparing heterogeneous cell samples (pig blood and tissue biopsy material) for flow microfluorometry (FMF) measurements. The very low fluorescence of cells labeled with fluorescently tagged antibodies requires monodisperse cell suspensions that are free of small debris and homogeneous. Procedures were developed for isolation, fixation, and conjugation

of spleen and white blood cell suspensions to assure compatibility between these procedures and maintenance of good single-cell suspensions. Numerous anticoagulants, red blood cell lysing agents and procedures, and several fixation methods were evaluated to provide procedures compatible with maintaining single-cell suspensions with minimal debris and still provide cell permeability to fluorescein-labeled antibody molecules. Buffy coat cell cultures were also considered. Although satisfactory protocols were developed, nonspecific binding of conjugate to uninfected cells decreased the sensitivity of FMF analysis below that of standard techniques. The present level of sensitivity requires that 10 percent of the cells in a sample be infected. Improved conjugate purity would increase the signal-to-noise ratio and make FMF a useful tool for studying virus replication in mammalian cells; this is being attempted.

Basic support experiments using the PK-15 cell system to determine if other areas of FMF applicability exist will continue. For the first time, a quantitative evaluation of conjugates can be accomplished using techniques developed for the proof-of-principle project. Quality evaluation of commercially produced conjugates is important for USDA licensing procedures and for evaluating our own conjugates. Conjugate evaluation is based on two parameters: (1) relative cell brightness or the amount of fluoresceinated antibody bound to a cell as compared with a "standard" conjugate, and (2) specificity as evidenced by the ratio of specifically to nonspecifically bound conjugate. Both parameters can be quantitated easily using the FMF.

Although instrumental development on this project has been reduced, new techniques of rapid cell identification and information processing developed in the section have been applied to the fluorescence analysis of randomly growing PK-15 cells infected with hog cholera virus. Recent developments permit measuring the ratio of cell fluorescence (total amount of fluorescent antibody bound) to cell volume. The resulting distributions (Fig. 1) for control and infected cells are both tighter (coefficient of variation decreases by approximately 2.0), indicating that larger, more mature cells do not produce more virus per cell than smaller cells. The improved coefficient of

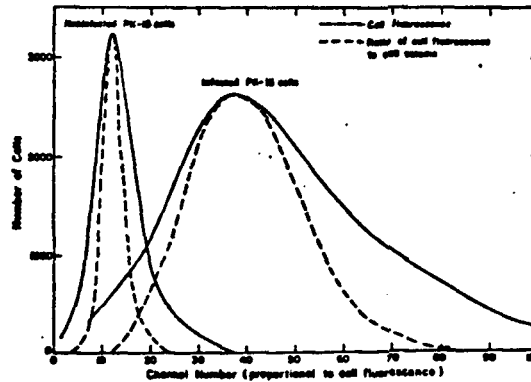


FIG. 1. Distributions for control and infected cells.

variation of the peaks is a result of cancelling the contribution of nonspecific binding which is proportional to cell volume.

Differences in light-scattering patterns were observed for hog cholera infected and noninfected PK-15 cells.² Light-scattering measurements were made with a new photometer³ described elsewhere in this report which uses high-speed film as the detector. Intensity of scattered radiation from suspensions of live infected and noninfected cells is shown in Fig. 2. In the angular range of 2.5 to 4.0°, overlap of the two curves is consistent with light-scatter theory and Coulter volume data that indicate the two cell populations are very similar in volume. At larger angles (4 to 25°), infected

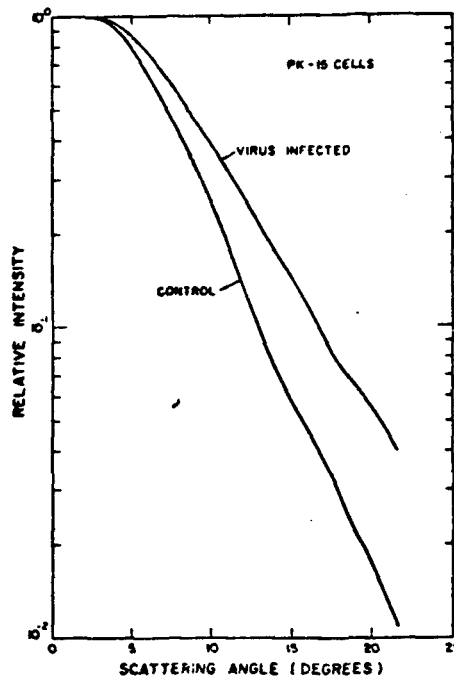


FIG. 2. Scattered radiation intensity for infected and noninfected cells.

cells scatter much more light (about 2.3 times at 20°) than noninfected cells. This difference in large angle light-scatter pattern is believed to be due to some change in internal structure between the two cell populations.

In response to a request for help from the Emergency Disease Task Force of the USDA, an effort is underway to investigate the applicability of our biophysical instrumentation for rapid differential diagnosis of Newcastle disease virus. The outbreak of a velogenic strain of the virus has resulted in the disease being declared a national emergency. The degree of polyploidy in chicken embryo fibroblasts after Newcastle infection is reported⁴ to correlate with the virulence of the virus. Therefore, a rapid, quantitative measurement of polyploidy with FMF should provide a rapid screening technique to identify differentially strains of Newcastle disease virus.

Effects of Temperature on the Mitotic Cycle of CHO Cells.--The purpose of this study is to make a detailed investigation into the effects of temperature on different phases of the CHO cell life cycle using FMF techniques for cell-cycle analysis.

Chinese hamster cells (CHO) in suspension culture were grown through two exponential growth cycles at three temperatures: 34, 37, and 40°C. Preliminary data suggest that, during the first cycle of cell growth after a 3° temperature change, most of the effects are on reaction rates. During the second cycle, when a steady state situation has been achieved, the effects are a consequence of changes in concentration of chemical reactants. This is evidenced by an apparent change in cell composition which was measured as a change in cell size. CHO cells growing at other than their optimum temperature were found to increase in volume.

Of particular interest is the observation that, upon a decrease in temperature (37 to 34°C), the percent of CHO cells in the G₁ phase of their life cycle increases from 46 to 61 percent, which is just the reverse for HeLa cells which show a decrease from 48 to 36 percent.⁵

Investigations with the Unique Mixoploid Cell Line, PK-15.--The unique DNA distribution of PK-15 cells, a mixoploid cell line, was reported in last year's annual report.¹ Clones that were diploid and tetraploid in DNA content (i.e., they differ by

a factor of 2 in DNA content but not in chromosome number) were isolated from the cell line. Because these two PK-15 clones were isolated from the same culture, we believe they either had exactly the same doubling time or their generation times were not equal but intercellular metabolic factors were being produced that differentially regulate cell doubling. Cells from the two clones were mixed in different ratios and allowed to grow through 6 passages. Their Feulgen-DNA distributions were then measured to determine if the two populations were growing at the same rate and maintaining the same ratios. Because the mixing ratios remained constant, we conclude that the two clones have the same doubling times and respond similarly to cell density. Further experiments are planned to compare these clones with regard to their chromosome banding pattern, response to temperature, and radiation.

REFERENCES

1. C. R. Richmond and G. L. Voelz, eds., Annual Report of the Biological and Medical Research Group (H-4) of the LASL Health Division, January through December 1971, Los Alamos Scientific Laboratory report LA-4923-PR (April 1972).
2. L. S. Cram and A. Brunsting, Fluorescence and light scattering measurements on hog cholera infected PK-15 cells. *Exp. Cell Res.* (1973), in press.
3. A. Brunsting and P. F. Mullaney, A light-scattering photometer using photographic film. *Rev. Sci. Instr.* 43, 1514-1519 (1972).
4. G. Poste, A. P. Waterson, G. Terry, D. J. Alexander, and P. Reeve, Cell fusion by Newcastle disease virus. *J. Gen. Virol.* 16, 95-97 (1972).
5. P. N. Rao and J. Engelberg, Effects of temperature on the mitotic cycle of normal and synchronized mammalian cells, In: "Cell Synchrony," Academic Press, New York (1966), pp. 332-352.

Normal and Tumor Cell Kinetic Studies Using Flow Microfluorometry (FMF)

Methods for studying the kinetics of proliferative cells from both normal and tumor tissues *in vivo* are of fundamental interest in addition to their possible application to the areas of chemotherapy and radiotherapy. Cell analysis and sorting instrumentation currently under development at the Los Alamos Scientific Laboratory can be used with

relative ease for kinetic studies. Basically, the procedure consists of (a) preparing single-cell suspensions from the tissue of interest using trypsinization procedures; (b) fixing single cells in methanol and formaldehyde mixture; and (c) staining fixed cells with acriflavine (fluorescent-Feulgen) for specific staining of cellular DNA. Other available techniques include the use of (a) the Coulter principle to determine the volume distribution of cells; (b) a signal from scattered light to gate the electronic system which measures fluorescence, thereby eliminating noise signals generated by debris in cell preparations; (c) a multiparameter cell separator to isolate cell populations with different DNA distributions; and (d) a combination of the above systems to measure directly the DNA content per unit cell volume. These techniques are described in detail in our annual report for 1971.¹

Our preliminary studies indicate that cell preparations for mouse tissues such as skin, intestinal epithelium, liver, spleen, and kidney that are considered important in radiotherapy can be made and their DNA distributions measured by FMF instrumentation. Figure 1 shows DNA distributions for different normal tissues that are considered to be some of the limiting tissues in radiation therapy. The noise caused by debris in the cell preparation and appearing in low channel numbers was not electronically gated out in these measurements. The DNA content of all these normal tissues is about the same and shows that a large fraction of cells is in the G_0 or G_1 state.

Dr. R. F. Kallman and associates^{2,3} have concluded from their studies with KHT sarcoma and EMT6 (mammary carcinoma) that a dose of 300 rads induces synchrony in the tumor cells, thereby causing cyclically fluctuating radiosensitivity changes as a function of time after exposure. Although it will be difficult to correlate results of DNA distribution with results of radiation sensitivity, it will be of interest to study the changes in DNA distributions in tumor cells in vivo with time after radiation exposure. KHT is a sarcoma that arose spontaneously at the base of the ear of a C3H/KM mouse in 1962 in Dr. Kallman's laboratory at Stanford University. This tumor line can be maintained by serial subcutaneous passage and has been studied extensively.^{4,5} A tumor of about 12 mm in

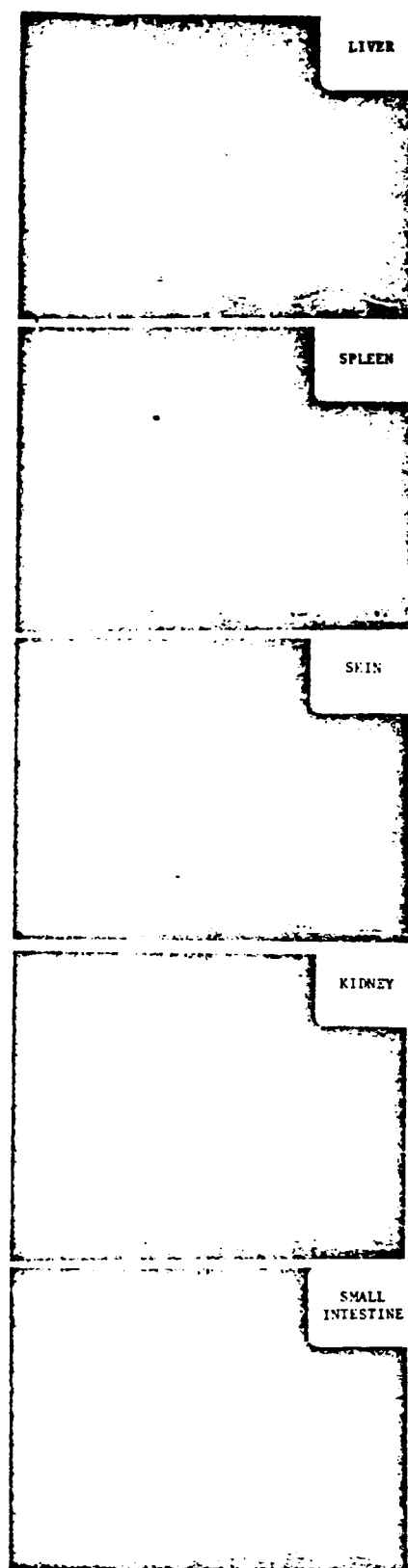


FIG. 1. DNA distribution of normal tissues in mice. The X axis is the channel number (proportional to DNA content in the cells), and the Y axis is the relative number of cells per channel.

diameter from a donor mouse is excised, placed in normal saline, and minced into small pieces about 1 mm^3 in volume. Tumor pieces are then transplanted onto the back of C3H mice via a small incision in the skin of the freshly shaven back. The tumor grows to about 1 cm in diameter on about the 12th day after transplantation. When the tumors were about 1 cm in diameter, the mice were anesthetized (0.1 ml/g body weight of Nembutal), and the tumors were exposed to X rays by shielding the remainder of the mouse. Mouse tumors exposed to 300 rads of 250-KVP X-rays were sacrificed at 0, 8, 12, 16, 22, 24, 26, and 30 hr after X-ray exposure, and cell preparations were made to measure DNA distribution. A few tissues were also exposed to 1500 or 3500 rads of X rays and were sacrificed at 24 hr after exposure. Tumor growth measurements suggest that 3500 rads is a curative dose. Two mice were used for each dose level and fixation time after exposure.

A scattered light signal was used to gate the noise signal arising from debris when the cells were used in the FMF instrumentation. All samples were measured to a total count of 50,000 cells. Figure 2 shows the results of DNA distributions at different times after 300 rads of exposure, where there are significant differences in DNA distribution. Microscopic examination showed that most of the cells were single and that the doublets were less than 5 percent in all samples. The first peak in the DNA distribution represents normal diploid cells in the tumor. The second peak, corresponding to the amount of DNA nearly twice that of normal diploid cells, is due to tumor cells in the G_1 phase. The third peak, corresponding to twice the amount of tumor cells in the G_1 phase, is due to tumor cells in the $G_2 + M$ phase. DNA distributions corresponding to cells in between G_1 and $G_2 + M$ tumor cells are due to cells in the S phase. When the cells in a tumor control sample were separated according to the DNA content in the cells using the cell separator, we found that the first peak in DNA distributions is due to leucocytes. It can be seen from Fig. 2 that the DNA distribution of tumors 8 and 12 hr after exposure to 300 rads, when compared to zero hour after exposure, has more cells in the $G_2 + M$ phase. This could be due to G_2 block caused by radiation. However, it can be seen that 12 hr

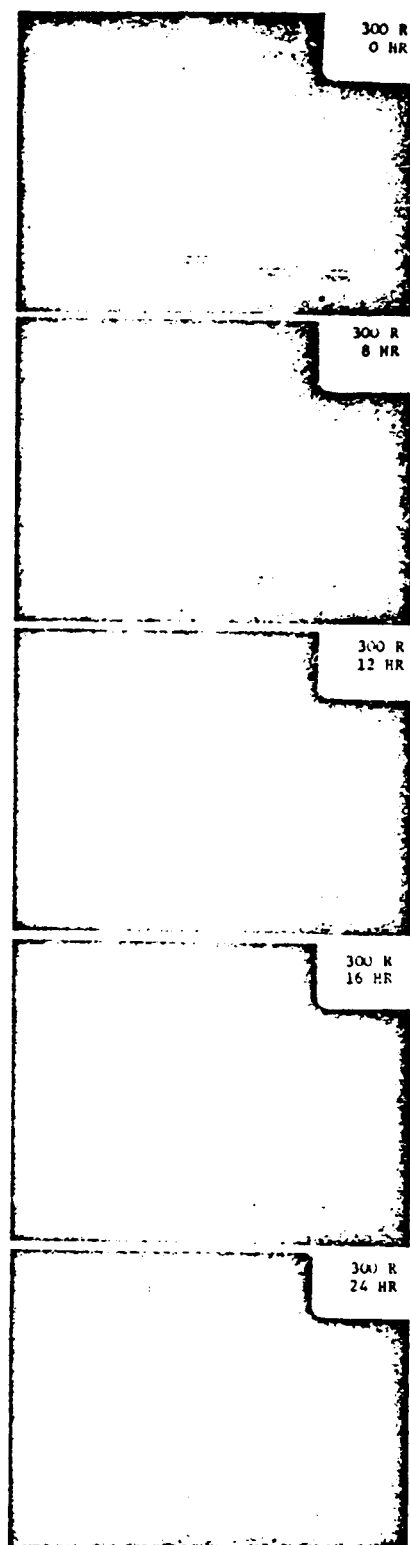


FIG. 2. DNA distribution of KHT sarcoma tumor cells at different times after exposure to 300 rads of X-rays.

after exposure the cells are beginning to divide and that at 24 hr after exposure to 300 rads DNA distribution looks very similar to that of the control. Figure 3 shows that when the cells are exposed to 1500 rads there still seems to be a small increase in cells in the $G_2 + M$ phase at 24 hr after exposure, whereas with 3500 rads nearly 50 percent of the cells are still in the $G_2 + M$ phase. One would expect this trend because with increasing dose the mitotic delay is increased. These results are in agreement with results of Kal⁶ using Rhabdomyosarcoma cells with impulse photometer instrumentation. Variations in DNA distribution among any two tumor samples treated in the same way were found to be remarkably similar. Thus, the difference in DNA distribution with dose and time after exposure are real. It can be concluded from these preliminary studies that FMF is a very good tool

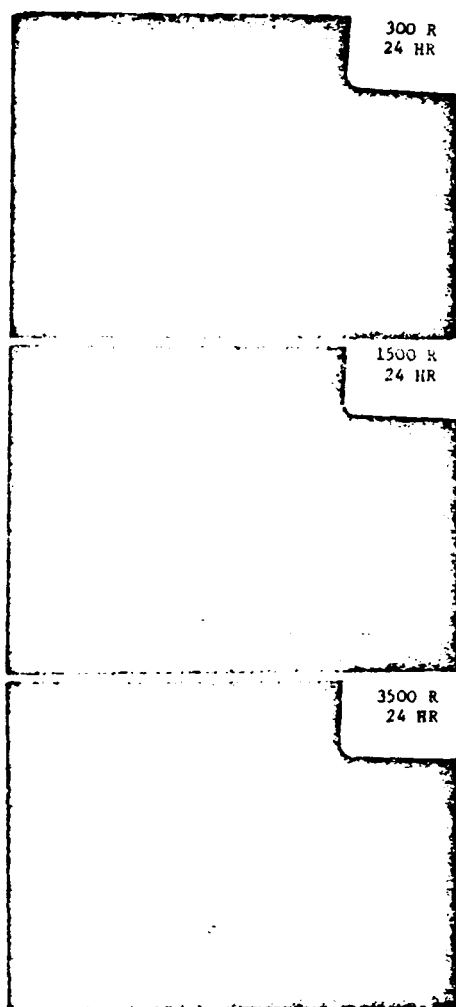


FIG. 3. DNA distribution of KHT sarcoma tumor cells after 24 hr of exposure to 300, 1500, and 3500 rads of X-rays.

to obtain quantitative information on tumor as well as normal cell kinetics after radiation treatment.

We propose to study the progression of normal and tumor cell populations in experimental mammals in addition to cells in culture when they are exposed to ionizing radiations such as X rays and later with negative pions. DNA distributions in patients treated with conventional radiations and later with negative pions could also be made whenever tumor biopsies are available. This type of measurement in experimental animals and possibly in some patients could give important information that may lead to optimum fractionation in radiotherapy and could also be used as a diagnostic modality to judge radiation effects after a given treatment and to plan future exposure.

REFERENCES

1. C. R. Richmond and G. L. Voelz, eds., Annual Report of the Biological and Medical Research Group (H-4) of the LASL Health Division, January through December 1971, Los Alamos Scientific Laboratory Report LA-4923-PR (April 1972).
2. R. F. Kallman and N. M. Blechen, Post irradiation cyclic radiosensitivity changes in tumors and normal tissues, In: "Proceedings of a Symposium on Dose Rate in Mammalian Radiation Biology (April 29-May 1, 1968)," AEC Division of Technical Information report CONF-680410, pp. 20.1-20.23.
3. S. C. Rockwell, Cellular Radiosensitivity, Cell Population Kinetics and Tumor Radiation Response in Two Related Mouse Mammary Carcinomas. Ph.D. Thesis, University of California, Berkeley.
4. L. M. Van Putten and R. F. Kallman, Oxygenation status of a transplantable tumor during fractionated radiation therapy. *J. Natl. Cancer Inst.* 40, 441-451 (1968).
5. R. F. Kallman, G. Silini, and L. M. Van Putten, Factors influencing the quantitative estimates of the *in vivo* survival of cells from solid tumors. *J. Natl. Cancer Inst.* 39, 539-549 (1967).
6. H. B. Kal, Distributions of cell volume and DNA content of Rhabdomyosarcoma cells growing *in vitro* and *in vivo* after irradiation. *Eur. J. Cancer* (1973), in press.

ISOTOPE APPLICATIONS SECTION

INTRODUCTION

Enriched concentrations of stable isotopes of the major elements of biological systems (i.e., carbon, hydrogen, nitrogen, and oxygen) have been available for many years. Except for deuterium, they were expensive and, therefore, not in great demand. Conversely, there was not much demand; therefore, the isotopes were expensive. This was, at least in part, because of the ready availability of the radioactive isotopes carbon-14 and tritium and, in particular, the early development of appropriate apparatus for their detection and quantitation. Without them, there would undoubtedly have been much greater use of the stable isotopes, not only of carbon and hydrogen but nitrogen and oxygen as well. However, even if materials had been readily available, they could not have been applied; only recently have sophisticated instrumentation developments started.

Several years ago the Division of Biomedical and Environmental Research recognized that, if it were not for the high price, carbon-13 could be used advantageously and perhaps widely as a tool in medical diagnoses of metabolic malfunctions involving such compounds as sugars. However, steps would have to be taken to surmount the cyclical barrier that stood in the way of exploiting potentials that rare stable isotopes such as carbon-13 had for enhancing the diagnostic powers of medicine. That is, high costs of separated isotopes precluded their use in large quantities, and absence of ongoing wide-scale use precluded reductions in cost of separating the isotopes that could accrue from plants designed and engineered for larger-scale production. It appeared that a three-pronged approach to the problem would have to be made whereby clinical advantages and supporting isotopic production methods would be developed, demonstrated, and given practical beginnings simultaneously. Although some research applications (e.g., in molecular biology, vibrational spectroscopy, and nuclear magnetic resonance) could use larger quantities of separated isotopes

than had been available up to now, if the prices were lower, the demand from these sources would probably be minor in comparison with that of even a single clinical application. Therefore, since inception of the carbon-13 project, development of applications of carbon-13 in clinical medicine has been of paramount importance, assisted by demonstrations in other fields of research of the utility, advantages, and unique characteristics of stable isotopes.

Foundation of the program rests on the capability to produce enriched isotopes in the quantities needed. The Los Alamos Scientific Laboratory's Inorganic Chemistry Group (CNC-4) has a long history of isotope separation. For some time it has been producing relatively large quantities of nitrogen-15, oxygen-16, oxygen-17, and oxygen-18 and was planning limited production of carbon-13 for chemical research. This experience, knowledge, and capability made it possible for a carbon-13 plant to be in operation in less than a year after initial interest was expressed by the Division of Biomedical and Environmental Research in 1969. The original 3-kg annual production rate has since been doubled, and further major expansion is in progress to meet the objectives of the program.^{1,2} An eventual, natural outcome should be commercial developments as markets are created and established.

During these initial years since start of the project, the Isotope Applications Section has established a number of required techniques and capabilities and has carried out investigations designed to further the broad as well as specific objectives of the program. A unique synthesis facility now exists which can provide the many labeled compounds needed (frequently on a large scale); high concentrations of carbon-13 have been incorporated into living systems (algae, yeast, mice) with observations that no deleterious effects of the isotope were apparent; applications of carbon-13 have been made to studies in biochemistry, primarily through utilization of carbon-13 nuclear

magnetic resonance (cmr), and clinical diagnostic trials have been initiated. There is continuing effort toward publicizing the potential of stable isotopes and in aiding, wherever possible, other investigators in making their initial applications. Perhaps one of our difficulties has been over-enthusiasm in this regard which has sometimes resulted in over-commitment of our available time and resources; better balance can certainly be anticipated as we acquire experience with each undertaking. A number of collaborative research projects are in progress with personnel at universities, research institutes, national laboratories, and other governmental organizations. In addition to producing the separated isotopes and providing various analytical services, Group CNC-4 is also a primary collaborator and participant in many of the activities.*

Dr. Walton W. Shreeve of the Medical Division, Brookhaven National Laboratory, was a LASL Visiting Staff Member from January to August. During this time, additional planning for various clinical applications of stable isotopes was carried out, and the first trials of carbon-13 in a glucose tolerance test were performed. LASL Visiting Staff Members (Short Term) participating and aiding in various projects, generally through visits of a few days, include Winslow Caughey (Arizona State University), Bruce Burnham (Utah State University), B. M. Tolbert (University of Colorado), G. H. Daub (University of New Mexico), L. O. Morgan (University of Texas), and R. T. Eakin (University of Texas). The section also continues to benefit from discussions and seminars presented by other visiting scientists.

PREPARATION OF COMPOUNDS LABELED WITH STABLE ISOTOPES

(D. G. Ott, E. G. Adame, V. S. Chavez, C. T. Gregg, J. L. Hanners, J. Y. Hutson, V. N. Kerr, V. H. Kollman, M. A. Nevarez, T. G. Sanchez, and T. W. Whaley)

Utilization of stable isotopes is almost

* The collaboration and cooperation of Dr. N. A. Matwyoff in all activities involving nuclear magnetic resonance (as well as other aspects of the stable isotopes program) is particularly acknowledged; also Drs. B. B. McInteer and T. A. Mills have been essential to various parts of the research program, in particular mass spectrometric isotopic analyses of carbon dioxide from the clinical trials as well as samples from other sources.

totally dependent on conversion of output from a separation facility into other chemical forms. Oxides from the enrichment process occasionally can be used directly; however, the bulk of requirements necessitates incorporation of enriched isotopes into organic compounds. There are needs for all degrees and combinations of labeling -- some compounds must be uniformly labeled, some specifically labeled in one or more particular molecular position; and some multiply labeled with more than one isotope, both uniformly and specifically. For some applications, high isotopic enrichment is required; for others, low enrichment is necessary or sufficient. The quantities of compounds needed can vary from milligrams to kilograms.

To meet these various and varied requirements efficiently, a synthesis facility is necessary which utilizes and effectively combines the methods of both organic and bio-synthesis. Each provides the other with starting materials, as well as furnishing ultimate products. As the capability is established for synthesis of a particular compound, the capability for production of others is automatically increased. The synthetic route chosen often depends (in addition to other considerations) on what experience, materials, or methods have become available through previous preparations, as well as what application might be likely in future syntheses.

The basic inorganic starting materials are the various oxides from the separation facility¹ (i.e., carbon monoxide for the carbon isotopes and nitric oxide for the nitrogen and oxygen isotopes). Carbon dioxide is readily available through oxidation of the monoxide, and water and ammonia are obtained through appropriate reductions of nitric oxide. The seven isotopes available to the current program from the production plant are carbon-12 (less than 10 ppm carbon-13), carbon-13 (less than 10 percent carbon-12), nitrogen-14 (less than 50 ppm nitrogen-15), nitrogen-15 (less than 5 percent nitrogen-14), oxygen-16 (less than 10 ppm oxygen-18), oxygen-17 (ca. 10 percent oxygen-16 and oxygen-18), and oxygen-18 (less than 5 percent oxygen-16).

Most of the compounds produced by the synthesis facility are for use in LASL research (including collaborative projects) primarily in biological, clinical, and chemical studies in progress in the

Biomedical Research Group (H-4) and the Chemistry-Nuclear Chemistry (CNC) Division. Provision of compounds needed in other programs throughout LASL should be considered an important function of our capability.

Through an interagency agreement between the U. S. Atomic Energy Commission and the National Institutes of Health, various labeled compounds were synthesized and supplied to the Chemistry and Life Sciences Laboratory, Research Triangle Institute, Research Triangle, North Carolina, for use in various research projects of the National Institute of General Medical Sciences. It is felt that similar arrangements could be mutually advantageous for the synthesis facility and for other organizations in need of compounds labeled with stable isotopes for various projects within the USAEC and other government agencies. Unnecessary duplication of effort, expertise, and facilities would be avoided, the capabilities for synthesis would actually be broadened, and many applications and developments could proceed which otherwise would be delayed or impossible.

Although there are real similarities between syntheses with radioactive isotopes (carbon-14, tritium, etc.) and the stable isotopes, there are also considerable differences. These are primarily a matter of scale; the preparations with stable isotopes are usually considerably larger. Many of the elegant schemes developed for carbon-14 are not applicable to carbon-13 at all — they simply will not scale up satisfactorily. On the other hand, the starting material common to both carbon-14 and carbon-13 syntheses, carbon dioxide, is more conveniently handled on the larger scale in a cylinder rather than from barium carbonate. Additionally, carbon-¹³C monoxide is the most readily available starting material, allowing utilization of reactions that are not practical for carbon-14.

Compounds labeled with stable isotopes exhibit differences from their isotope isomers in physical properties (e.g., density, molecular weight, and infrared and nuclear magnetic resonance spectra). These generally useful properties can be utilized in analytical procedures necessary for developing synthetic methods; these differences occasionally complicate common techniques which rely on comparison with standards (e.g., proof of identity by

infrared spectroscopy). Carbon-13 nuclear magnetic resonance (cmr) is, of course, very useful to the synthetic chemist. In addition, proton nuclear magnetic resonance (pmr), because of spin-spin coupling of protons with carbon-13, can often be used to study carbon-13 (for example, the acetic acids, methanol, and other simple products are routinely analyzed for ¹³C/¹²C ratios at each specific carbon atom using a simple pmr spectrometer).

Various preparations have been (and others will be) repeated several times because of unanticipated needs or continuing demand. Methanol and acetic acid have been produced on a more or less continuing basis, owing primarily to their applications as basic synthetic intermediates and also because of the large quantities required for yeast production. Tobacco plants are being maintained at various stages of development to ensure that unanticipated requirements for the simple carbohydrates which they afford can be met without undue delay.

Organic Synthesis

Table 1 gives a summary of isotopically labeled compounds which have been or are currently being produced, reasons for production, and various pertinent comments. Reaction sequences referred to in the table for their preparation are shown in Fig. 1. Naturally, there are many additional specific compounds which are necessary intermediates or which can be prepared by these same reactions, by obvious extensions, or by numerous combinations and permutations of the label; however, only those are listed which have been prepared or for which there is a current requirement.

The repertoire of developed methods for the efficient production of labeled compounds increases continuously. Each new synthesis has the additional benefit of simplification of a future problem. Particularly valuable are proven procedures for producing key synthetic intermediates containing one, two, and three isotopic atoms which can be used to introduce specific labels into a wide variety of more complicated molecules. Stocks of certain of the commonly used materials are being maintained, and several can be produced on a relatively large scale (i.e., many moles per week) when the demand exists (viz., methanol, acetic

TABLE 1. SUMMARY OF LABELED COMPOUNDS PREPARED BY CHEMICAL SYNTHESIS AND BIOSYNTHESIS

| Compound | Label(s) ^a | Method(s) ^a | Use | Status | Comments | Reference ^b |
|-------------------------------|-----------------------------------------------------------------------------|------------------------|-----------------------------------------------------------------------------------------------------|--------|---------------------------------------------------------------------------------------------------------------------------------------|------------------------|
| Acetic acid | All ^c 1,2- ¹² C ₂ 2- ¹² C | 2,3 | General synthetic intermediate Biological substrate Yeast substrate | f | Multimolar capacity Prepared for NIGMS | 3 |
| Acetic acid, anhydride | All ^d | 5,6 | Porphyrin labeling studies General synthetic intermediate | g | Cooperative project with W. Caughy, Arizona State University | 4,k |
| Acetic acid, methyl ester | All ^e | 7 | General synthetic intermediate | i | Prepared for M. Thompson, Agricultural Research Center, and P. Klein, Argonne National Laboratory | 1 |
| Acetic acid, phenyl ester | 1,2- ¹³ C ₂ | 8 | β-Sitosterol intermediate | g | | k |
| Acetone | 1,2- ¹³ C ₂ | 9 | General synthetic intermediate, isopropyl amine | i | Method of preparation being studied with assistance of G. Daub, University of New Mexico | 5 |
| Acetylene | 1,2- ¹³ C ₂ 1,2- ¹² C ₂ | 10 | Lithium acetylde and benzene intermediate | h | | |
| Alanine | All ^c ¹⁵ N | 11 | Clinical applications Studies on carbohydrate metabolism | i | Cooperative projects with W. Shreeve, Brookhaven National Laboratory, and D. Kipnis, Washington University Medical School | |
| Ammonia, ammonium chloride | ¹⁵ N | 12 | General synthetic intermediate | g | Ultimate nitrogen source for most nitrogen labeled compounds | 1 |
| L-Arginine | Guanido- ¹³ C- ¹⁵ N ₂ | 13 | Clinical and biochemical studies | h | Cooperative project with C. Solomons, University of Colorado Medical Center | 4 |
| Benzene | U- ¹³ C ₆ | 10 | Precursor of labeled aromatic compound Spectroscopic studies Cmr solvent | h | Being prepared for CNC-4 | 6 |
| Bromoacetic acid | U- ¹² C ₆ All ^c | 14 | Carboxymethylation of proteins General synthetic intermediate, glycine, EDTA, NTA | g | Cooperative project with CNC-4 | 4 |
| Bromoacetic acid, ethyl ester | All ^e | 15 | General synthetic intermediate, glycine | g | | 4 |
| n-Butyric acid | 1- ¹³ C | 3,4 | Intermediate in preparation of n-butyl-1- ¹³ C lithium for spec- troscopic studies | g | Cooperative project with E. Olson, University of South Dakota | k |

| Compound | Label(s) | Method(s) | Use | Status | Comments | Reference |
|-------------------------------------------------|------------------------------------------------------------------------|--------------------------------------|-----------------------------------------------------------------------------------------------|--------|-------------------------------------------------------------------------------------------------------------------------------------------------------|-----------|
| (Carbomethoxymethyl)trimethyl ammonium chloride | ^{13}C | 16 | Nmr studies of metal ion complexes Choline precursor | g | Prepared for CNC-4 | 4 |
| (Carboxymethyl)trimethyl ammonium hydrochloride | ^{13}C | 16 | Nmr studies of metal ion complexes | g | Prepared for CNC-4 | 4 |
| Chloroform | ^{12}C | 17 | Nmr solvent | h | Being prepared for CNC-4 Same method can be applied to chloroform- ^{13}C | 7 |
| Cyclopentadiene | ^{13}C | 18 | Nmr spectroscopic studies | g | Cooperative project with CNC-4 Label is scrambled in last step of synthesis | k |
| D,L-Cysteine | ^{13}C | 19 | Studies on structure of metallo-proteins Nmr studies on metal ion complexes Epr studies | g | Cooperative projects with M. Allison, Agricultural Research Service, and CNC-4 Cooperative project with W. Wolf, University of Southern California | 4 |
| Dimethylamine | $^{13}\text{C}_2$ - $^2\text{H}_6$ - ^{15}N | 20 | Polyisotopic intermediate | g | | 8 |
| Dimethylformamide (DMF) | $^{13}\text{C}_3$ - $^2\text{H}_7$ - ^{15}N - ^{18}O | 21 | Studies on polyisotopic molecules | i | | 9 |
| Ethanol | ^{13}C 2- ^{12}C | 22 22 | General synthetic intermediate Chloroform intermediate | h h | | 10 |
| Ethylenedinitrilotetra-(acetic acid) (EDTA) | ^{13}C $^{15}\text{N}_2$ | 23 | Nmr and nmr studies of metal ion complexes | g | Cooperative project with CNC-4 and CNC-2 | k |
| Fatty acids, long chain | ^{13}C | Biosynthesis (green algae) | Mass spectrometry studies Environmental tracers | i | Cooperative project with L. Varga, Oklahoma State University, and A. Harmon, AWU Graduate Student | k |
| Formaldehyde | ^{13}C | 24 | General synthetic intermediate, cysteine | g | | 11 |
| Formamide | ^{13}C | 25 | General synthetic intermediate, cyanide | g | | 1 |
| Formic acid, isopropyl ester | formyl- ^{13}C | 25 | General synthetic intermediate, cyanide, tryptophan, cyclopentadiene | g | Method applicable to other formate esters | k |
| D-Fructose | $^{13}\text{C}_6$ | Biosynthesis (tobacco, chard, canna) | Future studies on carbohydrate metabolism | f | Concomitant product in bio-synthesis of glucose- $^{13}\text{C}_6$ Intermediate for L-lactate- $^{13}\text{C}_3$ | 12 13 |

| <u>Compound</u> | <u>Label(s)</u> | <u>Method(s)^a</u> | <u>Use</u> | <u>Status</u> | <u>Comments</u> | <u>Reference^b</u> |
|---------------------------------|--------------------------------------------------------------------------------------|-----------------------------------------------|------------------------------------------------------------------------------------------------------------------------------------------------------------------------------|---------------|-----------------------------------------------------------------------------------------------------------------------------------------------------------------------------------------------------------------------------------------------|------------------------------|
| D-Galactose | ¹³ C U- ¹³ C ₆ | Biosynthesis (marine red algae) | Clinical applications Studies on galactose metabolism | h | Cooperative project with J. Shoop, P. Eaton, and D. Buckman, Uni- versity of New Mexico Medical School, and W. Shreeve, Brookhaven National Laboratory | 14 |
| D-Glucose | ¹³ C | 26 | Clinical applications Studies on glucose metabolism | h | Cooperative project with W. Shreeve, Brookhaven National Laboratory | k |
| D-Glucose | ¹³ C ₆ | Biosynthesis (tobacco, chard, canna) | Clinical applications Studies on glucose metabolism Biological substrate General synthetic intermediate | f | Cooperative project with J. Shoop and P. Eaton, University of New Mexico Medical School, and W. Shreeve, Brookhaven National Laboratory | 12 13 |
| Glycerol | ¹³ C ₃ | Biosynthesis (marine red algae) | General synthetic intermediate | h | Concomitant product in bio- synthesis of galactose-U- ¹³ C ₆ | 14 |
| Glycine | All ¹³ C 2- ¹³ C- ¹⁵ N | 27 | Clinical studies Studies on hemoglobin biosynthesis Studies on porphyrin biosynthesis Cmr studies on metal ion complexes | g | Cooperative projects with W. Nyhan, University of California Medical School; A. Hofmann, Mayo Clinic; P. Klein, Argonne National Laboratory; B. Burnham, Utah State University; J. DeGrazia, Stanford University; and CNC-4 | 4 |
| L-Histidine | ¹³ C 2- ¹³ C | 28 | Cmr studies on hemoglobin conformation Cmr studies of metal ion complexes | g | Cooperative project with CNC-4 | 4 |
| 3-Hydroxy-3-methylglutaric acid | ¹³ C methyl- ¹³ C 3-methyl- ¹³ C ₂ | 29 | Studies on cholesterol biosynthesis | i | Cooperative project with T. Scallan, University of New Mexico Medical School | k |
| Iodomethane | ¹³ C 12C ¹³ C- ² H ₃ | 30 | Studies on proton radiative capture reactions as analytical method for ¹³ C/ ¹² C General synthetic intermediate Polyisotopic intermediate | g | Cooperative project with A-1 | 15 |
| Isobutyric acid | ¹³ C 1- ¹³ C | 3,4 | Molecular rearrangement studies | g | Cooperative project with A. Fry, University of Arkansas | 1 |
| Isopropylamine | ¹³ C ₂ | 9 | Studies on metabolism of propanolol | i | Cooperative project with T. Gaffney, University of South Carolina Medical School | |
| Lactic acid | All ¹³ C | 11 | Clinical applications Studies on carbohydrate metabolism | i | Cooperative project with W. Shreeve, Brookhaven National Laboratory | |

| <u>Compound</u> | <u>Label(s)</u> | <u>Method(s)</u> ^a | <u>Use</u> | <u>Status</u> | <u>Comments</u> | <u>Reference</u> ^b |
|------------------------------|-----------------------------------------------------------------------------------------------------------------|-------------------------------|-------------------------------------------------------------------------|---------------|-----------------------------------------------------------------------------------------------------------------------------------------|-------------------------------|
| Lactose | 1- ¹³ C | 31 | Clinical applications Studies on lactose metabolism | i | Cooperative project with J. Shoop and P. Eston, University of New Mexico Medical School, and W. Shreeve, Brookhaven National Laboratory | 4 |
| Linoleic acid | 1- ¹³ C | 32 33 | Future studies on lipid metabolism | j | Synthetic method developed by E. Olson, AWU Faculty Participant | 16 17 |
| Lithium acetylide | 1,2- ¹³ C ₂ | 10 | General synthetic intermediate Contraceptive steroids | h | Being prepared for NIGMS | 18 |
| Malonic acid, dimethyl ester | All ^c | 34 | General synthetic intermediate | i | Synthetic method developed by E. Olson, AWU Faculty Participant | 17 |
| Mannose | 1- ¹³ C | 26 | Future studies on carbohydrate metabolism | h | Concomitant product in synthesis of glucose-1- ¹³ C | k |
| Methane | ¹³ C | 35 | General synthetic intermediate, cyanide | g | Multimolar capacity | 19 |
| Methanol | ¹³ C ¹² C | 36 37 | General synthetic intermediate, acetic acid, iodomethane Car solvent | f | Multimolar capacity Prepared for NIGMS and CNC-4 | 20 k |
| Methylamine | ¹³ C- ² H ₄ | 37 | Polyisotopic intermediate | g | | 4 |
| O-Methylisourea | ¹³ C- ² H ₃ - ¹⁵ N ¹³ C- ¹⁵ N ₂ | 38 13 | Polyisotopic intermediate General synthetic intermediate, arginine | g h | | 4 21 |
| Nitrilotriacetic acid (NTA) | All ^d ¹⁵ N | 39 | Car and nmr studies of metal ion complexes | g | Cooperative project with CNC-4 and CNC-2 | k |
| Oleic acid | 1- ¹³ C | 32 33 | Future studies on lipid metabolism | j | Synthetic method developed by E. Olson, AWU, Faculty Participant | 16 17 |
| Phthalimide, potassium salt | ¹⁵ N | 40 | General synthetic intermediate Synthesis of primary amines | g | | 4 |
| Pivalic acid | 1- ¹³ C | 3 | Molecular rearrangement studies | g | Cooperative project with A. Fry, University of Arkansas | 1 |
| Propionic acid | All ^c | 3,4 | Clinical applications General synthetic intermediate | i | Cooperative project with W. Nyhan, University of California, San Diego Medical School | |
| Pyridine | ¹⁵ N | 41 | Nmr spectroscopic studies Molecular rearrangement studies | h | Prepared for CNC-2 Being prepared for CNC-2 | 22 |

| <u>Compound</u> | <u>Label(s)</u> | <u>Method(s)^a</u> | <u>Use</u> | <u>Status</u> | <u>Comments</u> | <u>Reference^b</u> |
|-----------------|--------------------------------------------------------------------------------------------------------------|--------------------------------------|-------------------------------------------------------------------------------------------------------------|---------------|--------------------------------------------------------------------------------------------------------------------------------------------------------------------|------------------------------|
| Pyruvic acid | All ¹³ C | 11 | Studies on carbohydrate metabolism | 1 | Cooperative project with W. Shreeve, Brookhaven National Laboratory | |
| β-Sitosterol | 3,4- ¹³ C ₂ | 42 | Mass spectrometry studies on steroid metabolism Mechanistic studies on molecular rearrangement reactions | 8 | Cooperative project with P. Klein, Argonne National Laboratory Synthesis done by M. Thompson, Agricultural Research Center | 23 |
| Sodium cyanide | ¹³ C | 43 44 45 | General synthetic intermediate, glucose-1- ¹³ C, lactose | 8 | Large-scale production accomplished from methane Prepared for NIGMS Cyanide- ¹³ C- ¹⁵ N available from formamide dehydration | 24 25 |
| Starch | ¹³ C U- ¹³ C | Biosynthesis (tobacco) | Biological substrate Glucose-U- ¹³ C intermediate | f | Principal product from tobacco (excised leaf) photosynthesis | 12 13 |
| Sucrose | ¹³ C ₁₂ U- ¹³ C ₁₂ | Biosynthesis (tobacco, chard, canna) | Future studies on carbohydrate metabolism | f | Concomitant product in ¹³ C synthesis of glucose-U- ¹³ C Can be converted into glucose-U- ¹³ C and fructose-U- ¹³ C | 12 13 |
| Tetramethylurea | ¹³ C ₅ - ² H ₁₂ - ¹⁵ N ₂ - ¹⁸ O | 46 | Studies on polyisotopic molecules | i | | 26,27 |
| Tryptophan | ¹³ C 2- ¹³ C | 47 | Studies on tryptophan metabolism | h | Cooperative project with W. Shreeve, Brookhaven National Laboratory | 4 |
| Urea | ¹³ C ₁₅ ¹³ C- ¹⁵ N ₂ ¹² C | 48 48 48 | Precursor of labeled barbiturates Arginine intermediate Denaturing proteins for cmr studies | 8 h 8 | Prepared for NIGMS Prepared for CMC-4 | 28 |

^aSee Fig. 1 for method of preparation.

^bLiterature reference from which the synthetic method was adapted or on which it was based.

^cAll possible ¹³C isotope isomers.

^dAll symmetrical ¹³C isotope isomers.

^eAll possible ¹³C isotope isomers in acetate portion of molecule.

^fPrepared routinely on continuing basis.

^gPreparation completed to satisfy current requirements.

^hSynthesis of labeled compound currently in progress.

ⁱSynthetic method currently being developed.

^jSynthetic method developed but preparation of labeled compound not in progress.

^kSynthetic method developed by Isotope Applications Section.

^lStandard synthetic method.

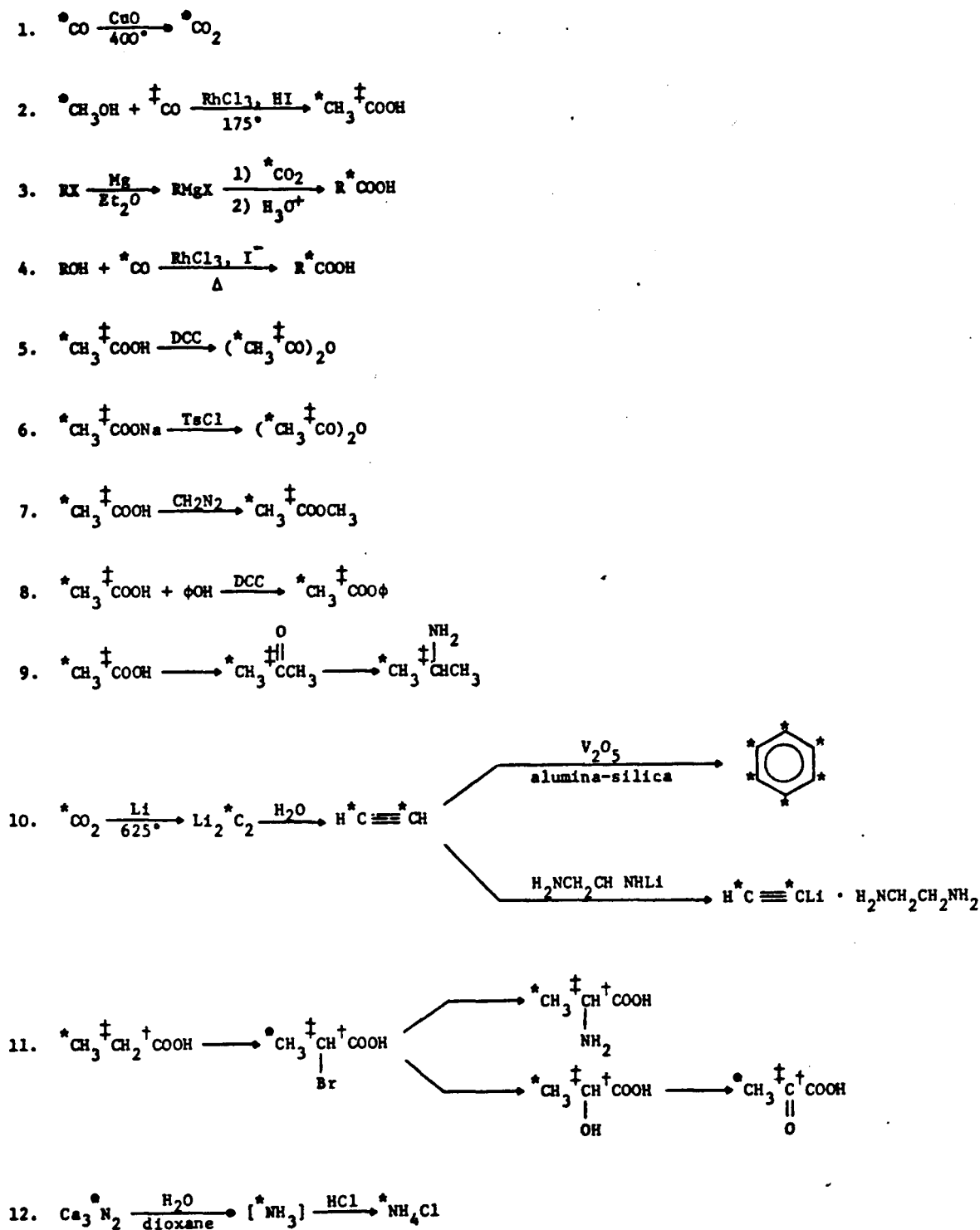
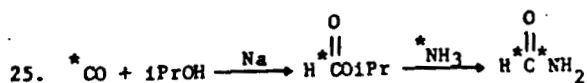
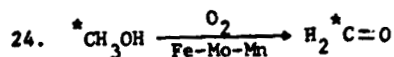
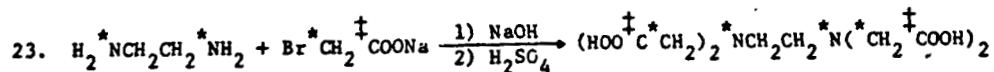
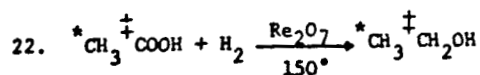
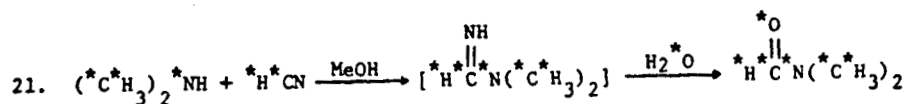
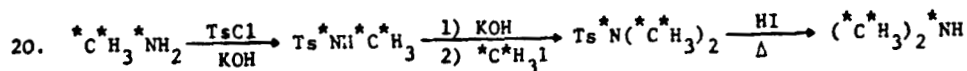
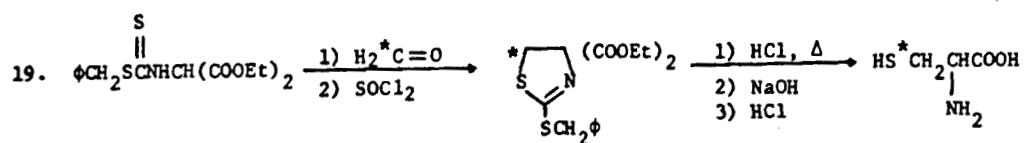
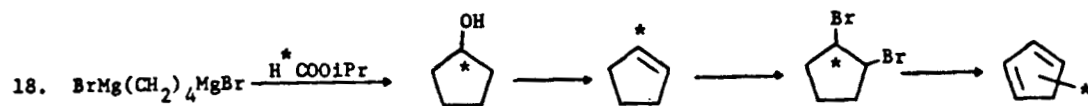
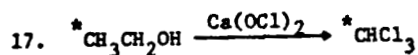
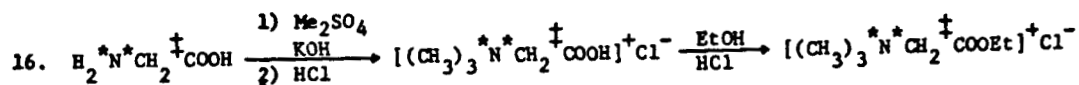
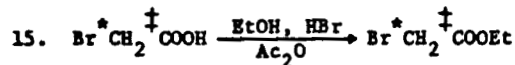
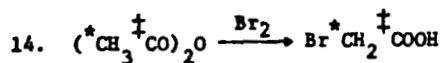
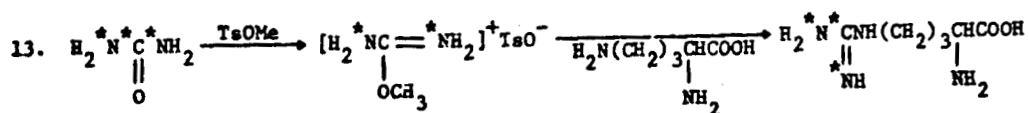
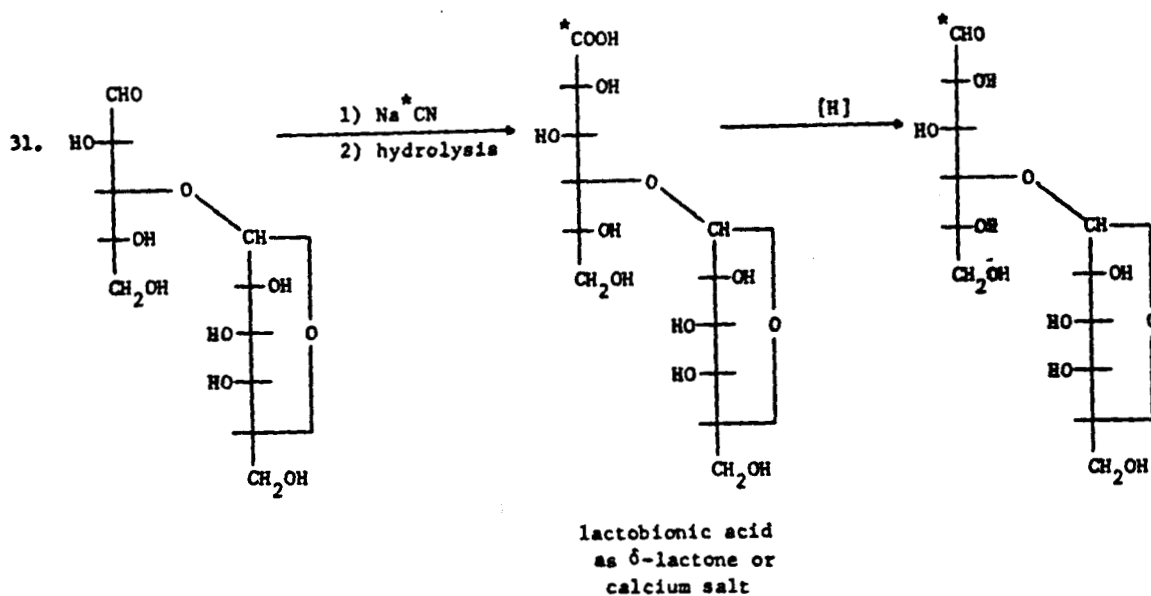
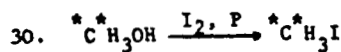
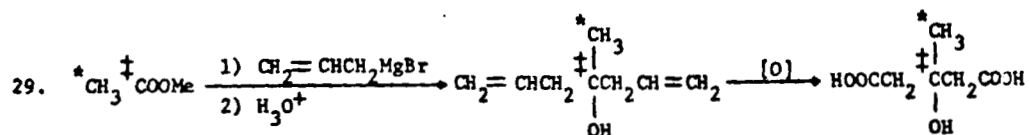
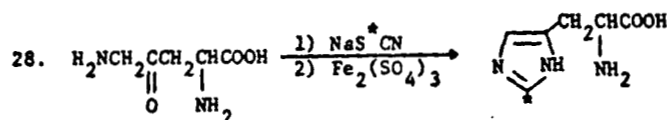
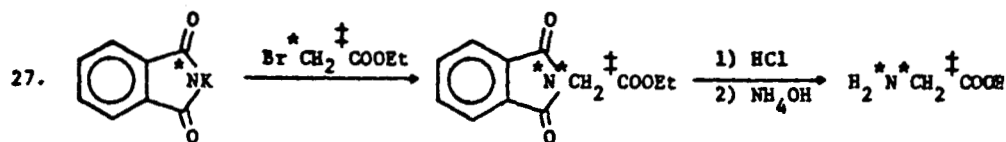
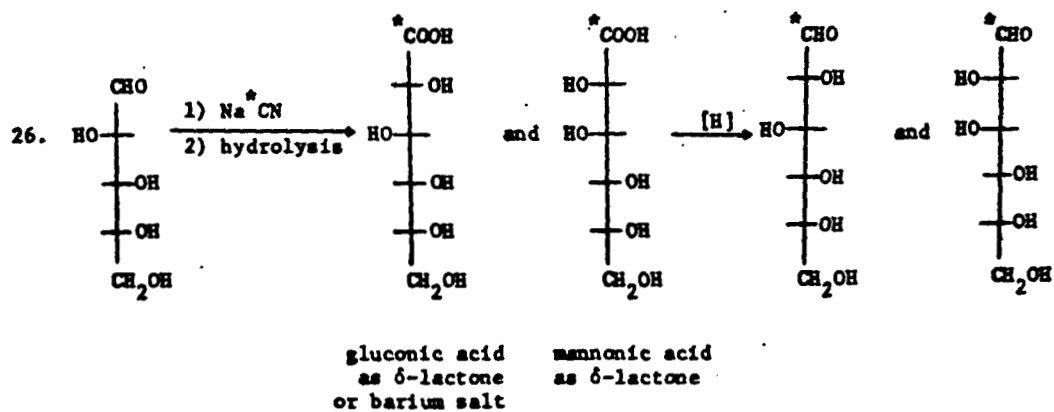
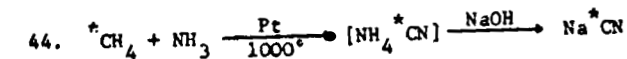
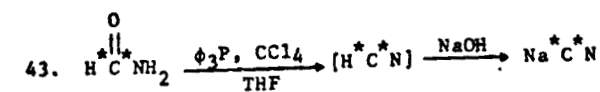
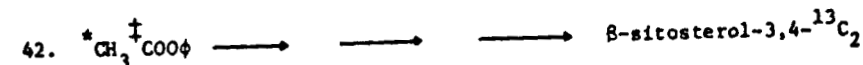
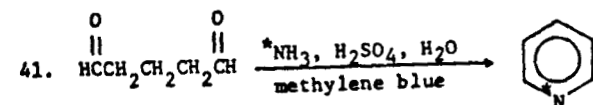
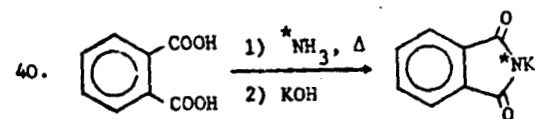
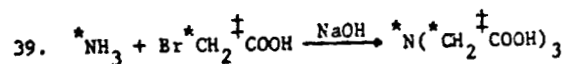
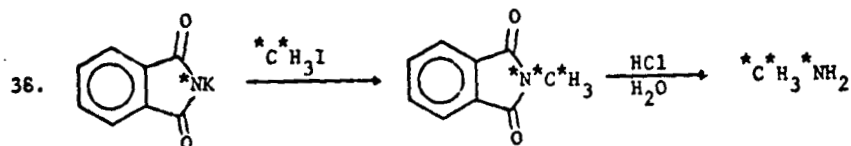
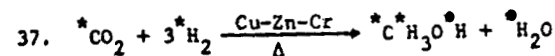
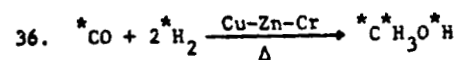
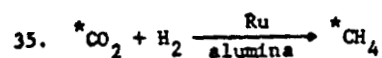
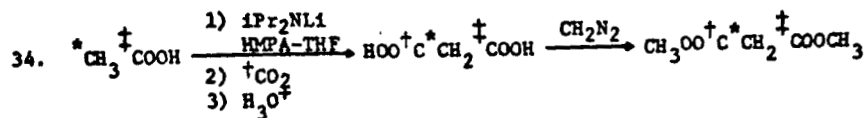
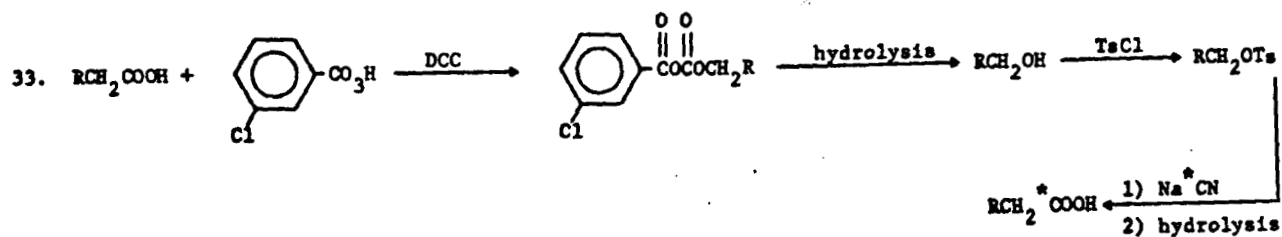
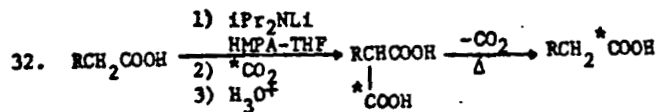
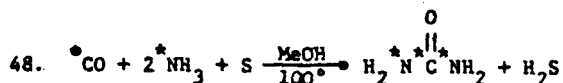
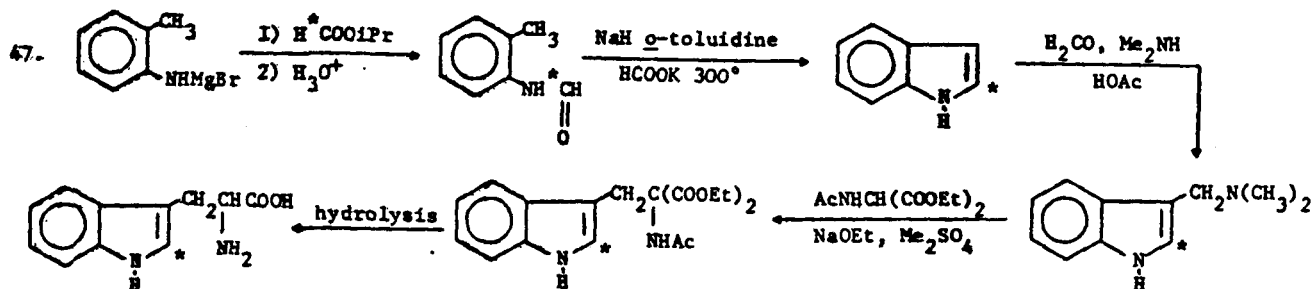
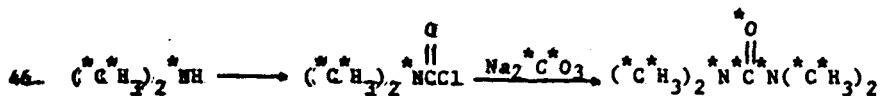
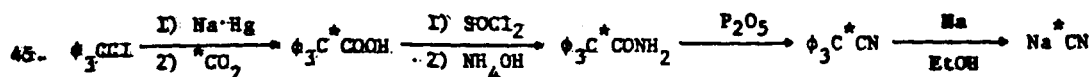


Fig. 1. Reaction sequences for preparation of labeled compounds. Isotopic labels have been indicated (*, †) to show both the position(s) of the isotopic atom(s) and the variety of isotopic compounds that can be prepared by a given synthetic method. Abbreviations used: R = alkyl group (Me = methyl, Et = ethyl, iPr = isopropyl), X = Cl, Br, I, DCC = dicyclohexylcarbodiimide, TsCl = p-toluenesulfonyl chloride, ϕ = phenyl = C₆H₅, TsOMe = methyl p-toluenesulfonyl anion, Ac₂O = acetic anhydride, [H] = reduction, [O] = oxidation, HMPA = hexamethylphosphoramide, THF = tetrahydrofuran, and Ac = acetyl = CH₃CO.









acids, methane, cyanide, methyl iodide, and certain others).

Relatively conventional laboratory glassware and apparatus and vacuum line techniques can be used generally for syntheses with stable isotopes. Owing to the extremely corrosive nature of rhodium carbonyls, preparations of carboxylic acids via carbonylation of alcohols are carried out in Hastelloy-C autoclaves (300-ml, 1-l., and 1-gallon capacities). These vessels are used for other types of pressure reactions as well. Stainless steel gas cylinders also serve as reaction vessels for less corrosive preparations (e.g., urea). Methanol is produced in lots of about 5 moles by catalytic hydrogenation of carbon dioxide in a specially constructed stainless steel apparatus. For preparation of methanol-¹²C, a second unit was constructed which is dedicated solely to carbon-12 to prevent contamination of this isotope isomer with carbon-13. A similar but smaller unit with about 1/50th the capacity, constructed of standard stainless steel fittings and tubing, is used for preparation of smaller amounts of polyisotopically substituted methanol (e.g., ¹³CD₃OD). An especially constructed apparatus is also used for synthesis of methane which forms the basis for isotopic cyanide production; methane will also be the required

intermediate for pyrolytic graphite-¹²C and graphite-¹³C. Figure 2 shows various items of apparatus devoted to relatively large-scale production of ¹²C- and ¹³C-labeled carboxylic acids, methanol and methane. The unit for synthesis of acetylene and benzene is shown in Fig. 3.

Biosynthesis

As is also encountered with organic synthesis, development of new procedures or combinations may

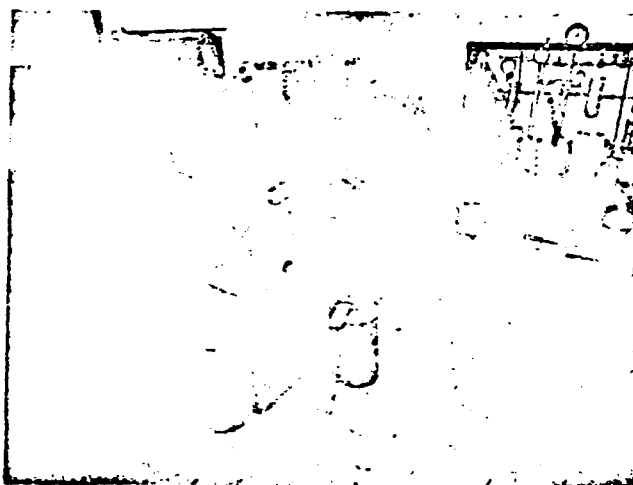


FIG. 2. Large-scale organic synthesis apparatus. Clockwise from lower left: 1-l. stirred autoclave, 1-gallon stirred autoclave, carbon-12 methanol unit, carbon-13 methanol unit, and methane unit.

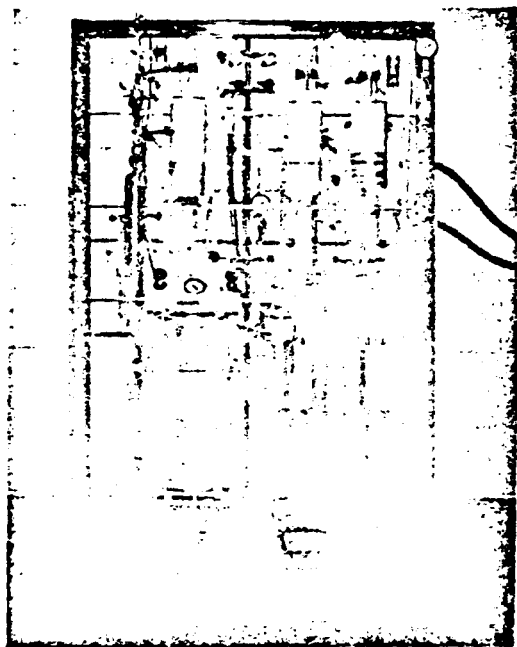


FIG. 3. Lithium carbide is prepared by reacting carbon dioxide with molten lithium in the reaction chamber (lower left). The acetylene liberated by treatment with water is purified and collected in a series of traps (upper portion) and can be transferred to storage vessels (lower right, rear) or converted to benzene on the vanadium oxide catalyst column (lower right, front).

be required for production of labeled materials through biosynthetic methods; often efficacious procedures perfected for radioactive isotope labeling are not entirely applicable with the amounts needed for stable isotope synthesis. For example, scaling up a procedure necessitating isolation and purification through chromatography when dozens of grams of product are involved may not be practical or even feasible. One of the major problems is not so much in finding a system which produces the desired products but one which also affords their isolation in a reasonable manner. Major emphasis the past year has been on development of methods and production of uniformly labeled carbon-13 sugars, in particular glucose-U-¹³C and galactose-U-¹³C, for applications in clinical trials.

Green algae.--Algae are appealing as a source of uniformly labeled compounds of biological importance because of their high incorporation efficiency of a simple carbon source, carbon dioxide. Efforts are being directed toward improving our previously attained production rates (ca. 1 g/l./day) using the large shaker apparatus by incorporation of high

intensity sodium vapor lamps into the 200-1. fermentor. This capability is desired for production of gram quantities of amino acids through collaboration with Dr. John Markley of Purdue University; in addition to application in this collaborative project, the amino acids are also desired in studies on histone biosynthesis in the Cellular and Molecular Radiobiology Sections. Other useful materials are concomitantly produced. Nucleotides will be utilized for investigations within the group and also in collaborations with Dr. William Rutter of the University of California Medical School, San Francisco. Fatty acids are needed as model compounds of carbon-13 in tracing environmental pollutants by Professor Lou Varga and Anthony Harmon (an AWU graduate student conducting this portion of his research in the section) of Oklahoma State University. Hopefully, the steroid fraction will serve as useful starting materials for applications in clinical studies and research by Dr. Duane Hagerman of the University of Colorado Medical School. The possibilities of using these organisms for production of glucose and galactose will also be investigated.

Yeast.--Analysis of the data obtained during the course of large-scale production of *Candida utilis* (for the mouse-feeding experiment conducted a year ago) is now being made. Acetic-1,2-¹³C acid served as the sole source of carbon. In Fig. 4 is

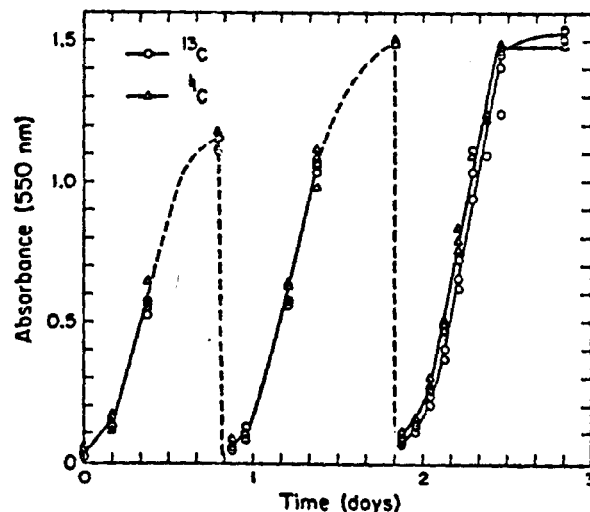


FIG. 4. Growth over 14 generations of yeast (*C. utilis*) metabolizing doubly labeled acetic-1,2-¹³C acid at 92.6 atom percent carbon-13 as the sole carbon source compared with yeast metabolizing normal abundance (1.1 atom percent carbon-13) acetate (3 flasks each).

shown the result of the first experiment ever made on the growth of *C. utilis* on highly enriched carbon-13, in this case, at 92.7 atom percent. Three spinner flasks contained the organism with acetic acid at normal abundance carbon-13 concentration (i.e., 1.1 atom percent); the other three flasks utilized the enriched substrate. The growth period was equivalent to 14 generations, during which no effect on growth rate of the high isotopic concentration can be discerned.

Figure 5 shows a typical experiment in which a yeast inoculum was grown up on normal carbon abundance acetate in a 14-l. fermentor and then transferred to the 200-l. fermentor and growth continued on doubly labeled acetic acid (80 atom percent carbon-13 in this experiment). There was no appreciable difference in lag period in the two media nor in the growth rates. These data are in contrast to results reported by other investigators²⁹ using the same labeled acetic acids but different growth rate measuring procedures; however, it was shown later³⁰ that the culture was, in fact, largely *C. krusei*, a typical fast growing impurity found in culture yeast propagations.

Growth of *C. utilis* on acetate (whether labeled or not) is biphasic. Figure 6 shows the growth curve and growth yield curve as functions of time for a typical experiment. The numbers accompanying the points of the growth yield curve are

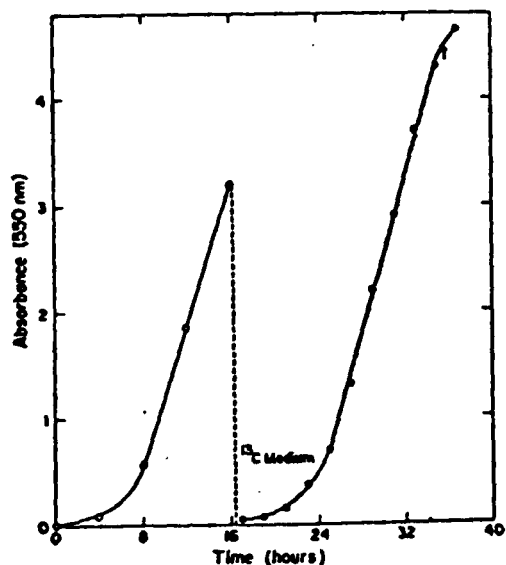


FIG. 5. Growth of yeast in a 14-l. fermentor on normal abundance acetate followed by inoculation into the 200-l. fermentor in a medium utilizing acetate at 80 atom percent carbon-13.

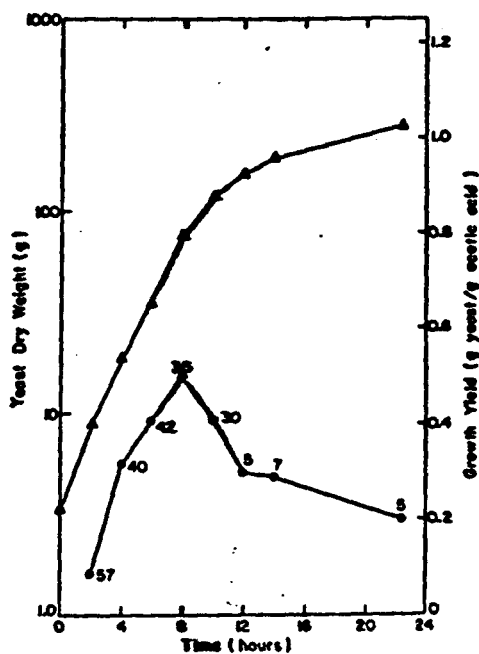


FIG. 6. Growth curve (absorbance at 550 nm, Δ) and growth yield curve (g yeast/g acetate, \circ) for *C. utilis* growing on acetic acid as sole carbon source. Numerals indicate percentages of budding.

the percentages of yeast cells budded. The initial rapid rise of the yield curve with a corresponding decline in budding rate was consistently observed. The peak marks the termination of the period of exponential cell growth which, typically, spanned the interval from 2 to 8 hr after inoculation of the culture. Following transition from exponential to linear growth, the growth yield and percentage of budding cells dropped sharply over a 4-hr period, then fell more slowly until the end of the experiment. Clearly, optimum incorporation of carbon-13 from acetate into yeast requires that growth be maintained somehow in the late exponential phase.

In the course of this series of experiments, over 1.8 kg of yeast was produced at an average carbon-13 enrichment of 80 atom percent. Nearly 6 kg of acetic acid was consumed for an average yield of 32 percent; most of the remaining carbon was recovered as respired carbon dioxide.

Candida utilis was also grown at 20 atom percent carbon-13 (optimized with respect to cmr spin-spin coupling considerations) by LASL Visiting Staff Member Dr. R. T. Eakin of the University of Texas. From this product was isolated 6-phosphogluconate dehydrogenase for kinetic and physical studies to measure the effects of varying levels of carbon-13

enrichment. Yeast hydrolysates were also used as carbon sources for growth of a mutant of *Neurospora crassa* which produces a high level of cytochrome c. This protein has now been purified and will also be used in isotope effects and physical studies.

Marine red algae.--Large-scale photosynthetic production of galactose-U-¹³C for clinical applications has come from incubation of thalli from *Gigartina corymbifera* and *Gigartina harveyana*. The red kelp are obtained fresh in 4- to 6-kg quantities from Pacific Bio-Marine Supply Company, Los Angeles, about 24 hr or less after they are harvested from the ocean. Photosynthetic incubation is carried out in the apparatus shown in Fig. 7 over a 24-hr period, after which the non-reducing galactoside, α-D-galactopyranosyl-2-glycerol, is extracted from the thalli. Except for scaling up of 4000- to 6000-fold, extractions are made essentially according to published procedures.³¹

The crude extract is then chromatographed on a Dowex 50W X8 (200- to 400-mesh, Ba⁺⁺) column, and the resulting pure galactoside is hydrolyzed with dilute trifluoroacetic acid. Galactose is obtained by crystallization, and the glycerol is recovered from the mother liquor. Another purification method involves acetylation of the crude galactoside, followed by isolation and deacetylation of the precipitated hexaacetate. Following removal of the acetyl groups with base, acid hydrolysis then yields galactose and glycerol. This latter method appears quite applicable on a small scale and for

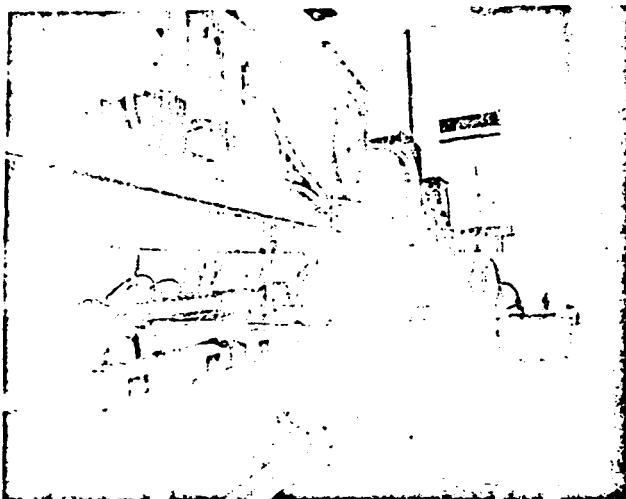
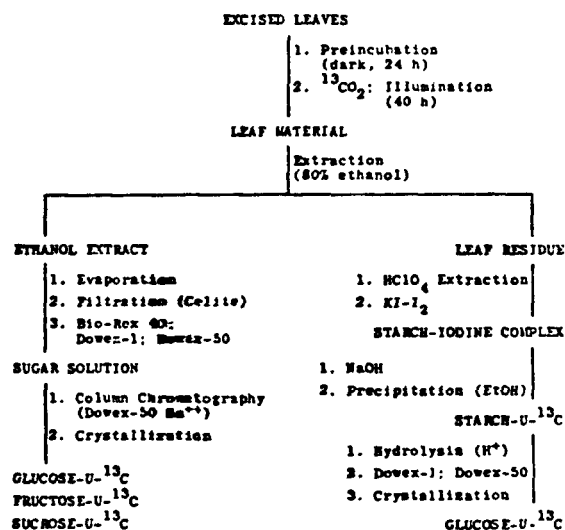


FIG. 7. Photosynthetic incubation apparatus. The 3 Lucite chambers have a total volume of ~100 l. and are mounted on a common oscillating mechanism.

analytical purposes, and the first method is applicable for large-scale preparations.

Initial experiments using 1- to 6-kg quantities of *Gigartina* did not result in as high yields as expected and, additionally, a greater amount of endogenous material was found in the product than reported.³¹ Although the experiments served the purpose of developing required procedures (and furnishing a limited amount of galactose-U-¹³C), minor modifications of our experimental procedures (particularly with respect to preincubation conditions) and procurement of uniform quality organisms should enhance production to the anticipated level of 25 g/week of galactose-U-¹³C at about 90 atom percent carbon-13.

Green plants.--As a source of uniformly labeled carbon-13 glucose, sucrose, and fructose, three green plant systems are being evaluated: *Nicotiana tobacum* L., variety Coker 319; Swiss chard, variety Burpee's Fordhook Giant; and *Canna indica*, variety Burpee's Dwarf Primrose Yellow. The most desirable system will be that which has the highest extractable yield of desired carbohydrate at the lowest manpower cost. To obtain the desired quantities of products, similar procedures described previously for carbon-13 labeling have been scaled up by several hundred fold, and more efficient and desirable methods of isolation and purification have been developed, as illustrated in the following scheme.



Tobacco plants are grown in the laboratory using soilless culture methods and artificial lighting (Fig. 8), following published procedures,^{32,33} from seed supplied by Professor C. D. Raper, North

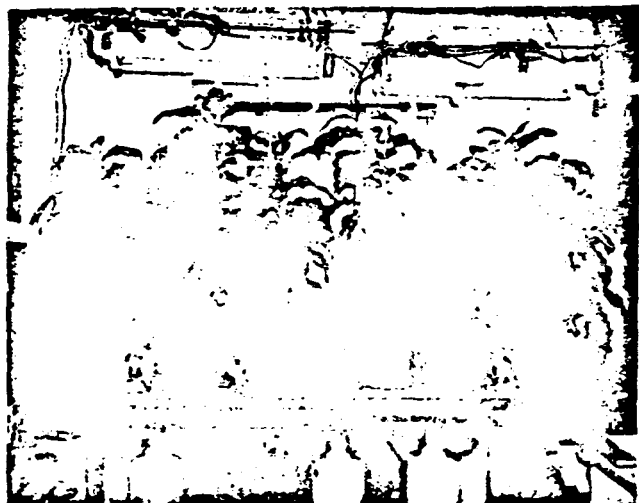


FIG. 8. Tobacco plants at about 3 months growing in the laboratory under soilless culture conditions. Nutrient addition and lighting cycles are automatically controlled. The excised leaves are used for photosynthetic production of carbon-13 labeled sugars.

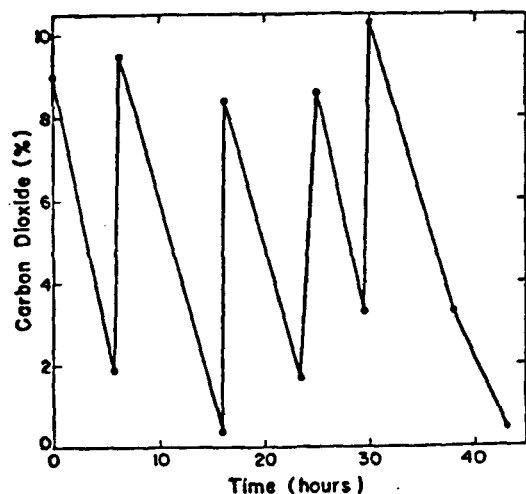


FIG. 9. Carbon dioxide uptake by excised tobacco leaves.

Carolina State University. During the course of the experiments with the first planting, about 8 kg of tobacco leaves were taken from 15 mature plants (growth period greater than 75 days). In each experiment, about 1 kg of leaves was excised and preincubated for 24 hr in the dark. Photosynthetic incubation with carbon-¹³C dioxide was carried out over approximately 40 hr (Fig. 9) in Lucite shaker boxes (see Fig. 7).

Leaves were removed from the chambers, frozen in liquid nitrogen to quench metabolism, and stored at 20°C. The free sugars and starch were extracted essentially as described by Putman *et al.*¹³ Starch was hydrolyzed with dilute trifluoroacetic acid to

glucose, which was recrystallized following evaporation of the solution. Glucose, sucrose, and fructose were separated chromatographically in 25-g quantities using a 5 x 100-cm column of Dowex 50W X8 (200- to 400-mesh, Ba⁺⁺) resin.³⁴ The sugars were characterized by enzymatic assay, by optical rotation, by gas chromatography of the trimethylsilyl derivatives, by ion exchange chromatography of the borate complexes, and by cmr (which also confirmed label uniformity).³⁵ The degree of enrichment of carbon-13 in the sugars was determined by mass spectrometric measurement of the ¹³C/¹²C isotope ratio in the carbon dioxide produced by wet combustion.

Eight incubations of tobacco leaves from the first planting produced the carbohydrates in yields shown in Table 2. The nature of ¹³C-containing byproducts remaining in the leaves after extraction has not been determined nor has the amount of extractable products in the leaf vines (these were removed from the leaves prior to extraction). With existing facilities, a steady-state production rate of approximately 50 g of crystalline glucose per week can be maintained at an estimated personnel cost of two man-hours per g. Plantings of tobacco are being made at intervals to ensure that a source of labeled glucose is readily available; the second crop is now mature and being used, and subsequent plantings are developing. Further details are described elsewhere.¹²

Experiments with Swiss chard and Canna have

TABLE 2. CARBON-13 LABELED CARBOHYDRATES PRODUCED BY TOBACCO LEAF PHOTOSYNTHESIS^a

| Product | g | Yield ^b | |
|----------|------------------|--------------------|---------|
| | | Percent | Percent |
| Starch | 155 ^c | | 33 |
| Glucose | 44 | | 10 |
| Fructose | 54 | | 12 |
| Sucrose | 21 | | 5 |

^a From 8 experiments which utilized 8.2 kg of excised leaves and 660 g of ¹³CO₂ at 83 atom percent ¹³C (average).

^b Based on ¹³CO₂; corrected for ca. 2 percent endogenous materials.

^c Moisture content 14 percent; hydrolysis and crystallization gave 130 g D-glucose.

been performed in essentially the same way as with tobacco, the main differences being that the length of time photosynthetic illumination is allowed to take place is reduced from 40 to 20 hr and that starch is not involved. The reduced time period is sufficient to produce the labeled carbohydrates³⁵ without incorporating large quantities of isotope in unextractable material. Three incubation experiments with Canna using 2.2 kg of mature leaves and three Swiss chard using 3.3 kg of leaves have been performed. Purification and analysis of the three major carbohydrates produced (glucose, fructose, and sucrose) are not yet complete; however, there is indication that, although the yields are quite good, neither Canna nor chard will prove superior to tobacco for our requirements.

STABLE ISOTOPES IN BIOMEDICAL RESEARCH

(D. G. Ott, C. T. Gregg, J. Y. Hutson, V. N. Kerr, V. H. Kollman, T. W. Whaley, and T. G. Sanchez)

Clinical Applications

The use of non-radioactive stable isotopes (in particular carbon-13) obviates various limitations encountered in application of radioactive isotopes in humans and would greatly enlarge the scope of isotopic tracer tests for pregnant women and children, for elective diagnostic procedures in large-scale populations, and for many basic physiological and pharmacological studies in healthy subjects. A current objective of the Isotope Applications Section is to foster and engage in efforts to demonstrate one or more clinical applications with high probability of widespread adoption and utilization of relatively large amounts of carbon-13. These initial tests have been selected on the basis of being both scientifically and clinically meaningful and technically feasible at the present stage of development of the program. Simplicity and reliability of testing from the standpoints of the nature of the organic compound used, clinical procedure, and technical measurement of the isotope in the biological products are other important considerations.

Collaborative relationships are being utilized to carry out the clinical procedures. Although Dr. Walton Shreeve of the Brookhaven National Laboratory was at LASL as a Visiting Staff Member from January to August to establish and conduct the first

clinical trials, as well as to initiate plans for additional tests, a research physician is not a permanent member of the staff, and a satisfactory clinical facility does not exist at LASL. Through Dr. Shreeve's efforts, cooperative ventures have begun with Dr. Phillip Eaton and Dr. Jon Shoop of the University of New Mexico School of Medicine at Albuquerque, which should entail extensive interaction between clinical staff members at this nearby institution and the LASL staff. Close coordination is being maintained with Dr. Shreeve following his return to Brookhaven. Other clinical trials are being encouraged through collaboration with other investigators [viz., Dr. Peter Klein of Argonne National Laboratory in conjunction with Dr. Alan Hoffman of Mayo Clinic (glycine-¹³C, for diverticulitis, etc.) and with Dr. William Nyhan of the University of California, San Diego (glycine-¹³C, for studies of glycinuria and aciduria in pediatric abnormalities); Dr. Clive Solomon and Dr. E. K. Cotton of the University of Colorado (arginine-¹³C/¹⁵N, for studies in cystic fibrosis); and Dr. David Kipnis of Washington University, St. Louis (alanine-¹³C, for amino acid/carbohydrate metabolism, particularly in pediatrics)].

In some cases, collaborations involve applications which are limited in clinical volume but particularly specific for employment of stable isotopes. We believe that, in addition to direct diagnostic applications, a broad usage in clinical and pharmacological research would further justify and stimulate production of stable isotopes and development of instrumentation. The latter can involve exploration of feasibility of new or unique methods of measurement (e.g., proton radiative capture reactions or nuclear magnetic resonance being actively pursued by LASL Groups A-1 and CNC-4, respectively) adapted for particular biological products in blood, urine, and perhaps tissues. Refinement and adaptation of existing techniques (e.g., mass spectrometry and infrared gas analysis) are also important functions in support of clinical studies.³⁶

Some metabolic diseases are common yet difficult to recognize either clinically or by laboratory tests. Even if recognized, the metabolic categories within and causes for disease entities need better elucidation. One of these diseases is diabetes.

Studies with ^{14}C -labeled compounds such as glucose and lactic acid have already been aimed toward early diagnosis and metabolic understanding of maturity-onset diabetes. As extensions of these studies, oxidation to expired carbon dioxide of glucose- ^{13}C is being tested when the labeled glucose is contained in the glucose load of an oral glucose tolerance test. Such a test embodies the principle of simplification of clinical procedure to encourage wide acceptance by patients in screening programs. Previous studies with ^{14}C -labeled glucose indicated that determination of isotopic carbon in exhaled carbon dioxide at various times following ingestion of the labeled glucose load did indeed show impaired carbohydrate metabolism in diabetic subjects. Extensions of these studies are now in progress utilizing glucose- ^{13}C , for which the Investigational New Drug Number 9002 was provided by the Food and Drug Administration. Figure 10 illustrates some selected results obtained for four subjects: a severe diabetic, a mild (adult-onset) diabetic, and two (non-diabetic) controls. Approximately a dozen tests have been performed; additional control subjects and patients suspected of diabetes will be studied similarly. However, present data seem to indicate that the test lacks sufficient specificity to diagnose mild diabetes. Application of glucose- ^{13}C in these studies (Food and Drug Administration

Investigational New Drug Number 8602), in consideration of involvement of C-1 in the various normal and abnormal metabolic pathways, could possibly be more discriminating than glucose- ^{13}C ; however, recent tests with glucose- ^{14}C , in conjunction with glucose- ^{13}C by Dr. Shreeve at Brookhaven, indicate that differentiation is still insufficient. Attention will now be directed toward investigation of ^{13}C -labeled L-lactic acid (and perhaps pyruvic acid and L-alanine) as likely materials for diagnosis of diabetes through isotopic analysis of breath carbon dioxide.

The oral dose of glucose- ^{13}C used in glucose tolerance studies was 40 g/m^2 of body area; the carbon-13 concentration was 2.1 atom percent (1.0 atom percent excess). Because the glucose- ^{13}C was synthesized at much higher enrichment, dilution with normal glucose was necessary. In adjusting isotopic concentrations in materials labeled with stable isotopes, consideration must be given to the amount of natural abundance isotope involved (another example of differences between use of stable isotopes and radioactive isotopes).

Galactose- ^{13}C should be available soon in quantities sufficient to proceed with clinical trials (following receipt of a FDA investigational new drug number) of a galactose tolerance test (oral administration) which also utilizes analysis of carbon dioxide in the breath as the diagnostic parameter. This test should be applicable to patients with hypothyroidism (for whom it could be a particularly needed functional test of tissue oxidative capacity) and to patients with hepatic cirrhosis (who also show impaired galactose tolerance).

Lactose- ^{13}C appears to be well suited for a major clinical application, since conversion of lactose- ^{14}C to carbon- ^{14}C dioxide *in vivo* has been shown to reveal readily the condition of intestinal lactase deficiency, which is probably a frequent cause of infant diarrhea as well as milk intolerance in children and adults. This is a highly prevalent condition in whites (10 to 20 percent) and even higher in Africans, Orientals, and American Indians. A widespread use of lactose- ^{13}C in pediatrics may be predicted. A study of the incidence of this genetic deficiency in Southwest Indian groups is indicated in the LASL area, particularly as it may

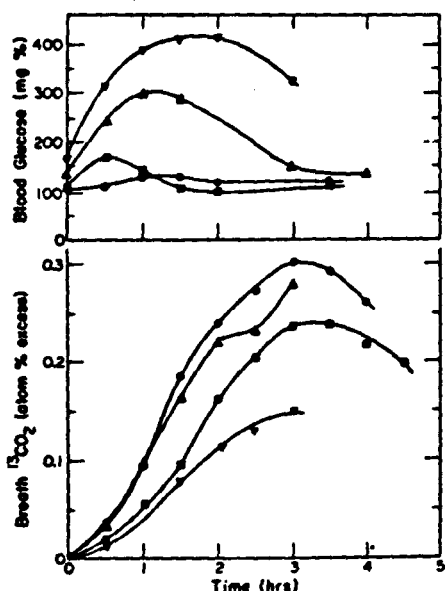


FIG. 10. Blood glucose levels and breath carbon- ^{13}C dioxide concentrations following oral administration of 40 g/m^2 of glucose- ^{13}C at 1.0 atom percent excess carbon-13: (Δ) severe diabetic; (∇) mild diabetic; (\circ) and (\bullet) control (nondiabetic) subjects.

be a cause of their common (and frequently fatal) infant diarrhes.

Biochemistry

Whole cell studies.--An interesting application of ^{13}C enrichment in biological systems was provided by examination of the cmr spectrum of yeast (*C. utilis*) at 78 atom percent ^{13}C . The spectrum of whole cells, at remarkably high resolution, is shown in Fig. 11a. Each of the numbered peaks can be assigned to a class of carbon atoms in the complex mixture. For example, peaks 19, 20, and 21 are methine carbons, peak 9 is in the expected position for the alpha carbon atoms of polypeptide chains, while peak 1 represents the terminal methyl carbons of long-chain fatty acids. Further studies were made on the water-soluble fraction from intact yeast cells (Fig. 11c), the residue remaining after exhaustive extraction with water (Fig. 11b), and finally with chloroform-methanol (not shown). These experiments are significant in that they establish the practicality of examining the ^{13}C -enriched fractions of complex biological mixtures even in suspensions of intact cells or crude extracts.

As an extension of this work, unlabeled yeast were allowed to metabolize glucose-1- ^{13}C with 10

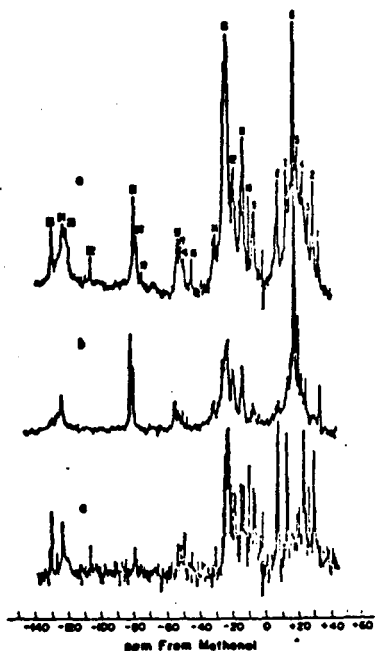


FIG. 11. Carbon-13 nuclear magnetic resonance spectra of *C. utilis* cells: (a) whole cells suspended in D_2O ; (b) cellular components remaining after exhaustive extraction with D_2O ; and (c) water-soluble components released by osmotic shock.

atom percent ^{13}C at C-1. The experiment was carried out under anaerobic conditions in the cmr sample tube, and spectra were accumulated at intervals by the fast Fourier transform method. The results are shown, in part, in Fig. 12. The actual spectra in the region of C-1 of glucose are shown for zero time and for pulse accumulations from 56 to 70 min and from 83 to 99 min. The insert summarizes the results of the complete experiment. The signal from C-1 progressively declines, while that of ethanol-2- ^{13}C gradually rises. The steady increase in a so far unidentified ^{13}C -compound is also shown. This signal may be that of intracellular glucose which might be expected to give a different signal from that of extracellular glucose. This important point is under further investigation.

Carbon- ^{13}C monoxide binding to various hemoglobins, cytochrome, and metalloporphyrins.--A number of studies on the cmr spectra of ^{13}CO bound to various molecules of biological importance have been carried out at LASL. Only a single peak is observed in the same spectral region whether the binding hemoglobin is in intact red cells, hemolysates, or solutions of previously crystallized hemoglobin (Table 3). Hemoglobins from man, mouse, and dog show the same behavior even under conditions

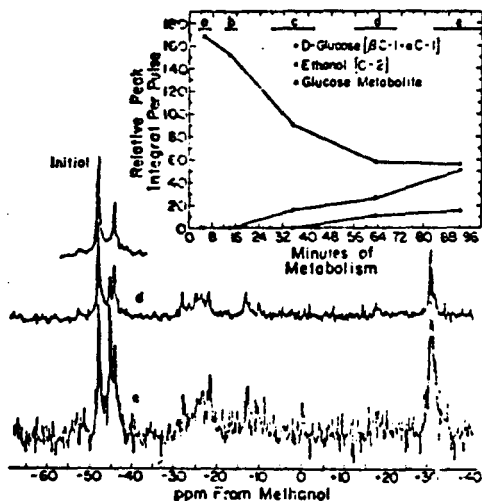


FIG. 12. Metabolism of glucose-1- ^{13}C by *C. utilis*: (a) 3 to 7 min after initiation of metabolism; (b) 12 to 16 min; (c) 28 to 42 min; (d) 56 to 70 min; and (e) 83 to 99 min. The spectra obtained during the initial time periods show only the signals corresponding to the carbon-13 substrate; the glucose C-1 region is illustrated. Signals in the region between -12 and -28 ppm are from the natural abundance carbon-13 in glucose carbons other than C-1.

TABLE 3. CARBON-13 CHEMICAL SHIFTS OF ¹³CO
COORDINATED TO SOME Fe(II) HEME PROTEINS AT 26°C

| System | Chemical shifts ^a |
|----------------------------------|------------------------------|
| Free CO | -51.2 |
| Fe(CO) ₅ | -82.5 |
| Protoporphyrin IX, dimethylester | -76.2 |
| Human whole blood | -77.4 (50 Hz) |
| Packed human red blood cells | -77.6 (55 Hz) |
| Human hemoglobin ^b | -77.2 (50 Hz) |
| Urea-denatured human hemoglobin | -76.7 (5 Hz) |
| Myoglobin | -78.6 (5 Hz) |
| Carboxymethyl cytochrome c | -75.8 (5 Hz) |
| Urea-denatured cytochrome c | -76.4 (5 Hz) |
| Rabbit whole blood | -77.5 -79.5 |

^aIn ppm from methanol; the numbers in parentheses are the full widths of the signals at half maximum intensity.

^bCrystallized from pooled human blood samples and redissolved in D₂O.

of acid or base denaturation or in 8 M urea. The spectrum of the ¹³CO bound to iron of cytochrome c or to synthetic iron porphyrins is the same as that of iron carbonyl or the complex biological molecules. As shown in Table 3, line widths for single-chain proteins like myoglobin and cytochrome c are much narrower than for intact hemoglobin. The hemoglobin line width for redissolved crystalline hemoglobin is the same as for hemoglobin in whole blood or packed red cells, while denaturation in 8 M urea causes a substantial narrowing of the hemoglobin line.

A recent paper³⁷ reported a spectrum with two equal peaks for ¹³CO bound to rabbit hemoglobin. These authors ascribe the two peaks to different binding of the ¹³CO by the hemoglobin alpha and beta chains. Our data suggest that the explanation given by the authors cannot be correct, but we have verified that rabbit hemoglobin does indeed show two peaks of bound ¹³CO. Two peaks of equal intensity ratio were observed in blood from the first of three 6-month-old male Dutch banded rabbits. The second rabbit showed an intensity ratio of the peaks of 4:5, while the third rabbit's blood gave two peaks of intensity 1:5. The most likely explanation is a population of two hemoglobins in the adult rabbit. Measurement of the amounts of fetal

hemoglobin in each rabbit showed that their blood contained 7.5, 5.5, and 4.5 percent fetal hemoglobin, respectively; however, this does not seem to account for the intensities of the two-banded spectrum. Samples of the blood of rabbits 1 and 3 have been sent to Dr. Stephen Shohat, University of California Medical School, San Francisco, where the hemoglobin components will be separated, measured, and returned to Los Alamos for further study. Since there is abundant evidence for heterogeneity in both alpha and beta chains of rabbit hemoglobin due to polymorphic alleles (rather than nonallelic genes), study of the ¹³CO binding by separated hemoglobins will explain, hopefully, the experimental observations.

Other animal studies.--In collaboration with Dr. Deither Neubert, Chairman of the Department of Embryonal Toxicology, Free University of Berlin, we have begun a study of the effects of high ¹³C enrichment on embryonal metabolism in mice. The first requirement of these investigations was production of precisely timed pregnancies in some 60 mice. In the first experiment, glucose-U-¹³C initially was given intravenously and subsequently by stomach tube to mice during the 8th and 9th days of pregnancy; in a second experiment, glucose was given during the 10th and 11th gestational days. In a third experiment, glucose-U-¹³C was given during day 11 of gestation with some of the animals being sacrificed at 8 hr after the first isotope administration and the remainder at 24 hr. In the last isotope experiment, mice in day 16 of gestation were used, and carbon-13 was administered at intervals for 8.5 hr for some of the animals and for 24 hr for the remainder. Additional nonisotopic experiments were performed to measure the effects on embryo resorption and blood glucose levels of various routes and time sequences of glucose administration.

After each isotopic experiment, the embryos were removed, weighed, then homogenized and separated into a variety of chemical fractions.³⁸ Maternal blood and liver were collected, as well as other maternal tissues in some experiments. Fetal livers were collected separately from the day 16 embryos. Labeled red blood cells were sent to Dr. Shohat's laboratory in San Francisco for examination of red cell membranes by cmr. Carbon-13 enriched, highly purified DNA was isolated from

some fractions and will be analyzed in the analytical ultracentrifuge and, if possible, by *cmr*. Crude RNA fractions (mostly ribosomal but probably also containing t-RNAs) were prepared along with a variety of liver glycogen samples. A labeled chromatin fraction, a histone fraction, and a DNA residue (after histone extraction) were prepared for *cmr* examination, and crude RNA polymerase was isolated from both normal carbon and isotopic carbon maternal and fetal nuclei. These samples are in addition to the crude acid-soluble fractions, etc.,³⁸ being made from a variety of maternal and fetal material obtained in the course of these experiments.

A number of benefits are expected from this approach. Carbon-13 labeled biological materials can be prepared from the mammalian material, and the effects of highly enriched carbon-13 can be studied on the very sensitive embryonal system. We also hope to develop methods for localizing the metabolic lesion caused by embryotoxic agents by noting changes in the patterns of carbon-13 incorporation (by *cmr*) when the embryotoxin and a carbon-13 substrate are given simultaneously. Moreover, we expect that the carbon-13 labeling may prove a powerful tool for isolating macromolecules formed *de novo* in a variety of synchronized biological systems, of which the mammalian embryo is the most complex example.

Biosynthetic pathways.--In a collaborative project with Dr. Milton Allison, U. S. Department of Agriculture, Ames, Iowa, it was found by application of *cmr* techniques that C-2 from acetate was incorporated by a rumen organism entirely into C-3 of isoleucine rather than C-2 as expected on the basis of known metabolic pathways. Further investigations are being carried out using both acetate-2-¹³C and acetate-1,2-¹³C. It is anticipated that considerable information about pathways of amino acid biosynthesis can be obtained through application of carbon-13 labeling and *cmr* in a more straightforward manner than is possible with mass spectroscopy or with radioactive labeling.

REFERENCES

1. R. E. Schreiber, ed., *ICONS at LASL*, Los Alamos Scientific Laboratory report LA-4759-MS (September 1971).
2. D. E. Armstrong, A. C. Briesmeister, B. B. McInteer, and R. M. Potter, A Carbon-13 Production Plant Using Carbon Monoxide Distillation. Los Alamos Scientific Laboratory report LA-4391 (April 1970).
3. F. E. Paulik and J. F. Roth, Novel catalysts for the low pressure carbonylation of methanol to acetic acid. *Chem. Comm.* 1578 (1968). Dutch Patent Application 6,804,850 (October 7, 1968).
4. A. Murray and D. L. Williams, "Organic Synthesis with Isotopes." Interscience Publishers, Inc., New York (1958).
5. J. E. Noakes, S. M. Kim, and J. J. Stipp, Chemical and counting advances in liquid scintillation age dating. In: *Proceedings of the Sixth International Conference on Radiocarbon and Tritium Dating*, Pullman, Washington (1965), p. 68.
6. J. E. Noakes, S. M. Kim, and G. A. Thomas, A chemical study of an ambient temperature catalytic benzene synthesis used in radiocarbon dating. Oak Ridge Institute of Nuclear Science report 46 (November 1964).
7. J. Ssuknewitsch and A. Tschiligarjan, Über die einwirkung von calciumhypochlorit auf organische verbindungen mit hydroxyl- und carbonylgruppen. I. *Mitteil: Calciumhypochlorit und die höheren primären alkohole.* *Ber.* 68B, 1210 (1935).
8. A. H. Dutton and F. Heath, The preparation of [¹⁴C]dimethylamine and [¹⁴C]dimethylnitrosamine. *J. Chem. Soc.* 1892 (1956).
9. P. L. DeBonneville, J. Strong, and V. T. Elkind, Nitrile groups. III. The preparation of N-substituted formamides and thioformamides from hydrogen cyanide. *J. Org. Chem.* 21, 772 (1956).
10. H. S. Broadbent, G. C. Campbell, W. J. Bartley, and J. H. Johnson, Rhenium and its compounds as hydrogenation catalysts. III. Rhenium heptoxide. *J. Org. Chem.* 24, 1847 (1959).
11. L. Luciani, Formaldehyde production. Italian Patent Application 675,778 (November 19, 1964).
12. V. H. Kollman, J. L. Hanners, J. Y. Hutson, T. W. Whaley, D. G. Ott, and C. T. Gregg, Large-scale photosynthetic production of carbon-13 labeled sugars: The tobacco leaf system. *Biochem. Biophys. Res. Commun.* (1973), in press.
13. E. W. Putman, W. Z. Hassid, G. Krotkov, and H. A. Barker, Preparation of radioactive carbon-labeled sugars by photosynthesis. *J. Biol. Chem.* 173, 785 (1948).
14. E. W. Putman and W. Z. Hassid, Structure of galactosylglycerol from *Iridaea laminarioides*. *J. Am. Chem. Soc.* 76, 2221 (1954).
15. H. S. King, Methyl iodide. In: "Organic Synthesis," *Coll. Vol. II*, John Wiley and Sons, Inc., New York (1943), p. 399.

16. D. B. Denney and N. Sherman, Degradation of acids to alcohols by the carboxy-inversion reaction. *J. Org. Chem.* 30, 3760 (1965).
17. P. E. Pfeffer, L. S. Silbert, and J. M. Chirinko, α Anions of carboxylic acids. II. The formation and alkylation of α -metalated aliphatic acids. *J. Org. Chem.* 37, 451 (1972).
18. O. F. Beumel and R. F. Harris, The preparation of lithium acetylde-ethylenediamine. *J. Org. Chem.* 28, 2775 (1963).
19. R. W. Buddemeier, A. Y. Young, A. W. Fairhall, and J. A. Young, Improved system of methane synthesis for radiocarbon dating. *Rev. Sci. Instr.* 41, 652 (1969).
20. P. Davies and F. Snowden, Production of oxygenated hydrocarbons. U. S. Patent 3,326,956 (June 20, 1967).
21. J. W. Janus, O-Alkylation of urea. *J. Chem. Soc.* 3551 (1955).
22. J. E. Colchester and J. A. Corran, Pyridine. British Patent 1,077,573 (August 2, 1967). *Chem. Abstr.* 68, 87171g (1968).
23. H. L. Otto, A. C. Besemer, and W. H. J. M. Wientjens, Synthesis of β -sitosterol-3- ^{14}C . *J. Labelled Compounds* 6, 111 (1970).
24. D. Baufl, S. Mlinko, and T. Palagyi, A new synthesis for the preparation of ^{14}C -labelled alkali cyanides. *J. Labelled Compounds* 7, 221 (1971).
25. E. Yamato and S. Sugasawa, Preparation of nitrile from primary amide. *Tetrahed. Lett.* 50, 4387 (1970).
26. J. K. Lawson and J. T. Croom, Dimethylamides from alkali carboxylates and dimethylcarbomoyl chloride. *J. Org. Chem.* 28, 232 (1963).
27. A. Fry, A tracer study of the reaction of isocyanates with carboxylic acids. *J. Am. Chem. Soc.* 75, 2686 (1953).
28. R. A. Franz and F. Applegath, A new urea synthesis. I. The reaction of ammonia, carbon monoxide and sulfur. *J. Org. Chem.* 26, 3304 (1961).
29. V. H. Kollman, W. H. Adams, J. R. Buchholz, C. W. Christenson, J. Langham, R. Price, and E. B. Fowler, Production of *Candida utilis* with 95 Atom Percent ^{13}C Acetic Acid as the Sole Carbon Source, Los Alamos Scientific Laboratory report LA-4551 (1971).
30. V. H. Kollman, unpublished results.
31. R. C. Bean, E. W. Putman, R. E. Trucco, and W. Z. Hassid, Preparation of ^{14}C -labeled D-galactose and glycerol. *J. Biol. Chem.* 204, 169 (1953).
32. C. D. Raper, Jr., W. H. Johnson, and R. J. Downs, Factors affecting the development of flue-cured tobacco grown in artificial environments. I. Effects of light duration and temperature on physical properties of fresh leaves. *Agronomy J.* 63, 283 (1971).
33. C. D. Raper, Jr., and C. B. McCants, Influence of nitrogen nutrition on growth of tobacco leaves. *Tob. Sci.* 11, 175 (1967).
34. J. K. N. Jones and R. A. Wall, The separation of sugars on ion-exchange resins. *Canad. J. Chem.* 38, 2290 (1960).
35. E. W. Putman and W. Z. Hassid, Isolation and purification of radioactive sugars by means of paper chromatography. *J. Biol. Chem.* 196, 749 (1952).
36. R. T. Eakin, L. O. Morgan, C. T. Gregg, and N. A. Matwiyoff, Carbon-13 nuclear magnetic resonance spectroscopy of living cells and their metabolism of a specifically labeled ^{13}C substrate. *FEBS Lett.* 28(3), 259 (1972).
37. R. B. Moon and J. H. Richards, Nuclear magnetic resonance studies of ^{13}CO binding to various heme globins. *J. Am. Chem. Soc.* 94, 5093 (1972).
38. R. Krowke, G. Siebert, and D. Neubert, Biochemical screening test with ^{14}C -glucose and ^{32}P -phosphate for the evaluation of embryotoxic effects *in vivo*. *Naunyn-Schmiedebergs Arch. Pharm.* 271, 274-288 (1971).

ANIMAL COLONY ACTIVITIES

INTRODUCTION

The LASL animal colony operations continued along the same lines as reported for 1971¹ with increased activities in the hot particle program and in the areas of pathology and disease surveillance. Day-to-day inventories of animals have not changed significantly over the previous year. Construction of a small flexible animal-holding facility in the TA-51 complex remote from the main laboratory building will begin in the spring. The facility will be constructed to house larger animals such as swine but can be converted for work with rodent species. The facility also will provide a location for isolation of animals brought to the LASL for short-term experiments by outside investigators using the biomedical beam at the CPAMFF.

DISEASE SURVEILLANCE

(P. M. LaBauve, M. R. Brooks, and L. M. Holland)

For several years a surveillance program has been in effect to aid in control of Pseudomonas aeruginosa and related pseudomonads in the mouse colony. A system utilizing chlorinated water (12 ppm) plus disposable bottle caps and twice weekly bottle changes has been in use since 1969.

Cages of mice are tested at time of changing by culturing water from the bottles on a special selective medium (Pseudosel, BBL). In addition, stool cultures are performed periodically on representative cages. Stock and breeding mice are tested at least quarterly, and mice used in radiation experiments are tested before and during the experiments, often weekly.

Incidence of positive cages was quite low during the first 6 months of 1972 (5 out of 749 cages). However, in June 1972, an outbreak occurred in one breeding room and was traced to a dirty air conditioning filter. Severe culling and regular testing have reduced the number of positive cages to quite low levels, and the outbreak has not spread to

other rooms. The situation responsible for this condition was corrected.

In addition to the Pseudomonas surveillance program, colony control studies are performed on a routine basis. Microbiological examinations for Mycoplasma, Pasteurella, and enteric pathogens are performed on all rodent and lagomorph species on a random basis, and all incoming animals are tested extensively during quarantine.

SUPPORT ACTIVITIES

(P. M. LaBauve, S. G. Carpenter, L. M. Holland, J. R. Prine, and R. H. Wood)

In any radiation lethality study involving larger laboratory species such as monkeys and dogs, infection plays a major role in all but the very highest dose rate exposures. Over the last year, we have made an attempt to define the bacteriological flora of rhesus monkeys (Macaca mulatta) before exposure to lethal irradiation and to determine what, if any, bacterial species can be recovered from the blood during the terminal stages of the experiment (see Mammalian Radiobiology Section of this report). Throat, fecal, and blood cultures are obtained from each of 10 monkeys just prior to start of radiation exposure. Both aerobic and anaerobic culture techniques are employed to identify significant species of bacteria. Table 1 shows the species identified and frequency of isolation.

The presence, in many of the monkeys, of the "trench mouth" organisms without clinical signs of the disease is of interest, as one of the signs of approaching terminal illness in monkeys is infection of and hemorrhage from the gums. Two of the animals had Shigella species in the throat, demonstrating the ability of the monkey to live with the constant presence of Shigella. Positive blood culture for Shigella in one animal and Staphylococcus epidermidis in three animals was attributed to contamination at the time the blood sample was drawn.

TABLE 1. INCIDENCE OF CERTAIN BACTERIAL SPECIES IN MONKEYS (MACACA MULATTA)

| <u>Bacterial species</u> | <u>Total number of isolations</u> | | |
|-------------------------------|-----------------------------------|--------------|--------------|
| | <u>Throat</u> | <u>Stool</u> | <u>Blood</u> |
| Proteus sp. | 6 | 6 | |
| Hemolytic staphylococci | 4 | 4 | |
| Nonhemolytic staphylococci | 2 | 2 | |
| Streptococcus viridans | 5 | 5 | |
| Borrelia and fusiform bacilli | 6 | 6 | |
| Shigella sp. | 4 | 2 | 1 1 |
| Clostridium perfringens | 9 | | 9 |
| Escherichia and Aerobacter | 10 | | 10 |
| Staphylococcus epidermidis | 3 | | 3 |
| Bacteriodes sp. | 3 | 1 | 2 |

TABLE 2. POSITIVE BLOOD CULTURES AT TERMINATION

| | |
|----------------------------|---|
| Staphylococcus epidermidis | 1 |
| Bacteroides | 1 |
| Clostridium perfringens | 1 |

The constant finding of Clostridium perfringens in the stool cultures is interesting but not surprising, as Clostridia are considered a normal inhabitant of the gastrointestinal tract of most mammals.² However, this observation is worthy of note, as Clostridium perfringens plays a role in tissue destruction found in the lethal gastric bloat syndrome of macaques.³

Table 2 shows the species of bacteria recovered from blood cultures of the same animals just prior to death. The largely negative results indicate that either the monkey does not suffer from a terminal bacteremia under these conditions or the timing of sampling was questionable. Results and methods of the entire experiment are to be reported elsewhere.

PATHOLOGY

(J. R. Prine, S. G. Carpenter, R. H. Wood, and L. M. Holland)

Pathology studies lend support to most of the programs utilizing animal models. During the first 11 months of calendar 1972, nearly 800 complete pathological examinations were performed on a variety of animals. Most of the work load is associated with the hot particle program which demands

detailed gross and histological studies on each animal. In addition, comparative radiation lethality studies involving dogs and monkeys call for complete pathology studies on individual animals.

One of the more important pathology activities is development of a technique for radiography of whole hamster lung utilizing ultrasoft X rays. This technique, which also preserves the tissue for later histological study, is explained in detail elsewhere in this report (The Hot Particle Project).

HAMSTER ANESTHESIA

(L. M. Holland, G. A. Drake, J. E. London, and J. S. Wilson)

Development of production-line techniques of microsphere injection utilizing the water pick⁴ requires that we anesthetize hamsters on a volume basis. Use of intraperitoneal pentobarbital led to death losses up to 10 to 12 percent during the immediate post-operative period in some instances and an additional few later deaths from injury to abdominal organs. To overcome this loss, we now use ketamine hydrochloride (Ketaset, Bristol Laboratories), a new anesthesia marketed for use in cats, that has the distinct advantage of being designed for intramuscular use. Ketamine hydrochloride has a wide margin of safety and acts very rapidly with an effective duration of 10 to 15 minutes. We have now used this drug in over 1000 hamsters, including some that were given a full anesthetic dose weekly for 12 weeks, and have observed no deleterious after-effects. With the use of this drug, our anesthetic losses have dropped from ~10 percent to less than 1 percent. A note on this application is in preparation for publication.

COMPLIANCE WITH FEDERAL LAWS

To our knowledge, we have remained in compliance with all federal laws governing the care and treatment of laboratory animals. The LASL's Biomedical Research Group has been accredited by the American Association for Laboratory Animal Care (AALAC) since 1966. Representatives from AALAC made a site visit for the purpose of updating our accreditation during November 1972.

REFERENCES

1. C. R. Richmond and G. L. Voelz, eds., Annual Report of the Biological and Medical Research Group (H-4) of the LASL Health Division, January through December 1971, Los Alamos Scientific Laboratory report LA-4923-PR, pp. 131-133.
2. D. W. Bruner, In: Hagan's Infectious Diseases of Domestic Animals, Fifth Ed., Comstock Publishing Associates, Ithaca, New York (1966).
3. W. M. Newton, P. D. Beamer, and H. E. Rhoades, Acute Bloat Syndrome in Stumptailed Macaques. Lab. Animal Sci. 21, 193-196 (1971).
4. L. M. Holland, G. A. Drake, J. E. London, and J. S. Wilson, Intravenous Injection with a Pulsed Dental Cleaning Device. Lab. Animal Sci. 21, 913-915 (1971).

APPENDIX

1972 BIBLIOGRAPHY FOR BIOMEDICAL RESEARCH GROUP

HOT PARTICLE PROJECT

Manuscript Submitted

M. J. Fulwyler, J. D. Perrings, and L. S. Cram, Production of Uniform Microspheres. *Rev. Sci. Instr.* (in press).

MOLECULAR RADIOBIOLOGY SECTION

Publications

P. Byvoet, G. R. Shepherd, J. M. Hardin, and B. J. Noland, Turnover of Labeled Methyl and Acetyl Groups in Histone Fractions of Cultured Mammalian Cells. *Federation Proc.* 31(2), 854 Abs (1972), Abstract No. 3563.

P. Byvoet, G. R. Shepherd, J. M. Hardin, and B. J. Noland, the Distribution and Turnover of Labeled Methyl Groups in Histone Fractions of Cultured Mammalian Cells. *Arch. Biochem. Biophys.* 148, 558-567 (1972).

U. Hollstein and P. L. Butler, Inhibition of Ribonucleic Acid Synthesis by Myxin. *Biochemistry* 11, 1345-1350 (1972).

R. L. Ratliff, Synthesis of Mixed Polynucleotides Containing Ribo- and Deoxyribonucleotides by Terminal Deoxynucleotidyl Transferase. *Federation Proc.* 31(2), 425 Abs (1972), Abstract No. 1165.

G. R. Shepherd, J. M. Hardin, B. J. Noland, and P. Byvoet, Turnover of Methyl, Acetyl, and Phosphoryl Groups in Histone Fractions of Cultured Mammalian Cells. *In: Abstracts of the First Rocky Mountain Regional Meeting of the American Chemical Society, Colorado State University, Fort Collins, Colorado (June 30-July 1, 1972), p. 13, Abstract No. 5.*

G. R. Shepherd, R. A. Walters, J. M. Hardin, and B. J. Noland, The Effects of X-Irradiation on Histone Acetylation and Methylation in Cultured Mammalian Cells. *Arch. Biochem. Biophys.* 149, 175-182 (1972).

D. A. Smith, A. M. Martinez, and D. L. Williams, Initiation of *In Vitro* RNA Synthesis with Oligodeoxyribonucleotides. *In: Abstracts of Papers of the 164th National Meeting of the American Chemical Society, New York City, New York (August 27-September 1, 1972), Abstract No. 71.*

G. F. Strniste, A. M. Martinez, and D. A. Smith, *In Vitro* Studies on the Synthesis of Ribonucleic Acid Using Ionizing Irradiated RNA Polymerase. *In: Abstracts of the 16th Annual Meeting of the Biophysical Society, Toronto, Ontario, Canada (February 24-27, 1972) 12, 155a (1972), Abstract No. SaPM-B16.*

G. F. Strniste and D. A. Smith, *In Vitro* Studies on the Synthesis of Ribonucleic Acid Using X-Irradiated RNA Polymerase. *In: Abstracts of the First Rocky Mountain Regional Meeting of the American Chemical Society, Colorado State University, Fort Collins, Colorado (June 30-July 1, 1972), p. 17, Abstract No. 18.*

Manuscripts Submitted

G. H. Daub, M. E. Ackerman, and F. N. Hayes, Anhydrous Hydrofluoric Acid as a Cyclizing Agent in the Preparation of Several Substituted Oxazoles from *N*-Aroyl- α -Aminoketones. *J. Org. Chem.* (in press).

D. M. Gray, R. L. Ratliff, and D. L. Williams, The Circular Dichroism of Poly d(AAT):d(ATT) and Poly r(AAU):r(AUU). A Test of the First-Neighbor Hypothesis. *Biopolymers* (submitted).

R. L. Ratliff, D. L. Williams, F. N. Hayes, and D. A. Smith, Preparation and Properties of the Repeating Sequence Polymer d(A-A-T)_n·d(A-T-T)_n. *J. Biol. Chem.* (submitted).

G. R. Shepherd, B. J. Noland, and J. M. Hardin, Structural Modifications of Histones in Cultured Mammalian Cells. *In: Proceedings of the International Meeting on "The Biochemistry of Gene Expression in Higher Organisms," Sydney, Australia*

(May 15-19, 1972). Australian and New Zealand Book Company and D. Reidel Publishing Company, Dordrecht, Holland (in press).

G. R. Shepherd, B. J. Noland, and J. M. Hardin, Turnover of Histone Acetyl Groups in Cultured Mammalian Cells. *Exp. Cell Res.* (in press).

G. R. Shepherd, J. M. Hardin, and B. J. Noland, Dephosphorylation of Histone Fractions of Cultured Mammalian Cells. *Arch. Biochem. Biophys.* (in press).

G. R. Shepherd, Evidence for the Biological Coupling of Biosynthesis and Internal Acetylation of Histone Fraction F2al in Cultured Mammalian Cells. *Biochim. Biophys. Acta* (in press).

J. E. Simpson, G. H. Daub, and F. N. Hayes, The Synthesis of Some 3',2''-Dioxamethylene Bridged p-Quaterphenyls and Related Compounds. *J. Org. Chem.* (submitted).

J. E. Simpson, G. H. Daub, and F. N. Hayes, The Synthesis of Some 2,2'-Dioxabridged Biphenyls and 1,1'-Binaphthyls. *J. Org. Chem.* (submitted).

G. F. Strniste, D. A. Smith, and F. N. Hayes, X-Ray Inactivation of the *Escherichia coli* DNA-Dependent RNA Polymerase in Aqueous Solution. I. Studies on Binding and Substrate Concentration Dependence in the Inactivation of Enzymatic Activity. *Biochemistry* (in press).

G. F. Strniste, D. A. Smith, and F. N. Hayes, X-Ray Inactivation of the *Escherichia coli* DNA-Dependent RNA Polymerase in Aqueous Solutions. II. Studies on Initiation and Fidelity of Transcription. *Biochemistry* (in press).

CELLULAR RADIOBIOLOGY SECTION

Publications

B. J. Barnhart and S. H. Cox, Replication and Sizing of Bacteriophage DNA: Membrane-Associated Functions in *Haemophilus influenzae*. In: Abstracts of the 72nd Annual Meeting of the American Society for Microbiology, Philadelphia, Pennsylvania (April 23-28, 1972), p. 202, Abstract No. V104.

L. L. Deaven and D. F. Petersen, Are Chromosomally Aneuploid Cells Genetically Aneuploid? In: Abstracts of Papers Presented at the Twelfth Annual Meeting of the American Society for Cell Biology, St. Louis, Missouri (November 8-11, 1972) 55, 57a (1972), Abstract No. 113.

M. D. Enger and R. A. Tobey, Effects of Iso-leucine Deficiency on Nucleic Acid and Protein Metabolism in Cultured Chinese Hamster Cells: Continued RNA and Protein Synthesis in the Absence of DNA Synthesis. *Biochemistry* 11, 269-277 (1972).

M. D. Enger and E. W. Campbell, Nascent Messenger-Like RNA Metabolism in Chinese Hamster Ovary Cells Cultured at Elevated Temperature. In: Abstracts of the 28th Annual Southwest Regional Meeting of the American Chemical Society, Baton Rouge, Louisiana (December 6-8, 1972), p. 33, Abstract No. 65.

L. R. Gurley, R. A. Walters, and R. A. Tobey, The Metabolism of Histone Fractions. IV. Synthesis of Histones during the G₁-Phase of the Mammalian Life Cycle. *Arch. Biochem. Biophys.* 148, 633-641 (1972).

L. R. Gurley and R. A. Walters, The Metabolism of Histone Fractions. V. The Relationship between Histone and DNA Synthesis after X-Irradiation. *Arch. Biochem. Biophys.* 153, 304-311 (1972).

L. R. Gurley, R. A. Walters, and R. A. Tobey, The Relationship of Histone Phosphorylation to the Cell Cycle. In: Abstracts of Papers Presented at the Twelfth Annual Meeting of the American Society for Cell Biology, St. Louis, Missouri (November 8-11, 1972) 55, 99a (1972), Abstract No. 198.

L. R. Gurley, R. A. Walters, and R. A. Tobey, The Independence of Histone Phosphorylation from DNA Synthesis. In: Abstracts of the 28th Annual Southwest Regional Meeting of the American Chemical Society, Baton Rouge, Louisiana (December 6-8, 1972), p. 34, Abstract No. 67.

A. E. Hampel, A. G. Saponara, R. A. Walters, and M. D. Enger, Low Molecular-Weight RNAs of Post-Ribosomal Particles: Evidence that the Particulate 4S RNAs Comprise a Differential Population of Transfer RNA. *Biochim. Biophys. Acta* 269, 428-440 (1972).

C. E. Hildebrand and R. A. Tobey, DNA-Membrane Associations in Cultured Chinese Hamster Cells. In: Abstracts of the 16th Annual Meeting of the Biophysical Society, Toronto, Ontario, Canada (February 24-27, 1972) 12, 249a (1972), Abstract No. Su-AM-E9.

P. M. Kraemer, Complex Carbohydrates of Mammalian Cells in Culture. In: Growth, Nutrition and Metabolism in Cells in Culture, Vol. 1 (G. H.

Rothblat and V. J. Cristofalo, eds.), Academic Press, New York (1972), pp. 371-426.

P. M. Kraemer, L. L. Deaven, H. A. Crissman, and M. A. Van Dilla, DNA Constancy Despite Variability in Chromosome Number. *In: Advances in Cell and Molecular Biology*, Vol. 2 (E. J. DuPrav, ed.), Academic Press, New York (1972), pp. 47-108.

P. M. Kraemer and R. A. Tobey, Cell-Cycle Dependent Desquamation of Heparan Sulfate from the Cell Surface. *J. Cell Biol.* 55, 713-717 (1972).

P. M. Kraemer, H. A. Crissman, and M. A. Van Dilla, Flow Microfluorometric (FMF) Studies of Plant Lectin Binding to Cultured Mammalian Cells. *In: Abstracts of Papers Presented at the Twelfth Annual Meeting of the American Society for Cell Biology*, St. Louis, Missouri (November 8-11, 1972) 55, 141a (1972), Abstract No. 281.

R. A. Tobey and H. A. Crissman, Preparation of Large Quantities of Synchronized Mammalian Cells in Late G₁ in the Pre-DNA Replicative Phase of the Cell Cycle. *Exp. Cell Res.* 75, 460-464 (1972).

R. A. Tobey, Arrest of Chinese Hamster Cells in G₂ following Treatment with the Anti-Tumor Drug Bleomycin. *J. Cell. Physiol.* 79, 259-265 (1972).

R. A. Tobey, H. A. Crissman, and P. M. Kraemer, A Method for Comparing Effects of Different Synchronizing Protocols on Mammalian Cell-Cycle Traverse: The Traverse Perturbation Index. *J. Cell Biol.* 54, 638-645 (1972).

R. A. Tobey, A Simple, Rapid Technique for Determination of the Effects of Chemotherapeutic Agents on Mammalian Cell-Cycle Traverse. *Cancer Res.* 32, 309-316 (1972).

R. A. Tobey, Effects of Cytosine Arabinoside, Daunomycin, Mithramycin, Azacytidine, Adriamycin, and Camptothecin on Mammalian Cell-Cycle Traverse. *Cancer Res.* 32, 2720-2725 (1972).

R. A. Tobey and H. A. Crissman, Use of Flow Microfluorometry in Detailed Analysis of Effects of Chemical Agents on Cell-Cycle Progression. *Cancer Res.* 32, 2726-2732 (1972).

R. A. Tobey, H. A. Crissman, and P. M. Kraemer, A Method for Comparing Effects of Different Synchronizing Protocols on Mammalian Cell-Cycle Traverse. *In: Abstracts of Papers Presented at the Twelfth Annual Meeting of the American Society for Cell Biology*, St. Louis, Missouri (November 8-11, 1972) 55, 99a (1972), Abstract No. 198.

R. A. Walters, L. R. Gurley, R. A. Tobey, M. D. Enger, and R. L. Ratliff, Effects of X-Irradiation on DNA Precursor Metabolism and DNA Replication in Chinese Hamster Cells. *In: Abstracts of Papers for the 20th Annual Meeting of the Radiation Research Society*, Portland, Oregon (May 14-18, 1972), pp. 25-26, Abstract No. CB-8.

R. A. Walters, L. R. Gurley, R. A. Tobey, M. D. Enger, and R. L. Ratliff, Effects of X-Irradiation on DNA Precursor Metabolism and DNA Replication in Chinese Hamster Cells. *In: Abstracts of the First Rocky Mountain Regional Meeting of the American Chemical Society*, Colorado State University, Fort Collins, Colorado (June 30-July 1, 1972), p. 17, Abstract No. 20.

R. A. Walters, R. L. Ratliff, L. R. Gurley, and M. D. Enger, The Effects of X-Irradiation on the Methylation of DNA from Chinese Hamster Ovary Cells. *In: Abstracts of the 28th Annual Southwest Regional Meeting of the American Chemical Society*, Baton Rouge, Louisiana (December 6-8, 1972), p. 34, Abstract No. 68.

Manuscripts Submitted

B. J. Barnhart, S. H. Cox, and R. T. Okinaka, Characterization of Defective Lysogeny in Haemophilus influenzae. *Virology* (submitted).

B. J. Barnhart and S. H. Cox, DNA Replication of Induced Prophage in Haemophilus influenzae. *J. Virol.* (submitted).

D. P. Bingham and B. J. Barnhart, Inhibition of Transformation by Antibodies against Competent Haemophilus influenzae. *J. Gen. Microbiol.* (in press).

L. L. Deaven and D. F. Petersen, The Chromosomes of CHO, an Aneuploid Chinese Hamster Cell Line: C-Band, C-Band, and Autoradiographic Analyses. *Chromosoma* (in press).

L. R. Gurley, R. A. Walters, and R. A. Tobey, Histone Phosphorylation in Late Interphase and Mitosis. *Biochem. Biophys. Res. Commun.* (in press).

L. R. Gurley, R. A. Walters, and R. A. Tobey, The Metabolism of Histone Fractions. VI. Differences in the Phosphorylation of Histone Fractions during the Cell Cycle. *Arch. Biochem. Biophys.* (in press).

L. R. Gurley, M. D. Enger, and R. A. Walters, The Nature of Histone fl Isolated from Polysomes. *Biochemistry* (in press).

C. E. Hildebrand and R. A. Tobey, DNA-Membrane Complexes in Cultured Chinese Hamster Cells. I. Nature of the DNA-Membrane Association. *J. Cell Biol.* (submitted).

C. E. Hildebrand and R. A. Tobey, DNA-Membrane Complexes in Cultured Chinese Hamster Cells. II. Involvement of DNA-Membrane Complexes in Temporal and Spatial Organization of DNA. *J. Cell Biol.* (submitted).

P. M. Kraemer, R. A. Tobey, and M. A. Van Dilla, Flow Microfluorometric Studies of Plant Lectin Binding to Mammalian Cells. I. General Features. *J. Cell. Physiol.* (submitted).

P. M. Kraemer and H. A. Crissman, Flow Microfluorometric Studies of Plant Lectin Binding to Mammalian Cells. II. Interference between Concanavalin A and Wheat Germ Agglutinin Sites. *J. Cell. Physiol.* (submitted).

A. G. Saponara and M. D. Enger, The Isolation from Ribonucleic Acid of Substituted Uridines Containing α -Aminobutyrate Moieties Derived from Methionine. *J. Biol. Chem.* (submitted).

R. A. Tobey, Production and Characterization of Mammalian Cells Reversibly Arrested in G_1 by Growth in Isoleucine-Deficient Medium. In: *Methods in Cell Physiology*, Vol. VI (D. M. Prescott, ed.), Academic Press, New York (in press).

MAMMALIAN RADIOBIOLOGY SECTION

Publications

W. H. Langham, Biological Implications of the Transuranium Elements for Man. *Health Phys.* **22**, 943-952 (1972).

C. R. Richmond and G. L. Voelz, eds., Annual Report of the Biological and Medical Research Group (H-4) of the LASL Health Division, January through December 1971. Los Alamos Scientific Laboratory report LA-4923-PR (1972).

J. F. Spalding and M. R. Brooks, Longevity and Mortality Distributions of Mice with and without X-Ray Exposure to 45 Generations of Male Progenitors. *Proc. Soc. Exp. Biol. Med.* **139**, 15-18 (1972).

J. F. Spalding and M. R. Brooks, Comparative Litter and Reproduction Characteristics of Mouse Populations with X-Ray Exposure, Including 45 Generations of Male Progenitors. *Proc. Soc. Exp. Biol. Med.* **141**, 445-447 (1972).

J. F. Spalding, N. J. Basmann, R. F. Archuleta, and O. S. Johnson, Comparative Effects of Dose Protraction by Fractionation and by Continuous Exposure. *Radiation Res.* **51**, 608-614 (1972).

J. F. Spalding, L. M. Holland, and J. R. Prine, Comparative Biological Effects of Protracted Cobalt-60 Irradiation in Beagles and Monkeys. In: *Abstracts of Papers for the 20th Annual Meeting of the Radiation Research Society, Portland, Oregon (May 14-18, 1972)*, pp. 35-36, Abstract No. Cd-12.

J. F. Spalding, L. M. Holland, and J. R. Prine, The Effects of Dose Protraction on Hematopoiesis in the Primate and Dog. *Life Sciences and Space Research COSPAR X*, 155-164 (1972).

Manuscripts Submitted

J. E. Furchner, C. R. Richmond, and J. E. London, Comparative Metabolism of Radionuclides in Mammals. VIII. Retention of 7 Beryllium in the Mouse, Rat, Monkey and Dog. *Health Phys.* (in press).

J. F. Spalding, L. M. Holland, J. R. Prine, P. M. LaBauve, and J. E. London, Comparative Effects of Dose Protraction and Residual Injury in Dogs and Monkeys. *Radiation Res.* (submitted).

PHYSICAL RADIOBIOLOGY SECTION

Publications

M. R. Raju, Physical and Radiobiological Aspects of π^- Mesons in Radiotherapy. Los Alamos Scientific Laboratory report LA-4931-MS (August 1972).

M. R. Raju, Physical and Biological Aspects of High LET Radiations with Reference to Radiotherapy. Los Alamos Scientific Laboratory report LA-5041-MS (September 1972).

Manuscripts Submitted

P. N. Dean, Estimation of Chest Wall Thickness in Lung Counting for Plutonium. *Health Phys.* (in press).

S. W. Jordan, P. N. Dean, and J. Ahlquist, Early Ultrastructural Effects of Ionizing Radiation. *J. Lab. Invest.* (in press).

BIOPHYSICS SECTION

Publications

A. Brunsting and P. F. Mullaney, Do Internal

Details of Mammalian Cells Influence Their Light Scattering Patterns? In: Abstracts of the 16th Annual Meeting of the Biophysical Society, Toronto, Ontario, Canada (February 24-27, 1972) 12, 141a (1972), Abstract No. SaPM-A6.

A. Brunsting and P. F. Mullaney, Differential Light Scattering: A Possible Method of Mammalian Cell Identification. J. Coll. Interface Sci. 39, 492-496 (1972).

A. Brunsting and P. F. Mullaney, A Light-Scattering Photometer Using Photographic Film. Rev. Sci. Instr. 43, 1514-1519 (1972).

A. Brunsting and P. F. Mullaney, Light Scattering from Coated Spheres: A Model for Biological Cells. Appl. Optics 11, 675-680 (1972).

A. Brunsting, Light Scattering from Mammalian Cells. Ph.D. Thesis, Department of Physics and Astronomy, University of New Mexico, Albuquerque, New Mexico. Los Alamos Scientific Laboratory report LADC-72-974 (June 1972).

A. Brunsting, Computer Analysis of Differential Light Scattering from Coated Spheres. Los Alamos Scientific Laboratory report LA-5032 (November 1972).

L. S. Cram and J. C. Hensley, Flow Microfluorometry for Fluorescent Antibody-Antigen Studies. In: Abstracts of the 16th Annual Meeting of the Biophysical Society, Toronto, Ontario, Canada (February 24-27, 1972) 12, 145a (1972), Abstract No. SaPM-A13.

D. M. Holm, L. S. Cram, and R. D. Hiebert, Instrumental Factors Influencing Resolution in Flow Microfluorometry. In: Abstracts of the 16th Annual Meeting of the Biophysical Society, Toronto, Ontario, Canada (February 24-27, 1972) 12, 144a (1972), Abstract No. SaPM-A12.

J. A. Steinkamp, M. J. Fulwyler, and J. R. Coulter, A New Multisensor Cell Analysis and Sorting System. In: Abstracts of the 16th Annual Meeting of the Biophysical Society, Toronto, Ontario, Canada (February 24-27, 1972) 12, 8a (1972), Abstract No. FPM-A4.

J. A. Steinkamp, M. J. Fulwyler, and M. A. Van Dilla, A High-Speed Electro-Optical Cell Analysis and Sorting System. In: 6th Albuquerque Section Instrumentation Symposium, Applications of Optical Electronics in Instrumentation, Instrument Society of America, Albuquerque, New Mexico (April 24-25, 1972), Abstract No. 3, Session III.

J. A. Steinkamp, M. A. Van Dilla, and A. Romero, Identification and Sorting of Human Leukocytes. In: Proceedings of the 25th Annual Conference on Engineering in Medicine and Biology 1972, Vol. 14 (1972), p. 82, Abstract No. 12.4.

T. T. Trujillo and M. A. Van Dilla, Adaptation of the Fluorescent Feulgen Reaction to Cells in Suspension for Flow Microfluorometry. Acta Cytol. 16, 26-30 (1972).

M. A. Van Dilla, Cell Analysis and Sorting by High-Speed Flow Methods. In: Abstracts of the 16th Annual Meeting of the Biophysical Society, Symposium on Biophysics of Cell Separation, Toronto, Ontario, Canada (February 24-27, 1972) 12, 7a (1972), Abstract No. FPM-A1.

Manuscripts Submitted

L. S. Cram and A. Brunsting, Fluorescence and Light Scattering Measurements on Hog Cholera-Infected PK-15 Cells. Exp. Cell Res. (in press).

D. M. Holm and L. S. Cram, An Improved Flow Microfluorometer for Rapid Measurements of Cell Fluorescence. Exp. Cell Res. (submitted).

R. O. Kelley, T. I. Baker, H. A. Crissman, and C. S. A. Henderson, Ultrastructure and Growth of Human Limb Mesenchyme (HLM) In Vitro. Anat. Record (submitted).

A. L. Kisch, R. O. Kelley, H. A. Crissman, and L. L. Paxton, DMSO Induced Reversion of Several Features of Polyoma Transformed BHK-21 Cells: Alterations in Growth and Morphology. J. Cell Biol. (submitted).

P. F. Mullaney and W. T. West, A Dual-Parameter Microfluorometer for Rapid Cell Analysis. Rev. Sci. Instr. (submitted).

J. A. Steinkamp, M. A. Van Dilla, and M. J. Fulwyler, Cell Analysis and Sorting: A New Multi-parameter Cell Sorter. Science (submitted).

J. A. Steinkamp, A. Romero, and M. A. Van Dilla, Multiparameter Cell Sorting: Identification of Human Leukocytes by Acridine Orange Fluorescence. Acta Cytol. (in press).

ISOTOPE APPLICATIONS SECTION

Publications

C. T. Gregg, Some Applications of ¹³C NMR to Biological Problems. In: Proceedings of Seminar on the Use of Stable Isotopes in Clinical Pharmacology, University of Chicago, November 10-11, 1971

(P. D. Klein and L. J. Roth, eds.). U. S. Atomic Energy Commission report CONF-711115 (August 1972), pp. 175-181.

C. T. Gregg, Some Aspects of the Energy Metabolism of Mammalian Cells. In: Growth, Nutrition and Metabolism in Cells in Culture, Vol. 1 (G. Rothblat and V. Cristofalo, eds.), Academic Press, New York (1972), pp. 83-136.

V. H. Kollman and C. T. Gregg, Preparation of Carbon-13 Labeled Sugars by Photosynthesis. In: J. Colorado-Wyoming Acad. Sci. VII(2-3), 20 (1972), Abstract No. 62.

D. G. Ott, Organic Synthesis and Biosynthesis. In: Proceedings of Seminar on the Use of Stable Isotopes in Clinical Pharmacology, University of Chicago, November 10-11, 1971 (P. D. Klein and L. J. Roth, eds.). U. S. Atomic Energy Commission report CONF-711115 (August 1972), pp. 15-32.

D. G. Ott, "Heavy" Mice. Lab World (January 1972), p. 72.

D. G. Ott, V. N. Kerr, and T. W. Whaley, Synthesis with Stable Isotopes. In: Abstracts of the First Rocky Mountain Regional Meeting of the American Chemical Society, Colorado State University, Fort Collins, Colorado (June 30-July 1, 1972), p. 34, Abstract No. 11.

C. E. Strouse, V. H. Kollman, and N. A. Matwiyoff, Carbon-13 NMR Spectra of Carbon-13 Enriched Chlorophylls a and b. Biochem. Biophys. Res. Commun. 46, 328-332 (1972).

T. W. Whaley and D. G. Ott, Simple Polyisotopic Molecules. In: Abstracts of the First Rocky Mountain Regional Meeting of the American Chemical Society, Colorado State University, Fort Collins, Colorado (June 30-July 1, 1972), p. 34, Abstract No. 12.

Manuscripts Submitted

V. H. Kollman, J. L. Hanners, J. Y. Hutson, T. W. Whaley, D. G. Ott, and C. T. Gregg, Large-Scale Photosynthetic Production of Carbon-13 Labeled Sugars: The Tobacco Leaf System. Biochem. Biophys. Res. Commun. (submitted).

N. A. Matwiyoff and B. F. Burnham, Carbon-13 NMR Spectroscopy of Tetrapyrroles. Ann. N. Y. Acad. Sci. (in press).

R. T. Eakin, L. O. Morgan, C. T. Gregg, and N. A. Matwiyoff, Carbon-13 Nuclear Magnetic Resonance Spectroscopy of Living Cells and Their Metabolism of a Specifically Labeled ¹³C Substrate. FEBS Letters (submitted).

TALKS PRESENTED AT SEMINARS AND MEETINGS

BY BIOMEDICAL RESEARCH GROUP STAFF

CELLULAR RADIOBIOLOGY SECTION

B. J. Barnhart and S. H. Cox, Replication and Sizing of Bacteriophage DNA: Membrane-Associated Functions in Haemophilus influenzae, presented at the 72nd Annual Meeting of the American Society for Microbiology, Philadelphia, Pennsylvania (April 23-28, 1972).

B. J. Barnhart and S. H. Cox, Prophage Excision in Haemophilus influenzae, presented at the Annual Regional Meeting of the Southwest Tri-State Branch of the American Society for Microbiology, El Paso, Texas (October 13-14, 1972).

L. L. Deaven, A Classical and a Modern Approach to Chromosome Structural Analysis, presented at the Department of Biophysics, Northern Michigan University, Marquette, Michigan (February 15, 1972).

L. L. Deaven, The Paradox of DNA Constancy in Heteroploidy, presented at the Department of Biophysics, Northern Michigan University, Marquette, Michigan (February 17, 1972).

L. L. Deaven, The Paradox of DNA Constancy in Heteroploid Cell Populations, presented at the Department of Biology, M. D. Anderson Hospital and Tumor Institute, University of Texas, Houston, Texas (July 26, 1972).

L. L. Deaven, Techniques for Banding Chromosomes with Giemsa Stain, presented at the Biomedical Division, Lawrence Livermore Laboratory, University of California, Livermore, California (October 27, 1972).

L. L. Deaven and D. F. Petersen, Are Chromosomally Aneuploid Cells Genetically Aneuploid? presented at the 12th Annual Meeting of the American Society for Cell Biology, St. Louis, Missouri (November 8-11, 1972).

M. D. Enger and E. W. Campbell, Nascent Messenger-Like RNA Metabolism in Chinese Hamster Ovary Cells Cultured at Elevated Temperature, presented at the 28th Annual Southwest Regional Meeting of the American Chemical Society, Baton Rouge,

Louisiana (December 6-8, 1972).

L. R. Gurley, R. A. Walters, and R. A. Tobey, The Relationship of Histone Phosphorylation to the Cell Cycle, presented at the 12th Annual Meeting of the American Society for Cell Biology, St. Louis, Missouri (November 8-11, 1972).

L. R. Gurley, R. A. Walters, and R. A. Tobey, The Independence of Histone Phosphorylation from DNA Synthesis, presented at the 28th Annual Southwest Regional Meeting of the American Chemical Society, Baton Rouge, Louisiana (December 6-8, 1972).

C. E. Hildebrand and R. A. Tobey, DNA-Membrane Associations in Cultured Chinese Hamster Cells, presented at the Annual Meeting of the Biophysical Society, Toronto, Canada (February 24-27, 1972).

P. M. Kraemer, DNA Constancy in Heteroploidy, presented at the University of Colorado Medical Center, Denver, Colorado (May 30, 1972).

P. M. Kraemer, Studies of the Cell Surface Utilizing Flow Microfluorometry, presented at a Drug Evaluation Branch program review, National Cancer Institute, Bethesda, Maryland (August 10, 1972).

P. M. Kraemer, H. A. Crissman, and M. A. Van Dilla, Flow Microfluorometric (FMF) Studies of Plant Lectin Binding to Cultured Mammalian Cells, presented at the 12th Annual Meeting of the American Society for Cell Biology, St. Louis, Missouri (November 8-11, 1972).

D. F. Petersen, Preclinical Experiments in Pion Radiobiology, presented at the Summer Oncology Course sponsored by the Edward Mallinckrodt Institute of Radiology, Washington University School of Medicine, St. Louis, Missouri (August 7, 1972).

D. F. Petersen, Cell Kinetics in Radiobiology (Round Table Discussion) and Cell-Cycle Analysis and Growth Properties of Chinese Hamster Cells, presented at the Summer Oncology Course sponsored by the Edward Mallinckrodt Institute of Radiology, Washington University School of Medicine, St. Louis,

Missouri (August 8, 1972).

R. A. Tobey, Differential Effects of Cytosine Arabinoside and Sodium Camptothecin on Initiation of DNA Synthesis, presented at the Upjohn Company, Kalamazoo, Michigan (February 25, 1972).

R. A. Tobey, Biochemical Properties of Chinese Hamster Cells Reversibly Arrested in G_1 in Isoleucine-Deficient Medium, presented at the Microbiology Seminar Series of the MSU/AEC Plant Research Laboratory, Michigan State University, East Lansing, Michigan (February 28, 1972).

R. A. Tobey, Determination of the Effects of Chemotherapeutic Agents on Mammalian Cell Traverse, presented at the MSU/AEC Plant Research Laboratory, Michigan State University, East Lansing, Michigan (February 29, 1972).

R. A. Tobey, Effects of Sub-Optimal Quantities of Isoleucine upon Macromolecular Synthesis in Chinese Hamster Cells, presented at the 23rd Annual Meeting of the Tissue Culture Association, Symposium on Cell Nutrition in Culture, Los Angeles, California (June 5-8, 1972).

R. A. Tobey, Detailed Analysis of Drug Effects on Mammalian Cell DNA Replication Utilizing Flow Microfluorometry, presented at a Drug Evaluation Branch program review, National Cancer Institute, Bethesda, Maryland (August 10, 1972).

R. A. Tobey, Use of Flow Microfluorometry in Analysis of Effects of Agents on Cell-Cycle Progression, presented at the Third Joint Working Conference sponsored by the Division of Cancer Treatment, National Cancer Institute, Hunt Valley Inn, Maryland (October 2-4, 1972).

R. A. Tobey, H. A. Crissman, and P. M. Kraemer, A Method for Comparing Effects of Different Synchronizing Protocols on Mammalian Cell-Cycle Traverse, presented at the 12th Annual Meeting of the American Society for Cell Biology, St. Louis, Missouri (November 8-11, 1972).

R. A. Walters, Effects of X-Irradiation on DNA Precursor Incorporation and DNA Replication in Chinese Hamster Cells, presented at the Biochemistry Department, University of New Mexico, Albuquerque, New Mexico (March 16, 1972).

R. A. Walters, The Effect of X-Irradiation on DNA Precursor Metabolism and DNA Replication in Chinese Hamster Cells, presented at Northern Illinois University, DeKalb, Illinois (May 4, 1972),

and at the Argonne National Laboratory, Argonne, Illinois (May 5, 1972).

R. A. Walters, L. R. Gurley, R. A. Tobey, M. D. Enger, and R. L. Ratliff, Effects of X-Irradiation on DNA Precursor Metabolism and DNA Replication in Chinese Hamster Cells, presented at the 20th Annual Meeting of the Radiation Research Society, Portland, Oregon (May 14-18, 1972).

R. A. Walters, L. R. Gurley, R. A. Tobey, M. D. Enger, and R. L. Ratliff, Effects of X-Irradiation on DNA Precursor Metabolism and DNA Replication in Chinese Hamster Cells, presented at the Rocky Mountain Regional Meeting of the American Chemical Society, Colorado State University, Fort Collins, Colorado (June 30-July 1, 1972).

R. A. Walters, R. L. Ratliff, L. R. Gurley, and M. D. Enger, The Effects of X-Irradiation on the Metabolism of DNA from Chinese Hamster Ovary Cells, presented at the 28th Annual Southwest Regional Meeting of the American Chemical Society, Baton Rouge, Louisiana (December 6-8, 1972).

MOLECULAR RADIOBIOLOGY SECTION

P. Byvoet, G. R. Shepherd, J. M. Hardin, and B. J. Noland, Turnover of Labeled Methyl and Acetyl Groups in Histone Fractions of Cultured Mammalian Cells, presented at the 63rd Annual Meeting of the American Society of Biological Chemists, Atlantic City, New Jersey (April 10-14, 1972).

G. R. Shepherd, Structural Alterations of Histones, presented at the Department of Biochemistry, University of New Mexico School of Medicine, Albuquerque, New Mexico (January 20, 1972).

G. R. Shepherd, Structural Alterations in Histones of Synchronized Mammalian Cells, presented at the Departments of Psychiatry and Pharmacology, University of Colorado Medical Center, Denver, Colorado (March 1, 1972), and at the Department of Molecular, Cellular and Developmental Biology, University of Colorado, Boulder, Colorado (March 2, 1972).

G. R. Shepherd, J. M. Hardin, B. J. Noland, and P. Byvoet, Turnover of Methyl, Acetyl, and Phosphoryl Groups in Histone Fractions of Cultured Mammalian Cells, presented at the Rocky Mountain Regional Meeting of the American Chemical Society, Colorado State University, Fort Collins, Colorado (June 30-July 1, 1972).

D. A. Smith, A. M. Martinez, and D. L. Williams, Initiation of *in vitro* RNA Synthesis with Oligodeoxyribonucleotides, presented at the 164th National Meeting of the American Chemical Society, New York City, New York (August 27-September 1, 1972).

G. F. Strniste, A. M. Martinez, and D. A. Smith, *In vitro* Studies on the Synthesis of Ribonucleic Acid Using Ionizing Irradiated RNA Polymerase, presented at the Annual Meeting of the Biophysics Society, Toronto, Canada (February 24-27, 1972).

G. F. Strniste, *In vitro* Studies on the Synthesis of Ribonucleic Acid Using Ionizing Irradiated RNA Polymerase, presented at St. Olaf College, Northfield, Minnesota (March 23, 1972).

G. F. Strniste and D. A. Smith, *In vitro* Studies on the Synthesis of Ribonucleic Acid Using X-Irradiated RNA Polymerase, presented at the Rocky Mountain Regional Meeting of the American Chemical Society, Colorado State University, Fort Collins, Colorado (June 30-July 1, 1972).

BIOPHYSICS SECTION

A. Brunsting and P. F. Mullaney, Do Internal Details of Mammalian Cells Influence Their Light Scattering Patterns? presented at the Annual Meeting of the Biophysical Society, Toronto, Canada (February 24-27, 1972).

L. S. Cram and J. C. Mensley, Flow Microfluorometry for Fluorescent Antibody-Antigen Studies, presented at the Annual Meeting of the Biophysical Society, Toronto, Canada (February 24-27, 1972).

L. S. Cram and H. A. Crissman, DNA of Mammalian Cells: High-Speed Flow Microspectrofluorometry, presented at Cold Spring Harbor Laboratory, Cold Spring Harbor, New York (July 11, 1972).

H. A. Crissman, Cell Preparative Considerations in the General Operative Features of Flow Microfluorometry, presented at a Drug Evaluation Branch program review, National Cancer Institute, Bethesda, Maryland (August 10, 1972).

H. A. Crissman, Flow Microfluorometry: Principles and Applications for Cell Biology, presented at the University of New Mexico School of Medicine, Albuquerque, New Mexico (October 3, 1972).

D. M. Holm, L. S. Cram, and R. D. Hiebert, Instrumental Factors Influencing Resolution in Flow Microfluorometry, presented at the Annual Meeting

of the Biophysical Society, Toronto, Canada (February 24-27, 1972).

P. K. Horan, Parameters of Virus Infection as Studied by Flow Microfluorometry, presented at the Meeting on the Molecular Biology of SV40, Polyoma and Adeno Viruses (August 16-19, 1972), and Herpes Virus Meeting (August 20-24, 1972), Cold Spring Harbor Laboratory, Cold Spring Harbor, New York.

P. K. Horan, Flow Microfluorometry as Applied to Cancer Diagnosis, presented at the National Cancer Institute, Bethesda, Maryland (August 28, 1972).

P. F. Mullaney, High-Speed Cell Analysis Research at the Los Alamos Scientific Laboratory, presented at the Canadian AEC/Biophysical Society meeting, Nuclear Research Establishment, AEC of Canada, Pinawa (Winnipeg), Canada (January 13-14, 1972).

C. R. Richmond, Non-Uniform Dose Distribution in Tissues: Fact and Fancy, presented at the Fall Meeting of the Rio Grande Chapter of the Health Physics Society, Albuquerque, New Mexico (November 3, 1972).

J. A. Steinkamp, M. J. Fulwyler, and J. R. Coulter, A New Multisensor Cell Analysis and Sorting System, presented at the Annual Meeting of the Biophysical Society, Toronto, Canada (February 24-27, 1972).

J. A. Steinkamp, M. J. Fulwyler, and M. A. Van Dilla, A High-Speed Electro-Optical Cell Analysis and Sorting System, presented at the Conference on Applications of Optical Electronics in Instrumentation sponsored by the Instrument Society of America and the University of New Mexico, Albuquerque, New Mexico (March 30-31, 1972).

J. A. Steinkamp, M. A. Van Dilla, and A. Romero, Identification and Sorting of Human Leukocytes, presented at the 25th Annual Conference on Engineering in Medicine and Biology, Bal Harbour, Florida (October 1-5, 1972).

M. A. Van Dilla, Cell Analysis and Sorting by High-Speed Flow Methods, presented at the Annual Meeting of the Biophysical Society, Symposium on Biophysics of Cell Separation, Toronto, Canada (February 24-27, 1972).

M. A. Van Dilla, The Cell Sensing and Analysis Program at Los Alamos, presented at the Conference on Quantitative Fluorescence Techniques as Applied

in Cell Biology, Seattle, Washington (March 27-31, 1972).

M. A. Van Dilla, Cell Analysis and Cell Sorting, presented at the Biophysics Department, University of California, Berkeley, California (May 2, 1972).

M. A. Van Dilla, Flow System Cell Analysis, presented at the 1972 Engineering Foundation Conference on "Engineering in Medicine — Automatic Cytology," Saxtons River, Vermont (August 7-11, 1972).

M. A. Van Dilla and J. A. Steinkamp, Electronic Cell Sorting and Applications to Cell Biology and Exfoliative Cytology, presented at the Symposium on Recent Developments in Research Methods and Instrumentation sponsored by the National Heart and Lung Institute, National Institutes of Health, Bethesda, Maryland (November 30, 1972).

MAMMALIAN RADIOBIOLOGY SECTION

J. F. Spalding, L. M. Holland, and J. R. Prine, Comparative Biological Effects of Protracted Cobalt-60 Irradiation in Beagles and Monkeys, presented at the 20th Annual Meeting of the Radiation Research Society, Portland, Oregon (May 14-18, 1972).

PHYSICAL RADIOBIOLOGY SECTION

P. N. Dean, Estimation of Chest Wall Thickness in Lung Counting for Plutonium, presented at the Annual Meeting of the Health Physics Society, Las Vegas, Nevada (June 12-16, 1972).

P. N. Dean, Visualization of Pion Stopping Region, presented at the National Meeting on Applications of Optical Instruments in Medicine, Chicago, Illinois (November 29-30, 1972).

M. R. Raju, Physical and Radiobiological Aspects of π^- Mesons with Reference to Radiotherapy, presented at the M. D. Anderson Hospital and Tumor Institute, University of Texas, Houston, Texas (July 6, 1972).

M. R. Raju, Negative Pions in Radiotherapy: Physical and Radiobiological Aspects, presented at the Sloan Kettering Institute, New York City, New York (July 24, 1972).

M. R. Raju, Negative Pions in Radiotherapy, presented at the Third International Conference on Medical Physics and Medical Engineering, Goteborg, Sweden (July 30-August 4, 1972).

M. R. Raju, Physical and Radiobiological

Aspects of Heavy Charged Particles and Their Potential Use in Radiotherapy, presented at a Refresher Course of the Radiological Society of North America, Chicago, Illinois (November 29-30, 1972).

C. Richman, Studying Pion Beams for Cancer Therapy, presented at the Annual Meeting of the New Mexico Division of the American Cancer Society, Albuquerque, New Mexico (September 9, 1972).

K. L. Swinth and P. N. Dean, Intercalibration for Low-Energy Photon Measurements, presented at the Annual Meeting of the Health Physics Society, Las Vegas, Nevada (June 12-16, 1972).

ISOTOPE APPLICATIONS SECTION

C. T. Gregg, Carbon Pathways: Glycolysis and Related Fermentations, presented at the Department of Microbiology, University of New Mexico School of Medicine, Albuquerque, New Mexico (October 13, 1972).

C. T. Gregg, Carbon Pathways: TCA, Glyoxylate Cycle, presented at the Department of Microbiology, University of New Mexico School of Medicine, Albuquerque, New Mexico (October 18, 1972).

C. T. Gregg, Electron Transport, presented at the Department of Microbiology, University of New Mexico School of Medicine, Albuquerque, New Mexico (October 20, 1972).

V. H. Kollman and C. T. Gregg, Preparation of Carbon-13 Labeled Sugars by Photosynthesis, presented at the Annual Meeting of the Botanical Sciences Section, Southwestern and Rocky Mountain Division, American Association for the Advancement of Science, and the Colorado-Wyoming Academy of Science, Colorado State University, Fort Collins, Colorado (April 26-29, 1972).

D. G. Ott, Stable Isotopes and the Synthetic Chemist, presented at the Department of Chemistry, University of New Mexico, Albuquerque, New Mexico (March 24, 1972).

D. G. Ott, V. N. Kerr, and T. W. Whaley, Synthesis with Stable Isotopes, presented at the Rocky Mountain Regional Meeting of the American Chemical Society, Colorado State University, Fort Collins, Colorado (June 30-July 1, 1972).

D. G. Ott, Biomedical Applications of Stable Isotopes of Carbon, Oxygen, and Nitrogen, presented at the Laboratory of Nuclear Medicine, University of California, Los Angeles, California (December 12, 1972).

W. W. Shreeve, Lipogenesis from Carbon-14

Labeled Carbohydrates in vivo in Humans, presented
at the University of New Mexico School of Medicine,
Albuquerque, New Mexico (April 28, 1972).

T. W. Whaley and D. G. Ott, Simple Polyisotopic

Molecules, presented at the Rocky Mountain Regional
Meeting of the American Chemical Society, Colorado
State University, Fort Collins, Colorado (June 30-
July 1, 1972).

RESEARCH INTERESTS OF BIOMEDICAL RESEARCH GROUP DIRECTIVE STAFF MEMBERS

- E. C. Anderson, Ph.D., University of Chicago (1949)
Electronic spectrometry of cell population distributions
Analysis of cell growth and division dynamics by mathematical and computer models
Biochemistry of mammalian cell life cycle
Biological effects of hot particles
- B. J. Barnhart, Sc.D., Johns Hopkins University (1962)
Biochemistry of bacterial genetic transformation
Photobiology: Bacterial responses to ultraviolet light and DNA repair processes
- L. S. Cram, Ph.D., Pennsylvania State University (1969)
Macromolecular structure and ultraviolet radiation action
High-speed cellular analysis and biomedical instrumentation
- P. N. Dean, M.A., Rice University (1958)
Low-level radioactivity counting
Radiological physics
Computer applications
- M. D. Enger, Ph.D., University of Wisconsin (1964)
Mammalian RNA synthesis and modification
- J. E. Furchner, Ph.D., University of New Mexico (1955)
Metabolism of radionuclides
Internal emitters
Radiation protection guides
- C. T. Gregg, Ph.D., Oregon State University (1959)
Energy metabolism of cultured cells
Biochemical applications of stable isotopes
- L. R. Gurley, Ph.D., University of North Carolina (1964)
Histone chemistry and metabolism
- F. N. Hayes, Ph.D., Northwestern University (1949)
Radiation chemistry and biology of nucleic acids
- C. E. Hildebrand, Ph.D., Pennsylvania State University (1970)
Synthesis of cell-free protein
- D. E. Hoard, Ph.D., University of California (1957)
Organic synthesis of oligodeoxynucleotides
Effects of radiation on nucleic acids
- L. M. Holland, D.V.M., Colorado State University (1958)
Laboratory animal medicine
Hematology and surgery
Mammalian radiobiology
- P. K. Horan, Ph.D., Pennsylvania State University (1970)
Tumor cell diagnosis using LASL cell sorter techniques
- J. H. Jett, Ph.D., University of Colorado (1969)
Nuclear physics applications and instrumentation for radioactivity counting
Computer applications for data analysis and system control
- P. M. Kraemer, Ph.D., University of Pennsylvania (1964)
Structure and function of mammalian cell-surface complex carbohydrates
- P. F. Mullaney, Ph.D., University of Delaware (1965)
Optical cell sensing
Light scattering by cells
Simultaneous measurement of multicellular parameters
- D. G. Ott, Ph.D., Washington State University (1953)
Organic syntheses with isotopes
Nucleotide chemistry
Biochemical applications of stable isotopes
- D. F. Petersen, Ph.D., University of Chicago (1954)
Biochemistry of mammalian cell life cycle
Synchronization of mammalian cell cultures

- J. R. Prine, D.V.M., Texas A and M University (1951)
 Board certified veterinary pathologist
 Pathology of small laboratory animals and primates
 Radiation pathology
- R. L. Ratliff, Ph.D., St. Louis University (1960)
 Isolation of DNA polymerase and deoxy-nucleases
 Enzymatic synthesis of polynucleotides
- M. R. Raju, Sc.D., Andhra University (1961)
 Dosimetry and radiobiology of high LET radiations in general, with reference to radiotherapy
 Dosimetry and radiobiology of negative pions
 Application of FMF instrumentation to normal and tumor cell kinetics
- C. Richman, University of California, Berkeley (1943)
 Dosimetry and radiobiology of negative pions
- C. R. Richmond, Ph.D., University of New Mexico (1958)
 Metabolic kinetics and biological effects of radionuclides
 Water and electrolyte metabolism
 Mammalian radiobiology
- A. G. Saponara, Ph.D., University of Wisconsin (1964)
 Isolation and characterization of minor nucleotides from mammalian cell nucleic acids
- G. R. Shepherd, Ph.D., Stanford University (1961)
 Cellular differentiation
 Structure and function of histones
 Structure of chromatin
- D. A. Smith, Ph.D., University of Southern California (1964)
 Nucleic acid enzymology
 Ultracentrifugation
 Molecular radiobiology
- J. F. Spalding, Ph.D., Texas A and M University (1953)
 Somatic and genetic effects of ionizing radiation from external sources
- J. A. Steinkamp, Ph.D., Iowa State University (1970)
 Electronic instrumentation design and testing
 Electromagnetic radiation monitoring
 Identification of cells by fluorescent methods
 Automated cell analysis and sorting and biomedical instrumentation
- R. A. Tobey, Ph.D., University of Illinois (1963)
 Biochemical regulation of mammalian cell-cycle events
- M. A. Van Dilla, Ph.D., Massachusetts Institute of Technology (1951)
 Cell microfluorometry: DNA distribution in cell populations
 Light scattering by cells
 Cell volume spectrometry
- R. A. Walters, Ph.D., Colorado State University (1967)
 Biochemistry of radiation effects on mammalian cells
 Analytical biochemistry of macromolecules
- T. W. Whaley, Ph.D., University of New Mexico (1971)
 Organic scintillators
 Organic synthesis with stable isotopes
- D. L. Williams, M.S., University of Colorado (1944)
 Organic synthesis of oligodeoxynucleotides

COMMITTEES ASSOCIATED WITH THE BIOMEDICAL RESEARCH PROGRAM

The Interdivisional Steering Committee for the Isotopes of Carbon, Oxygen, Nitrogen, and Sulfur (ICONS) Program provides guidance for both Groups CNC-4 and H-4. Committee members are:

N. A. Matwiyoff (CNC-4), Chairman
B. B. McInteer (CNC-4)
J. D. Seagrave (P-DOR)
C. T. Gregg (H-4)
D. G. Ott (H-4)

Consultation to this group is provided by numerous individuals, including:

J. S. Kirby-Smith (USAEC/DBER)
B. Tolbert (University of Colorado)
T. O. Morgan (University of Texas)
L. Roth (University of Chicago)
P. Stout (University of California, Davis)

Efforts began late in 1971 to organize an advisory committee for the purpose of providing expert advice to the Director of the Laboratory on the scientific merit and future direction of the more fundamental segments of the overall Laboratory's biomedical research program. Composition of the Advisory Committee for Biomedical Research is such that emphasis will be directed toward the more basic and fundamental aspects of the overall biomedical program. This is important because, since the early 1960's with encouragement of the AEC's Division of Biology and Medicine (now the Division of Biomedical and Environmental Research), a significant fraction of the Laboratory's biomedical research effort has been directed toward a continuing program in biology which is more fundamentally and generally oriented toward AEC/DBER interests on the basis of the argument that progress in biology is essential to the development of a strong program in radiobiology. At the time of writing this report, plans are being made to hold the second meeting of this advisory committee. Composition of the committee is given below:

Dr. Arthur B. Pardee (Chairman)
Professor of Biochemical Sciences
Princeton University
Princeton, New Jersey

Dr. Phillip P. Cohen
Professor of Physiological Chemistry
University of Wisconsin
Madison, Wisconsin

Dr. Robert M. Bock
Professor of Molecular Biology
University of Wisconsin
Madison, Wisconsin

Dr. William J. Rutter
Department of Biochemistry and Biophysics
University of California
San Francisco, California

Dr. David E. Kuhl
Professor of Radiology
University of Pennsylvania
Philadelphia, Pennsylvania

Dr. Leo K. Bustad, Director
Radiobiology Laboratory and
Comparative Oncology Laboratory
University of California, Davis
Davis, California

This advisory committee represents the enormous pool of expertise and experience in the areas of transport and organization of biochemical events in living systems; tumor cell kinetics in radiotherapy; radiology; biochemistry; molecular biology, transfer RNA chemistry; physiological chemistry; fundamental cancer research, pathology; chemotherapy; biomedical instrumentation; and enzyme mechanism studies. This group has proved to be extremely valuable in providing technical advice and program direction to virtually all phases of our overall biomedical research program.

Another committee that relates strongly to Group H-4 is the Clinton P. Anderson Mason Physics

Facility (CPAMPF) Biomedical Steering Committee. The main committee and its numerous subcommittees, comprised of LASL personnel and members of the general scientific community, provide a broad base of competence and experience from numerous disciplines. Members of the main committee and its subcommittees are as follows:

CPAMPF Biomedical Steering Committee

Dr. Paul Todd (Chairman)
Department of Biophysics
Pennsylvania State University
University Park, Pennsylvania

Dr. C. R. Richmond (Alternate)
Los Alamos Scientific Laboratory
Los Alamos, New Mexico

Dr. Chaim Richman (Member at Large)
Los Alamos Scientific Laboratory
Los Alamos, New Mexico

Dr. M. M. Kligerman (Member at Large)
Los Alamos Scientific Laboratory
Los Alamos, New Mexico

and
University of New Mexico
Albuquerque, New Mexico

Dr. Henry S. Kaplan (Member at Large)
Department of Radiology
Stanford University Medical Center
Stanford, California

Dr. H. Rodney Withers (Member at Large)
M. D. Anderson Hospital and
Tumor Institute
Texas Medical Center
Houston, Texas

Dr. Louis Rosen (Member at Large)
Los Alamos Scientific Laboratory
Los Alamos, New Mexico

Dr. A. M. Koehler (Member at Large)
Cyclotron Laboratory
Harvard University
Cambridge, Massachusetts

Dr. David Hussey (Member at Large)
Department of Radiotherapy
M. D. Anderson Hospital
and Tumor Institute
Texas Medical Center
Houston, Texas

Dr. Clarence C. Lushbaugh
Medical Division
Oak Ridge Associated Universities, Inc.
Oak Ridge, Tennessee

Subcommittee on Facility and Beam Line

Dr. Paul M. Franke, Jr. (Co-Chairman)
Los Alamos Scientific Laboratory
Los Alamos, New Mexico

Dr. Richard L. Hutson (Co-Chairman)
Los Alamos Scientific Laboratory
Los Alamos, New Mexico

Dr. Arvid S. Lundy (Alternate)
Los Alamos Scientific Laboratory
Los Alamos, New Mexico

Dr. M. M. Kligerman
Los Alamos Scientific Laboratory
Los Alamos, New Mexico

and
University of New Mexico
Albuquerque, New Mexico

Dr. George D. Oliver, Jr.
Department of Radiology
Washington University School of Medicine
St. Louis, Missouri

Subcommittee on Physical and Biological Dosimetry

Dr. Lawrence H. Lanzl (Chairman)
Department of Radiology
University of Chicago
Chicago, Illinois

Dr. M. R. Raju (Alternate)
Los Alamos Scientific Laboratory
Los Alamos, New Mexico

Dr. Peter R. Almond
Physics Department
M. D. Anderson Hospital
and Tumor Institute
Texas Medical Center
Houston, Texas

Subcommittee on Radioisotope Research

Dr. Jon D. Shoop (Chairman)
University of New Mexico
School of Medicine
Albuquerque, New Mexico

Dr. Harold A. O'Brien (Alternate)
Los Alamos Scientific Laboratory
Los Alamos, New Mexico

Dr. James J. Reidy
Department of Physics
University of Mississippi
University, Mississippi

Subcommittee on Nuclear Medicine and Diagnostic Procedures

Dr. Robert D. Moseley, Jr. (Chairman)
Department of Radiology
Bernalillo County Medical Center
Albuquerque, New Mexico

Mr. Phillip N. Dean (Alternate)
Los Alamos Scientific Laboratory
Los Alamos, New Mexico

Dr. Jon D. Shoop
University of New Mexico
School of Medicine
Albuquerque, New Mexico

Subcommittee on Cell and Tumor Radiobiology

Dr. Larry L. Schenken (Chairman)
Radiation Physics and Biology
Mayo Clinic
Rochester, Minnesota

Dr. D. F. Petersen (Alternate)
Los Alamos Scientific Laboratory
Los Alamos, New Mexico

Dr. H. R. Withers
M. D. Anderson Hospital
and Tumor Institute
Texas Medical Center
Houston, Texas

Dr. M. M. Eikind
Department of Radiation Biology
Hammersmith Hospital
London, England

Dr. George M. Mahn
Department of Radiology
Stanford University Medical Center
Stanford, California

Subcommittee on Radiobiology and Pathology

Dr. Charles R. Key (Chairman)
University of New Mexico
School of Medicine
Albuquerque, New Mexico

Dr. John F. Spalding (Alternate)
Los Alamos Scientific Laboratory
Los Alamos, New Mexico

Dr. Robert A. Anderson
Department of Pathology
University of New Mexico
School of Medicine
Albuquerque, New Mexico

Dr. M. M. Kligerman
Los Alamos Scientific Laboratory
Los Alamos, New Mexico
and
University of New Mexico
Albuquerque, New Mexico

Dr. F. Bing Johnson
University of Colorado
School of Medicine
Denver, Colorado

Dr. Robert F. Kallman
Department of Radiology
Stanford University School of Medicine
Palo Alto, California

Dr. C. C. Lushbaugh
Medical Division
Oak Ridge Associated Universities, Inc.
Oak Ridge, Tennessee

Subcommittee on Therapy

Dr. Max L. M. Boone (Chairman)
Department of Radiology
Arizona Medical Center
Tucson, Arizona

Dr. M. M. Kligerman (Alternate)
Los Alamos Scientific Laboratory
Los Alamos, New Mexico
and
University of New Mexico
Albuquerque, New Mexico
Dr. David Hussey
Department of Radiotherapy
M. D. Anderson Hospital
and Tumor Institute
Texas Medical Center
Houston, Texas

Dr. Charles C. Rogers
Department of Radiology
Medical College of Virginia
Health Sciences Center
Richmond, Virginia
Dr. Malcolm A. Bagshaw
Department of Radiology
Stanford University Medical Center
Stanford, California